PUBLISHED WEEKLY

VOL. 241 NO. 2 JUNE 4, 1982

THIS ISSUE COMPLETES VOL. 241

JOURNAL OF

CHROMATOGRAPHY

INTERNATIONAL JOURNAL ON CHROMATOGRAPHY, ELECTROPHORESIS AND RELATED METHODS

ELSEVIER SCIENTIFIC PUBLISHING COMPANY
AMSTERDAM

JOURNAL OF CHROMATOGRAPHY

Scope. The *Journal of Chromatography* publishes papers on all aspects of chromatography, electrophoresis and related methods. Contributions consist mainly of research papers dealing with chromatographic theory, instrumental development and their applications. The section *Biomedical Applications*, which is under separate editorship, deals with the following aspects: developments in and applications of chromatographic and electrophoretic techniques related to clinical diagnosis (including the publication of normal values); screening and profiling procedures with special reference to metabolic disorders; results from basic medical research with direct consequences in clinical practice; combinations of chromatographic and electrophoretic methods with other physicochemical techniques such as mass spectrometry. In *Chromatographic Reviews*, reviews on all aspects of chromatography, electrophoresis and related methods are published.

Submission of Papers. Papers in English, French and German may be submitted, in three copies. Manuscripts should be submitted to: The Editor of *Journal of Chromatography*, P.O. Box 681, 1000 AR Amsterdam, The Netherlands, or to: The Editor of *Journal of Chromatography, Biomedical Applications*, P.O. Box 681, 1000 AR Amsterdam, The Netherlands. Review articles are invited or proposed by letter to the Editors and will appear in *Chromatographic Reviews* or *Biomedical Applications*. An outline of the proposed review should first be forwarded to the Editors for preliminary discussion prior to preparation. Submission of an article is understood to imply that the article is original and unpublished and is not being considered for publication elsewhere. For copyright regulations, see below.

Subscription Orders. Subscription orders should be sent to: Elsevier Scientific Publishing Company, P.O. Box 211, 1000 AE Amsterdam, The Netherlands. The *Journal of Chromatography* and the *Biomedical Applications* section can be subscribed to separately.

Publication. The *Journal of Chromatography* (incl. *Biomedical Applications, Chromatographic Reviews* and *Cumulative Author and Subject Indexes, Vols. 221–230, 231–240* and *241–250*) has 25 volumes in 1982. The subscription prices for 1982 are:

J. Chromatogr. (incl. *Chromatogr. Rev.* and *Cum. Indexes Vols. 221–230, 231–240 and 241–250*) + *Biomed. Appl.* (Vols. 227–251):
Dfl. 3625.00 plus Dfl. 500.00 (postage) (total *ca.* US$ 1650.00)

J. Chromatogr. (incl. *Chromatogr. Rev.* and *Cum. Indexes Vols. 231–240* and *241–250*) only (Vols. 234–251):
Dfl. 2826.00 plus Dfl. 360.00 (postage) (total *ca.* US$ 1274.50)

Biomed. Appl. (incl. *Cum. Indexes Vols. 221–230*) only (Vols 227–233):
Dfl. 1050.00 plus Dfl. 140.00 (postage) (total *ca.* US$ 476.00).

Journals are automatically sent by airmail to the U.S.A. and Canada at no extra costs, and to Japan, Australia and New Zealand, with a small additional postal charge. Back volumes of the *Journal of Chromatography* (Vols. 1 through 226) are available at Dfl. 173.00 (plus postage). Claims for issues not received should be made within three months of publication of the issue. If not, they cannot be honoured free of charge. For customers in the U.S.A. and Canada, wishing additional bibliographic information on this and other Elsevier journals, please contact Elsevier Science Publishing Company Inc., Journal Information Center, 52 Vanderbilt Avenue, New York, NY 10017. Tel: (212) 867-9040.

Abstracts/Contents Lists published in Analytical Abstracts, Biochemical Abstracts, Biological Abstracts, Chemical Abstracts, Chemical Titles, Current Contents/Physical, Chemical & Earth Sciences, Current Contents/Life Sciences, Index Medicus, Mass Spectrometry Bulletin, and Science Citation Index.

See page 3 of cover for Publication Schedule, Information for Authors, and information on the News Section and Advertisements.

Printed in The Netherlands

CONTENTS

(Abstracts/Contents Lists published in Analytical Abstracts, Biochemical Abstracts, Biological Abstracts, Chemical Abstracts, Chemical Titles, Current Contents/Physical, Chemical & Earth Sciences, Current Contents/Life Sciences, Index Medicus, Mass Spectrometry Bulletin, and Science Citation Index)

(Continued overleaf)

Notes

Letters to the Editor

HPLC 600

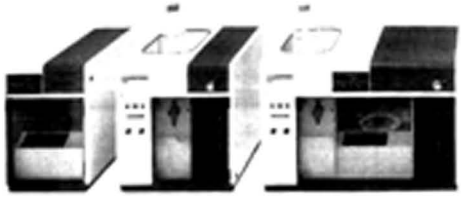

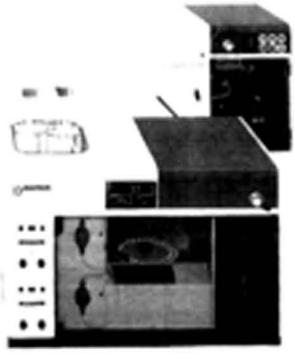

KONTRON
Your partner in modern HPLC

KONTRON AG
Analytical Division
Bernerstrasse Süd 169
CH-8048 Zürich

Australia (Sydney)	(02) 9383433	Germany (Munich)	(08165) 771	Netherlands (Maarssen)	(03465) 60894
Austria (Vienna)	(0222) 670631	Great Britain (St. Albans)	(0727) 66222	Spain (Madrid)	(01) 7291155
Canada (Mississauga)	(416) 6781151	Italy (Milan)	(02) 50721	Sweden (Täby)	(08) 7567330
France (Vélizy)	(3) 9469722	Japan (Tokyo)	(03214) 5371	Switzerland (Zurich)	(01) 435 4111

U.S.A.: Kontron Electronics Inc., 630 Price Avenue, Redwood City/California 94063, (415) 3611012

Gain Access to the Largest Known Collection of Mass Spectra— 1982 REGISTRY OF MASS SPECTRAL DATA

John Wiley & Sons announces the June publication of their 1982 Registry of Mass Spectral Data. It will provide direct access to approximately 70,000 spectra of 55,000 different compounds. This will be the largest known collection of mass spectra, and is nearly double the size of the current mass spectral database.

The spectra have been compiled and checked by Professor Fred W. McLafferty, who has been involved with the development of Wiley's Mass Spectral database since its first publication in 1968 in collaboration with Professor Sixten Abrahamsson and the late Professor Einar Stenhagen.

Chemists and other scientists may gain access to the spectra in several ways:

1. By obtaining Wiley's spectral database through their instrument supplier.
2. By purchasing the tape directly from Wiley and loading it into a local computer or spectrometer.
3. By accessing the database online through Cornell Computer Services.

Quantity and resale price schedules are quoted on request. The tape is available in a variety of industry standard formats for use with local software. Identification of unknown compounds is optimized, however, if **PBM/STIRS** matching and interpretive programs are utilized. The **PBM/STIRS** software was developed by Professor Fred W. McLafferty's group at Cornell and may be obtained from: **DECUS**, Digital Equipment Computer Users Society, Maynard, Massachusetts; the Quantum Chemistry Program Exchange, Indiana University; and the American Society for Mass Spectrometry.

The 1982 tape is scheduled for release in June. The initial retail price is $4,000 for a single tape. Wiswesser notations and CAS registry numbers are available as an option (for an extra charge). Owners of the current tape may replace it with the new tape at a discounted price.

The Registry of Mass Spectral Data is available from John Wiley & Sons, Electronic Publishing Division, 605 Third Avenue, New York, New York 10158. Telephone (212) 850-6331. A detailed prospectus is available at no charge.

Mr. Myer Kutz, Database Publisher
John Wiley & Sons, Inc.
605 Third Avenue
New York, New York 10158

1807 175 YEARS 1982

Dear Mr. Kutz:

Please send me full details of the 1982 Registry Of Mass Spectral Data on magnetic tape. I am interested in:

____ Purchasing the tape for use in my laboratory or institution.
____ Obtaining the tape through my instrument supplier, who is _____
____ Accessing the tape online.
____ Licensing for redistribution.

NAME _____
AFFILIATION _____
ADDRESS _____
CITY _____ STATE _____ ZIP CODE _____
TELEPHONE _____

3-6397

Reader service card

JOURNAL OF

CHROMATOGRAPHY

INTERNATIONAL JOURNAL ON CHROMATOGRAPHY, ELECTROPHORESIS AND RELATED METHODS

use this card for more information on advertisements and news items

I would like to receive, without any obligation, further information on

News items: _____

Advertisements: _____

I am especially interested in the fields as indicated below:

- ☐ 6040 Analytical Chemistry
- ☐ 6050 Chromatography
- ☐ 6150 Mass Spectrometry
- ☐ 6140 Spectroscopy
- ☐ 6240 Pharmaceutical Chemistry
- ☐ 6241 Medicinal Chemistry
- ☐ 6242 Clinical Chemistry
- ☐ 6260 Environmental Chemistry

Name: _____

Position: _____

Address: _____

_____

please use envelope; mail as printed matter

ELSEVIER SCIENCE PUBLISHERS

Advertising department

P.O. BOX 211,

1000 AE AMSTERDAM – THE NETHERLANDS

please use envelope; mail as printed matter

ELSEVIER SCIENCE PUBLISHERS

Advertising department

P.O. BOX 211,

1000 AE AMSTERDAM – THE NETHERLANDS

Reader service card

JOURNAL OF

CHROMATOGRAPHY

INTERNATIONAL JOURNAL ON CHROMATOGRAPHY, ELECTROPHORESIS AND RELATED METHODS

use this card for more information on advertisements and news items

I would like to receive, without any obligation, further information on

News items: _____

Advertisements: _____

I am especially interested in the fields as indicated below:

- ☐ 6040 Analytical Chemistry
- ☐ 6050 Chromatography
- ☐ 6150 Mass Spectrometry
- ☐ 6140 Spectroscopy
- ☐ 6240 Pharmaceutical Chemistry
- ☐ 6241 Medicinal Chemistry
- ☐ 6242 Clinical Chemistry
- ☐ 6260 Environmental Chemistry

Name: _____

Position: _____

Address: _____

_____

Journal of Chromatography, 241 (1982) 237–256
Elsevier Scientific Publishing Company, Amsterdam — Printed in The Netherlands

CHROM. 14,780

IDENTIFICATION AND EVALUATION OF RETENTION MECHANISMS IN GAS–LIQUID CHROMATOGRAPHIC SYSTEMS*

R. N. NIKOLOV
Institute of Chemical Technology, Central Research Laboratory, 1156 Sofia (Bulgaria)
(First received September 1st, 1981; revised manuscript received January 30th, 1982)

SUMMARY

A procedure for identification of the retention mechanisms in gas–liquid chromatographic systems is proposed. It is based on the introduction of a sorption model for these systems, in which the presence of two layers of liquid stationary phase on the support is assumed. First a multimolecular layer of highly oriented molecules adjacent to the solid surface is formed, followed by a second bulk layer. The partition properties of both layers were expected to be different due to their structural peculiarities. An appropriate retention equation assuming all probable sorption retention mechanisms is derived. Problems attendant upon the application of this equation for identification purposes are discussed. The knowledge of some experimental parameters and the employment of a suitable computer program lead to unequivocal identification of solute retention mechanisms as well as to determination of partial partition coefficients. The reliability of the identification procedure was verified with published and new experimental data. Calculated partition coefficients allowed to the evaluation of the relative contributions of the identified mechanisms to the solute retention. The results obtained are in good agreement with the requirements of the introduced sorption model.

INTRODUCTION

A previously derived retention equation

$$E = \sum_i K_i S_i \tag{1}$$

was found to be applicable for all column chromatographic systems[1]. Here E is the so-called integral retention effect, representing the net retention volume per gram of packing; K_i are the appropriate partial partition coefficients and S_i the corresponding

* Presented at the *3rd Danube Symposium on Chromatography, Siófok, August 31–September 3, 1981*. The majority of the papers presented at this symposium has been published in *J. Chromatogr.*, Vol. 241, No. 1 (1982).

0021-9673/82/0000–0000/$02.75

specific phase characteristics of the packing. Hence eqn. 1 accounts in a most general form for the mixed retention mechanisms in a chromatographic system.

In gas–liquid chromatography (GLC) a commonly accepted approach is to consider the mixed retention mechanisms as a result of interfacial adsorption effects in addition to the dissolution in the liquid stationary phase (LSP)[2-13]. Then, the contributions of all sorption phenomena to the solute retention are generally expressed in a three-term equation

$$E = V_L K_L + A_{GL} K_{GL} + A_{LS} K_{GLS} \quad (2)$$

where V_L is the volume of LSP while A_{GL} and A_{LS} are the gas–liquid and liquid–solid interfacial areas, respectively. Usually, all these quantities are expressed per gram of packing. The partition coefficients K_L, K_{GL} and K_{GLS} correspond to dissolution in the LSP and to adsorption at the gas–liquid and liquid–solid interfaces. For some GLC systems the reduced forms of eqn. 2

$$E = V_L K_L + A_{GL} K_{GL} \quad (3)$$

or

$$E = V_L K_L + A_{LS} K_{GLS} \quad (4)$$

are also employed with the assumption that only two mechanisms contribute to the retention[2-4,6].

An important problem concerning the application of retention equations is the correct determination of their terms, *i.e.*, the exact identification of retention mechanisms acting in the GLC system investigated. This originates in the necessity to find a solution of the so-called inverse retention problem[14], which means determining the partition coefficients if the integral retention effect and the specific phase characteristics are known. A particular case of the inverse retention problem is related to thermodynamic measurements by GLC when an accurate value of K_L must be obtained from a system with mixed retention mechanisms[11,15].

Usually, the dimensionality of retention equations is intuitively determined without guarantee of their correct presentation. Hence, the development of new approaches for this purpose is of pronounced interest. It is of note that Weiner *et al.*[16] considered factor analysis to be potentially able to solve the problem. Unfortunately, the example chosen was not complex enough to demonstrate the power of the method.

In the present paper a procedure for identification of the retention mechanisms in GLC systems is proposed. It is based on the introduction of a sorption model specific to these systems. The application of the procedure requires knowledge of some experimental parameters as well as employment of an appropriate computer program.

THEORETICAL

State of liquid stationary phase on the support

The loading of solid support with a film of LSP leads to a perceptible modification of the film properties in comparison with the bulk phase[17-23]. The cause for

this phenomenon appears to be the specific orientation of molecules in the multimolecular structurally modified liquid layer. Principally, the orientation of molecules can take place up to a considerable thickness of LSP film, gradually falling off with the distance from the support surface. Beyond the effective thickness of this modified liquid layer, the loaded LSP retains the properties of bulk phase.

The existence of a highly oriented liquid layer in the vicinity of the solid surface is a manifestation of the so-called "long-range" interaction forces[24,25] which arise at interfaces and sometimes cause inexplicable behaviour of molecules. Briefly, two different layers could be distinguished at sufficient LSP amount on the support:

(i) a multimolecular layer of highly oriented LSP molecules, adjacent to the solid surface and denoted here as the *structured* layer

(ii) a *bulk* LSP layer covering the structured one

If the solute molecules show propensity towards adsorption at the liquid–solid interface they could displace the adsorbed phase molecules because of a larger affinity to the solid surface. Following a two-dimensional adsorption model, the adsorbed solute molecules will be considered to have direct contact with the support. On the other hand, those dispersed in the structured LSP layer will be treated as dissolved molecules similarly to these in the bulk phase. However, a noticeable difference in the partition properties of both layers could be expected due to their structural peculiarities.

Sorption model of GLC systems

Let us consider a section of a GLC packed column. It is supposed that the packing consists of a usual wide-pore non-silanized solid support loaded with a LSP. The phase amount is adequate to guarantee complete coverage of solid surface with a multimolecular liquid film. The amount of packing in the section is considered to be 1 g, so that the specific phase characteristics listed below are expressed per gram of packing. V_G, V_L, V_S and V_B are the volumes of the gas phase, total LSP, structured and bulk LSP layers respectively, and A_{GL} and A_{LS} are the corresponding gas–liquid and liquid–solid interfacial areas. Then, the general retention equation assuming all probable sorption mechanisms can be presented in the form

$$E = V_S K_S + V_B K_L + A_{GL} K_{GL} + A_{LS} K_{GLS} \tag{5}$$

where K_S and K_L could be interpreted as "structured" and "bulk" partition coefficients, respectively.

Eqn. 5 is valid under conditions of infinite dilution whereas K_i are constants at a given temperature. Thorough examination shows the complex nature of K_S and K_{GLS}, with respect to the solute distribution between phases having no immediate contact. In fact

$$K_S = K_{BS} K_L \tag{6}$$

$$K_{GLS} = K_{SA} K_S \tag{7}$$

where K_{BS} is the partition coefficient between structured and bulk LSP layers and K_{SA} is that between liquid–solid interface and structured layer. A combination of eqns. 6 and 7

$$K_{GLS} = K_{SA} K_{BS} K_L \tag{8}$$

enables the rigorous evaluation of the liquid–solid adsorption by means of K_{SA}.

The non-equal possibilities of obtaining data for all phase characteristics makes eqn. 5 inapplicable in practice. Thus, A_{GL} and A_{LS} can be determined experimentally, while V_S and V_B cannot. However,

$$V_S + V_B = V_L \tag{9}$$

where V_L is usually known. Combining eqns. 5 and 9 we obtain

$$E = V_S(K_S - K_L) + V_L K_L + A_{GL}K_{GL} + A_{LS}K_{GLS} \tag{10}$$

where only V_S cannot be determined by an appropriate experimental technique.

In fact V_S is a function of V_L and LSP film thickness, d. With increase of V_L, starting from zero, d increases gradually to the utmost effective thickness, d_S, of the structured layer. Consequently, d_S is considered here as a measure of the mean distance to which the long-range forces affect the LSP bulk proporties and then:

$$V_S \approx V_L, \text{ whereas } d < d_S \tag{11}$$

With further increase of V_L formation of the LSP bulk layer starts. Then, d_S remains constant while d increases and a satisfactory evaluation of V_S could be obtained from:

$$V_S = A_{LS}d_S, \text{ when } d \geqslant d_S \tag{12}$$

Taking into account eqns. 11 and 12, eqn. 10 can be presented in the form

$$E = V_L K_L + \delta V_L(K_S - K_L) + (1 - \delta)\, A_{LS}\,[d_S(K_S - K_L)] + \\ + A_{GL}K_{GL} + A_{LS}K_{GLS} \tag{13}$$

where:

$$\delta = 1, \text{ when } d < d_S \tag{13a}$$

or

$$\delta = 0, \text{ when } d \geqslant d_S \tag{13b}$$

Similarly, for K_L, K_{GL} and K_{GLS} the quantities

$$K_S - K_L = K_{SL} \tag{13c}$$

and

$$d_S(K_S - K_L) = K_{DSL} \tag{13d}$$

are to be considered as constant terms under infinite dilution and at a given temperature. They are independent of the variations of phase characteristics in a certain GLC system. Introducing the new eqns. 13c and 13d into eqn. 13, we obtain the final form:

$$E = V_L K_L + \delta V_L K_{SL} + (1 - \delta)\, A_{LS}K_{DSL} + A_{GL}K_{GL} + A_{LS}K_{GLS} \tag{14}$$

Eqn. 14 involves all probable retention mechanisms in accordance with the introduced sorption model of GLC systems. It can be interpreted as a general retention equation that permits the development of a procedure for identification of the retention mechanisms.

Problems of identification

The use of eqn. 14 gives rise to some experimental and mathematical problems. Prior to proceeding to the identification of the retention mechanisms, it will be shown how these problems can be overcome.

Experimental problems. Eqn. 14 is linear with five unknowns (K_L, K_{SL}, K_{DSL}, K_{GL} and K_{GLS}) which can be determined only by solution of a system of minimum five linear equations. This requires knowledge of the phase characteristics (V_L, A_{GL} and A_{LS}) for a minimum of five column packings prepared from identical LSP and solid support at different liquid loadings[14]. Each solute must be chromatographed on each packing at the required constant temperature, thus obtaining a set of integral retention effects, E. Hence, it is necessary to arrange a large number of precise chromatographic experiments, the basic problems being:

determination of minimal amount of LSP providing eqn. 14 is still valid and exact determination of V_L, A_{GL} and A_{LS}

Experience with wide-pore supports with specific surface area 1–4 $m^2\ g^{-1}$ indicates that approximately 1% LSP is adequate to cover the surface with a layer thicker than one molecular diameter[26]. Obviously, such a packing could be the first in a series of packings with increased liquid loadings. For determination of V_L the so-called evaporation method[27,28] is recommended, since this requires minimal time and yields satisfactory accuracy. Usually, the BET technique or the continuous flow method is applicable for determining both A_{GL} and A_{LS}, the latter being considered here as the specific surface area of the support.

To avoid difficulties with area measurements some workers do not use such experimental data, especially when their interest is focused on the calculation of K_L only[6,11,29]. However, to identify the retention mechanisms in a GLC system it is obligatory to employ A_{GL} and A_{LS}. In this case, a modified BET technique offering considerable accuracy with small surface areas can be recommended[30], and has successfully been applied[26,31].

Mathematical problems. It is well known that solute retention in GLC systems is not always a result of mixed mechanisms. For some solutes there exist the so-called "pure" systems in which dissolution in the LSP is the unique mechanism of retention. Then, the retention equation takes the forms

$$E = V_L K_L \tag{15}$$

or

$$E = V_S K_S + V_B K_L \tag{16}$$

Since the application of eqn. 14 is meaningless in such cases, the first mathematical problem is to establish when it can be applied. In other words, it is necessary to examine whether solute retention results from mixed mechanisms or not.

Let us represent eqn. 5 in the form:

$$E = V_L\bar{K}_L + I_A \tag{17}$$

where

$$I_A = A_{GL}K_{GL} + A_{LS}K_{GLS}$$

Here $\bar{K}_L$ is considered as a mean value between K_S and K_L, so that $V_L\bar{K}_L = V_SK_S + V_BK_L$. It will be shown later that such an approximation is quite acceptable because $K_S \approx K_L$.

If adsorption effects contribute to the solute retention, *i.e.*, if $I_A > 0$ an E *vs.* V_L plot would give a curve convex to the abscissa for small V_L values. Then, applying regression analysis to eqn. 17 the latter can be tested for linear correlation between E and V_L. If precise experimental data are used the obtained straight line with slope $\bar{K}_L$, intercept I_A and correlation coefficient R will be the first step in estimating the presence or absence of mixed mechanisms. Obviously, if $\bar{K}_L > 0$, $R \approx 1$ and the absolute value of I_A does not exceed the standard error of estimation (S.E.E.) for E (*i.e.*, $|I_A| \leqslant$ S.E.E. > 0), it means $I_A = 0$. Consequently, the solute retention is due to the solution only (absorption mechanisms) and eqn. 17 has to be reduced to eqns. 15 or 16. If $\bar{K}_L > 0$, $R << 1$ and $I_A >$ S.E.E. > 0, it is to be accepted that retention results from mixed mechanisms. Then, the application of eqn. 14 is reasonable.

It could happen that $\bar{K}_L \leqslant 0$, $|R| < 1$ and $I_A >>$ S.E.E. > 0. The fact that I_A is too large indicates the action of at least one adsorption mechanism while the negative $\bar{K}_L$ means that absorption may not be absent. It is clear that a linear correlation on the basis of the non-linear eqn. 17 leads principally to a decreased slope, $\bar{K}_L$. Hence, if $\bar{K}_L$ is *a priori* small and I_A extremely large, an incorrect evaluation of $\bar{K}_L$ by regression analysis is quite possible. A recommended approach in such cases is to apply directly eqn. 14 that can give an unequivocal answer.

Briefly, to identify mixed retention mechanisms in a GLC system the application of eqn. 14 is required. It is necessary to compose a "suitable" system of linear equations. That is the second important mathematical problem.

Whether the system of equations will be a "suitable" one or not will depend on the selection of δ values in the particular equations. Expressions 13a and 13b show the dependence of δ on the relation between LSP film thickness, d, and structured layer effective thickness, d_S. Usually, d is given by the approximation

$$d = V_L/A_{LS} \tag{18}$$

while d_S is unknown. This makes impossible a direct compilation of the "suitable" system, but does not exclude the possibility of "finding" it among the set of several similar systems based on eqn. 14.

To that purpose, the first equation must be related to the serial packing containing minimal amount of LSP. Each successive equation will correspond to a more heavily loaded packing than the previous one and the last equation will correspond to the packing with greatest loading. Supposing d_S to be within the interval of d values for two "neighbouring" packings, the unequivocal selection of δ values in all equations

will be facilitated. Since d_S could lie between the d values of any pair of "neighbouring" serial packings, a set of similar systems of equations can be obtained.

For example, with a series of p column packings where $p \geqslant 5$, following eqn. 18 we obtain for each packing:

$$d^i = V_L^i / A_{LS}^i \; (i = 1, 2, \ldots, m, n, \ldots, p) \tag{18a}$$

Supposing $d^m < d_S \leqslant d^n$ (where $n = m + 1$) and taking into account eqns. 13a, 13b and 14, the general form for similar systems can be written as follows:

$$\begin{aligned}
&V_L^1 K_L + V_L^1 K_{SL} + 0 + A_{GL}^1 K_{GL} + A_{LS}^1 K_{GLS} = E^1 \\
&\vdots \\
&V_L^m K_L + V_L^m K_{SL} + 0 + A_{GL}^m K_{GL} + A_{LS}^m K_{GLS} = E^m \\
&V_L^n K_L + 0 + A_{LS}^n K_{DSL} + A_{GL}^n K_{GL} + A_{LS}^n K_{GLS} = E^n \\
&\vdots \\
&V_L^p K_L + 0 + A_{LS}^p K_{DSL} + A_{GL}^p K_{GL} + A_{LS}^p K_{GLS} = E^p
\end{aligned} \tag{19}$$

Principally, the maximum number of these systems can be $p - 1$. However, in the case when d_S is supposed to fall into intervals $(d^1, d^2]$ or $(d^{p-1}, d^p]$ the corresponding systems contain linear dependent equations and cannot be solved. Hence, the real number of similar systems is limited to $p - 3$, among which one is the so-called "suitable" system. Its solution enables further identification of the retention mechanisms and the problem here reduces to discovery of this system. To do this, the solutions of all $p - 3$ systems must be obtained. Then, an appropriate test for K_i and d_S values in conformity with a logical system of criteria permits the unequivocal determination of the "suitable" system of equations.

Prior to considering the principles of the system of criteria, a note concerning the mathematical approach to solution of the similar systems is needed. Since the systems are approximate (because of the presence of experimentally determined quantities) their solutions are strongly influenced by the computational method employed. It was shown elsewhere[14] that methods of matrix algebra give the best results, the latter being least-squares averaged. Such an approach leads to possibly the best approximate solution.

System of criteria. In order to discover the "suitable" system of equations it is necessary to define the fundamental physical relationships which as criteria are to be obeyed by the unknowns in system 19. Failure to satisfy any one of these criteria is an indication of perturbation in the system of equations. Such a perturbation could be caused either by an incorrect assumption in the location of d_S within a certain interval $(d^m, d^n]$ or by the absence of some mechanism whose contribution to the solute retention is take into account through the corresponding term.

The fundamental criterion for testing the solution of system 19 is the inequality

$$K_L > 0 \tag{20}$$

whose physical sense is obvious. Further, a reliable K_L value must obey all equations of the system. Since the adsorption contributions to retention are smallest in case of the most heavily loaded, *i.e.*, p-th packing, it is clear that fulfilment of the additional criterion

$$K_L \leqslant E^p / V_L^p \tag{21}$$

will enable a reasonable K_L value to be obtained.

In the case of criteria 20 and 21, the relation

$$K_S > 0 \tag{22}$$

is relevant. The coefficient K_S is analogous to K_L and characterizes the partition properties of the structured LSP layer. Moreover, K_S and K_L appear to be approximately equal, thus the satisfaction of inequality 22 will be obligatory in case of a "suitable" system.

Significant for the correct evaluation of d_S are the criteria:

$$d_S > 0 \tag{23}$$

and

$$d^m < d_S \leqslant d^n \; (m = 2, 3, \ldots, p - 2; \; n = m + 1) \tag{24}$$

While inequality 23 reflects a clear physical requirement for d_S, the fulfilment of criterion 24 denotes a correct location of d_S within the interval considered. Hence, from a mathematical point of view this is a reliable indication for final discovery of the "suitable" system.

To continue with the identification procedure, the values of K_{GL} and K_{GLS} have to be examined. If they satisfy the inequalities

$$K_{GL} > 0 \tag{25}$$

and

$$K_{GLS} > 0 \tag{26}$$

the solute is retained by all possible sorption mechanisms and the corresponding K_i values obtained represent the solution of the so-called inverse retention problem.

If $K_{GL} < 0$ and/or $K_{GLS} < 0$, the system of equations is perturbed and the calculated K_S, K_L and d_S are non-reliable. Their correct values can be determined by solving the systems of equations based on properly reduced variants of eqn. 14. For example, if $K_{GL} > 0$ and $K_{GLS} < 0$, the appropriate equation will be

$$E = V_L K_L + \delta V_L K_{SL} + (1 - \delta) A_{LS} K_{DSL} + A_{GL} K_{GL} \tag{27}$$

while when $K_{GL} < 0$ and $K_{GLS} > 0$, it will be:

$$E = V_L K_L + \delta V_L K_{SL} + (1 - \delta) A_{LS} K_{DSL} + A_{LS} K_{GLS} \tag{28}$$

To compose the set of similar systems corresponding to any one of the above equations, the same procedure as for the system 19 must be followed. The fulfilment of criteria 20–24 is required in order to discover the "suitable" system of equations and if criterion 25 or 26 is also obeyed the identification procedure is completed.

In case of $K_S \leqslant 0$ for all similar systems of equations, the observed perturbation could be due to identical or nearly equal partition properties of both the structured and the bulk LSP layers with respect to the solute. This means that all the similar systems are inexpedient and others, based on the alternatively valid eqns. 2, 3 or 4, must be composed and solved.

An appropriate computer program incorporating the system of criteria was written to facilitate the identification procedure. Experimental data of Pecsok *et al.*[3] were used to test the program. Their experiments concerned nineteen solutes with different functional groups chromatographed at 25°C in the system β,β'-thiodipropionitrile (TDPN)–firebrick (42–60 mesh). Unfortunately, data for V_L, A_{GL} and A_{LS} were recalculated from the amount of LSP and those for A_{GL} were interpolated from a plot of A_{GL} *vs.* LSP percentage. Results of the program verification are shown in Table I. They will be discussed later together with the results of the present experiments.

EXPERIMENTAL

Materials

Celite 545 (BDH, Poole, Great Britain), 60–80 mesh, with specific surface area 1.92 $m^2\ g^{-1}$ was used as solid support. Non-polar Apiezon M and moderately polar Carbowax 4000 (both from Carlo Erba, Milan, Italy) were the liquid stationary phases.

Twelve individual solutes, *n*-octane, cyclohexane, benzene, 1-propanol, 2-propanol, 1-butanol, 2-methyl-1-propanol, 2-butanone, 4-methyl-2-pentanone, chlorobenzene and thiophene, were selected for the chromatographic experiments. Except for cyclohexane, chlorobenzene and thiophene (E. Merck, Darmstadt, G.F.R.), all of 99% purity, the other solutes (Poly Science Corporation, Niles, IL, U.S.A.) were of minimum 99.5% purity. Pure hydrogen (99,95%) dried with molecular sieve 5A was used as carrier gas.

Apparatus

A Fractovap Model B gas chromatograph (Carlo Erba, Milan, Italy) with thermistor detector was employed. The instrument was home-modified to ensure constant column and detector temperatures within ± 0.02°C. Stainless-steel columns were 2 m × 3 mm I.D. A 1-mV Model 194 electronic recorder (Honeywell, Newhouse, Great Britain) was used for registration of chromatographic peaks.

Procedures

Initially, a series of six packings containing different LSP amounts within 1–18% was prepared for both Apiezon M and Carbowax 4000. In addition, a new series of four packings with Carbowax 4000 whose amount varied within 1–5% was examined in order to verify the GLC sorption model. To prepare each packing a certain amount of support was thoroughly dried at 150°C under vacuum at 2×10^{-4} Torr

for 4 h. The LSP deposition was accomplished from dilute solution in analytical grade solvents using a rotating vacuum-evaporator. Conditioning at 150 C for 16 h was carried out for each column.

The LSP amount in the packings was determined after completion of the chromatographic experiments. An accuracy of ± 0.05–$\pm 0.1\%$ was achieved by means of the evaporation method[28]. Using the method of Bliznakov *et al.*[30], LSP specific surface areas were measured with a reproducibility in three determinations within $\pm 1.5\%$.

All chromatographic experiments were carried out at 70 C. On-column injections of solutes were made with a 1-μl Hamilton microsyringe. For each solute, three to five samples of different amounts were chromatographed on all serial packings.

In order to ensure exact retention time determinations the recorder a.c. supply was additionally stabilized and the chart speed was suitably chosen for each solute. The reproducibility achieved was within $\pm 0.06\%$, allowing accurate determination of integral retention effects within $\pm 0.2\%$.

RESULTS AND DISCUSSION

Partial partition coefficients of nineteen solutes in the system TDPN–firebrick calculated at 25°C are presented in Table I. This system was chosen for verification of

TABLE I

CALCULATED PARTIAL PARTITION COEFFICIENTS FOR IDENTIFIED RETENTION MECHANISMS ON β,β'-THIODIPROPIONITRILE–FIREBRICK AT 25 C ACCORDING TO EXPERIMENTAL DATA[3]

Solute	K_S	K_L	K_{GL}	K_{GLS}	K_{SA}	D^*_{SL}	d_S
	–	–	(10^{-6} cm)	(10^{-6} cm)	(10^{-6} cm)	(%)	(10^{-6} cm)
n-Hexane	9.3	9.2	64.4			(0.8)	
2-Methylpentane	6.7	6.7	53.0			(−0.9)	
3-Methylpentane	8.7	8.7	52.8			(−0.7)	
2,3-Dimethylbutane	7.4	7.4	48.2			(−0.7)	
n-Heptane	20.7	20.6	188			0.5	
2,2,4-Trimethylpentane	17.2	17.3	233			−0.6	
Cyclopentane	16.2	16.1	21.0			0.6	
Cyclohexane	32.5	32.3	58.3			0.6	
Methylcyclopentane	21.2	21.3	53.0			(−0.9)	
Hexene-1	20.2	14.5	73.6			39.3	1.9
Cyclohexene	94.2	85.8	72.9			9.8	2.0
Benzene	441	421	116			4.8	2.4
Diethyl ether	26.9	31.9	56.4			−15.7	2.0
n-Butyl ethyl ether	99.9	56.0	386			78.4	2.8
Propionaldehyde	299	246	109			21.4	2.3
Isobutyraldehyde	270	317	91.4	137	0.51	−14.7	2.1
Ethyl acetate	465	442	481			5.2	1.9
Acetone	427	447	247			− 4.3	2.0
Methyl ethyl ketone	769	808	526			− 4.9	1.9

* $D_{SL} = 10^2(K_S - K_L)/K_L$. All values in parentheses were obtained from unrounded K_S and K_L respectively, while the others were from those values listed in the table.

the computer program, *i.e.*, of the identification procedure described. In agreement with the observations of Pecsok *et al.*[3] it was found that paraffins and cycloparaffins are retained by both dissolution in LSP and adsorption at the gas–liquid interface. For these solutes the absolute values, $|D_{SL}|$, of the deviations of K_S from K_L were less than 1%. Simultaneously, the d_S values obtained were always greater than the LSP film thickness in the most heavily loaded packing, failing to satisfy criterion 24. In accordance with the accuracy of the published data, it was decided to neglect D_{SL} values within $\pm 1\%$ and to consider $K_S = K_L$. Nevertheless, both coefficients are presented in Table I, while the incorrect d_S values are omitted in order to indicate the perturbation. Hence, both the structured and the bulk LSP layers have equal partition properties towards the hydrocarbons considered.

On the contrary, hexene-1, cyclohexene and benzene are retained by means of two absorption and one adsorption mechanisms. Their $|D_{SL}|$ values are large, varying within 5–39%. Without exception $K_S > K_L$, thus indicating the more intensive interactions in the structured layer. The third retention mechanism is connected with gas–liquid interfacial adsorption of the solutes, their K_{GL} values being nearly equal to those obtained by Pecsok *et al.*[3].

It is of particular interest to consider the behaviour of the polar oxygen-containing compounds. Except for isobutyraldehyde, all solutes are retained by means of dissolution in both layers as well as by adsorption at the gas–liquid interface. Liquid–solid adsorption is observed only with isobutyraldehyde and could be explained in terms of eventual hydrogen bonding of the α-H atom, due to the so-called hyperconjugation effect. In all cases K_S clearly deviates from K_L, while K_{GL} values remain approximately the same as reported by Pecsok *et al.*[3].

A noticeable difference is observed in K_S to K_L ratio for the pairs propionaldehyde–isobutyraldehyde and diethyl ether–*n*-butyl ethyl ether. The explanation can be found in the difference between both the steric factors (for the first pair) and the molecular polarizabilities (for the second), which affect the solute interactions with the LSP.

Further, calculated d_S values are presented in Table I for those solutes retained (among others) by two absorption mechanisms. Principally, the effective thickness of the structured layer does not depend on the solute nature. As shown the d_S values are of similar magnitude, the mean value together with the standard deviation being $(2.1 \pm 0.3) \times 10^{-6}$ cm. The observed range is due to the absence of original experimental data for V_L, A_{GL} and A_{LS}, as mentioned above. Nevertheless, these results allow a positive estimation of both the identification procedure and the corresponding computer program.

To demonstrate the ability of the proposed procedure to solve problems of mixed retention mechanisms under complicated conditions, the following experiments were carried out. Two conventional GLC systems were chosen under conditions of reduced adsorption contributions to the retention. Small specific surface area of the support and relatively high temperature were employed, thus complications with the identification were expected.

Plots of A_{LS} and A_{GL} *vs.* V_L for both Apiezon–Celite and Carbowax–Celite systems are shown in Fig. 1a and 1b, respectively. No significant dependence of A_{GL} on the nature of the LSP is observed, while A_{LS} varies because of difference in the LSP density. The final results of application of the identification procedure will be considered in detail separately for each system.

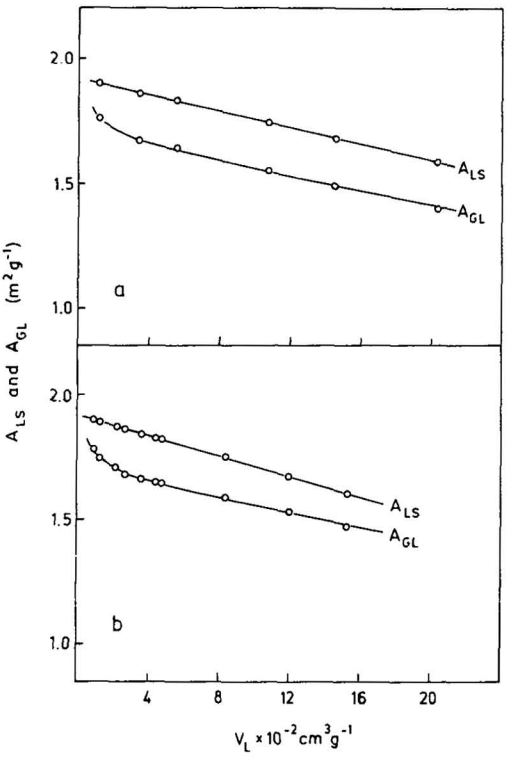

Fig. 1. Dependence of liquid–solid and gas–liquid interfacial specific surface areas on liquid stationary phase volume per gram of packing: a, Apiezon M–Celite 545; b, Carbowax 4000–Celite 545 (systems A and B).

System Apiezon M–Celite 545

As reported in Table II, *n*-octane, cyclohexane, benzene, chlorobenzene and thiophene are retained only by dissolution in the LSP. These solutes have large K_L values and show no tendency to adsorb at the gas–liquid or liquid–solid interfaces. In the case of benzene this behaviour is contradictory to the results of Komaita *et al.*[32], who found adsorption at a squalane–alumina interface. However, the present result can be explained in terms of the substantial difference in the supports (Celite *vs.* alumina) as well as in the liquid phases employed (Apiezone *vs.* squalane). Also it is known that the non-polar Apiezon M contains a definite amount of polymeric methyl phenyl ethers[33], which adsorb preferably on the support surface, thus invalidating the competition of solutes such as benzene, chlorobenzene and thiophene.

On the contrary, alcohols and ketones show relatively poor solubility in the LSP and a definite propensity towards liquid–solid adsorption. This behaviour is in agreement with some previous observations[5,34], but contradicts others, according to which alcohols and ketones adsorb also at the gas–liquid interface when saturated hydrocarbons are used as liquid phases[10,11]. In the present investigation no gas–liquid adsorption was observed. As pointed out by Conder[13], this could indicate absence of infite dilution for the solutes chromatographed. However, it seems more

TABLE II

CALCULATED PARTIAL PARTITION COEFFICIENTS FOR IDENTIFIED RETENTION MECHANISMS ON SYSTEM APIEZON M–CELITE 545 AT 70°C

Solute	K_L	K_{GLS} ($\cdot 10^{-6}$ cm)	K_{SA} ($\cdot 10^{-6}$ cm)
n-Octane	356.7		
Cyclohexane	117.5		
Benzene	107.5		
1-Propanol	24.18	78.5	3.25
2-Propanol	10.97	24.0	2.19
1-Butanol	57.47	245	4.26
2-Butanol	33.26	88.2	2.65
2-Methyl-1-propanol	45.92	145	3.16
2-Butanone	34.50	19.5	0.57
4-Methyl-2-pentanone	131.6	118	0.90
Chlorobenzene	541.9		
Thiophene	116.0		

reasonable that gas–liquid adsorption does not contribute to the retention of alcohols and ketones because of the higher temperature of the present experiments (70 *vs.* 30 or 40°C for investigations discussed by Conder).

K_S values are not presented in Table II because it was found $K_S < 0$ for all solutes. This fact, as already discussed, demonstrates the approximately equal partition properties of both structured and bulk LSP layers, so that K_S and K_L cannot be distinguished. A cursory inspection of the K_{SA} values indicates that alcohols adsorb more strongly than ketones. This parallels the hydrogen-bonding tendency of the solutes considered, and is responsible for their adsorption on the support surface. The more pronounced adsorption of primary alcohols in comparison with secondary ones is due to the well known steric factors.

Systems Carbowax 4000–Celite 545

As pointed out above, a series of six packings loaded within 1–18% was prepared (system A). The results obtained by application of the identification procedure are presented in Table III. *n*-Octane and cyclohexane were retained by means of both dissolution in LSP and adsorption at the gas–liquid interface. In fact K_S and K_L were identical, their deviations, $|D_{SL}|$, being smaller than 0.5%. Calculated d_S values were greater than the LSP thickness in the most heavily loaded packing of the series. In other words the behaviour of these hydrocarbons was the same as that on TDPN–firebrick.

All other solutes were retained by means of two absorption and one adsorption mechanisms (at the gas–liquid interface). No liquid–solid adsorption was identified. A relatively small but clear difference between K_S and K_L was observed for each of these solutes. The corresponding $|D_{SL}|$ values were not so large as in the system TDPN–firebrick, but they were essentially greater than 0.5%. In accordance with the accuracy of the present experimental data, it was accepted that there was a difference between K_S and K_L only if $|D_{SL}| > 0.5\%$. It is seen in the table that $|D_{SL}| < 2\%$, thus indicating the small difference in the partition properties of both LSP layers at 70°C.

TABLE III

CALCULATED PARTIAL PARTITION COEFFICIENTS FOR IDENTIFIED RETENTION MECHANISMS IN SYSTEM A AND ESTIMATED DEVIATIONS OF K_S AND K_{GL} IN COMPARISON WITH SYSTEM B

All experiments at 70°C. Both A and B contain Carbowax 4000–Celite 545 packings in different loadings: A within 1–18%, and B within 1–5%.

Solute	*System A*				*Comparison with system B*		
	K_S	K_L	K_{GL} ($\cdot 10^{-6}$ cm)	d_S ($\cdot 10^{-6}$ cm)	D_{SL} (%)	D_S (%)	D_{GL} (%)
n-Octane	46.03	45.88	16.8		0.33	0.57	−1.2
Cyclohexane	28.81	28.69	4.21		0.42	0.81	−1.8
Benzene	138.5	137.2	8.50	2.7	0.95	−0.52	1.5
1-Propanol	246.1	242.7	31.7	2.9	1.40	0.34	0.97
2-Propanol	114.3	116.2	19.4	2.8	−1.64	−0.44	1.3
1-Butanol	512.8	505.5	45.0	2.9	1.44	0.31	−0.74
2-Butanol	220.6	224.6	26.1	2.7	−1.78	−0.29	1.1
2-Methyl-1-propanol	353.6	350.7	38.6	2.8	0.83	0.18	−1.0
2-Butanone	103.4	101.9	11.9	2.9	1.47	−0.37	1.7
4-Methyl-2-pentanone	206.1	210.1	20.5	2.8	−1.90	−0.33	1.4
Chlorobenzene	830.7	825.6	16.2	3.0	0.62	0.31	−1.4
Thiophene	221.6	220.0	7.28	2.9	0.73	−0.26	−1.9

Because of the high temperature at which the solutes were chromatographed, their gas–liquid interfacial adsorption was weak, reflected in the relatively small K_{GL} values. Nevertheless, this adsorption mechanism was clearly identified without any complications.

In contrast to the system TDPN–firebrick, calculated d_S values for system A show a noticeable constancy with small standard deviation: $(2.8 \pm 0.1) \times 10^{-6}$ cm. This fact could be considered as evidence for a properly developed GLC sorption model. However, for final verification, an additional Carbowax–Celite system (system B) was examined under the same chromatographic conditions.

Four packings loaded within 1–5% were prepared in order to obtain only a structured layer coating on the support. This means that the LSP film thickness in the most heavily loaded packing should not exceed the calculated d_S middle value. If the sorption model is adequate the integral retention of solutes should be controlled by the equation

$$E = V_S K_S + A_{GL} K_{GL}$$

where V_S is now equal to the total LSP volume per gram of packing. A solution of the corresponding system of four linear equations should give K_S and K_{GL} values nearly equal to those obtained for system A.

In Table III the D_S and D_{GL} deviations are calculated as follows:

$$D_i = 10^2(K_i^A - K_i^B)/0.5(K_i^A + K_i^B)$$

where the superscripts A and B refer to the corresponding chromatographic systems, while *i* indicates S or GL respectively. Except for *n*-octane, cyclohexane and benzene, $|D_S|$ is less than 0.5%, thus being also smaller than the respective $|D_{SL}|$. In fact the K_S^B values are identical with K_S^A, while the differences between K_S^A and K_L^A are obviously greater. Coincidence of K_{GL} values for the solutes in both systems is also observed, so that $|D_{GL}| < 2\%$. These observations agree well with the sorption model, and confirm its reliability as a basis of the identification procedure developed. The latter appears to be an useful tool allowing one to solve problems of mixed retention mechanisms in GLC systems even under complex conditions.

As mentioned above, a correct identification of the retention mechanisms leads immediately to solution of the inverse retention problem. The partial partition coefficients obtained permit evaluation of the contributions of these mechanisms to the integral solute retention. Results for the systems Apiezon–Celite and Carbowax–Celite (system A) are presented in Table IV. For each solute the partial retention effects (PRE) are indicated in accordance with the corresponding retention mechanisms identified on the packings of both systems. All calculated values are percentages, thus allowing comparison of relative contributions to solute retention.

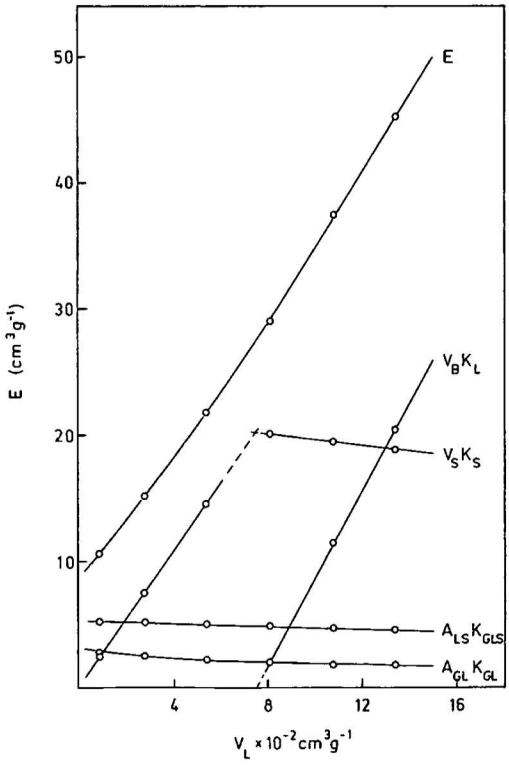

Fig. 2. Variation of partial retention effects and integral retention with liquid stationary phase volume per gram of packing for isobutyraldehyde on β,β′-thiodipropionitrile–firebrick at 25°C.

TABLE IV

RELATIVE CONTRIBUTIONS OF PARTIAL RETENTION EFFECTS (PRE) TO INTEGRAL RETENTION IN VARIOUS PACKINGS OF SYSTEMS APIEZON M–CELITE 545 AND CARBOWAX 4000–CELITE 545 (SYSTEM A), BOTH AT 70°C

Solute	*Apiezon M–Celite 545*							*Carbowax 4000–Celite 545 (system A)*					
	PRE	*% LSP*						*PRE*	*% LSP*				
		0.9899	*2.880*	*4.729*	*9.119*	*12.30*	*17.27*		*1.000*	*2.921*	*4.771*	*9.090*	*13.05*	*16.67*
n-Octane	$V_L K_L$	100.0	100.0	100.0	100.0	100.0	100.0	$V_L K_L$	58.3	81.5	87.8	93.4	95.5	96.6
								$A_{GL} K_{GL}$	41.7	18.5	12.2	6.6	4.5	3.4
Cyclohexane	$V_L K_L$	100.0	100.0	100.0	100.0	100.0	100.0	$V_L K_L$	76.5	91.7	94.7	97.2	98.3	98.7
								$A_{GL} K_{GL}$	23.5	8.3	5.3	2.8	1.7	1.3
Benzene	$V_L K_L$	100.0	100.0	100.0	100.0	100.0	100.0	$V_S K_S$	89.4	96.4	97.7	56.2	37.5	28.2
								$V_B K_L$				42.7	61.7	71.3
								$A_{GL} K_{GL}$	10.6	3.6	2.3	1.1	0.8	0.5
1-Propanol	$V_L K_L$	15.8	36.0	48.4	65.5	72.6	79.7	$V_S K_S$	80.1	92.6	95.4	59.7	40.1	30.2
	$A_{LS} K_{GLS}$	84.2	64.0	51.6	34.5	27.4	20.3	$V_B K_L$				37.9	58.2	68.5
								$A_{GL} K_{GL}$	19.9	7.4	4.6	2.4	1.7	1.3
2-Propanol	$V_L K_L$	22.0	45.1	58.1	73.8	79.9	85.5	$V_S K_S$	75.0	90.3	94.0	56.5	37.8	28.5
	$A_{LS} K_{GLS}$	78.0	54.9	41.9	26.2	20.1	14.5	$V_B K_L$				40.4	60.1	69.9
								$A_{GL} K_{GL}$	25.0	9.7	6.0	3.1	2.1	1.6

1-Butanol	$V_L K_L$	12.6	30.0	41.7	59.1	66.9	75.0	$V_S K_S$	85.5	94.8	96.8	60.2	40.4	30.4
	$A_{LS} K_{GLS}$	87.4	70.0	58.3	40.9	33.1	25.0	$V_B K_L$				38.2	58.5	68.8
								$A_{GL} K_{GL}$	14.5	5.2	3.2	1.6	1.1	0.8
2-Butanol	$V_L K_L$	18.8	40.8	53.5	70.0	76.5	82.9	$V_S K_S$	81.5	93.1	95.7	55.0	36.7	27.6
	$A_{LS} K_{GLS}$	81.2	59.2	46.5	30.0	23.5	17.1	$V_B K_L$				42.8	61.8	71.3
								$A_{GL} K_{GL}$	18.5	6.9	4.3	2.2	1.5	1.1
2-Methyl-1-propanol	$V_L K_L$	16.1	36.6	48.9	66.1	73.1	80.2	$V_S K_S$	82.2	93.5	96.0	57.6	38.6	29.0
	$A_{LS} K_{GLS}$	83.9	63.4	51.1	33.9	26.9	19.8	$V_B K_L$				40.4	60.0	69.9
								$A_{GL} K_{GL}$	17.8	6.5	4.0	2.0	1.4	1.1
2-Butanone	$V_L K_L$	51.9	76.5	84.2	91.6	93.8	95.8	$V_S K_S$	81.9	93.3	95.8	59.9	40.2	30.3
	$A_{LS} K_{GLS}$	48.1	23.5	15.8	8.4	6.2	4.2	$V_B K_L$				38.0	58.3	68.6
								$A_{GL} K_{GL}$	18.1	6.7	4.2	2.1	1.5	1.1
4-Methyl-2-pentanone	$V_L K_L$	40.7	67.1	77.3	87.4	90.6	93.5	$V_S K_S$	84.0	94.2	96.4	57.2	38.1	28.6
	$A_{LS} K_{GLS}$	59.3	32.9	22.7	12.6	9.4	6.5	$V_B K_L$				40.9	60.6	70.5
								$A_{GL} K_{GL}$	16.0	5.8	3.6	1.9	1.3	0.9
Chloro-benzene	$V_L K_L$	100.0	100.0	100.0	100.0	100.0	100.0	$V_S K_S$	96.3	98.8	99.3	62.8	41.8	31.4
								$V_B K_L$				36.8	57.9	68.4
								$A_{GL} K_{GL}$	3.7	1.2	0.7	0.4	0.3	0.2
Thiophene	$V_L K_L$	100.0	100.0	100.0	100.0	100.0	100.0	$V_S K_S$	94.0	98.0	98.8	60.6	40.5	30.4
								$V_B K_L$				38.7	59.1	69.3
								$A_{GL} K_{GL}$	6.0	2.0	1.2	0.7	0.4	0.3

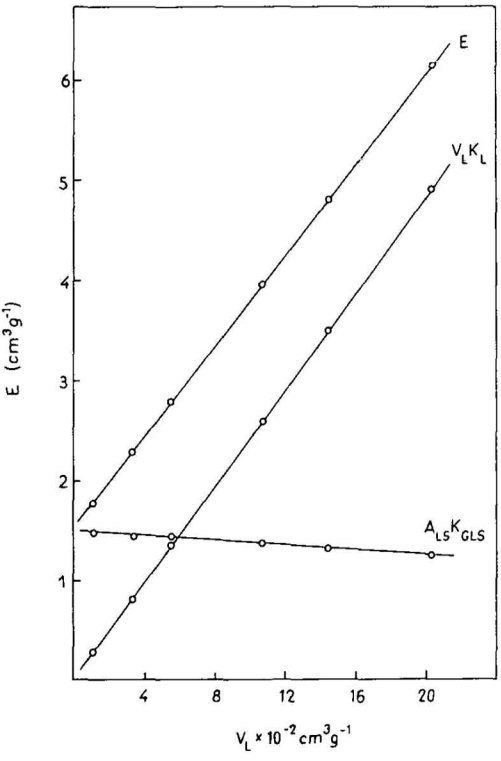

Fig. 3. Variation of partial retention effects and integral retention with liquid stationary phase volume per gram of packing for 1-propanol on Apiezon M–Celite 545 at 70°C.

It follows from Table IV that liquid–solid adsorption of polar solutes contributes to their integral retention in the Apiezon–Celite system. Even in the case of the most heavily loaded packing the adsorption contributions vary between 4 and 25%. On the contrary, in the Carbowax–Celite system the gas–liquid adsorption contributes moderately to the retention of all solutes, decreasing rapidly with increasing LSP loading. Considerable contributions varying between 3 and 42% are observed only in the packing with smallest amount of LSP. The most pronounced retention effect is due to dissolution in both the structured and/or the bulk LSP layers.

To demonstrate the variation of integral retention, E, and that of PRE with V_L, plots are presented in Figs. 2–4 for selected solutes. Fig. 2 shows absolute contributions of all mechanisms to the integral retention of isobutyraldehyde in the system TDPN–firebrick. As expected, with increasing V_L the $V_S K_S$ contribution increases until the structured layer achieves its maximum thickness, d_S. After the appearance of the bulk LSP layer, $V_S K_S$ decreases slowly since $V_S = A_{LS} d_S$, where A_{LS} decreases with increasing V_L and d_S remains constant. Apparently, the dependence of $V_S K_S$ on V_L can be represented by means of two straight lines, illustrating the variation of this contribution before and after completion of the structured layer respectively. The intersection of both lines corresponds to that V_L value at which formation of the bulk

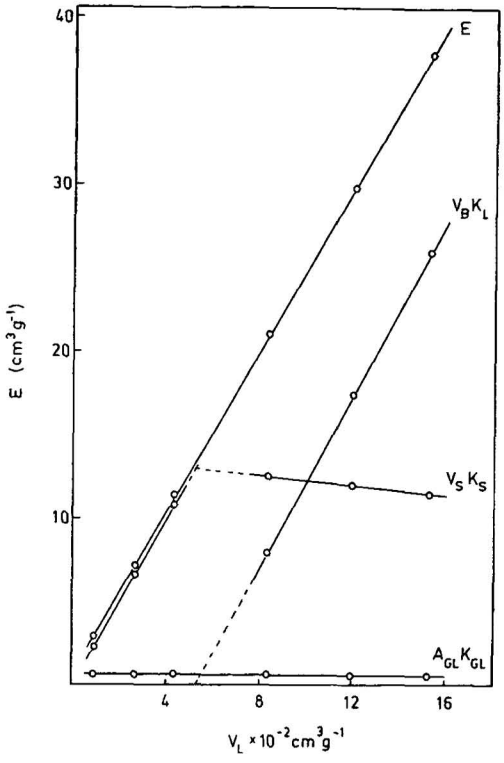

Fig. 4. Variation of partial retention effects and integral retention with liquid stationary phase volume per gram of packing for 1-propanol on Carbowax 4000–Celite 545 (system A) at 70°C.

layer starts, *i.e.*, this point is the origin of the $V_B K_L$ retention contribution. Simultaneously, the contributions $A_{GL}K_{GL}$ and $A_{LS}K_{GLS}$ parallel the corresponding dependences of A_{GL} and A_{LS} on V_L. Regardless of the small K_{SA} for isobutyraldehyde, its liquid–solid adsorption contributes more to the integral retention than the adsorption at the gas–liquid interface.

Figs. 3 and 4 show the behaviour of PRE for 1-propanol on Apiezon–Celite and Carbowax–Celite respectively. Since in the former system $K_S = K_L$ the contribution of the unique absorption mechanism is indicated in Fig. 3 as $V_L K_L$. As discussed above, the $A_{LS}K_{GLS}$ contribution decreases with increasing V_L, remaining as a considerable part of the integral retention. On the other hand, the situation on Carbowax–Celite (system A) is quite different resulting in two absorption mechanisms. Fig. 4 shows that for 1-propanol $V_S K_S$ and $V_B K_L$ follow similar dependences on V_L to those in Fig. 2. Moreover, the contribution of $A_{GL}K_{GLS}$ is essentially small, while that of $A_{LS}K_{GLS}$ is completely absent.

In conclusion, the introduced GLC sorption model has allowed a reliable procedure to be developed which needs no investigator's intuition for identification of the retention mechanisms. The application of this procedure leads immediately to solution of the inverse retention problem, resulting in a set of precisely calculated partition coefficients. The latter permits one to evaluate absolute and/or relative contributions of identified mechanisms to the integral solute retention.

ACKNOWLEDGEMENTS

The author gratefully acknowledges useful discussion with Professor Dr. B. Alexiev, Department of Organic Chemistry of the Institute of Chemical Technology, Sofia. He is also indebted to Mrs. M. Shopova and Mrs. L. Petkova, all ex-students of the same Institute, for their experimental assistance.

REFERENCES

1 R. N. Nikolov, in E. Kováts (Editor), *Column Chromatography (Proc. Symp., Lausanne, October 7–10, 1969)*, Ed. Swiss Chemists' Ass., 1970, p. 156.
2 R. L. Martin, *Anal. Chem.*, 33 (1961) 347.
3 R. L. Pecsok, A. de Yllana and A. Abdul Karim, *Anal. Chem.*, 36 (1964) 452.
4 D. E. Martire, *Anal. Chem.*, 38 (1966) 244.
5 P. Urone and J. F. Parcher, *Anal. Chem.*, 38 (1966) 270.
6 J. R. Conder, D. C. Locke and J. H. Purnell, *J. Phys. Chem.*, 73 (1969) 700.
7 V. G. Berezkin, V. P. Pakhomov, V. S. Tatarinsky and V. M. Fateeva, *Dokl. Akad. Nauk SSSR*, 180 (1968) 1135.
8 J. F. K. Huber and R. G. Gerritse, *J. Chromatogr.*, 58 (1971) 137.
9 Z. Suprynowicz, A. Waksmundzki and W. Rudziński, *J. Chromatogr.*, 67 (1972) 21.
10 R. L. Pecsok and B. H. Gump, *J. Phys. Chem.*, 71 (1967) 2202.
11 H. L. Liao and D. E. Martire, *Anal. Chem.*, 44 (1972) 498.
12 V. G. Berezkin and V. M. Fateeva, *J. Chromatogr.*, 58 (1971) 73.
13 J. R. Conder, *Anal. Chem.*, 48 (1976) 917.
14 R. N. Nikolov, *Chromatographia*, 4 (1971) 565.
15 J. R. Conder, *J. Chromatogr.*, 39 (1969) 273.
16 P. H. Weiner, H. L. Liao and B. L. Karger, *Anal. Chem.*, 46 (1974) 2182.
17 J. S. Rowlinson, in A. Goldup (Editor), *Gas Chromatography 1964*, Institute of Petroleum, London, 1965, p. 213.
18 D. H. Everett, in A. Goldup (Editor), *Gas Chromatography 1964*, Institute of Petroleum, London, 1965, p. 219.
19 A. Di Corcia, A. Liberti and R. Samperi, *Anal. Chem.*, 45 (1973) 1228.
20 F. Bruner, P. Ciccioli, G. Crescentini and M. T. Pistolesi, *Anal. Chem.*, 45 (1973) 1851.
21 J. Serpinet, *J. Chromatogr.*, 68 (1972) 9.
22 J. Serpinet, *J. Chromatogr.*, 77 (1973) 289.
23 J. Serpinet, *Chromatographia*, 8 (1975) 18.
24 A. W. Adamson, *Physical Chemistry of Surfaces*, Wiley-Interscience, New York, 3rd Ed., 1976, p. 305.
25 J. R. Conder and C. L. Young, *Physicochemical Measurement by Gas Chromatography*, Wiley-Interscience, Chichester, 1979, p. 516.
26 R. N. Nikolov, *Chromatographia*, 6 (1973) 451.
27 N. D. Petsev, R. N. Nikolov and A. Kostova, *J. Chromatogr.*, 93 (1974) 369.
28 R. N. Nikolov, N. D. Petsev and A. D. Stefanova, *Chromatographia*, 9 (1976) 81.
29 D. C. Locke, *Advan. Chromatogr.*, 14 (1976) 87.
30 G. M. Bliznakov, I. V. Bakardjiev and E. M. Gocheva, *J. Catal.*, 18 (1970) 260.
31 R. N. Nikolov, *Chromatographia*, 7 (1974) 6.
32 T. Komaita, K. Naito and S. Takei, *J. Chromatogr.*, 114 (1975) 1.
33 H. Rotzsche and M. Hofmann, in E. Leibnitz and H. G. Struppe (Editors), *Rukovodstvo po Gazovoj Khromatografii*, Izd. Mir, Moskow, 1969, p. 176.
34 J. F. Parcher and C. L. Hussey, *Anal. Chem.*, 45 (1973) 188.

Journal of Chromatography, 241 (1982) 257–268
Elsevier Scientific Publishing Company, Amsterdam — Printed in The Netherlands

CHROM. 14,645

COMPARISON OF STATIONARY PHASE FORMATION IN RP-FOR METHANOL–WATER SYSTEMS

CLEMENT R. YONKER, THOMAS A. ZWIER* and MICHAEL F. BURKE*
Department of Chemistry, University of Arizona, Tucson, AZ 85721 (U.S.A.)
(First received July 29th, 1981; revised manuscript received November 3rd, 1981)

SUMMARY

A proposed model for a ternary stationary phase system for RP-18 and RP-8 is evaluated. The stationary phase is a combination of bonded organic moiety, silica substrate and associated solvent molecules. The volume and composition of the stationary phase were found to vary under changing mobile phase conditions. Stationary phase formation by solvation of the bonded organic moiety is different but related for RP-18 and RP-8. Selectivity (α) was also seen to plateau for RP-18 and RP-8 at different values. The overall stationary phase formation was found to be dependent on the chain length of the bonded organic moiety and residual silanol activity for RP-18 and RP-8.

INTRODUCTION

Since the development and implementation of chemically bonded phases for chromatographic separations[1], the structure, composition and volume of the stationary phase have been shrouded in uncertainty. The structure of the stationary phase is dependent on the initial silane starting material, *e.g.*, trichlorosilanes, polymerization and cross-linking; dichlorosilanes, polymerization; and monochlorosilanes, no polymerization. The composition is defined by the organic moiety attached to the silica surface through the silane, be it an octydecyl, octyl or propylamine group. The volume of the stationary phase (V_S) is of fundamental importance in chromatography, as seen in the equation

$$V_R = V_m + KV_s \tag{1}$$

where V_R is the retention volume of the solute and V_m is the volume of mobile phase in the column. The need for an actual value of V_s can be circumvented by using the retention factor (k') (ref. 2), which is defined by the equation

$$k' = \frac{t_r - t_0}{t_0} \tag{2}$$

* Present address: The Upjohn Company, 7000 Portage Road, Kalamazoo, MI 49001, U.S.A.

0021-9673/82/0000–0000/$02.75

where t_0 is the breakthrough time for a non-retained species and t_r is the retention time of a solute species. The relationship between K and k' is

$$k' = K \cdot \frac{V_s}{V_m} \tag{3}$$

Therefore, the use of k' assumes that the phase ratio is constant, which is not proved to be a valid assumption[3]. It is therefore of considerable interest to know the actual volume of the stationary phase as a function of the mobile phase composition and the bonded material.

The measurement of V_s has been undertaken by many workers[3–7]. Melander *et al.*[3] estimated the relative magnitude of the phase ratio between columns showing homoenergetic retention by plots of ln k'_A *versus* ln k'_B, where k' is the retention factor for a solute under similar conditions for columns A and B. Sander and Field[4] estimated the phase ratio using a geometric model of the silica surface based on manufacturer's information on silanol surface coverage and percentage of carbon bonded to the surface. From a knowledge of the phase ratio, which could be calculated by one of the above-mentioned methods, V_s can be determined for any column once V_m is accurately known. Berendsen *et al.*[5] studied various methods for the determination of t_0, the elution time of a non-retained component, by using salts, deuterated mobile phase components and linearization of a homologous series. They demonstrated that the most satisfactory method for determination of t_0 and thus V_m was by linearization of a homologous series. They also showed that t_0 changed for a column on varying the percentage of organic modifier in the mobile phase. McCormick and Karger[6] and Slaats *et al.*[7] measured the distribution isotherms of methanol, acetonitrile and tetrahydrofuran (THF) between the bonded organic moiety and the mobile phase for varying ratios of non-aqueous modifier in the mobile phase. These investigators showed an enrichment of the stationary phase by the non-aqueous modifier. Ruckert and Samuelson[8] first studied the distribution of both water and organic modifiers between aqueous mobile phases and in ion-exchange resins. Tilly-Melin *et al.*[9] measured both the change in V_m and the enrichment of the stationary phase by the non-aqueous modifier. They related the two together for RP-8 with acetonitrile as the non-aqueous modifier from 10 to 60% (v/v).

As the work by the above investigators demonstrates, the formation of the stationary phase is a dynamic process under control of the mobile phase. In the debate concerning the underlying mechanism of the separation process in reversed-phase chromatography (RPC), the mechanisms of a solvophobic effect and partitioning have been proposed. The hydrophobic effect consideres the bonded phase as a passive receptor for the solute. The solvation of the bonded moiety serves no role in retention except to present a barrier between the organic moiety and the solute. Scott and Kucera[10] investigated if the solute displaces the solvent layer absorbed to the stationary phase, as would occur in a hydrophobic mechanism, and found no solvent displacement.

All the above-mentioned work supports the view of the stationary phase being a ternary combination of bonded organic moiety, absorbed solvent molecules and residual silanols on the silica surface. The solvation of the bonded organic moeity by the non-aqueous modifier should be viewed as a dynamic process dependent on the

moiety present and the substrate to which the moiety is bonded. This dynamic process must be considered in the overall separations mechanism in RPC. In this work a study was undertaken to compare the enrichment of the bonded organic moeity by methanol for RP-8 and RP-18, and the possible role solvation plays in the selectivity of the separations process.

EXPERIMENTAL

By linearization of a homologous series of alcohols, following the procedure set forth by Berendsen *et al.*[5], one obtains an equation for a line:

$$t_{rN+1} = \alpha t_{rN} - t_0 (\alpha - 1) \tag{4}$$

Plotting t_{rN+1} (retention time of the $N + 1$-carbon homologue *versus* t_{rN} (retention time of the N-carbon homologue), t_0 can be determined from the slope of the line α (relative retention) and the intercept. The elution time of a non-retained solute, t_0, can be expressed as V_m, the volume of mobile phase in the column by multiplying t_0 by the flow-rate through the column. The change in t_0 (Fig. 3) is inversely related to the change in volume of the stationary phase, V_s. Thus, the measurement of V_m will be sensitive to volume changes in V_s owing to solvation of the bonded moiety and or substrate by the non-aqueous modifier.

The alcohols in this study were obtained from Aldrich (Milwaukee, WI, U.S.A.), except for methanol (Fisher Scientific, Fair Lawn, NJ, U.S.A.), and were used without further purification. The alcohols included methanol, ethanol, 1-propanol, 1-butanol, 1-pentanol, 1-hexanol, 1-heptanol, 1-octanol, 1-nonanol, 1-decanol, 1-dodecanol, 1-tetradecanol, 1-hexadecanol and 1-octadecanol. Depending on the mobile phase composition, a selected series of alcohols were used as solutes, *e.g.* methanol–water (20:80) for RP-18; the alcohols used as solutes were ethanol ($\bar{t}_r$ = 114.5 sec), *n*-propanol ($\bar{t}_r$ = 181.4 sec), *n*-butanol ($\bar{t}_r$ = 401.7 sec) and *n*-pentanol ($\bar{t}_r$ = 1176.3 sec). The solutes were dissolved in the mobile phase before being injected on to the column. The columns employed were slurry packed in the laboratory [100 × 4.6 mm I.D. LiChrosorb RP-18 and RP-8, 10 μm particle size (MCB, Cincinnati, OH, U.S.A.)]. The solvent delivery system was an Altex Model 420 with 110a pumps (Beckman Instruments, Irvine, CA, U.S.A.). The detector was a Waters R403 differential refractometer with a 10-μl flow cell (Waters Assoc., Milford, MA, U.S.A.). The solvents were methanol and doubly distilled water, which were filtered, mixed by volume and sonicated for 15 min prior to use. The column and detector were both thermostated at 25°C in a water-jacket. Prior to making flow-rate measurements, the column was equilibrated with approximately 200 column volumes of the appropriate solvent. After equilibration was complete, the probes were injected (concentrations were *ca.* 2.5 μl/ml) and their retention times were measured by a System I computing integrator (Spectra-Physics, San Jose, CA, U.S.A.) to 0.1 sec. The average of five replicate injections was used in calculating t_0. The extra column volume was determined by injecting methanol–water (8:2) into 100% methanol with the column removed.

The total amount of methanol extracted from the column was determined using a Varian Model 1700 gas chromatograph with a flame-ionization detector. The

column was a 1:1 (w/w) mixture of Poropak Q and R in a 6 ft. × 1/4 in. I.D. copper column at 185°C, with nitrogen as the carrier gas at a flow-rate of 25 ml/min. The detector and injector temperatures were 200°C, respectively. Water was determined using a Gow-Mac Model 550 GC with a thermal conductivity detector. A 4 ft. × 1/4 in. I.D. copper column of Poropak R was used at 140°C with helium as the carrier gas at a flow-rate of 25 ml/min. The detector bridge current was 200 mA at 200°C and the injector temperature was 180°C. After measuring V_m, the column was flushed with approximately 48.75 ml of dioxane (distilled from potassium hydroxide) at 2 ml/min into a 50-ml volumetric flask containing 1.00 ml of isopropanol as internal standard. The contents of the flask were brought to volume with dioxane. An injection volume of 3 μl was used. Peak areas were measured with a Spectra-Physics Autolab Minigrator and the appropriate area ratios from at least three injections were averaged for the determination of the amount of solvent extracted. The volume of solvent extracted was determined from a calibration graph relating a known amount of methanol to the peak-area ratio of methanol to isopropanol. Subtracting the percentage of methanol in V_m and extra-column volume from the gas chromatographic (GC) measurement, the amount of modifier in the solvation layer can be determined by the equation

$$V_T = \%MV_m + \%MV_{ec} + V_s \tag{5}$$

where V_T is the total amount of modifier measured by GC, V_m is the volume of mobile phase in the column measured by eqn. 2, $\%M$ is the volume percentage of modifier in the mobile phase, V_{ec} is the extra-column dead volume and V_s is the volume of the solvation layer of stationary phase. The amount of water extracted was determined in the same manner. The validity of these measurements are borne out by those of Westerlund and Theodorsen[11], who used RP-8 with methanol–buffer (40:60) as the mobile phase and determine 0.18 ml/g of methanol in the stationary phase. This value is within the experimental error of our own measured value using methanol–water (40:60) with RP-8 (see Table II).

RESULTS AND DISCUSSION

The model of the stationary phase, as proposed, is a combination of silica substrate, bonded organic moiety and solvation layer consisting of mobile phase components. The interaction of the mobile phase with the silica substrate and bonded moiety controls the composition and volume of the solvation layer. The influence of the mobile phase on the formation of the stationary phase for RP-18 and RP-8 can be seen in Tables I and II and Figs. 1 and 2. In general, during solvation the organic moeity can selectively enrich the stationary phase in lipophilic non-aqueous modifiers through dispersion interactions, while residual silanols also influence the uptake of aqueous and non-aqueous modifiers with hydrogen bonding capabilities such as those normally used in RPC, *e.g.*, water, methanol, acetonitrile and THF.

The data in Tables I and II have been normalized by the surface area of the packing material. This normalization by surface area [RP-8 250 m^2/g, RP-18 150 m^2/g (see ref. 12)] allows one to compare the two packing materials with respect to the effect of chain length and residual silanols. Surface coverage and degree of derivatization are

TABLE I

INFLUENCE OF MOBILE PHASE ON FORMATION OF STATIONARY PHASE FOR RP-18

RP-18: surface area 150 m^2/g; pore size 150 Å; length of chain C_{18}; carbon content 19.8%; functional group bonded dimethyloctyldecylchlorosilane; calculated degree of derivatization 42%; surface coverage 5.5 μmol C/m^2; weight in column 0.8948 g.

Parameter	*Methanol–water composition of mobile phase*					
	0:100	*20:80*	*40:60*	*60:40*	*80:20*	*100:0*
t_0 (sec)	67.18	61.95	54.85	49.72	49.68	46.91
V_m (ml)	1.12	1.03	0.914	0.829	0.828	0.782
V_{CH_3OH} in stationary phase (ml/g) ($\pm$0.03)	0.00	0.04	0.16	0.25	0.30	0.37
V_{CH_3OH} in stationary phase (μmol/m^2) ($\pm$5.60)	0.00	7.24	25.7	40.5	49.1	61.4
V_{H_2O} in stationary phase (ml/g) ($\pm$0.03)	0.27	0.04	0.08	0.09	0.03	0.00
V_{H_2O} in stationary phase (μmol/m^2) ($\pm$11.1)	101	16.3	31.1	34.8	10.4	0.00
V_s total volume in stationary phase (ml/g) ($\pm$0.04)	0.27	0.09	0.24	0.34	0.33	0.373
V_s, total volume in stationary phase (μmol/m^2) ($\pm$12.4)	101	23.5	56.8	75.3	59.5	61.4
α	4.06	3.48	2.59	1.90	1.54	1.46
Methanol in stationary phase (%, v/v, total)	0	50	65	72	91	$\approx$100

TABLE II

INFLUENCE OF MOBILE PHASE ON FORMATION OF STATIONARY PHASE FOR RP-8

RP-8: surface area 250 m^2/g; pore size 100 Å; length of chain C_8; carbon content 12.2%; functional group bonded dimethyloctylchlorosilane; calculated degree of derivatization 30%; surface coverage 4.0 μmol C/m^2; weight in column 0.7344 g.

Parameter	*Methanol–water composition of mobile phase*				
	0:100	*20:80*	*40:60*	*60:40*	*80:20*	*100:0*
t_0 (sec)	77.61	67.94	62.61	57.29	45.3	
V_m (ml)	1.29	1.13	1.04	0.955	0.755	
V_{CH_3OH} in stationary phase (ml/g) ($\pm$0.04)	0.00	0.07	0.18	0.37	0.72	
V_{CH_3OH} in stationary phase (μmol/m^2) ($\pm$4.10)	0.00	7.25	17.9	37.0	71.8	
V_{H_2O} in stationary phase (ml/g) ($\pm$0.04)	0.25	0.05	0.08	0.13	0.19	
V_{H_2O} in stationary phase (μmol/m^2) ($\pm$9.10)	54.6	10.9	18.2	29.3	42.0	
V_s total volume in stationary phase (ml/g) ($\pm$0.06)	0.25	0.12	0.26	0.50	0.91	
V_s, total volume in stationary phase (μmol/m^2) ($\pm$10.0)	54.6	18.2	36.1	66.3	114	
α	3.62	3.18	2.40	1.75	1.71	
Methanol in stationary phase (%, v/v, total)	0	60	69	74	79	

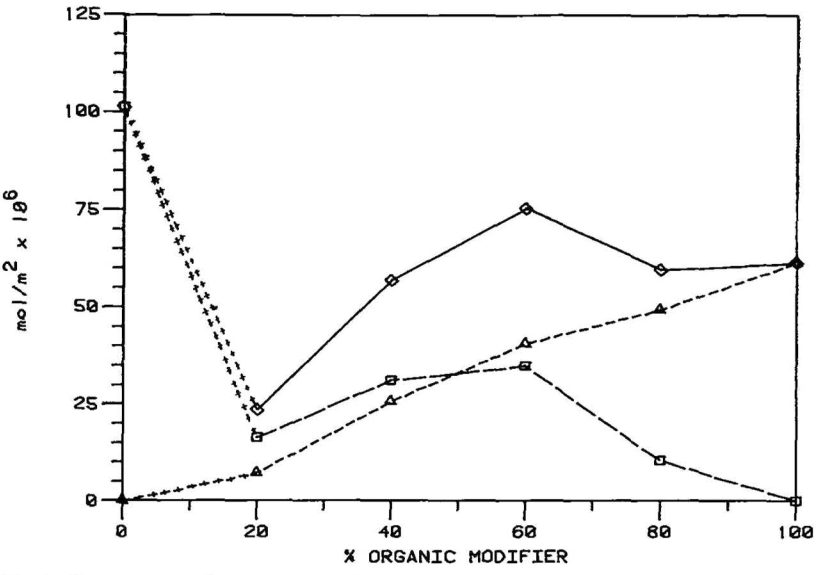

Fig. 1. Concentration of solvent absorbed into the stationary phase *versus* percentage of organic modifier in the mobile phase for RP-18. Individual points are connected for clarity. △, Methanol; □, water; ◇, total.

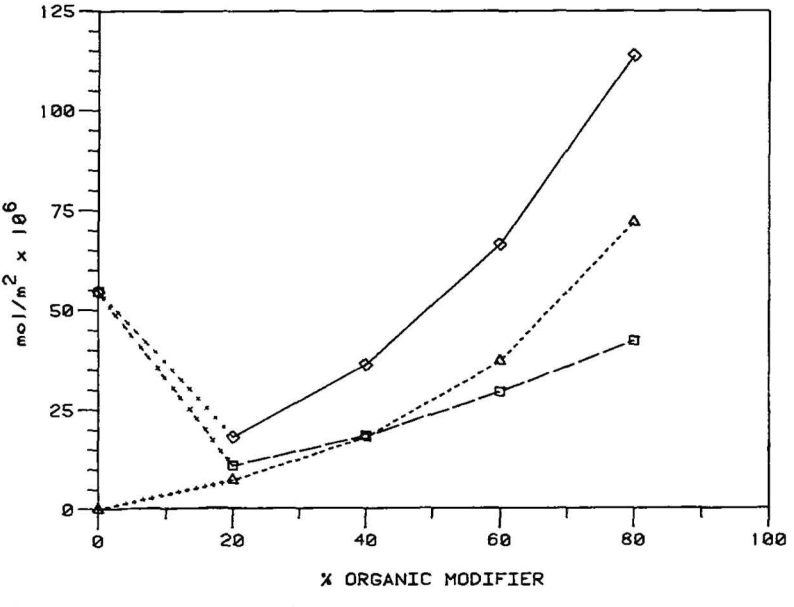

Fig. 2. Concentration of solvent absorbed into the stationary phase *versus* percentage of organic modifier in the mobile phase for RP-8. Individual points are connected for clarity. Symbols as in Fig. 1.

also important points to consider when comparing two different packing materials. If one assumes a geometric model of the silica surface in which there are eight accessible silanol groups per 100 Å^2 (refs. 13 and 14), then the maximum surface coverage would be 13.3 μmol C/m^2. For RP-18, the surface coverage is 5.5 μmol C/m^2, and the degree of derivatization is *ca.* 42%. For RP-8, the surface coverage is 4.0 μmol C/m^2 and the degree of derivatization is *ca.* 30%. These values are not absolute but are dependent on the geometric model chosen, but the trends in surface coverage and degree of derivatization are significant.

In order to understand the solvation mechanism of RP-8, one must begin with a geometric model of its surface. With the assumption of 8 silanols per 100 Å^2, it is reasonable to assume that the bonded structure for these sites will be the one of lowest energy for the number of sites occupied by the silane. That is, the monochlorosilanes will bind as far away from each other as possible. These sites will be at the corners of an isosceles triangle with the base *ca.* 10.0 Å and the sides *ca.* 11.2 Å long. The remaining silanols are either sterically hindered from any interactions or hydrogen bonded to the solvent present, *e.g.*, water, methanol, acetonitrile or THF. This geometric model accounts for 3 silanols per 100 Å^2 for silane binding. The RP-8 surface with 30% derivatization has 2.5 silanols per 100 Å^2 which are chemically bonded; this is in close agreement with the above postulated model. Therefore, a comparison between the model and the RP-8 surface can be undertaken. The physical phenomena inherent in this model will manifest themselves for the case of RP-8 through the amount of structuring of the bonded moiety by the loss of degrees of freedom on bonding to the surface, and the residual silanol activity of the surface.

Under 100% aqueous conditions, the C_8 chain will tend to increase the entropy of the surrounding water molecules by decreasing its surface area through intermolecular and intramolecular interactions[15]. Intramolecular interactions are limited owing to the rigidity imparted to the molecule on binding to the surface, and the limits imposed by the C_8 chain length. This structuring of the C_8 moiety on binding to the surface is borne out through ^{13}C nuclear magnetic resonance investigations of the RP-8 surface[16]. Intermolecular interactions are restrained owing to the limits imposed by the geometric model of the surface. The distance between C_8 moieties as determined from the model are 10.0 and 11.2 Å, respectively, while the C_8 chain length is *ca.* 12.0 Å. The C_8 chain will have difficulty undergoing efficient intermolecular interactions with neighboring chains, because of the C_8 chain length and the distance between bonded chains. Also, the hydrophilic surface, from the remaining silanols, will not allow a close approach of the lipophilic C_8 chain. Both of these reasons will combine in decreasing the amount of C–C overlap for efficient dispersion interactions between C_8 chains. As the percentage of methanol increases in the mobile phase (0–20%), there is enough methanol present to overcome the weak interchain dispersion interactions and solvate the C_8 chains. This results in the enrichment of the non-aqueous modifier in the stationary phase under low methanol concentrations as seen in Table II, for 20% methanol in the stationary phase. On solvation by methanol, the RP-8 assumes a "brush"-like structure, with the mobile phase having direct access to the residual silanols on the silica surface. As the concentration of methanol in the mobile phase increases above 20%, the solvation of the RP-8 surface is dominated by its residual silanols. Any solvent molecules that can effectively hydrogen bond to the residual silanols present between the C_8 chains will be brought into the

stationary phase. Methanol and water, being hydrogen-bond donors or acceptors, will bring other water and methanol molecules with them into the stationary phase. Therefore, hydrogen bonding is the chemical driving force behind stationary phase formation. This mechanism is dependent on mass action: the higher the percentage of methanol in the mobile phase, the more methanol can be brought into the stationary phase by solvent molecules already present, and the more methanol brought into the stationary phase, the more water can be brought along with it. A synergistic effect is prevalent between the methanol and water, which aids the stationary phase formation. This explains the results in Table II and Fig. 2 of the continuing increase in the water present in the stationary phase throughout the entire mobile phase compositional range. Dispersion interactions between C_8 and methanol play a major role in solvation for low concentrations of methanol modifier (between 0 and 20%). Once methanol has initially solvated the C_8 chain, opening the C_8 structure by breaking any weak interchain dispersion interactions, the synergistic effect due to the residual silanols on the surface takes over and continues throughout the solvent compositional range.

RP-18 has the same geometric surface model of 8 silanols per 100 Å, but the bonding arrangement of the silanes are different. In order to explain the experimental data of RP-18 in which *ca.* 3.3 sites per 100 Å are bonded by silanes, a model of the RP-18 system must have at least four non-sterically hindered silanols with which to chemically bond through. An arrangement of this nature can be made within the constraints of 100 $Å^2$ by making the silanols be at the corners of a square with free silanols surrounding them. This proposed model will have four unhindered silanols for binding, with four silanol groups remaining. One consequence of this model is that the C_{18} chains are bonded closer to one another than the C_8 chains. So, unlike the RP-8 material, the carbon chains in RP-18 are long enough to undergo effective intermolecular interactions, and probably weaker intramolecular interactions even with the first 6–8 carbons being rigid due to bonding. This picture of the surface is similar to Lochmuller's[16].

The solvation of RP-18 is a meld of two mechanisms. The first is a mechanism similar to RP-8 involving the residual surface silanols, and the second involves the increased dispersion interactions for RP-18 due to the larger carbon surface area of the chain as compared to RP-8. From 0–60% methanol modifier concentrations the solvation is similar to RP-8 in that residual silanols on the surface not sterically hindered by the C_{18} chains dominate the solvation. This mimics the RP-8 solvation process with one major exception, which occurs at low methanol modifier concentrations, $<20\%$. For RP-18 under low methanol modifier concentrations, most of the intramolecular interactions and all of the intermolecular interactions between chains are intact. Therefore, the methanol does not open the C_{18} structure as it does the C_8 structure, with the resulting increase in methanol solvation for RP-8 over RP-18. The residual silanols between the clumps of C_{18} chains dominate the solvation mechanism up to *ca.* 70% methanol modifier concentration through their ability to hydrogen bond with either water or methanol. As the percentage of methanol in the mobile phase increases, the intermolecular interactions between chains are "unzipped" from top to bottom by the mass action effect of the methanol. When the solvent-chain interactions overcome the intra- and intermolecular interactions of the chain, the C_{18} becomes more erect and "brush"-like. This "brush"-like structure increases the

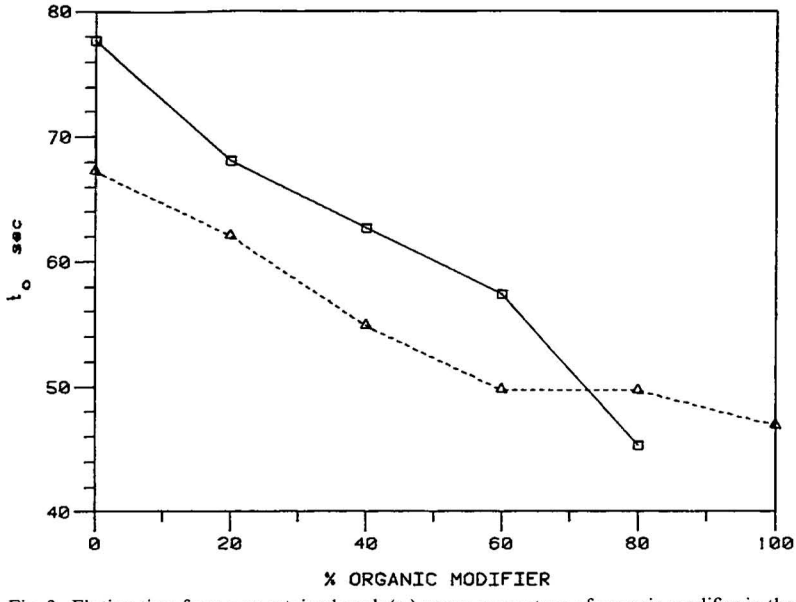

Fig. 3. Elution time for a non-retained peak (t_0) *versus* percentage of organic modifier in the mobile phase for RP-18 (△) and RP-8 (□). t_0 was determined by eqn. 4.

ability of the C_{18} chain to undergo dispersion interactions with methanol, as there is a larger carbon surface area available for Van der Waals' interactions with solvent molecules for C_{18} than for C_8. This increased solvation of the C_{18} by the second mechanism is reflected in the more "liquid"-like spectra seen in ^{13}C nuclear magnetic resonance experiments[16]. At *ca.* 70% methanol in the mobile phase the second mechanism of solvation begins to dominate. This "unzipping" of the C_{18} interactions is completed and methanol now has access to the increased carbon surface area. Methanol can effectively solvate the C_{18} with a resulting "brush"-like structure. These events will cause an enrichment of the C_{18} in organic modifier. Also, with the more open structure methanol can remove any water from between the chains. This hypothesis explains the jump in the percentage of methanol in the stationary phase which is seen in Table I for RP-18 at an 80% concentration of methanol modifier.

There is one final point to be discussed which is relevant to both RP-18 and RP-8, and that is stationary phase formation at 100% water in the mobile phase. From Tables I and II a large stationary phase volume is found at this value for the mobile phase composition. A possible explanation for this observation is two-fold: (1) the residual silanols present on the silica surface are involved in hydrogen bonding with the water present from the mobile phase and (2) water can be trapped on the substrate surface by a "tent" of C_{18} or C_8 chains. This trapping of water is caused by the "freezing" of the bonded chains. This "freezing" of the bonded chains results from the intra- and/or intermolecular interactions amongst the chains themselves. Such interactions would be expected to be energetically favorable when compared only with the interactions between the water matrix and the hydrocarbon. At 100% water in the mobile phase an adsorption mechanism is most likely responsible for chromatographic retention, in contrast to a partition mechanism in a solvation layer.

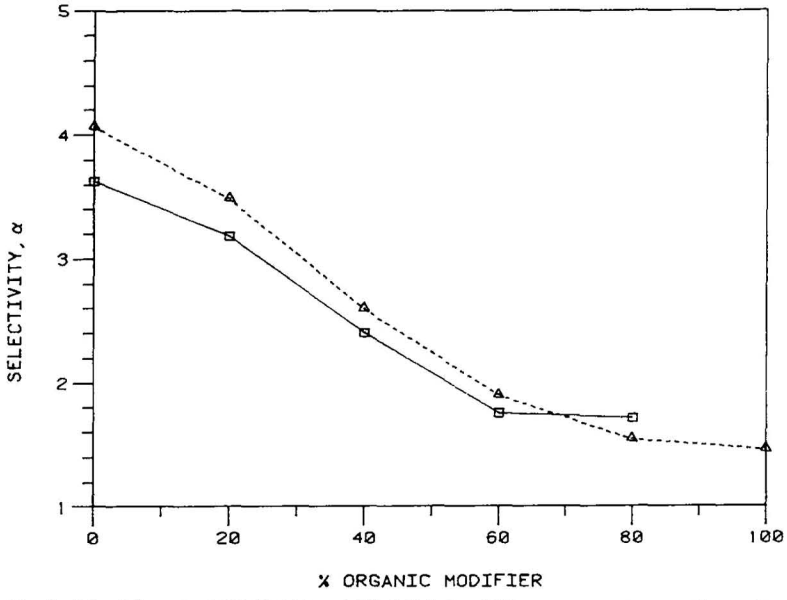

Fig. 4. Selectivity (α) of RP-18 ($\triangle$) and RP-8 ($\square$) for ΔCH_2 *versus* percentage of organic modifier in the mobile phase. α was determined by eqn. 4.

Further work is being carried out to determine the exact mechanism which is responsible for chromatographic selectivity at 100% water in the mobile phase and also the conditions under which a partitioning mechanism begins to contribute.

Another interesting phenomenon is the change in α between RP-8 and RP-18 (see Fig. 4). The relative retention (α) in this experiment is based on the selectivity of the stationary phase for a change of one methylene group, ΔCH_2, in the homologous series of alcohols. RP-18 has the highest initial selectivity (Table I), but a cross-over occurs at approximately 70% methanol, and from then on RP-8 has the largest α value. A possible explanation for this cross-over of α between packing materials is the effect of surface coverage and chain length in controlling the stationary phase composition. The enrichment of the stationary phase with non-aqueous modifier does have a definite effect on the separations process. The higher the concentration of methanol in the stationary phase, the more "non-polar" the stationary phase appears to the solute, relative to the mobile phase (see Tables I and II). The more "non-polar" the stationary phase, the smaller the difference in free energy of transfer ($\Delta\Delta G_{2-1}$) for a change of one methylene group between the N and $N + 1$ homologues. Thermodynamically, $\Delta\Delta G_{2-1} = -RT\ln\alpha$ (ref. 6); if $\Delta G_2 < \Delta G_1$, then $\alpha > 1$ or $k'_2 > k'_1$. If $\Delta G_2 = \Delta G_1$, then $\Delta\Delta G_{2-1} = 0$, and $\alpha = 1$ or $k'_2 = k'_1$, and no separation of these two solutes will occur under this set of stationary and mobile phase conditions. The more "non-polar" the stationary phase becomes owing to enrichment of the non-aqueous modifier by the bonded moiety, the less discrimination the stationary phase has for the change in one dispersion interaction (ΔCH_2). Thus α approaches unity or the retention times of the two solutes become more equal.

RP-8 has the greater concentration of methanol in the stationary phase up to

70% methanol modifier concentration, and therefore RP-8 will have a smaller selectivity for ΔCH_2 than RP-18. At 70% and higher methanol modifier concentrations the concentration of methanol in the stationary phase is kept constant for RP-8 owing to the synergistic effect of the methanol and water for the RP-8 materials. At this point RP-8 then becomes the more selective packing material for a ΔCH_2 group because it appears more "polar" to the mobile phase than does RP-18. At methanol modifier concentrations above 70%, RP-18 can effectively enrich the stationary phase in methanol, owing to the "unzipping" of the C_{18} chains. This presents a larger carbon surface area to the solvent molecules for undergoing dispersion interactions, thus presenting to the solutes, a more "non-polar" stationary phase than the mobile phase, with a concomitant decrease in selectivity for a ΔCH_2 group for RP-18.

The α values of both RP-8 and RP-18 plateau at 1.7 and 1.5, respectively. These plateaus are reached for both packing materials, at a point where the enrichment of the stationary phase in methanol no longer changes the overall selectivity characteristics of the stationary phase for ΔCH_2 group, which for methanol occurs at higher modifier concentrations, because of the weakness of the dispersion interaction of methanol compared with more "non-polar" solvents such as acetonitrile, THF and dioxane[2]. The strength of the dispersion interaction of the solvent will ultimately govern how rapidly a bonded chain will be solvated and when the α plateau will be reached.

In conclusion, solvation and stationary phase formation for RP-18 and RP-8 are dynamic processes controlled through a combination of two mechanisms. The extent of control exercised by these two mechanisms is dependent on the residual silanol activity and length of carbon chain bonded to the surface. For RP-8 the low surface coverage by the silane allows the residual silanols to dominate stationary phase formation. Dispersion interactions between the solvent and C_8 chain dominate stationary phase formation only at low methanol modifier concentrations, whereas for RP-18, with its higher surface coverage and longer carbon chain, residual silanols play a decreasing role in stationary phase formation for methanol modifier concentrations from 0 to 60%. The increased carbon surface area of the C_{18} chain plays an increasing role in stationary phase formation for methanol modifier concentrations from 0 to 100%, with the cross-over point between these two mechanisms occurring at *ca.* 70% methanol for RP-18. The data presented in this paper can be contrasted with the work of McCormick and Karger[6], where for RP-8 the reported minimum V_m was found at *ca.* 60% methanol in the mobile phase. The differences probably result from the different manner in which t_0 has been measured. The linearization of a homologous series of *n*-alcohols depends only on the retention of the solute species for the determination of t_0. Therefore, V_m is independent of the possible retention of any mobile phase component. If V_m^{max} values for the data reported in Tables I and II are chosen at 0% organic modifier, *i.e.*, no solvation, then for RP-18 $V_m^{max} = 1.12 \pm 0.07$ ml and for RP-8 $V_m^{max} = 1.29 \pm 0.07$ ml. These values are reasonable when compared with the values reported and calculated from McCormick and Karger[6] and Berendsen *et al.*[5].

These results clearly show that the selectivity of a bonded material is determined by the extent of solvation of the substrate materials as well as the bonded moiety. Solvation of the stationary phase is dependent on the specific and non-specific interactions of the mobile phase components for the substrate and bonded moiety.

Further investigations involving other organic modifiers should provide a better understanding of the question of relative solvent strengths in determining the chromatographic characteristics of bonded materials.

ACKNOWLEDGEMENTS

T.A.Z. acknowledges the partial support of the work provided by his receipt of a University of Arizona Graduate College Fellowship. M. F. B. acknowledges the partial support of the work by an unrestricted grant from Chevron Research.

REFERENCES

1 R. E. Majors, *J. Chromatogr. Sci.*, 18 (1980) 488.
2 B. L. Karger, L. R. Snyder and Cs. Horváth, *An Introduction to Separation Science*, Wiley, New York, 1973, pp. 272 and 131.
3 W. Melander, J. Stoveken and Cs. Horváth, *J. Chromatogr.*, 199 (1980) 35.
4 L. C. Sander and L. R. Field, *Anal. Chem.*, 52 (1980) 2009.
5 G. E. Berendsen, P. J. Schoenmakers, L. De Galan, G. Bigh, Z. Varga-Puchone and J. Inczedy, *J. Liquid Chromatogr.*, 11 (1980) 1669.
6 R. M. McCormick and B. L. Karger, *Anal. Chem.*, 52 (1980) 2249.
7 E. H. Slaats, W. Markovski, J. Fekete and H. Poppe, *J. Chromatogr.*, 207 (1981) 299.
8 H. Ruckert and O. Samuelson, *Acta Chem. Scand.*, 11 (1957) 303.
9 A. Tilly-Melin, Y. Askemark, K. G. Wahlund and G. Schill, *Anal. Chem.*, 51 (1979) 976.
10 R. P. W. Scott and P. Kucera, *J. Chromatogr.*, 142 (1977) 213.
11 D. Westerlund and A. Theodorsen, *J. Chromatogr.*, 144 (1977) 27.
12 K. J. Stetzenbach, *Ph.D. Dissertation*, University of Arizona, Tucson, AZ, 1980.
13 K. K. Unger, *Porous Silica*, Elsevier, Amsterdam, 1979, p. 7.
14 R. K. Iler, *The Chemistry of Silica*, Wiley, New York, 1979, p. 624.
15 Cs. Horváth, W. Melander and I. Molnár, *J. Chromatogr.*, 125 (1976) 129.
16 T. A. Zwier and M. F. Burke, in preparation.
17 C. H. Lochmuller and D. R. Wilder, *J. Chromatogr. Sci.*, 17 (1979) 574.

Journal of Chromatography, 241 (1982) 269–280
Elsevier Scientific Publishing Company, Amsterdam — Printed in The Netherlands

CHROM. 14,646

INVESTIGATION OF STATIONARY PHASE FORMATION FOR RP-18 USING VARIOUS ORGANIC MODIFIERS

CLEMENT R. YONKER, THOMAS A. ZWIER* and MICHAEL F. BURKE*
Department of Chemistry, University of Arizona, Tucson, AZ 85721 (U.S.A.)
(First received August 12th, 1981; revised manuscript received November 3rd, 1981)

SUMMARY

Additional support for a model of the stationary phase consisting of solvent molecules absorbed to both the bonded organic moiety and residual silanols on the silica surface is presented. The enrichment of the stationary phase by the bonded organic moiety in solvents having a large solvent strength for C_{18} was observed. Stationary phase formation for RP-18 is seen to be dependent on two mechanisms, whereas for RP-8 stationary phase formation is under the control of the residual silanols present on the surface. A relationship between ln θ (phase ratio) and stationary phase formation was derived and evaluated for the solvents methanol, acetonitrile and tetrahydrofuran (THF). Acetonitrile is shown to have anomalous behavior when compared with methanol and THF. A qualitative relationship between α and solvent strength is also developed and discussed.

INTRODUCTION

In a previous paper[1], the formation of the stationary phase was found to be dependent on both the solvation of the bonded moiety and the residual silanols on the substrate surface for RP-18 and RP-8. The efficiency with which the bonded carbon chain can undergo solvation is dependent on the Van der Waals interactions between the bonded moiety and the solvent. For RP-18 and RP-8 dispersion interactions between the mobile phase and the chain are one driving force in the mechanism behind stationary phase formation. Therefore, one could predict a greater solvation of a bonded carbon chain by solvents whose dispersion interactions are large. This hypothesis has been given support by workers who have studied the absorption isothersm for solvents commonly used in reversed-phase chromatography (RPC), *i.e.*, methanol, acetonitrile and tetrahydrofuran (THF)[2,3]. The solvation of the bonded moiety should result in a change in the volume of the stationary phase (V_s) together with enrichment of the stationary phase in solvent molecules capable of undergoing more effective dispersion interactions. Berendsen *et al.*[4], have addressed the question of change in stationary phase volume on changing the percentage of organic modifier

* Present address: The Upjohn Company, 7000 Portage Road, Kalamazoo, MI 49001, U.S.A.

0021-9673/82/0000–0000/$02.75

in methanol–water systems for various bonded phase columns. Additional supporting evidence can be found in the works of Tilly-Melin *et al.*[5] for LiChrosorb RP-8 and Westerlund and Theodorsen[6] for LiChrosorb RP-8 and Spherisorb ODS. One can deduce from the above work that the phase ratio (θ), which is defined as V_s/V_m, where V_m is the volume of mobile phase in the column, changes with varying mobile phase compositions.

The phase ratio is another important parameter that must be taken into account in any separation process. As stated above and from the data presented later in this paper (see Tables I–III), θ can change with varying mobile phase composition. For chromatographic separation processes a general equation can be derived to describe the phenomena that occur[7]:

$$V_R = V_m + K_D V_s \tag{1}$$

where K_D is the distribution coefficient, defined as

$$K_D = k'/\theta \tag{2}$$

where k' is the retention factor. One can see from eqn. 2 that the distribution coefficient is reciprocally related to the phase ratio and the retention factor is proportional to the phase ratio. The retention factor is most often reported for chromatographic separations with the assumption being made that the phase ratio is constant throughout the mobile phase compositional range used. The data presented in this paper prove this is not the case, θ cannot necessarily be considered constant and this effect on the separation processes must be taken into account.

In RPC k' has been found to fit an equation of the form

$$k' = Ae^{-B(\%\text{Org})} \tag{3}$$

where A and B are constants and %Org is the percentage of organic modifier in the mobile phase[8]. On rearranging eqn. 3, one obtains

$$\ln k' = \ln A - B(\%\text{Org}) \tag{4}$$

$\ln k'$ is a linear function of the percentage of organic modifier in the mobile phase. Substituting eqn. 2 into eqn. 4, we obtain

$$\ln K_D\theta = \ln A - B(\%\text{Org}) \tag{5}$$

and rearranging,

$$\ln \theta = \ln A/K_D - B(\%\text{Org}) \tag{6}$$

Eqn. 6, relating $\ln \theta$ to the percentage of organic modifier in the mobile phase, predicts there to be a linear relationship between the two variables.

In this work we have studied the enrichment of LiChrosorb RP-18 by methanol, acetonitrile and THF at organic modifier concentrations from 0 to 100%. The

effect that this enrichment has on stationary phase volume, the phase ratio and the selectivity of RP-18 is discussed.

EXPERIMENTAL

The experimental details have already been described[1], but exceptions were made for the determination of acetonitrile in the stationary phase. In the gas chromatographic (GC) measurement of the amount of acetonitrile in the stationary phase, methanol was used as the internal standard because of the co-elution of acetonitrile and isopropanol. Therefore, a calibration graph was constructed of volume of acetonitrile *versus* peak-area ratio of acetonitrile to methanol, for 1 ml of methanol as internal standard and from 0.0 to 1.4 ml of acetonitrile diluted to 50 ml with dioxane. The determination of both the elution time of a non-retained component, t_0, and the amount of THF in the stationary phase was carried out as described in the previous paper[1].

RESULTS AND DISCUSSION

From Fig. 1 and Tables I–III, it can be seen that t_0 changes on increasing the percentage of organic modifier in the mobile phase. Fig. 1 also shows that t_0 is also dependent on which organic solvent is used in the mobile phase. This change in t_0 or V_m on using different organic solvents in the mobile phase must require a compensating change in the volume of the stationary phase. Using the model of the stationary phase as proposed in the previous paper[1], the stationary phase was considered to be a

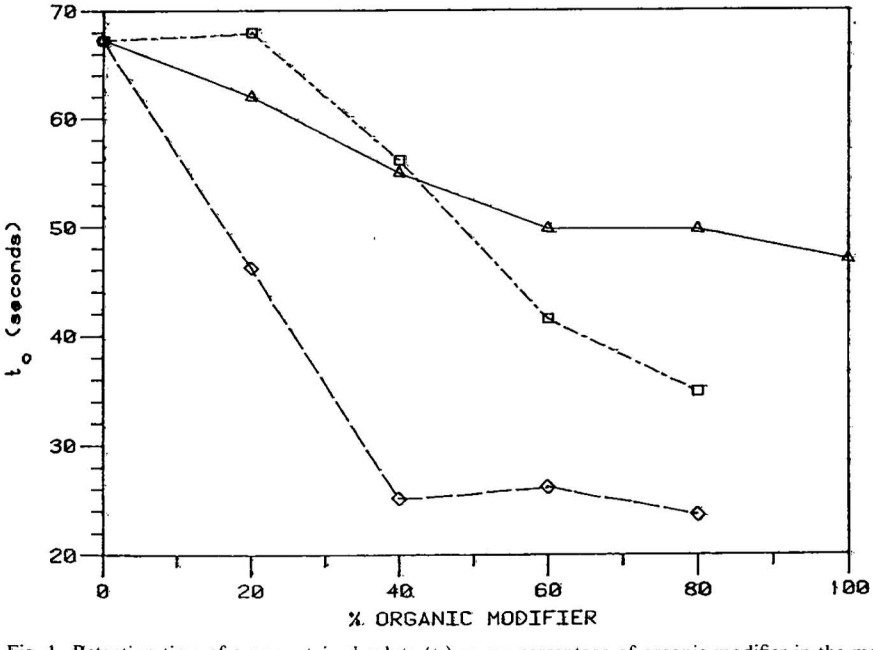

Fig. 1. Retention time of a non-retained solute (t_0) *versus* percentage of organic modifier in the mobile phase for methanol (△), acetonitrile (□) and THF (◇).

TABLE I

EFFECT OF METHANOL–WATER MOBILE PHASE COMPOSITION ON FORMATION OF RP-18 STATIONARY PHASE

RP-18: surface area 150 m^2/g; pore size 150 Å; length of chain C_{18}; carbon content 19.8 %; functional group bonded dimethyloctyldecylchlorosilane; calculated degree of derivatization 42 %; surface coverage 5.5 μmol C/m^2; weight in column 0.8948 g.

Parameter	*Methanol–water composition*					
	0:100	*20:80*	*40:60*	*60:40*	*80:20*	*100:0*
t_0 (sec)	67.18	61.95	54.85	49.72	49.68	46.91
V_m (ml)	1.12	1.03	0.91	0.83	0.83	0.78
Volume of methanol present in stationary phase (ml/g) ($\pm$0.03)	0.00	0.04	0.16	0.25	0.30	0.37
Volume of water present in stationary phase (ml/g) ($\pm$0.03)	0.27	0.04	0.08	0.09	0.03	0.00
Total volume of stationary phase (ml/g) ($\pm$0.04)	0.27	0.09	0.24	0.34	0.33	0.37
α	4.06	3.48	2.59	1.90	1.54	1.46
Methanol in stationary phase (%, v/v)	0	50	65	72	91	100
Phase ratio (θ)	0.22	0.08	0.24	0.37	0.35	0.43

TABLE II

EFFECT OF ACETONITRILE–WATER MOBILE PHASE COMPOSITION ON FORMATION OF RP-18 STATIONARY PHASE

Parameter	*Acetonitrile–water composition*					
	0:100	*20:80*	*40:60*	*60:40*	*80:20*	*100:0*
t_0 (sec)	67.18	67.88	56.12	41.47	34.89	–
V_m (ml)	1.12	1.13	0.94	0.69	0.58	–
Volume of acetonitrile present in stationary phase (ml/g) ($\pm$0.03)	0.00	0.10	0.19	0.39	0.50	–
Volume of water present in stationary phase (ml/g) ($\pm$0.03)	0.27	0.00	0.04	0.14	0.13	0.04
Total volume of stationary phase (ml/g) ($\pm$0.04)	0.27	0.10	0.23	0.53	0.63	–
α	4.06	2.99	1.97	1.55	1.43	–
Acetonitrile in stationary phase (%, v/v)	0	–	84	73	80	–
Phase ratio (θ)	0.22	–	0.21	0.69	0.96	–

TABLE III

EFFECT OF THF–WATER MOBILE PHASE COMPOSITION ON FORMATION OF RP-18 STATIONARY PHASE

Parameter	*THF–water composition*					
	0:100	*20:80*	*40:60*	*60:40*	*80:20*	*100:0*
t_0 (sec)	67.18	46.17	25.14	26.16	23.68	–
V_m (ml)	1.12	0.76	0.41	0.43	0.38	–
Volume of THF present in stationary phase (ml/g) ($\pm$0.03)	0.00	0.21	0.49	0.61	0.71	–
Volume of water present in stationary phase (ml/g) ($\pm$0.03)	0.27	0.16	0.29	0.19	0.06	0.00
Total volume of stationary phase (ml/g) ($\pm$0.04)	0.27	0.37	0.78	0.80	0.77	–
α	4.06	2.80	1.49	1.14	1.09	–
THF in stationary phase (%, v/v)	0	57	63	76	92	–
Phase ratio (θ)	0.27	0.44	1.70	1.70	1.80	–

ternary system containing the bonded organic moiety and solvent molecules adsorbed by both the bonded moiety and residual silanols on the silica substrate. The solvation of the bonded moiety (in this case, for RP-18, the bonded phase is octyldecyldimethylchlorosilane) depends on the intermolecular interactions between the solvent molecules and the bonded chain.

Intermolecular interactions between the solvent and the chain can be either specific or non-specific. For RP-18 non-specific interactions are the main driving force behind solvation of the C_{18} chain. Therefore, the stronger the non-specific dispersion interactions a solvent molecule can undergo the more effectively that solvent molecule can interact with the C_{18} chain. V_s is seen to increase throughout the entire mobile phase compositional range owing to the ability of the C_{18} to be solvated by the non-aqueous modifier. As V_s increases, V_m must decrease to keep the total volume for the column constant. These data for RP-18 are supported by work of Karger and McCormick[2] for RP-8.

If the enrichment of RP-18 by solvent molecules from the mobile phase is truly dependent on dispersion interactions, then for the three solvents commonly used in RPC, *i.e.*, methanol, acetonitrile and THF, the amount of modifier absorbed should follow the order of increasing dispersion interactions, which is methanol < acetonitrile < THF[9]. From Fig. 2, the volume of organic modifier absorbed by the C_{18} increases in the order methanol < acetonitrile < THF. This view is a simplification of the overall solvation process for RP-18. Non-specific interactions play a major role in stationary phase formation, but one also needs to consider the specific interactions between the solvent molecules of the mobile phase and the residual silanols on the silica surface. Comparing the specific intermolecular interactions of solvent molecules with residual silanols, the most prominent will be the solvent's acid–base properties, *i.e.*, its ability to be either a hydrogen-bond donor or acceptor

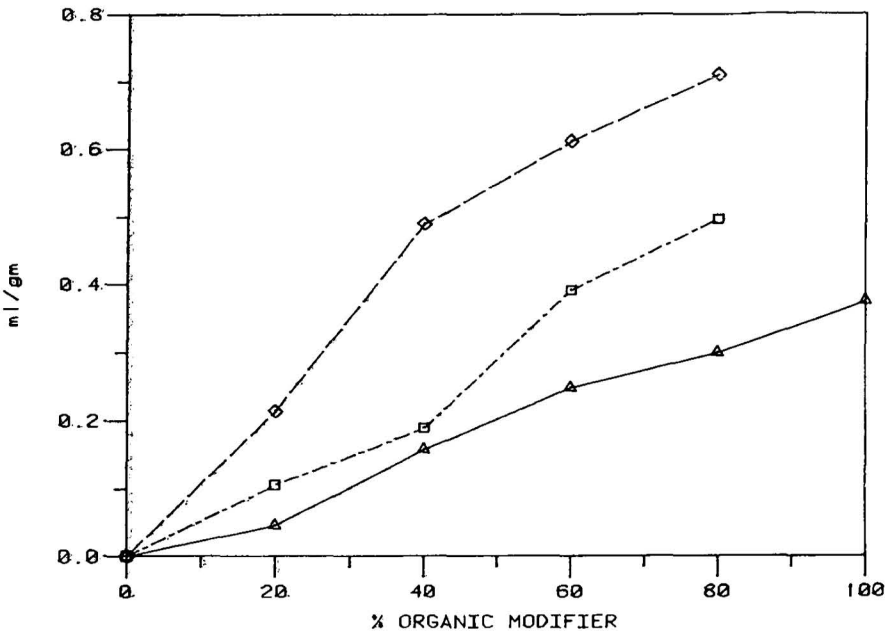

Fig. 2. Concentration of organic modifier in the stationary phase (ml/g) *versus* percentage of organic modifier in the mobile phase for methanol (△), acetonitrile (□) and THF (◇).

when interacting with the silanol. The hydrogen-bond donor strengths of the three solvents based on regular solution theory (Hildebrand solubility parameters) are ranked methanol ≫ THF = acetonitrile, while the hydrogen-bond acceptor strengths of the solvents follow the order methanol > THF > acetonitrile[9]. If one was to base the solvation of a non-bonded silica surface on the acid–base properties of these three solvents the solvation order would be methanol ≫ THF ≈ acetonitrile. Non-bonded silanols are present on the surface and they can enter into the retention process, as demonstrated by Horvath and Nahum[8]. Therefore, the solvation of the silanols must be considered with the solvation of the C_{18} chain in stationary phase formation. These specific interactions play a minor role in stationary phase formation for RP-18; as seen from Fig. 2, the absorption of organic modifier is under the control of the bonded carbon chain. However, under very low surface coverage conditions the specific intermolecular interactions between the solvent molecules and the silanols could dominate stationary phase formation.

Fig. 3 depicts the amount of water found in the stationary phase for the three solvents used. The amount of water in the stationary phase is seen to be dependent on the solvent used and the percentage of that particular solvent in the mobile phase; this has also been demonstrated for batch extraction methods[10]. For ease of discussion, Fig. 3 can be divided into three regions: (I) from 20 to 50%, (II) from 50 to 70% and (III) from 70 to 100% organic modifier concentrations. In region I the amount of water in the stationary phase is dependent on the hydrogen-bonding characteristics of the solvent and on the solubility parameter of the solvent for C_{18}. Therefore, THF, having the greatest ability to solvate the C_{18} chain and reasonable hydrogen-bond

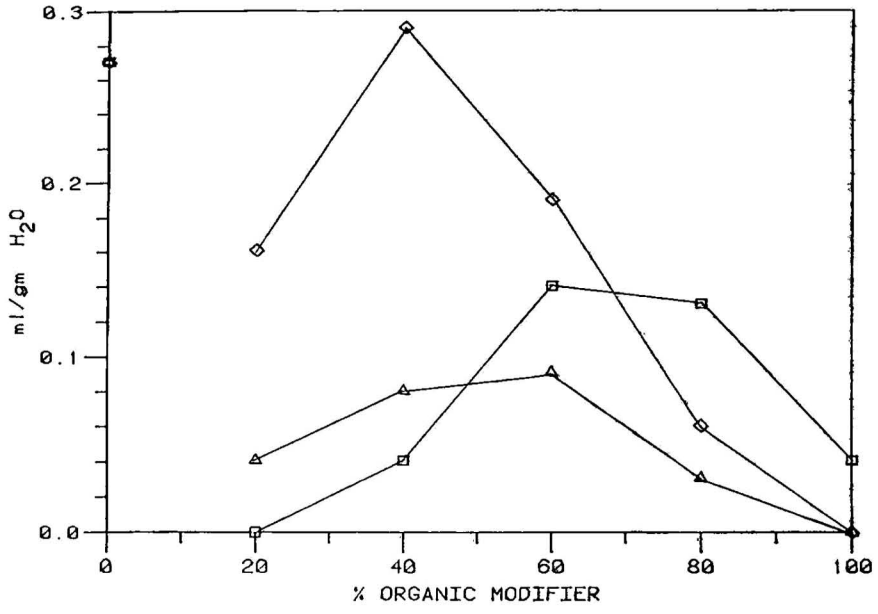

Fig. 3. Concentration of water in the stationary phase (ml/g) *versus* percentage of organic modifier concentration in the mobile phase for methanol (△), acetonitrile (□) and THF (◇).

acceptor properties, brings the most water with it upon formation of the stationary phase. Methanol, on the other hand, has the weakest dispersive interaction for C_{18}, but it is easily the strongest hydrogen bonder of the three solvents. Thus, even though a smaller amount of methanol will solvate the C_{18} compared with THF and acetonitrile, methanol will bring over with it a larger percentage of water than THF or acetonitrile (see Table I). Whereas acetonitrile has a dispersive interaction for C_{18} slightly larger than that of methanol, but it is the weakest of the three solvents in hydrogen-bond strength. Thus acetonitrile will bring the smallest amount of water into the stationary phase compared with methanol and THF. For 20% acetonitrile, we report essentially 0.00 ml/g of water in the stationary phase. We feel that there was water present in the stationary phase, but only a very small amount. In region II in Fig. 3, for methanol and THF the amount of water in the stationary phase is seen to decrease, whereas for acetonitrile there is an increase in the amount of water present. A possible explanation is as the amount of methanol and THF increases in the stationary phase a mass-action effect takes over. These solvents can effectively compete with and displace water from the residual silanols present. THF can displace water because of the overwhelming amount of it in the stationary phase and its hydrogen-bonding ability, whereas for methanol, the smaller amount present in the stationary phase can more easily displace water because of its stronger acid–base properties. Acetonitrile, owing to its weaker hydrogen-bonding strength and dispersive interactions, cannot overwhelm the water by its presence in the stationary phase or displace it from the residual silanols. Therefore, water will increase in concentration in the stationary phase with acetonitrile as organic modifier. Finally, in region III, the mechanism for the removal of water from the stationary phase is the organic

solvents mass-action effect, which overwhelms any water left associated with the residual silanols and the solvent's hydrogen-bonding ability. Therefore, acetonitrile, having the weakest hydrogen-bonding ability and a similar solvating ability for C_{18} as methanol, cannot displace all of the water from the residual silanols.

Overall, the amount of water found in the stationary phase was observed to be dependent on the organic modifiers solvent strength for C_{18}, and on the solvent's hydrogen-bonding capabilities. Methanol and THF display very similar curves in Fig. 3, with acetonitrile showing anomalous behavior in comparison with these two solvents. The anomalous behavior of acetonitrile will manifest itself through selectivity and the overall separation processes.

One final point to be discussed, which is relevant for RP-18, is stationary phase formation with 100% water as the mobile phase. From Tables I–III and Fig. 4, a large stationary phase volume is found at this mobile phase composition. A possible explanation for this observation is two-fold: (1) the residual silanols present on the silica surface are involved in hydrogen-bonding with the water present in the mobile phase and (2) water can be trapped on the substrate surface by a "tent" of C_{18} chains. This trapping of water is caused by the "freezing" of the bonded chains. The "freezing" of the bonded chains results from the intra- and/or intermolecular interactions amongst the chains themselves. Such interactions would be expected to be energetically favorable when compared only with interactions between the water matrix and the hydrocarbon. With 100% water as the mobile phase an adsorption mechanism is probably responsible for chromatographic retention in contrast to a partition mechanism in a solvation layer.

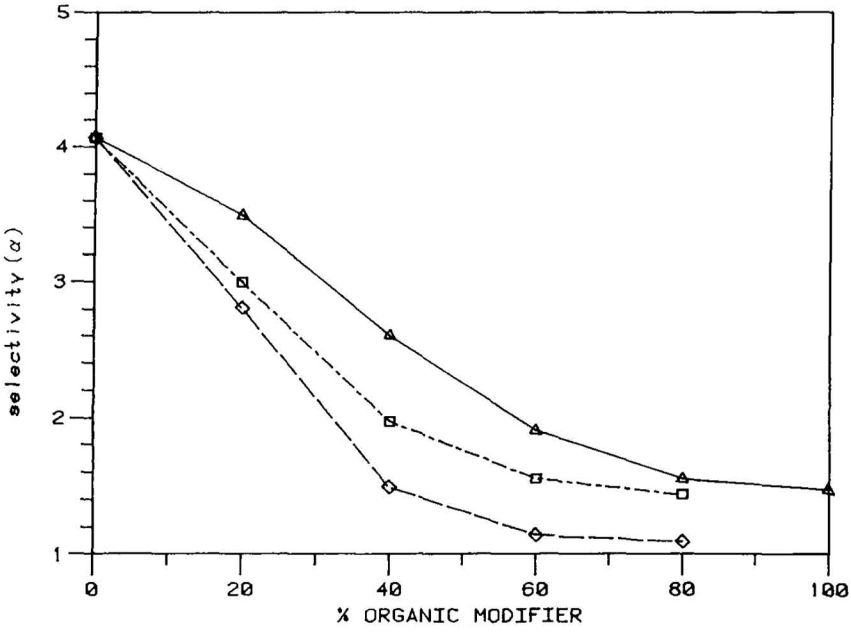

Fig. 4. Selectivity (α) *versus* percentage of organic modifier in the mobile phase for methanol (△), acetonitrile (□) and THF (◇).

The selectivity (α) of the stationary phase for the homologous series of alcohols used as probes is indicative of the effect that solvation and therefore the composition of the stationary phase has on the separation process. Selectivity in these experiments is based on the change of one methylene group (ΔCH_2) in the *n*-alcohol chain. The effect on α of enrichment of the stationary phase by the organic modifier is depicted in Fig. 4. Two features of these curves are clearly evident: (1) α gradually reaches a plateau value and (2) this plateau value and the rate at which the plateau is reached are solvent dependent. A possible explanation for the above mentioned features is that the stationary phase becomes enriched by the solvent (see the values in Tables I–III, for the volume of organic modifier in the stationary phase) and appears less "polar" to the solute, *i.e.*, the absorbed solvent molecules in the stationary phase are a stronger solvent for the solute than the mobile phase. Therefore, the value for ΔCH_2 will be greatest for the largest difference in solvent strength between the stationary phase and the mobile phase.

When eluent molecules with different solubility parameters solvate the bonded phase, they create stationary phases with different solvent strengths. The stationary phases formed by methanol, acetonitrile and THF will have different selectivities based on their abilities to discriminate between a ΔCH_2 group. Methanol, with a dispersive interaction solubility parameter of 6.2 (ref. 9), will undergo the least effective interaction with a methylene group, whereas THF, whose solubility parameter is 7.6 (ref. 9), will undergo the most effective interaction with a methylene group. The ability of acetonitrile to interact with a methylene group is between those of methanol and THF. Therefore, methanol will see the greatest difference between two solutes differing by a ΔCH_2. This difference can be expressed by the change in free energy of selecting between the two solutes, and is expressed by the equation

$$\Delta\Delta G_{N+1-N} = -RT \ln \alpha \tag{7}$$

where the assumption is made that the change in the free energy of transfer of the solutes from the mobile phase to the stationary phase is due only to the addition of one methylene group from the *N*-carbon homologue to the $N + 1$-carbon homologue. Table IV lists these changes in free energy and it can be seen that the largest free energy change for a ΔCH_2 group is for methanol and the smallest is for THF. Therefore, the order of selectivity shown in a column of data points is determined by the solvent's solubility parameter for the particular interaction being investigated. Selectivity and solvent strength are reciprocally related, but the rate at which the α

TABLE IV

$\Delta\Delta G_{N+1-N}$ VALUES FOR ALCOHOL HOMOLOGUES AT 25°C EXPRESSED IN cal/mole FROM EQN. 7

Solvent	*Concentration of solvent (%)*					
	0	*20*	*40*	*60*	*80*	*100*
Methanol	−830	−738	−564	−380	−256	−224
Acetonitrile	−830	−649	−402	−260	−212	–
THF	−830	−610	236	− 78	− 51	–

plateau is approached is proportional to solvent strength, owing to the ability of the stronger solvent to solvate the C_{18} chain more efficiently.

For methanol–water and THF–water the largest difference in solvent strength occurs at 0% modifier concentration, the difference becoming smaller as one continues to 100% modifier concentration. Therefore, α is largest in the beginning and decreases with increasing percentage of organic modifier. The α values reach a plateau when the enrichment of the stationary phase by a solvent no longer contributes to a change in the differences of the solvent strengths between the stationary and mobile phases.

The selectivity of acetonitrile is not as easily analysed as those of methanol and THF because of its anomalous behavior during stationary phase formation, as discussed earlier concerning the amount of water found in the stationary phase. However, a qualitative statement can be made for the selectivity in acetonitrile–water systems. The selectivity of acetonitrile–water seems to follow the solvent strength for C_{18} because these selectivity values fall between those for methanol and THF (see Fig. 4).

In summary, selectivity for a ΔCH_2 group through a compositional range of one solvent is controlled by the solvent strength of the stationary phase as compared with the solvent strength of the mobile phase. In comparison, at any one specific mobile phase composition the selectivity is reciprocally related to the dispersion interaction solubility parameter for that specific solvent with respect to the bonded moiety.

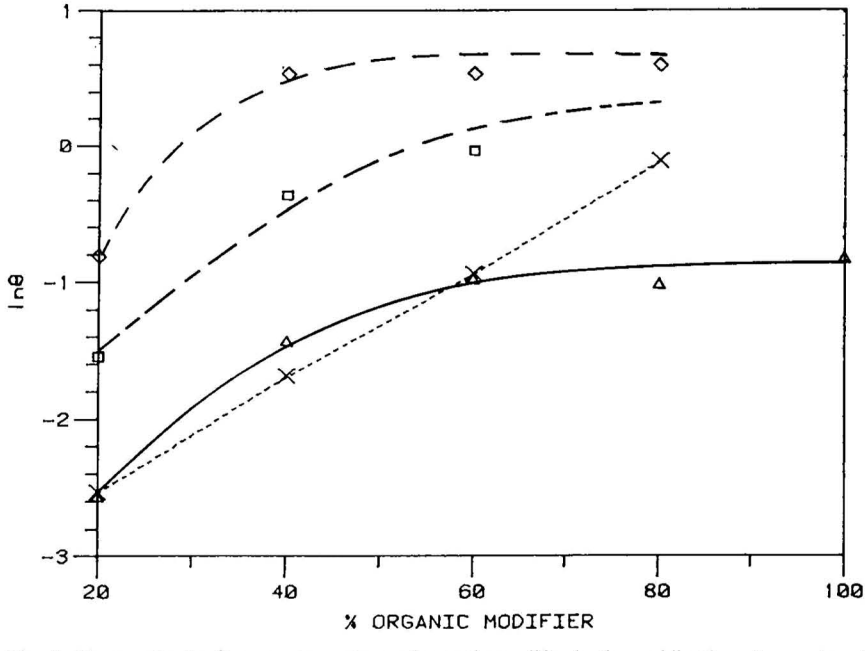

Fig. 5. Phase ratio (ln θ) *versus* percentage of organic modifier in the mobile phase for methanol (△), acetonitrile (□) and THF (◇). Data from ref. 1 for methanol and RP-8 (×) are also included for ease of comparison.

The above arguments on the dependence of the selectivity on the composition of the stationary phase again raise the question of the role of the volume of the stationary phase and therefore the phase ratio. A plot of the data in Tables I–III in the format of eqn. 6 can be seen in Fig. 5. Previous data for RP-8 (ref. 1) have also been included for comparison. The linear relationship predicted in eqn. 6 does not occur for RP-18 using the three solvents investigated, as there are two mechanisms controlling the formation of the stationary phase: (A) the solvation of the bonded organic moiety, which is dependent on non-specific interactions between the solvent and the bonded phase, and (B) the solvation of the substrate surface, which is dependent on specific interactions between the solvent and the surface. We have previously reported[1] that the solvation mechanism of RP-8 for methanol–water systems is dependent on process B. Therefore, one can conclude that the linear regions in the curves for RP-18 in Fig. 5 are dominated by stationary phase formation under control of the substrate surface. The transition between the linear region and the plateau region of the curves is where both mechanisms A and B are competing on equal terms in determining the composition of the stationary phase. The plateau region is controlled by the bonded moiety enriching itself in solvent molecules process A. Therefore, by plotting ln θ *versus* percentage of organic modifier one can tell more about the processes involved in stationary phase formation and the extent to which these two processes dominate.

In analysing Fig. 5, the stationary phase formation of THF–water systems is dominated by the enrichment of the bonded moiety in THF above *ca.* 40% THF in the mobile phase. Methanol, on the other hand, having a weaker dispersive interaction, does not reach its plateau until *ca.* 60%. In contrast, for acetonitrile over the entire compositional range there is no clear dominance of one stationary phase mechanism over the other.

Comparing eqn. 4 with eqn. 6, from the intercept of these two plots one can calculate K_D for a particular solute. This statement must be qualified because first of all a plot of ln θ *versus* percentage of organic modifier must be linear, and as both intercepts are determined from logarithmic plots the errors in these values will be magnified on solving for K_D. However, K_D values within an order of magnitude of their true values can be obtained by this method.

In conclusion, the stationary phase formation of RP-18 was found to be a combination of two mechanisms, non-specific interactions between the solvent-bonded moiety and specific interactions of the solvent with the substrate surface. The point at which the former mechanism begins to dominate stationary phase formation is related to the dispersive interaction solubility parameter: the stronger the solvent strength for C_{18} the earlier ln θ begins to plateau. Selectivity was also found to be dependent on solvent strength, which ultimately relates to the solubility parameter of a particular solvent for the bonded moiety. It is interesting that for both methanol and THF the α plateau and the ln θ plateau begin roughly at the same percentage of organic modifier. Acetonitrile was found to behave differently from methanol and THF both in the amount of water found in the stationary phase and in the mechanism of stationary phase formation. The conclusions in this paper further support our proposed model of a ternary stationary phase, and the hypotheses of stationary phase formation in RP-8 and RP-18 reported earlier. It should be noted that this approach to the question of selectivity in bonded phase chromatography emphasizes the active role of the stationary phase which results from the solvation of the bonded moiety

and the substrate by the components of the mobile phase.

Further investigations of stationary phase formation and its relationship to the solubility parameter of a solvent are being undertaken in order to gain a greater insight into the overall separation processes. Special emphasis is being placed on the role of ternary solvent mixtures and the role of temperature in stationary phase formation.

ACKNOWLEDGEMENTS

T. A. Z. acknowledges the partial support of the work provided by his receipt of a University of Arizona Graduate College Fellowship. M. F. B. acknowledges the partial support of the work by an unrestricted grant from Chevron Research.

REFERENCES

1 C. R. Yonker, T. A. Zwier and M. F. Burke, *J. Chromatogr.*, 241 (1982) 257.
2 B. L. Karger and R. M. McCormick, *Anal. Chem.*, 52 (1980) 2249.
3 E. H. Slaats, W. Markovski, J. Fekete and H. Poppe, *J. Chromatogr.*, 207 (1981) 299.
4 G. E. Berendsen, P. J. Schoenmakers, L. De Galan, G. Bigh, Z. Varga-Puchony and J. Inczedy, *J. Liquid Chromatogr.*, 11 (1980) 1669.
5 A. Tilly-Melin, Y. Askemark, K. G. Wahlund and G. Schill, *Anal. Chem.*, 51 (1979) 976.
6 D. Westerlund and A. Theodorsen, *J. Chromatogr.*, 144 (1977) 27.
7 A. J. P. Martin and R. L. M. Synge, *Biochem. J.*, 35 (1941) 1358.
8 A. Nahum and Cs. Horváth, *J. Chromatogr.*, 203 (1981) 53.
9 B. L. Karger, L. R. Snyder and Cs. Horváth, *An Introduction to Separation Science*, Wiley, New York, 1973, p. 273.
10 K. J. Stetzenbach, *Ph.D. Dissertation*, University of Arizona, Tucson, AZ, 1980.

Journal of Chromatography, 241 (1982) 281–286
Elsevier Scientific Publishing Company, Amsterdam — Printed in The Netherlands

CHROM. 14,733

EVALUATION OF THE SELECTIVITY OF SOME ORGANO-SUBSTITUTED LAYER SILICATES*

S. V. BONDARENKO*, A. I. ZHUKOVA and Yu. I. TARASEVICH
Institute of Colloid Chemistry and Chemistry of Water of the Ukrainian Academy of Sciences, 42 Prospekt Vernadskoho, Kiev 165 (U.S.S.R.)
(First received September 3rd, 1981; revised manuscript received January 11th, 1982)

SUMMARY

The thermodynamic characteristics of the adsorption of individual C_8 alkylbenzenes on organo-substituted layer silicates and chromatograms of separation of artificial three- and four-component mixtures on these sorbents have been obtained by gas adsorption chromatography. The separation properties of chromatographic columns containing modified minerals have been determined, and it was established that with highly dispersed silicates (montmorillonite and fluorhectorite) the selectivity of the sorbent contributes considerably to the separation. It is shown that, depending on the type of modifying cations, the selectivity of organo-substituted layer silicates is determined by either the enthalpic or the entropic component of the Gibbs free energy change on adsorption.

INTRODUCTION

The separation of organic compounds with narrow boiling ranges is one of the most difficult problems in analytical gas chromatography. Multi-component sorbents based on organo-substituted clay minerals have been used successfully for this purpose[1–5]. The complicated composition of the sorbent makes it difficult to establish the role of each of the components in chromatographic separation and therefore there are no clear requirements for the characteristics of the organic complexes used. In order to work them out, a systematic investigation of the selectivity of organo-substituted clay minerals with respect to hydrocarbons of narrow boiling range is necessary.

It is known[6] that the separation properties of a chromatographic packed column with respect to substances that have similar boiling points is determined by the efficiency of the column itself and the selectivity of the sorbent. The latter, in accordance with Herington's equation[7], is directly connected with the retention volumes of adsorbates, which are proportional to the Gibbs free energy change in the

* Presented at the *3rd Danube Symposium on Chromatography, Siofok, August 31–September 3, 1981*. The majority of the papers presented at this symposium have been published in *J. Chromatogr.*, Vol. 241, No. 1 (1982).

0021-9673/82/0000–0000/$02.75

system[8]. Therefore, if the separation efficiency of the column is determined mainly by the selectivity of the sorbent, it may be possible to calculate the potential separation efficiency of a packed column from the retention volumes of individual components of the mixture to be separated. Also, by measuring the different constituents of the Gibbs free energy, the role of the structure of the modifying layer in determining the selectivity of the sorbent may be established.

EXPERIMENTAL

Pyzhevsky montmorillonite, kovdorsky vermiculite and synthetic fluorhectorite, the basic characteristics of which are listed in Table I, were used. A standard sample of Bentone-245 was used for comparison. The minerals were modified with alkylammonium and alkylpyridinium chlorides and bromides. The methods for obtaining organo-substituted samples were analogous to those reported earlier[9].

The amounts of sorbed organic substances were determined by the combustion method[10]. The specific surface areas of the sorbents with respect to water and *n*-hexane were determined from adsorption isotherms obtained by the microbalance method. The gas chromatographic conditions were described earlier[11].

RESULTS AND DISCUSSION

The determination of the separation properties of columns containing the investigated sorbents showed that with highly dispersed minerals (montmorillonite, fluorhectorite) the selectivity of the sorbents contributes considerably to the separation. This was indicated by the relationship between the relative retention volumes of the components to be separated using the modified samples of the minerals and the separation ability of the columns. Table II shows that the degree of separation of a mixture of *p*-xylene and ethylbenzene by cetylpyridinium-montmorillonite is higher

TABLE I

PHYSICO-CHEMICAL CHARACTERISTICS OF LAYER SILICATES

Property	*Mineral*		
	Montmorillonite	*Fluorhectorite*	*Vermiculite*
Cation-exchange capacity (mg-equiv./g)	0.90–1.0	0.75–0.82	1.40–1.50
Basic cation in exchange complex	Ca^{2+}	Na^{+}	Mg^{2+}
Elementary charge (charge units)	0.39	0.65	0.85
Exchange position area (Å^2)	60.0	37.7	27.5
Effective surface area determined from adsorption of water (m^2/g)	420–480	280	470–500
External surface area determined from adsorption of hexane (m^2/g)	30–40	20	8–10
Particle size (μm)	0.03–0.3	–	3–5

TABLE II

EFFICIENCY (NUMBER OF THEORETICAL PLATES, N), SELECTIVITY (V_{rel}) AND SEPARATION ABILITY (K_1, K_b) OF CHROMATOGRAPHIC COLUMNS CONTAINING MODIFIED MINERALS

Sorbent	*Temperature (°C)*	N	*p-Xylene Ethylbenzene*		*m-Xylene p-Xylene*		
			V_{rel}	K_b	V_{rel}	K_b	K_1
Bentone-245	93	2000	1.04	0.25	1.20	0.98	1.70
Cetyltrimethylammonium-montmorillonite	110	1880	0.97	0	1.26	–	3.50
Cetylpyridinium-montmorillonite	93	1070	0.92	0.84	1.17	0.98	1.79
Cetylpyridinium-fluorhectorite	94	1360	0.90	0.93	1.05	0.95	1.60
Cetylpyridinium-vermiculite	99	670	0.97	0.06	1.12	0.60	–

than by Bentone-245 (K_b = 0.84 and 0.25, respectively), which correlates with the relative retention volumes of the mixture on these sorbents (0.92 and 1.04), but not with the number of theoretical plates, N (1070 and 2000). An analogous situation is observed on comparing the separation criteria and the efficiency of columns containing cetylpyridinium-fluorhectorite and Bentone-245 with respect to the same pair of hydrocarbons. With a column containing cetyltrimethylammonium-montmorillonite, which gives a slightly different value of N to the column containing Bentone-245, the mixture of *p*-xylene and ethylbenzene is hardly separated; this is due to the insufficient difference in the retention volumes of the sorbates. At the same time, the separation criterion, K_1, for the *m*-xylene–*p*-xylene mixture on cetyltrimethylammonium-montmorillonite exceeds the K_1 values obtained with other sorbents. This agrees with the highest values of V_{rel} (Table III) of the sorbates when they are adsorbed by cetyltrimethylammonium-montmorillonite.

As the separation ability of highly dispersed adsorbents is determined by their selectivity, the preliminary investigation of the adsorption thermodynamics of individual substances allows a more certain determination of the potential separation properties of the sorbents. The chromatograms in Figs. 1 and 2 confirm that when analysing hydrocarbon mixtures over a narrow temperature range the same yields of the components and, to some extent, the same degree of separation remain, which may be expected from the differences in the retention volumes of individual sorbates. The retention volumes and heats of adsorption of *o*-, *m*- and *p*-xylene on cetyltrimethylammonium-montmorillonite ($\bar{Q}_a$ = 47, 52 and 46 kJ/mol, respectively) confirm the high separation ability of this sorbent with respect to the mixture examined. In fact, Fig. 1 shows that for this sorbent all three isomers are separated from each other and the peaks of *m*- and *p*-xylene are further apart than when other organocomplexes are used as sorbents (Fig. 2).

From the thermodynamic point of view, the selectivity of organo-substituted layer silicates is due in some instances to differences in the enthalpies and in other instances to differences in the entropies of adsorption of individual hydrocarbons.

TABLE III

RELATIVE RETENTION VOLUMES (V_{rel}) AND ENTHALPIES OF ADSORPTION ($\Delta\bar{Q}_a$, kJ/mol) of AROMATIC HYDROCARBONS ON ORGANO-SUBSTITUTED LAYER SILICATES AT 150°C

Sample mixture	*Bentone-245*		*Montmorillonite*						*Vermiculite*				*Cetylpyridinium-fluorhectorite (a = 1.39)**	
			*Cetylpyridinium- (a = 1.41)**		*Cetylammonium- (a = 1.36)**		*Cetyltrimethyl-ammonium- (a = 1.54)**		*Cetylpyridinium- (a = 1.34)**		*Cetylammonium- (a = 1.24)**			
	V_{rel}	$\Delta\bar{Q}_a$	V_{rel}	$\Delta\bar{Q}_a$	V_{rel}	$\Delta\bar{Q}_a$	V_{rel}	$\Delta\bar{Q}_a$	V_{rel}	$\Delta\bar{Q}_a$	V_{rel}	$\Delta\bar{Q}_a$	V_{rel}	$\Delta\bar{Q}_a$
m-Xylene *p*-xylene	1.20	0	1.17	1	1.11	3	1.26	6	1.12	0	1.17	2	1.05	0
p-Xylene-ethylbenzene	1.04	0	0.92	−1	1.00	−3	0.97	−2	0.97	−1	0.98	0	0.90	0

* a = Modifier sorbed in mg-equiv./g.

TABLE IV

SPECIFIC RETENTION VOLUMES (V_s, cm^3/m^2), ISOSTERIC ENTHALPIES ($\bar{Q}_a$, kJ/mol) AND DIFFERENTIAL ENTROPIES ($-\Delta\bar{S}_a$, J/mol·°K) OF ADSORPTION OF AROMATIC HYDROCARBON ON ORGANO-SUBSTITUTED LAYER SILICATES AT 150°C

Adsorbate	*Bentone-245*			*Montmorillonite*						*Vermiculite*						*Cetylpyridinium-fluorhectorite (1.39 mg-equiv./g)*		
	V_s	$\bar{Q}_a$	$-\Delta\bar{S}_a$	*Cetylpyridinium- (1.41 mg-equiv./g)*			*Cetylammonium- (1.36 mg-equiv./g)*			*Cetylpyridinium- (1.34 mg-equiv./g)*			*Cetylammonium- (1.25 mg-equiv./g)*					
				V_s	$\bar{Q}_a$	$-\Delta\bar{S}_a$	V_s	$\bar{Q}_a$	$-\Delta\bar{S}_a$	V_s	$\bar{Q}_a$	$-\Delta\bar{S}_a$	V_s	$\bar{Q}_a$	$-\Delta\bar{S}_a$	V_s	$\bar{Q}_a$	$-\Delta\bar{S}_a$
Benzene	0.29	44	72	0.73	40	53	–	–	–	3.38	46	55	1.82	34	32	1.30	42	53
Toluene	0.47	46	72	0.94	43	58	–	–	–	4:66	49	59	2.79	38	38	–	–	–
Ethylbenzene	0.70	51	79	1.44	45	59	0.82	38	47	6.58	54	68	4.69	43	47	2.50	44	54
p-Xylene	0.75	51	80	1.32	44	58	0.82	41	54	6.37	53	66	4.73	42	43	2.35	45	56
m-Xylene	0.90	51	78	1.55	45	60	0.91	44	60	7.11	53	65	5.57	44	46	2.63	45	55
o-Xylene	0.97	51	76	1.60	45	59	0.87	42	56	7.58	53	65	5.32	44	46	2.75	45	54

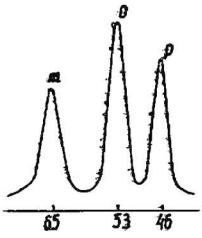

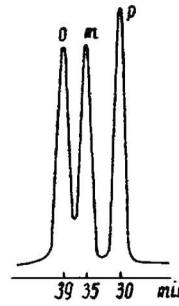

Fig. 1. Separation of artificial three-component mixture on cetyltrimethylammonium-montmorillonite. p = *p*-Xylene; m = *m*-xylene; o = *o*-xylene.

Fig. 2. Separation of artificial three-component mixture on Bentone-245. Symbols as in Fig. 1.

Therefore, the highest values of V_{rel} for the *m*-xylene–*p*-xylene system using cetyltrimethylammonium-montmorillonite correlate with the highest values of $\Delta\bar{Q}_a$ (Table III). The relative enthalpies of adsorption and retention volumes of *m*- and *p*-xylene on cetylammonium-montmorillonite and -vermiculite are lower. For these adsorbents, the series of increasing retention volumes of dialkylbenzene isomers correlates with the series of increasing enthalpies of adsorption. Therefore, the enthalpic factor plays the main role in the change in free energy when adsorption on organo-derivatives of these adsorbents takes place, and the separation effect is due mainly to the difference in the enthalpies of adsorption of the isomers. These differences are connected with the fact that the centres of Van der Waals forces of the molecular chains of the adsorbed structural isomers are not at the same distances from the solid surfaces[8,12]. Also, the different arrangements of the substituents in the benzene ring change the electronic density distribution in the skeleton of the ring, resulting in different energies of interaction between the sorbate molecules and the active centres of the adsorbents. However, the differences in the interactions between alkylbenzene molecules and the surfaces of the adsorbents depend rather on the accessibility of the active centres of the organo-complexes for the molecules adsorbed than on the dipole moment. This is confirmed by the discrepancy between the series of increasing enthalpies of adsorption of xylene isomers on the organo-substituted minerals (for cetyltrimethylammonium- and cetylammonium-montmorillonite *m*- > *o*- > *p*-) and the series of increasing dipole moments of the sorbate molecules (*o*- > *m*- > *p*-).

With cetylpyridinium-substituted layer silicates and Bentone-245, there is virtually no difference in the enthalpies of adsorption of xylene isomers (Table III). Therefore, the selectivity of these sorbents is determined by the same difference that is observed in the entropies of adsorption of the hydrocarbons examined (Table IV). The predominating influence of the entropic factor in separations on the sorbents is apparently connected with the fact that modifying groups with a cyclic function (cetylpyridinium) form geometrically less homogeneous layers on the surface. This creates conditions for greater differences in the entropies of rotation of xylene isomers when adsorption takes place; the symmetrical molecules of *p*-xylene lose more rotational degrees of freedom than *m*-xylene on adsorption and, as a result, are eluted first from the column.

Taking as a basis earlier investigations[5,9] and considering the relatively small

increase in the retention volumes of benzene on organo-substituted sorbents in comparison with the unsubstituted sorbents[13], it can be concluded that the separation of aromatic hydrocarbons takes place mainly at the external surface of modified layer silicates. Moreover, under the gas chromatographic conditions used (temperature 100–150°C and degree of surface coverage not exceeding 0.05), the polarity of the active centres of the modifying layer and its micro-relief would apparently affect the adsorption process. This assumption was supported by the fact that an increase in the enthalpy of adsorption of xylenes from 36–39 to 44–45 kJ/mol was observed on a montmorillonite sample that had been washed with aqueous ethanol in order to remove excess of sorbed cetylpyridinium groups.

In conclusion, this work indicates that under the gas chromatographic conditions used, the potential separation efficiency of highly dispersed sorbents may be determined from the thermodynamic adsorption characteristics of individual substances. The same thermodynamic characteristics allow the determination of the effect of the components of the Gibbs free energy change on adsorption on the selectivity of organo-substituted layer silicates.

REFERENCES

1 M. A. Hughes, D. White and A. L. Roberts, *Nature (London)*, 184 (1959) 1796.
2 D. White, in W. F. Bradley (Editor), *Clays and Clay Minerals, Proceedings of the 12th National Conference on Clays and Clay Minerals, Atlanta, Georgia, September 30–October 2, 1963*, Pergamon Press, Oxford, New York, 1964, p. 257.
3 W. H. Slabaugh and R. W. Vasofsky, *Clays Clay Miner.*, 23 (1975) 458.
4 R. W. Vasofsky and W. H. Slabaugh, *J. Colloid Interface Sci.*, 55 (1976) 342.
5 V. G. Berezkin, V. S. Gavrichev, L. N. Kolomiyets, A. A. Korolev, V. N. Lipavskii, N. S. Nikitina and V. S. Tatarinskii, *Gazovaya Khromatografiya v Neftekhimii*, Nauka, Moscow, 1975, p. 200.
6 A. V. Kiselev and Y. I. Yashin, *Adsorbtsionnaya Gazovaya i Zhidkostnaya Khromatografiya*, Khimiya, Moscow, 1979, p. 21.
7 E. F. G. Herington, in D. H. Desty (Editor), *Vapour Phase Chromatography*, Butterworths, London, 1957, p. 5.
8 A. V. Kiselev and Y. I. Yashin, *Gazo-adsorbtsionnaya Khromatografiya*, Nauka, Moscow, 1967, p. 116.
9 A. I. Zhukova, S. V. Bondarenko and Y. I. Tarasevich, *Neftekhimiya*, 21 (1981) 765.
10 J. L. McAtee, Jr., *Amer. Mineral.*, 44 (1959) 1230.
11 S. V. Bondarenko, A. I. Zhukova and Y. I. Tarasevich, *Ukr. Khim. Zh.*, 46 (1980) 370.
12 A. N. Korol, *Nepodvizhnaya Faza v Gazo-zhidkostnoi Khromatografii*, Naukova Dumka, Kiev, 1969, p. 116.
13 M. Taramasso and F. Veniale, *Control Miner. Petrol.*, 21 (1969) 53.

Journal of Chromatography, 241 (1982) 287–294
Elsevier Scientific Publishing Company, Amsterdam — Printed in The Netherlands

CHROM. 14,719

STUDY OF ADSORPTION FROM SOLUTIONS BY COLUMN CHROMATOGRAPHY*

S. A. BUSEV, S. I. ZVEREV, O. G. LARIONOV and E. S. JAKUBOV*
Chromatography Laboratory, Institute of Physical Chemistry, Academy of Sciences of the U.S.S.R., Lenin Avenue, 117312 Moscow V-312 (U.S.S.R.)

(First received September 3rd, 1981; revised manuscript received January 11th, 1982)

SUMMARY

A column chromatographic method is proposed for obtaining data on equilibrium characteristics of adsorption; the method makes it possible to obtain in a single chromatographic experiment the excess adsorption isotherm of binary solution over the whole range of concentrations. The potentials and limitations of the method with respect to equilibrium data and thermodynamic characteristics of adsorption systems are discussed. A comparison with static experimental data is made.

INTRODUCTION

The development of industrial separation and purification processes requires data on equilibrium partition coefficients and adsorption kinetics. The information on partition coefficients is usually obtained by measuring static adsorption isotherms of mixtures to be separated. This method has a number of advantages but is very time consuming. In equilibrium chromatography, elution curves provide information about adsorption isotherms[1,2]. Therefore, some workers have used chromatography for the determination of adsorption isotherms of gases and vapours[3–10]. In connection with progress in high-performance liquid chromatography (HPLC) the method has been applied to adsorption from liquid mixtures[11–14]. This paper deals with the potential of the method.

THEORETICAL

The method is based on the well known equation of concentration point movement:

$$\left(-\frac{\partial x}{\partial V}\right) = \frac{1}{m\alpha + f'(x)} \tag{1}$$

* Presented at the *3rd Danube Symposium on Chromatography, Siofok, August 31–September 3, 1981*. The majority of the papers presented at this symposium has been published in *J. Chromatogr.*, Vol. 241, No. 1 (1982).

0021-9673/82/0000–0000/$02.75

where x is the distance covered by a concentration point φ when the eluent (volume V) passes through the column, m is the mass of an adsorbent in the column, f′ is the first derivative of the adsorption isotherm at the point with equilibrium concentration φ and α is the free volume of the column.

From eqn. 1 we can obtain an expression for the calculation of adsorption at the point with concentration φ:

$$f(\varphi) = \frac{1}{m} \int_0^{\varphi} (V\varphi - \alpha)\, d\varphi \tag{2}$$

Thus, knowing only the elution curve for the separation of component A from component B it is in principle possible to calculate the adsorption isotherm of the binary mixture A–B over the entire range of concentrations.

However, the use of eqn. 2 raises a number of problems:

(1) Two types of adsorption isotherm can be distinguished when studying adsorption of solutions by the static method: a surface excess isotherm and an absolute content adsorption isotherm. The surface excess, n_1^e, can be found directly from an adsorption experiment if the initial and the equilibrium concentrations of the solution, the mass of the adsorbent and the amount of the solution are known:

$$n_1^e = \frac{n^0 \Delta x_1}{m} \tag{3}$$

where n^0 is the amount of the substance in the solution, m is the mass of the adsorbent and Δx_1 is the change in concentration of the solution due to adsorption. The absolute content of the substance in the adsorption solution, n_i^s, is related to the surface excess as follows:

$$n_1^s = n_1^e + (n_1^s + n_2^s)\, x_1 \tag{4}$$

To take advantage of this expression, an additional relationship, $n_1^s = f(n_2^s)$, should be known. The questions arise of the derivative of which adsorption isotherm is to be used in eqn. 1 and the type of adsorption that is measured in the chromatographic experiment. These questions were first considered in refs. 15 and 16, where it was shown that $f(\varphi)$ in eqn. 2 is the surface excess isotherm and α is the free volume of the column, including the volume of the adsorbent pores. Thus, it is the surface excess that is determined in the chromatographic experiment, just as in static measurements.

(2) Eqn. 1 has been derived for the equilibrium adsorption on the assumption that the broadening effects due to diffusion and mass transfer are absent. To what extent is this assumption justified? It is known from experience in and the theory of liquid chromatography that to meet these conditions it is necessary to use micron-sized particles, suitable methods for column packing, optimal flow-rates and special experimental units that reduce the extra-column broadening to a minimum. It should be noted that it is not always possible to meet the first two conditions.

(3) With steep adsorption isotherms (strong specific interactions), the amount adsorbed is already large at low concentrations and, as can be seen from eqn. 1, the

elution time may be very long for small concentrations. Also, the tail of the elution curve is too long, and therefore large amounts of solvents and long times are required for elution; finally, to reduce errors of integration of eqn. 2 it is necessary to detect accurately very low concentrations, which substantially limits the potential of the method.

EXPERIMENTAL

Surface excess isotherms were obtained at 303°K by a chromatographic procedure described previously[13]. All measurements were carried out on AC charcoal (Barnebey Cheney, U.S.A.) with Dubinin's parameters $W_0 = 0.38$ and $B_{benzene} = 0.75 \cdot 10^{-6}$ (where W_0 is the volume of the adsorption space, *i.e.*, the micropore volume, and B is the basic structure characteristic of the porous structure of the adsorbent[18]), and with volumes of micropores, mesopores and macropores of 0.38, 0.04 and 0.17 cm^3/g, respectively. The components of the binary solutions were benzene, 2,2,4-trimethylpentane, ethanol and carbon tetrachloride (all analytical-reagent grade).

RESULTS AND DISCUSSION

We carried out experiments to test the limits of the application of the method as regards adsorption isotherm measurements[13,14]. It has been shown that for systems with zero excess adsorption it is virtually impossible to avoid broadening of the elution curves because of the finite time of diffusion and mass transfer. As a result, the surface excess quantity, calculated from the elution curve, is not zero for systems that exhibit zero adsorption excess in the static experiment. This leads to elevated values of adsorption from eqn. 2. In particular, appreciable errors arise for systems of low selectivity.

Fig. 1 shows adsorption isotherms obtained from the elution curve with no account being taken of the broadening effects. It can be seen that for the system carbon tetrachloride–isooctane the surface excess amount obtained in the dynamic experiment exceeds the value from the static experiments by about 30%. Thus, a

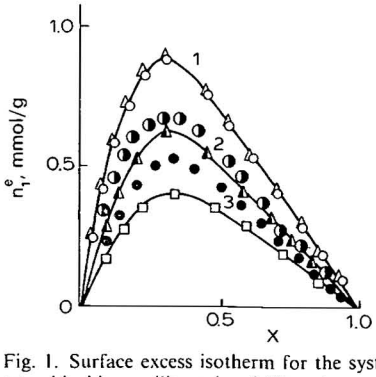

Fig. 1. Surface excess isotherm for the systems (1) benzene–isooctane on silica gel, (2) benzene–carbon tetrachloride on silica gel and (3) carbon tetrachloride–isooctane on silica gel. ○, ◑, ●, No broadening taken into account; △, ◭, □, broadening taken into account.

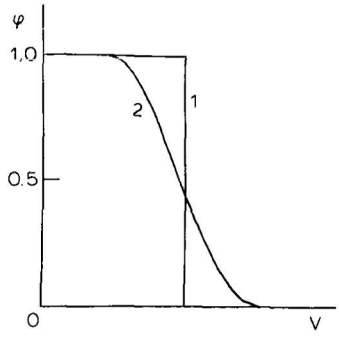

Fig. 2. Elution curve in ideal chromatography for (1) $\chi_{(\varphi)}^{(x)} = 0$ and (2) $\chi_{(\varphi)}^{(x)} > 0$, where χ is excess adsorption in ml/g.

correction for elution curve broadening is necessary in order to obtain a correct adsorption value.

The theoretical allowance for the band broadening processes requires a knowledge of a great number of physico-chemical parameters of the system, and in most instances this requires additional independent measurements. Again, one cannot evaluate the contribution of extra-column effects to the broadening, the effects being a characteristic of the liquid chromatographic (LC) system used. Therefore, an attempt has been made to develop a sufficiently simple and convenient empirical method of allowing for elution curve broadening.

We proceeded from the fact that in the case of a zero excess adsorption isotherm the band broadening is due to all factors with the exception of the adsorption isotherm itself. Fig. 2 shows schematically the ideal chromatographic elution curves for both a zero adsorption isotherm (curve 1) and non-zero one (curve 2). A schematic representation of the same curves in a real chromatographic experiment is shown in Fig. 3.

From the mass balance conditions, the areas under curves 1 and 2 (ideal and real chromatography) must be the same. From eqn. 2, it follows that the adsorption isotherm can be calculated from an ideal chromatogram with the help of the expression

$$f(\varphi) = \frac{1}{m} \int_0^{\varphi} (V_2 - V_1)\, d\varphi \tag{5}$$

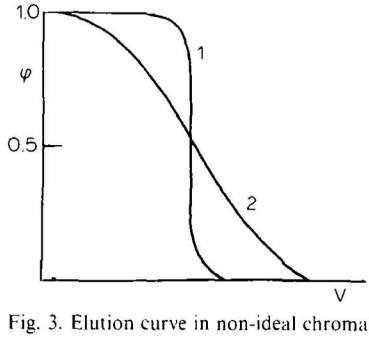

Fig. 3. Elution curve in non-ideal chromatography for (1) $\chi_{(\varphi)}^{(x)} = 0$ and (2) $\chi_{(\varphi)}^{(x)} > 0$.

We have assumed that the deformation of the elution curve due to the non-ideal chromatographic process should be the same both in the case of a zero adsorption isotherm and in the case of a non-zero one. Therefore, in non-ideal chromatography the elution volumes of appropriate concentrations obtained in a real chromatographic experiment for the system under study and for one where the excess adsorption is known to be zero should be introduced into eqn. 5. The criterion for zero adsorption is identity of the elution curves obtained when eluting component 1 by component 2 and *vice versa*. Fig. 1 shows the adsorption values (triangles) calculated with allowance for the broadening effects according to the above method. It can be seen that the dynamic adsorption data agree with the static data. The proposed correction method enabled us to use a very simple and cheap experimental unit and adsorbents with a particle size of 50–100 μm.

As has already been mentioned, another limitation of the method is that with steep isotherms very low concentrations have to be detected. Moreover, one can never be certain whether all of the substance has been eluted from the column. This gives rise to errors in the determination of adsorption. If a well designed LC system is available that ensures accurate volume measurements, this problem may be solved on the basis of mass balance computation. On the one hand, the volume of a substance in the column can be obtained by integrating the elution curve for the system with zero excess adsorption; on the other hand, the volume must be equal to that which is eluted in the case of a system with a non-zero excess adsorption. Equality of the volumes in both instances indicates complete elution of the substance from the column, and conversely, a difference indicates that the substance remains partially in the column. If the minimum concentration, φ_{min}, that can be adequately detected is known, than the amount of the non-desorbed substance corresponding to this concentration may be calculated from the relationship

$$\int_0^{\varphi_{min}} V_2 \, d\varphi = \int_0^1 V_1 \, d\varphi - \int_{\varphi_{min}}^1 V_2 \, d\varphi \tag{6}$$

However, in order to take advantage of eqn. 6, very accurate volume measurements are required and the experiments must be carried out carefully; otherwise, the discrepancy between the amounts of the substance eluted in the "zero" run and in the "main" run would be ascribed to the adsorption. In consequence, a serious error may be introduced in the result. Therefore, in practice it is convenient to take advantage of the following approach.

According to eqn. 5,

$$f(\varphi) = \frac{1}{m} \int_0^{\varphi} (V_2 - V_1) \, d\varphi$$

where V_1 and V_2 are true elution volumes. Let the elution curves $V_i'(\varphi)$ be measured. If the errors in V_2' and V_1' are ΔV_2 and ΔV_1, respectively, than eqn. 5 can be written in the form

$$\frac{1}{m} \int_0^{\varphi} (V_2' - V_1') \, d\varphi = \frac{1}{m} \int_0^{\varphi} (V_2 - V_1) \, d\varphi + \frac{1}{m} \int_0^{\varphi} (\Delta V_2 - \Delta V_1) \, d\varphi \tag{7}$$

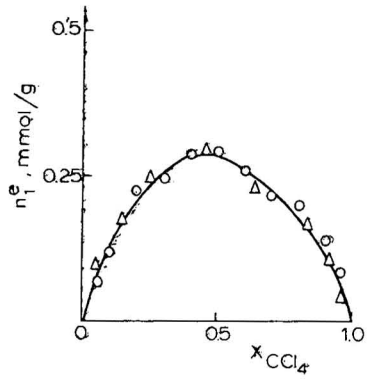

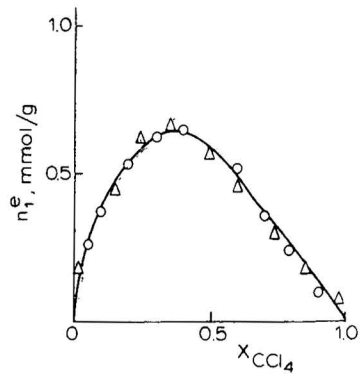

Fig. 4. Surface excess isotherm for the system carbon tetrachloride–isooctane on silica gel. O, Chromatographic method of measurement; △, static method of measurement[17].

Fig. 5. Surface excess isotherm for the system carbon tetrachloride–isooctane on charcoal. O, Chromatographic method of measurement; △, static method of measurement.

According to eqn. 5 the first integral of the right-hand side of eqn. 7 is the excess adsorption. When $\varphi = 1$, the excess adsorption is zero and we have

$$\frac{1}{m}\int_0^1 (V_2' - V_1')\,\mathrm{d}\varphi = \frac{1}{m}\int_0^1 (\Delta V_2 - \Delta V_1)\,\mathrm{d}\varphi \tag{8}$$

As practice has shown, the largest errors in V_2' and V_1' are introduced when the substance in the column is changed, *i.e.*, with the shapes of the elution curves in parallel runs coinciding, one can observe their relative displacement along the V axis. Therefore, it can be assumed that $\Delta V_2 - \Delta V_1 =$ constant. Then,

$$\frac{\Delta V_2 - \Delta V_1}{m} = \frac{1}{m}\int_0^1 (V_2' - V_1')\,\mathrm{d}\varphi \tag{9}$$

In order to eliminate uncertainty related to the fact that the detection is actually limited to the concentration φ_{min}, it is expedient to have one experimental point measured by the static adsorption technique at the lowest detectable concentration. Finally, we can write

$$f(\varphi) = \frac{1}{m}\int_0^{\varphi} (V_2 - V_1)\,\mathrm{d}\varphi = f(\varphi_{min}) + \frac{1}{m}\int_{\varphi_{min}}^{\varphi} (V_2' - V_1')\,\mathrm{d}\varphi - \frac{1}{m}\int_{\varphi_{min}}^{1} (V_2' - V_1')\,\mathrm{d}\varphi \tag{10}$$

Figs. 4 and 5 compare adsorption data obtained by the static and the dynamic techniques. The peculiar case is the determination of adsorption isotherms in the case of

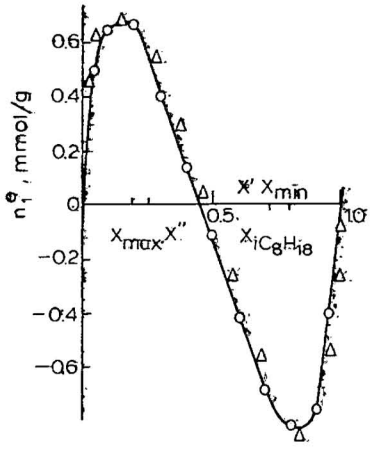

Fig. 6. Surface excess isotherm for the system isooctane–ethanol on charcoal. O, Chromatographic method of measurement; △, static method of measurement.

S-shaped adsorption isotherms (Fig. 6). In this instance concentration points of $\varphi < \varphi_{max}$ and $\varphi > \varphi_{min}$ are moving at speeds greater than those of maximum and minimum points. Therefore, for example, for the system isooctane–ethanol, upon elution all concentration points at $\varphi > \varphi_{max}$ are washed out as a sharp self-narrowing front and only the points on the isotherm up to $\varphi = \varphi'$ can be calculated from the elution curve. Therefore, in the calculation the whole adsorption isotherm, the curve of the elution of ethanol from isooctane should be taken into account. In this instance concentration points at $\varphi > \varphi_{min}$ are eluted in the form of a broadened front, whereas all points at $\varphi < \varphi_{min}$ appear as a self-narrowing front. From such a curve the adsorption isotherm can be found only for the concentration points at $1 > \varphi > \varphi''$.

Figs. 7–10 compare the data obtained from the static (triangles) and the dynamic (circles) adsorption experiments. There is fairly good agreement between the results.

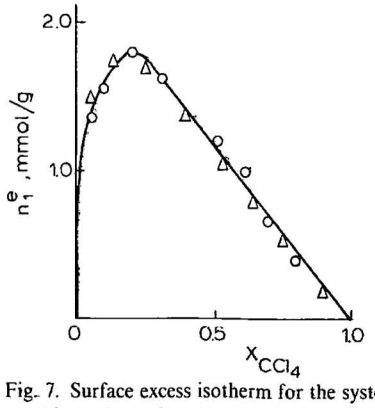

Fig. 7. Surface excess isotherm for the system carbon tetrachloride–ethanol on charcoal. O, Chromatographic method of measurement; △, static method of measurement.

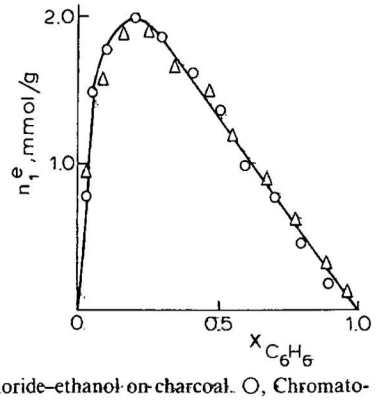

Fig. 8. Surface excess isotherm for the system benzene–ethanol on charcoal: O, Chromatographic method of measurement; △, static method of measurement.

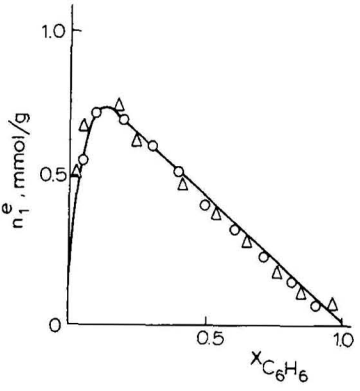

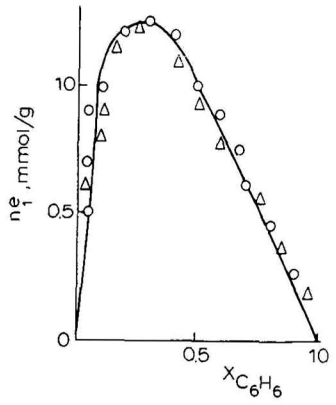

Fig. 9. Surface excess isotherm for the system benzene–carbon tetrachloride on charcoal. ○, Chromatographic method of measurement; △, static method of measurement.

Fig. 10. Excess adsorption isotherm for the system benzene–isooctane on charcoal. ○, Chromatographic method of measurement; △, static method of measurement.

CONCLUSION

The proposed method allows one to make measurements in the absence of extraneous gases with high accuracy over a wide range of temperatures and pressures. Also, unlike the static technique, the measurements can be easily automated. Studies of adsorption isotherms for benzene–isooctane, benzene–carbon tetrachloride, ethanol–benzene and ethanol–isooctane solutions on the same adsorbents gave similar results.

REFERENCES

1 D. De Vault, *J. Amer. Chem. Soc.*, 65 (1943) 592.
2 J. N. Wilson, *J. Amer. Chem. Soc.*, 62 (1940) 1583.
3 E. Glueckauf, *J. Chem. Soc.*, (1947) 1302.
4 E. Glueckauf, *Discuss. Faraday Soc.*, 7 (1947) 199.
5 N. M. Turkeltaub, *Nov. Med.*, 26 (1952) 45.
6 S. J. Gregg and R. Stock, in D. H. Desty (Editor), *Gas Chromatography 1958*, Butterworths, London, 1958, p.-F44.
7 G. Ya. Gaziev, M. I. Yanovskii and V. V. Brazhnikov, *Kinet. Katal.*, 1 (1960) 548.
8 E. Wicke, *Angew. Chem.*, B19 (1947) 15.
9 L. D. Beljakova, A. V. Kiselev and N. V. Kovaleva, *Zh. Fiz. Khim.*, 42 (1968) 2276.
10 A. V. Kiselev and Ya. I. Yashin, *Gas–Solid Chromatography*, Nauka, Moscow, 1967, p. 73.
11 C. S. Sharma and T. Fort, Jr., *J. Colloid Interface Sci.*, 43 (1973) 36.
12 A. A. Zhukhovitskii, A. F. Shljakhov and A. V. Sokolov, *Zavod. Lab.*, 41 (1975) 25 and 159.
13 S. I. Zverev, O. G. Larionov and K. V. Chmutov, *Zh. Fiz. Khim.*, 48 (1974) 1556 and 2101.
14 S. A. Busev, O. G. Larionov and K. V. Chmutov, *Zh. Fiz. Khim.*, 54 (1980) 991.
15 W. M. Smith and A. Van Den Hock., *Rec. Trav. Chim. Pays-Bas*, 76 (1957) 561.
16 G. G. Bayle and A. Klinkenberg, *Rec. Trav. Chim. Pays-Bas*, 75 (1957) 593.
17 S. I. Zverev, O. G. Larionov and K. V. Chmutov, *Zh. Fiz. Khim.*, 48 (1974) 2350.
18 B. P. Bering, M. M. Dubinin and V. V. Serpinskii, *J. Colloid Interface Sci.*, 21 (1966) 378.

Journal of Chromatography, 241 (1982) 295–304
Elsevier Scientific Publishing Company, Amsterdam — Printed in The Netherlands

CHROM. 14,737

LIGAND-EXCHANGE GAS CHROMATOGRAPHIC SEPARATION OF ANILINE BASES

KAZUMI FUJIMURA*, MASANOBU KITANAKA and TEIICHI ANDO
Department of Industrial Chemistry, Faculty of Engineering, Kyoto University, Sakyo-ku, Kyoto 606 (Japan)
(Received September 25th, 1981)

SUMMARY

Chromosorb G AW DMCS, coated with manganese(II) stearate, was used as column packing in ligand-exchange gas chromatography, and found to be more suitable for the separation of aniline bases than zirconium phosphate microcrystalline gels in the manganese(II) form, because the former has a lower adsorptivity and gives more symmetrical sharp peaks than the latter. From the comparison of retention data of aniline bases obtained on the manganese(II) stearate column with those obtained on the zirconium phosphate column, the retention order was found to be affected not only by the gas-phase basicity and the molecular configuration of the sample compound, but also by the surface structure of the metal support.

INTRODUCTION

Ligand-exchange liquid chromatography is now a well established method for separation of complex-forming organic compounds. It has, however, some drawbacks such as metal leakage from the stationary phase and the difficulty in adjusting the metal concentration in the stationary phase. In gas chromatography (GC), the former cannot occur and the latter can easily be overcome by impregnating or coating the support with a suitable amount of metal salt, instead of using a stationary phase bonded with a limited amount of chelating moiety.

Recent studies on ligand-exchange GC using zirconium phosphate microcrystalline gels as a metal support have shown that the use of a metal capable of forming a labile complex with the sample as well as with the mobile phase ligand is effective in improving the peak shape and reducing peak tailing. However, the peak tailing due to physical adsorption on the matrices of metal supports could not be eliminated completely, although the technique of gradient elution was useful in reducing the tailing of later peaks[1]. This means that better peak resolutions would not be obtained unless metal supports having more inert surface are used.

In the present study, Chromosorb G AW DMCS, coated with manganese(II) stearate, was selected as a stationary phase, and comparison was made between the retention behaviour of a number of aniline bases on this column and that on a

0021-9673/82/0000–0000/$02.75

zirconium phosphate column in the Mn^{2+} form.

Gas chromatographic separation of aniline bases has been achieved by many workers in partition[2-12] or adsorption[13,14] modes, but to our knowledge has never been tried in a ligand-exchange mode.

EXPERIMENTAL

Reagents

The aniline bases used in the present study are listed in Table I. They were of the highest purity available and were used without further purification as 1% solutions in *n*-hexane. Test solutions were prepared so as to contain 1% of each component.

Manganese(II) stearate was purified by recrystallization from benzene. Chromosorb G AW DMCS (80–100 mesh), used as a support of manganese(II) stearate, was obtained from Johns-Manville (Denver, CO, U.S.A.). Zirconium phosphate microcrystalline gel, Bio-Rad ZP-1, also used as a metal support, was purchased from Bio-Rad Labs. (Richmond, CA, U.S.A.).

Karl Fischer reagent, Mitsubishi SS (titre 3.0 mg water per ml), and the absorbing solvent, Mitsubishi ME (a mixture of dry methanol and ethylene glycol), were purchased from Mitsubishi Chemical Industries (Tokyo, Japan).

Column preparation

Manganese(II) stearate column. Chromosorb G AW DMCS was coated with 3% (w/w) manganese(II) stearate in the following way. A solution of manganese stearate in refluxing benzene was cooled to room temperature and then added to Chromosorb G AW DMCS. The mixture was stirred gently for 10 min, and the solvent was evaporated slowly under reduced pressure by use of a rotary evaporator, to leave the packing material. After rinsing with *n*-hexane and drying in air at room temperature, the packing was equilibrated with ammonia vapour for 24 h in a dish in a desiccator containing 14% ammonia at the bottom. After air-drying, the packing was sieved to 80–100 mesh and was placed in a glass spiral column (3 m × 4 mm I.D.) by suction. The packed column was conditioned at 80°C for 24 h by use of nitrogen containing ammonia and water vapour as carrier gas at a flow-rate of 15 ml/min. The detector was then connected and the conditioning was continued until the baseline was stable.

Zirconium phosphate column. Microcrystalline gel as received was treated with a 20% aqueous solution of manganese nitrate to convert its ionic form into the manganese(II) form. It was washed with distilled water until the filtrate was free from manganese, and then air-dried. Equilibration of the gel with ammonia vapour, packing of the gel into a column and conditioning of the column were performed as described above.

Apparatus and procedure

A 0-23 Hitachi gas chromatograph (Hitachi, Tokyo, Japan), equipped with a hydrogen flame ionization detector, was used isothermally in single-column mode. The injection port and the detector were kept at the same temperature as the column bath.

Nitrogen containing ammonia and water vapour, employed as the carrier gas, was obtained by passing nitrogen over the surface of aqueous ammonia, and was fed into the column through the injection port. The container of aqueous ammonia was placed in a thermostat and was kept at a constant temperature.

The concentration of ammonia and/or water vapour in the carrier gas was controlled by changing either the concentration of ammonia solution in the container or the temperature of the thermostat. The concentration of ammonia in the carrier gas was measured by absorbing the gas at the column outlet in a standard solution of hydrochloric acid for 3 min and titrating the excess of acid with sodium hydroxide. Water in the carrier gas was determined by absorbing the gas in absolute methanol containing glacial acetic acid for 30 min, and titrating the solution with Karl Fischer reagent. The apparatus used for titration was a Kyoto Electric Manufacturing MK-S titrator (Kyoto, Japan), the end-point being detected by the dead-stop method.

Sample solution (usually 0.4 μl) was injected into the top of the column using a 10-μl syringe. The column hold-up volume was measured from the retention time of methane and the flow-rate of the carrier gas.

RESULTS AND DISCUSSION

Adsorption on zirconium phosphate matrices

To examine the adsorption on zirconium phosphate, some N-monoalkyl-substituted anilines were chromatographed on NH_4^+ or Mn^{2+} columns packed with microcrystalline zirconium phosphate gels with nitrogen gas containing ammonia and water vapour as mobile phase. As can be seen from Fig. 1, the NH_4^+ gave larger

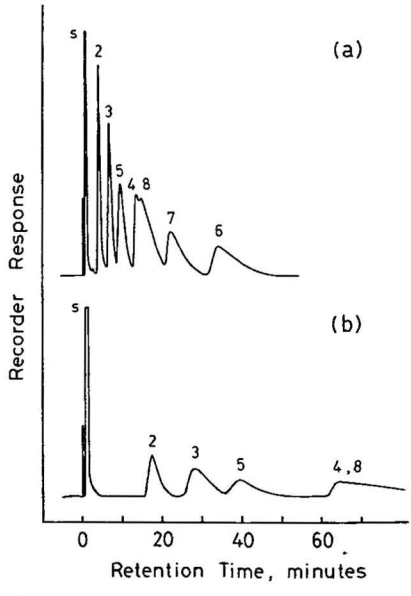

Fig. 1. Chromatograms of a mixture of N-monoalkyl-substituted anilines on zirconium phosphate (60–80 mesh) in Mn^{2+} form (a) and NH_4^+ form (b) at 80°C. Column: 3 m × 4 mm I.D. Flow-rate: 20.0 ml/min. Ammonia concentration (μmol/ml) in mobile phase; 0.70 (a); 0.73 (b). Water concentration (μmol/ml) in mobile phase: 0.09 (a); 0.10 (b). Peak identification as in Table I (s = solvent).

retention times and severer peak tailing than the Mn^{2+} form, under the same chromatographic conditions. This means that zirconium phosphate matrices exhibit a very high adsorptivity, since the retention of aniline bases on the NH_4^+ form cannot be based on complex formation between the sample and NH_4^+.

The adsorption on zirconium phosphate matrices can be explained in terms of hydrogen bond formation between the oxygen atom in zirconium phosphate and the amino hydrogen atom in the aniline bases. On the contrary, the retention of aniline bases on the Mn^{2+} form may be attributed primarily to complex formation; the adsorption due to hydrogen bonding is decreased on this column, because the active surface of the zirconium phosphate matrix is covered partially with bulky octahedral manganese ammine complexes formed with ammonia in the mobile phase.

The above rationalization is supported by the finding that in the absence of mobile phase ligands such as ammonia and/or water none of the aniline bases tested could be eluted from the column, whether in the NH_4^+ form or in the Mn^{2+} form, within a reasonable time.

The peak tailing observed in Fig. 1a suggests that the adsorption due to hydrogen bonding still remains even on the Mn^{2+} form. Although not indicated in Fig. 1, some samples showed different elution orders between the NH_4^+ and Mn^{2+} forms. Thus, chloro- and fluoroanilines were eluted in the order *o-* < *m-* < *p*-isomers on the NH_4^+ form, and *o-* < *p-* < *m*-isomers on the Mn^{2+} form. This variation may be ascribed to the difference in retention mechanism on the two forms.

Effect of ammonia concentration on retention on zirconium phosphate

The adjusted retention times, t'_R, of some N,N-dialkyl-substituted anilines and xylidines measured on a column of zirconium phosphate in the Mn^{2+} form are shown in Fig. 2 as a function of the ammonia concentration in the mobile phase. The water

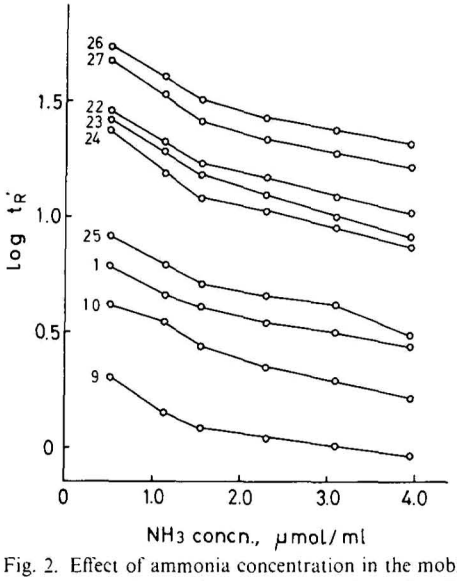

Fig. 2. Effect of ammonia concentration in the mobile phase on log t'_R of some N,N-dialkyl-substituted anilines and xylidines. Column: 3 m × 4 mm I.D. Packings: zirconium phosphate (60–80 mesh), Mn^{2+} form. Column temperature: 80 C. Flow-rate: 15.5 ml/min. Line identification as in Table I.

concentration was kept in the range 0.82–0.97 μM/ml throughout the measurement. Fig. 2 shows an approximately linear relationship between log adjusted retention time (t'_R) and the ammonia concentration, with a small but distinct change of the slope at an ammonia concentration of about 1.5 μM/ml. It also shows that the elution order as well as the peak resolution do not vary with the ammonia concentration, because the slope, *i.e.*, the decrease of t'_R with a unit increase of ammonia concentration, is nearly equal for all samples examined.

These findings suggest that the retention of aniline bases on a zirconium phosphate column (Mn^{2+}) is governed by the concentration of mobile phase ligands, and that the elution order and the peak resolution of aniline bases depend on their inherent nature.

TABLE I

ANILINE BASES USED AND THEIR ADJUSTED RETENTION TIMES (MIN) ON CHROMOSORB G AW DMCS WITH AND WITHOUT MANGANESE(II) STEARATE AT 75°C

Column: 3 m × 4 mm I.D. Flow-rate: 10.0 ml/min.

		Column			
		Coated with 3% manganese(II) stearate			*Not coated*
NH_3 concn. in mobile phase (μmol/ml)		1.20	4.69	–	1.14
H_2O concn. in mobile phase (μmol/ml)		0.13	0.15	–	0.11
No.	*Compound*				
1	Aniline	2.9	2.5	5.6	0.45
2	N-Methylaniline	4.0	3.5	6.3	0.40
3	N-Ethylaniline	6.2	5.4	9.4	0.54
4	N-*n*-Propylaniline	12.2	10.7	18.7	0.94
5	N-Isopropylaniline	6.7	5.8	10.3	0.58
6	N-*n*-Butylaniline	27.0	23.5	41.0	1.84
7	N-Isobutylaniline	16.7	15.1	25.8	1.23
8	N-*sec.*-Butylaniline	13.0	11.8	20.1	1.00
9	N,N-Dimethylaniline	4.5	3.8	6.8	0.37
10	N,N-Diethylaniline	11.3	9.8	17.3	0.83
11	N,N-Di-*n*-propylaniline	37.8	32.7	57.6	2.40
12	N,N-Di-*n*-butylaniline	–	–	–	7.80
13	*o*-Fluoroaniline	1.9	1.6	3.0	0.25
14	*m*-Fluoroaniline	3.5	3.1	6.2	0.48
15	*p*-Fluoroaniline	3.8	3.2	8.0	0.63
16	*o*-Chloroaniline	7.2	6.5	11.7	0.61
17	*m*-Chloroaniline	16.5	14.8	29.8	1.56
18	*p*-Chloroaniline	19.0	16.9	39.0	1.96
19	*o*-Toluidine	5.2	4.4	8.6	0.61
20	*m*-Toluidine	6.6	5.4	11.8	0.80
21	*p*-Toluidine	6.9	5.8	14.6	0.91
22	2,3-Xylidine	14.9	12.2	25.8	1.46
23	2,4-Xylidine	12.3	10.0	21.9	1.23
24	2,5-Xylidine	11.9	9.7	19.3	1.11
25	2,6-Xylidine	9.8	8.0	14.8	0.83
26	3,4-Xylidine	19.7	15.4	40.3	2.25
27	3,5-Xylidine	14.9	11.9	26.7	1.47

Retention behaviour on manganese(II) stearate-coated column

In an attempt to reduce the peak tailing due to physical adsorption on active metal support surfaces, use was made of Chromosorb G AW DMCS coated with manganese(II) stearate, instead of zirconium phosphate (Mn^{2+}). Table I lists the retention times of aniline bases, measured on columns of Chromosorb G AW DMCS coated with and without manganese(II) stearate, together with the chromatographic conditions.

As had been expected, the retention times on the non-coated column were very short and there was no pronounced difference among the samples, whereas those on the coated column increased without any change in the elution order with a decrease of the ammonia concentration in the mobile phase, as was the case on zirconium phosphate (Mn^{2+}). It is considered that the retention of aniline bases on a manganese(II) stearate-coated Chromosorb column is not based on partition, but on the interaction between the manganese and the amino group of the amines, since manganese(II) stearate (m.p. 112°C) acts as a solid at the column temperature of 75°C, at which the adjusted retention times were measured. A manganese(II) stearate-coated Chromosorb column differs from a zirconium phosphate column (Mn^{2+}) in the following way: all samples tested could be eluted, although with relatively long retention times, from a coated column even when neither ammonia nor water is present in the mobile phase. This may be explained by the smaller total amount of manganese as well as by the weaker interaction between the supports or matrices and the aniline bases on the coated column compared with the zirconium phosphate column.

It is to be noted, however, that the concentration of the mobile phase ligands, especially that of ammonia, greatly affects not only the retention time but also the peak resolution. Fig. 3 shows a poorer peak resolution and a severer peak tailing caused by the absence of ammonia and water vapour in the mobile phase.

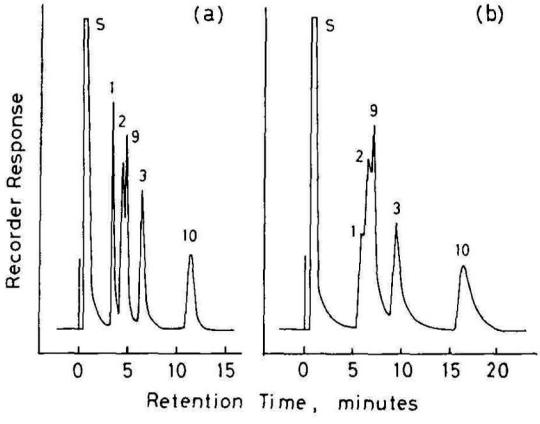

Fig. 3. Chromatograms of a mixture of some N-monoalkyl-substituted and N,N-dialkyl-substituted anilines at 75 C. Column: 3 m × 4 mm I.D. Packings: 3% manganese stearate coated on Chromosorb G AW DMCS (80–100 mesh). Flow-rate: 10.1 ml/min. Ammonia concentration (μmol/ml) in mobile phase: 1.20 (a); none (b). Water concentration (μmol/ml) in mobile phase: 0.13 (a); none (b). Peak identification as in Table I.

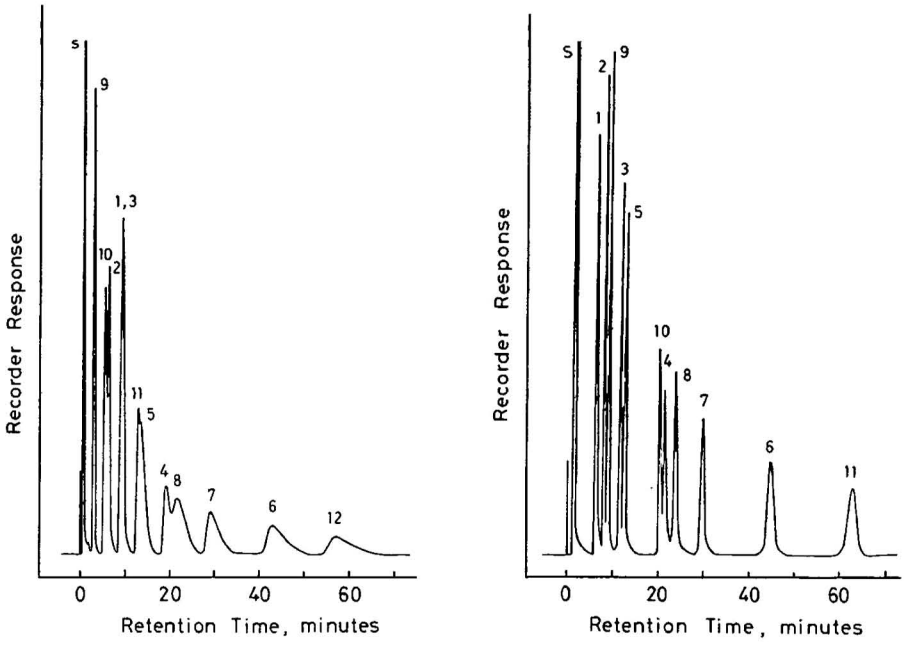

Fig. 4. Separation of N-alkyl-substituted anilines on zirconium phosphate (60–80 mesh), Mn^{2+} form at 90°C. Column: 3 m × 4 mm I.D. Flow-rate: 24.8 ml/min. Ammonia concentration in mobile phase: 3.07 μmol/ml. Water concentration in mobile phase: 0.20 μmol/ml. Peak identification as in Table I.

Fig. 5. Separation of N-alkyl-substituted anilines with 3% manganese stearate coated on Chromosorb G AW DMCS (80–100 mesh) at 80°C. Column: 3 m × 4 mm I.D. Flow-rate: 21.8 ml/min. Ammonia concentration in mobile phase: 2.89 μmol/ml. Water concentration in mobile phase: 0.13 μmol/ml. Peak identification as in Table I.

Comparison of column efficiency and selectivity

Chromatographic separation of aniline bases was performed by use of a manganese(II) stearate-coated Chromosorb column and a zirconium phosphate column (Mn^{2+}) under the most suitable conditions. The chromatograms obtained are shown in Figs. 4–7. Comparison of Fig. 5 with Fig. 4 and of Fig. 6b with Fig. 6a shows that the manganese stearate-coated Chromosorb column gives sharper and more symmetrical peaks, although there is still a slight peak tailing at a later peak (No. 26) in Fig. 6b. While the peak tailing on the zirconium phosphate column may be attributed to the adsorption on the zirconium phosphate matrix and/or to the slow rate of the ligand exchange reaction, only the latter can be responsible for the peak tailing on the manganese stearate-coated column. It may be concluded, therefore, that the column of manganese stearate coated on Chromosorb G AW DMCS is superior in efficiency to the column of zirconium phosphate (Mn^{2+}).

On the other hand, there is a difference in the elution order between the two kinds of columns. As can be seen from Fig. 5, N,N-dialkyl-substituted anilines are generally more strongly retained on the manganese stearate-coated Chromosorb column than on the zirconium phosphate column (Mn^{2+}). For example, N,N-di-*n*-propylaniline (11) is eluted from the coated column after, but from the zirconium

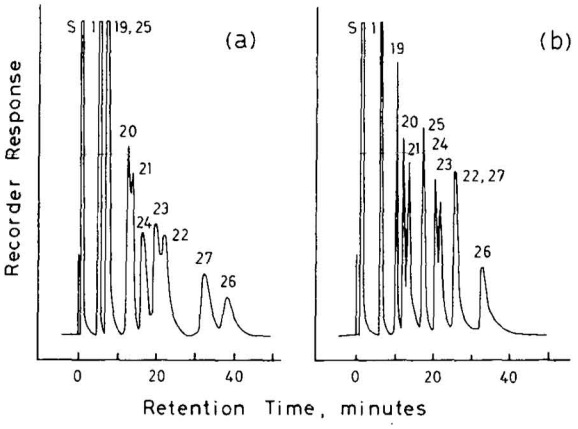

Fig. 6. Separation of aniline, toluidines and xylidines on (a) zirconium phosphate (60–80 mesh), Mn^{2+} form, and (b) manganese stearate coated on Chromosorb G AW DMCS (80–100 mesh). Chromatographic conditions for (a) and (b) as for Figs. 4 and 5, respectively. Peak identification as in Table I.

phosphate column before, N-monoalkyl-substituted anilines (5, 4, 8, 7, 6), the retention times of which are nearly the same on either column. Another example is N,N-di-*n*-butylaniline, which cannot be eluted within 150 min from the coated column under the conditions shown in Fig. 5.

It is to be noted that the same elution order is observed within the homologous series of aniline bases; the order is 2 < 3 < 5 < 4 < 8 < 7 < 6 for N-monoalkyl-substituted anilines and 9 < 10 < 11 < 12 for N,N-dialkyl-substituted anilines irrespective of the column. These orders agree with that of the carbon chain lengths of the alkyl groups in the homologues and are opposite to the order of bulkiness of the alkyl groups within isomers. The mechanism of retention thus seems to be similar on the two columns. The differences between the two columns in elution order, as shown in Figs. 4 and 5, is probably due to the difference in selectivities of the metal supports used.

It has been shown that in ligand-exchange chromatography the retention behaviour of sample compounds depends largely on their gas-phase basicity as well as on their molecular configuration; the smaller the gas-phase basicity of the aniline derivative and the bulkier the moiety around the amino nitrogen, the shorter is the retention time. Although very few gas-phase basicities of aniline derivatives are known, it can be expected from the data pertaining to aliphatic amines that the gas-phase basicity of alkyl-substituted anilines increases with an increase of the alkyl chain length as well as with the number of the alkyl substituents[15–17]. For aniline bases carrying isomeric alkyl groups, the gas-phase basicity is expected to follow the order *tert.*- > *sec.*- > *iso*- > *n*-alkyl-substituted anilines.

Experimentally, however, the elution order of N-propyl- and N-butylaniline isomers does not agree with the above expectation on either column. This is probably due to the steric hindrance to complex formation. Furthermore, aniline was eluted from the zirconium phosphate column (Mn^{2+}) after N,N-dimethyl-, N,N-diethyl- and N-methylanilines, although it had the shortest retention time on the manganese stearate-coated Chromosorb column as expected. Again, this may be explained in

terms of steric factors, since microcrystalline zirconium phosphate gels are of a smaller pore size than Chromosorb G. The above findings strongly suggest that the elution order of N-substituted anilines in ligand-exchange GC is determined by the balance of the effects of gas-phase basicity and steric bulk.

When a manganese stearate-coated Chromosorb column is used, the hydrophobic interaction, or the Van der Waals interaction, between the stearate group and the alkyl chain in the sample can also affect the sample retention. This is evidenced by the retention times of aliphatic and aromatic hydrocarbons, which have no coordination sites; their retention times increase with increasing carbon number. For example, the retention times of benzene, toluene, ethylbenzene and isopropylbenzene were 1.89, 2.19, 2.71 and 3.25 min, respectively, and those of methane, *n*-pentane, *n*-hexane, *n*-heptane and *n*-decane were 1.63, 1.72, 1.80, 1.96 and 4.64 min, respectively, under the conditions cited in Fig. 5.

Toluidine and xylidine isomers showed similar retention behaviour as N-alkyl-substitited anilines. As Fig. 6 shows, toluidine isomers are eluted in the order of *o*- < *m*- < *p*-isomer from either column. This order is the opposite to that of their ionization potentials, which in turn are closely related to their proton affinities or basicities in the gas phase[18,19]. In contrast, the bulkiness effect is the dominant factor determining the elution order of xylidine isomers; 2,6-xylidine, whose nitrogen atom is completely shielded by the two adjacent methyl groups, has the shortest retention time, followed by 2,5-, 2,4-, 2,3-, 3,5- and 3,4-xylidine. This order is the same as that of the distance between the amino group and the nearest methyl group. The elution order of 3,4- and 3,5-xylidines is the opposite to that of their ionization potentials.

It is interesting to note that the pairs 24/23 and 22/27 showed better separation on a zirconium phosphate column than on a coated column, whereas the paris 23/22, 20/21 and 19/25 showed better separation on a coated column than on a zirconium phosphate column. Of additional interest is the behaviour of 2,6-xylidine on a zirconium phosphate column. It elutes before *m*- and *p*-toluidines because of its larger steric hindrance to complex formation on the microcrystalline structure, in spite of

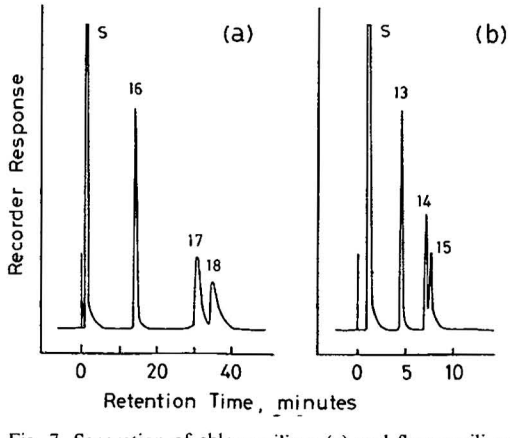

Fig. 7. Separation of chloroanilines (a) and fluoroanilines (b) with 3% manganese stearate coated on Chromosorb G AW DMCS (80–100 mesh) at 80°C. Chromatographic conditions for (a) as for Fig. 5, and for (b): column 3 m × 4 mm I.D.; flow-rate, 16.1 ml/min; ammonia concentration in mobile phase, 2.03 μmol/ml; water concentration in mobile phase, 0.15 μmol/ml. Peak identification as in Table I.

the expected larger gas-phase basicity than those of toluidines.

The separation of chloro- and fluoroaniline isomers was best achieved on a coated column as shown in Fig. 7. Fluoroanilines are retained lesser strongly than chloroanilines, with the same elution order, *o*- < *m*- < *p*-isomer. On a zirconium phosphate column the orders both changed to *o*- < *p*- < *m*-isomer and the peak resolution decreased. These orders do not agree with the one expected from the ionization potentials of chloroanilines, *i.e.*, *p*- < *o*- < *m*-isomer.

CONCLUSIONS

The work reported here has demonstrated that metal stearate-coated Chromosorb G AW DMCS is a much more useful stationary phase for the ligand-exchange GC separation of aniline bases than zirconium phosphate in a metal ion form; the latter fails to give sharp symmetrical peaks because of its high adsorptivity based on hydrogen bonding, whereas the former gives better peak shape and resolution because of its decreased adsorptivity caused by complex formation.

The elution order of samples has been found to depend on the surface structure of the supports or matrices of the metal, as well as on the complex-forming ability of the sample and the steric hindrance to complex formation, which in turn are closely related to the gas-phase basicity of the sample and its molecular configuration, respectively. It has also been suggested that not only complex formation but also hydrophobic interaction plays a role in determining the retention of aniline bases, when the metal stearate-coated stationary phase is used. This column cannot be used, however, in an adsorption chromatographic mode, because the peak resolution is markedly decreased in the absence of mobile phase ligands, although all the samples tested in this study could be eluted under such conditions.

REFERENCES

1 K. Fujimura and T. Ando, *Anal. Chem.*, 49 (1977) 1179.
2 J. S. Parson and J. C. Morath, *Anal. Chem.*, 36 (1964) 237.
3 K. J. Bombaugh, *Anal. Chem.*, 37 (1965) 72.
4 H. G. Henkel, *J. Gas Chromatogr.*, 3 (1965) 320.
5 A. R. Cooper, C. W. P. Crowne and P. G. Farrell, *J. Chromatogr.*, 27 (1967) 362.
6 W. J. Irvine and M. J. Saxby, *J. Chromatogr.*, 43 (1969) 129.
7 E. Townley, I. Perez and P. Kabasakalian, *Anal. Chem.*, 42 (1970) 947.
8 S. M. Farroha and S. S. Emeish, *Talanta*, 22 (1975) 121.
9 G. O. Wood and R. G. Anderson, *Amer. Ind. Hyg. Ass. J.*, 36 (1975) 538.
10 B. E. Bowen, *Anal. Chem.*, 48 (1976) 1584.
11 D. E. Bradway and T. Shafik, *J. Chromatogr. Sci.*, 15 (1977) 322.
12 R. F. Moseman, *J. Chromatogr.*, 166 (1978) 397.
13 J. J. Franken, C. Vidal-Madjar and G. Guiochon, *Anal. Chem.*, 43 (1971) 2034.
14 J. M. H. Daemen, W. Dankelman and M. E. Hendriks, *J. Chromatogr. Sci.*, 13 (1975) 79.
15 R. Yamdagni and P. Kebarle, *J. Amer. Chem. Soc.*, 95 (1973) 3504.
16 C. Agami, *Bull. Soc. Chim. Fr.*, (1974) 869.
17 J. E. Bartmess, J. A. Scott and R. T. McIver, Jr., *J. Amer. Chem. Soc.*, 101 (1979) 6046.
18 D. H. Aue, H. M. Webb and M. T. Bowers, *J. Amer. Chem. Soc.*, 94 (1972) 4726.
19 B. G. Ramsey and F. A. Walker, *J. Amer. Chem. Soc.*, 96 (1974) 3314.

Journal of Chromatography, 241 (1982) 305–323
Elsevier Scientific Publishing Company, Amsterdam — Printed in The Netherlands

CHROM. 14,749

DIRECT ANALYSIS OF ^{13}C ABUNDANCE IN PLANT CARBOHYDRATES BY GAS CHROMATOGRAPHY–MASS SPECTROMETRY

HIROSHI KOUCHI

Division of Plant Nutrition, National Institute of Agricultural Sciences, Kannon-dai, Yatabe-cho, Tsukuba, Ibaraki 305 (Japan)

(Received December 16th, 1981)

SUMMARY

A method for the direct analysis of ^{13}C abundance in several kinds of plant carbohydrates by gas chromatography–mass spectrometry (GC–MS) has been developed. The analysis was conducted with the quasi-molecular ion peak and its isotopic species obtained by chemical ionization with isobutane as a reagent gas, and the results are given both as ^{13}C content (atom%) and as the distribution of labelled molecules (mole%). The precision of ^{13}C measurements was within $\pm 2\%$ for ^{13}C abundance from 2 to 10 atom% and less than $\pm 1\%$ for ^{13}C abundance above 10 atom%. Contents of ^{13}C obtained by this method for soluble carbohydrates in corn leaves fed $^{13}CO_2$ were in good agreement with the results obtained with an infrared ^{13}C analyser.

Using this method, the incorporation of ^{13}C assimilated photosynthetically into several carbohydrates in soybean plants and their translocation into roots and nodules were investigated and it was shown that the GC–MS method was applicable as a routine method for the ^{13}C analysis of many plant metabolites in ^{13}C tracer experiments.

INTRODUCTION

The use of ^{13}C as a tracer in the study of plant physiology has developed in recent years. In spite of the disadvantage that the detection of ^{13}C as a stable isotope is much less sensitive than that of the radioactivity of ^{14}C, the application of ^{13}C in numerous branches of plant science should be developed increasingly in the future because first, the use of ^{13}C avoids the biological hazards of and the complicated restrictions accompanying the use of ^{14}C compounds, and second, the results are obtained directly in the form of an isotope ratio, which is more useful for the investigation of metabolic processes, especially the rate of turnover or translocation of metabolites.

The abundance of ^{13}C in biological materials has generally been measured with a mass spectrometer designed for isotope analysis or, more recently, by infrared absorption spectrometry[1]. In these methods, the sample is combusted by appropriate methods and ^{13}C content is determined by measuring the $^{13}CO_2$ to $^{12}CO_2$ ratio, so

0021-9673/82/0000–0000/$02.75

that the sample must be purified carefully prior to analysis in order to prevent the simultaneous combustion of contaminants, and also relatively large amounts of sample are required. Hence, these methods have not necessarily been adequate for the ^{13}C analysis of small amounts of biological compounds such as carbohydrates, organic acids and amino acids.

Gas chromatography–mass spectrometry (GC–MS) is considered to be the best method for the analysis of stable isotopes in trace amounts of biological compounds. In particular, the direct analysis of isotopically labelled compounds without any combustion or digestion process has the great advantage that it can determine the isotope ratio and also provide structural information on molecules and the intermolecular distribution of isotopes. The application of GC–MS to stable isotope analysis has been investigated since the early days of the development of GC–MS[2,3], and several workers reported its application in biochemistry and medicine[4,5]. However, most of this work was aimed at the quantification of isotopically labelled or non-labelled compounds with the aid of tracer molecules in which the position and abundance of particular isotopes was known previously, or was aimed at obtaining qualitative information on the positions of tracer atoms in molecules by analysis of appropriate fragment ion peaks. Thus, little work on either theoretical or methodological aspects of the routine analysis of stable isotope in compounds separated gas chromatographically has been done with the purpose to chase the fate of tracer atoms in metabolic process.

The direct analysis of stable isotopes in molecules by GC–MS involves the measurement of the intensities of several isotopic species of molecular, quasi-molecular or fragment ion peaks. In GC–MS, a relatively wide mass range is scanned rapidly at a rate of a few milliseconds per mass unit for small gas chromatographic peaks with a continuously varying intensity, so that the precision and accuracy of the intensities measured for each ion peak are much poorer than those in other methods for stable isotope analysis. Because of this disadvantage, GC–MS has not been adopted for the routine analysis of isotope ratios in biological materials generally containing isotopes in low abundance. In this regard, as suggested by Caprioli *et al.*[6], a quadrupole mass analyser has some advantages with respect to precision and accuracy over the magnetic deflection type mass spectrometer, mainly because of its extremely high switching rate of mass dispersion. However, the quadrupole instrument has the disadvantage that the practical sensitivity decreases rapidly in high mass regions. Most biological compounds, for analysis by gas chromatography, must be converted into volatile forms such as trimethylsilyl derivatives, which have relatively high molecular weights, so that for the direct analysis of these compounds it seems to be preferable today to use a magnetic deflection type mass spectrometer.

On the other hand, Sano *et al.*[7] developed a technique of mass fragmentography for monitoring continuously $^{12}CO_2$ and $^{13}CO_2$ from a pyrolyser for the continuous combustion of effluents from a gas chromatographic column. This method is expected to provide a better precision of ^{13}C measurement and also it is very attractive as it allows possible improvements to the simultaneous measurement of ^{13}C and ^{15}N abundance in doubly labelled compounds by an appropriate combustion method[8]. However, this method is not released from the apprehensions to reduce the accuracy of ^{13}C abundance owing to contamination and/or incomplete combustion, and also provides no structural information.

The precision and accuracy of the peak intensities in mass spectra have been greatly improved in recent years with a combination of GC–MS and computer systems that allow rapid repeat scanning and data acquisition with high performance. Therefore, although the limit of precision inherent in the direct analysis of isotope ratios by GC–MS should be borne in mind, it would seem to be valuable to investigate the possibility of using GC–MS for the routine measurement of isotope contents in various biological compounds with regard to the level of precision required in tracer experiments.

We have therefore investigated the direct GC–MS analysis of the ^{13}C contents of some plant metabolites labelled with ^{13}C assimilated photosynthetically and in this paper we discuss its application to the study of the fate of photosynthetic products in higher plants.

CALCULATION OF ^{13}C CONTENT FROM MASS SPECTRAL DATA

Biological molecules in tracer experiments are generally considered to be mixtures of molecules containing a varying number of isotopes. For example, ^{13}C-labelled glucose obtained by photosynthesis in $^{13}CO_2$ is a mixture of molecular species in which 0–6 carbon atoms are substituted by ^{13}C. In such mixtures, data on the distribution of isotopic molecular species are required in order to evaluate the isotope abundance. Thus, isotope contents of molecules are determined with complex arithmetic manupulations from data on the intensities of all possible isotopic species of molecular or fragment ion peaks. In a particular instance in which it is assumed that the isotopes are uniformally, *i.e.*, randomly, distributed in molecules, the equation proposed by VandenHeuvel *et al.*[9] could be used, which requires the intensities of only two ion peaks, *viz.*, M and M + 1 corresponding to the non-labelled molecule and the molecule containing only one heavy isotope, respectively. However, in a short-time labelling experiment, it is evident that this assumption of random distribution is by no means justified. On the other hand, Biemann[2] discussed in detail an approximate method using all of the peak intensities corresponding to each isotopic species, based on the assumption that the ratios of the intensity of the isotope peak at M + 1, M + 2, ..., etc., to the intensity of peak at M are same in both unenriched and enriched materials. This assumption is approximately justified in most instances but the resulting error is not small if the contribution of particular isotopes to the natural abundance of each isotopic molecular species is not negligible in comparison with that of other isotopes in the molecule.

The method for the evaluation of the ^{13}C content (in atom%) and the distribution of isotopic molecular species (in mole%) devised in this work can be outlined as follows.

An empirical expression C_nT was initially introduced, corresponding to the molecular or fragment ion peaks concerned, where C_n corresponds to n carbon atoms expected to incorporate ^{13}C as a tracer and T contains all of the other elements in molecule. For example, the quasi-molecular (MH^+) ion peak (m/e = 628) of the trimethylsilyl (TMS) derivative of glucose oxime, which is obtained by chemical ionization with isobutane as a reagent gas, is expressed as C_6T, where T is $C_{18}H_{63}O_6NSi_6$. Various isotopic species of T are denoted by T^0, T^1, T^2, ..., etc., each with one mass unit difference, where T^0 is one containing no heavy isotope. The

abundance of T^i ($i = 0, 1, 2, \ldots$) depends on the natural abundance of the isotopes of each element constituting T and is considered to be identical in unenriched and enriched molecules.

Let M be the mass number of C_nT containing no heavy isotope, then the molecular species corresponding to each isotopic ion peak with mass number at M, M + 1, M + 2, ..., M + n are as follows:

$$\begin{aligned}
&\mathrm{M}: && {}^{12}C_nT^0\\
&\mathrm{M}+1: && {}^{13}C^{12}C_{n-1}T^0,\ {}^{12}C_nT^1\\
&\mathrm{M}+2: && {}^{13}C_2{}^{12}C_{n-2}T^0,\ {}^{13}C^{12}C_{n-1}T^1,\ {}^{12}C_nT^2\\
&\vdots\\
&\mathrm{M}+n: && {}^{13}C_nT^0,\ {}^{13}C_{n-1}{}^{12}CT^1, \ldots,\ {}^{12}C_nT^n
\end{aligned}$$

Let A_i ($i = 0, 1, 2, \ldots, n$) be the abundance of T^i and B_i the abundance of isotopic species of the molecule to be analysed in which i carbon atoms in n are substituted by ^{13}C. Then, the intensity R_i ($i = 0, 1, 2, \ldots, n$) of the ion peak at M, M + 1, M + 2, ..., M + n is related to A_i and B_i by the following equations:

$$\left.\begin{aligned}
R_0 &= k(A_0B_0)\\
R_1 &= k(A_0B_1 + A_1B_0)\\
R_2 &= k(A_0B_2 + A_1B_1 + A_2B_0)\\
&\vdots\\
R_n &= k(A_0B_n + A_1B_{n-1} + \ldots + A_nB_0)
\end{aligned}\right\} \qquad (1)$$

where k is a proportionality constant depending on the amounts of sample injected and the ionization efficiency. It should be noted that the ionization efficiencies of the ion peaks concerned are assumed to be identical for all labelled species of the same molecule.

Dividing each equation in eqn. 1 by the first equation in the series, $R_0 = k(A_0B_0)$, gives nth-order simultaneous equations:

$$\left.\begin{aligned}
R_1' &= A_1' + B_1'\\
R_2' &= A_2' + A_1'B_1' + B_2'\\
R_3' &= A_3' + A_2'B_1' + A_1'B_2' + B_3'\\
&\vdots\\
R_n' &= A_n' + A_{n-1}'B_1' + \ldots + B_n'
\end{aligned}\right\} \qquad (2)$$

where

$$\left.\begin{aligned} R_i' &= R_i/R_0 \\ B_i' &= B_i/B_0 \\ A_i' &= A_i/A_0 \qquad (i = 1, 2, \ldots, n) \end{aligned}\right\} \tag{3}$$

R_i' are the relative intensities of each of the ion peaks of isotopic species of C_nT based on $R_0 = 1$.

Eqns. 2 are solved for B_i' and the abundance of labelled molecules, $B_0, B_1, \ldots, B_n$ are obtained with

$$\left.\begin{aligned} B_0 &= 1\Big/\left(\sum_{i=1}^{n} B_i' + 1\right) \\ B_i &= B_0 B_i' \qquad (i = 1, 2, \ldots, n) \end{aligned}\right\} \tag{4}$$

as the sum of molecular abundance, $\sum_{i=0}^{n} B_i$ must be equal to unity. Then, the ^{13}C content, X (atom %), is calculated with

$$X = \frac{1}{n} \sum_{i=1}^{n} iB_i \cdot 100 \tag{5}$$

The abundances of $T^0, T^1, \ldots, T^n$ can be calculated theoretically from the natural abundances of the isotopes of each element in T. However, as discussed later, the peak intensities measured by a mass spectrometer contain some systematic errors considered probably to be due to contamination of small peaks by electrical noise and/or background noise (see Tables I and II). Therefore, it is preferable to use the A_i' values determined experimentally by the analysis of unenriched molecules.

It is assumed initially that ^{13}C is distributed randomly in unenriched molecules. This assumption is entirely reasonable as isotope discrimination occurring naturally is negligible for the level of precision achieved with GC–MS analysis. Let a and b be the natural abundance of ^{12}C and ^{13}C, respectively, $(a + b = 1)$ and the probability of finding any molecule with a certain number of atoms of ^{12}C and ^{13}C will be the appropriate term of the binomial expansion

$$(a + b)^n = a^n + {}_nC_1 a^{n-1} b + {}_nC_2 a^{n-2} b^2 + \ldots + b^n \tag{6}$$

where

$${}_nC_i = \frac{n(n-1)\ldots(n-i+1)}{i!}$$

Therefore, the B_is in eqns. 1 are substituted by

$$B_i \equiv {}_nC_i a^{n-i} b^i \qquad (i = 0, 1, 2, \ldots, n) \tag{7}$$

Let K_i ($i = 1, 2, \ldots, n$) be the intensities of the M + 1, M + 2, ... M + n peaks relative to the intensity of the M peak in the unenriched molecule; the resulting equations corresponding to eqns. 2 are

$$\left.\begin{aligned} K_1 &= A'_1 + {}_nC_1 e \\ K_2 &= A'_2 + {}_nC_1 e A'_1 + {}_nC_2 e^2 \\ K_3 &= A'_3 + {}_nC_1 e A'_2 + {}_nC_2 e^2 A'_1 + {}_nC_3 e^3 \\ &\vdots \\ K_n &= A'_n + {}_nC_1 e A'_{n-1} + {}_nC_2 e^2 A'_{n-2} + \ldots + e^n \end{aligned}\right\} \tag{8}$$

where $e = b/a$. If the official value of ^{13}C natural abundance, $b = 0.01107$, is adopted, then e is calculated to be 0.011194.

Eqns. 8 are solved for A'_i and the resulting values are used for eqns. 2 for an enriched sample.

The abundances A_i ($i = 0, 1, 2, \ldots, n$) of T^0, T^1, T^2, ..., T^n are determined in the same manner as shown in eqns. 4. Here, the assumption that $\sum_{i=0}^{n} A_i = 1$ is not entirely justified because A_{n+1}, A_{n+2}, ..., etc., are very small but not zero. However, the resulting error is not large and also this approximation has no effect on the calculation of ^{13}C abundance in enriched materials because eqns. 2 require values of A'_i but not of A_i.

EXPERIMENTAL

Preparation of trimethylsilyl derivatives

A solution containing 1–5 mg of carbohydrates was evaporated *in vacuo* completely to dryness over phosphorus pentoxide. Aliquots (about 200 μl) of anhydrous pyridine containing hydroxylamine hydrochloride (25 mg/ml) were added to the residue and reaction was carried out at 75°C for 1 h to give oximes of reducing sugars. After cooling to room temperature, 1 ml of TMS-HT (Tokyo Kasei Kogyo, Tokyo, Japan) was added and the mixture was allowed to stand overnight at room temperature to give trimethylsilyl (TMS) derivatives. A few microlitres of the clear supernatant solution were injected into the gas chromatograph.

Preparation of ^{13}C-labelled plant carbohydrates

Corn plants were grown in phytotron (25°C, natural light) for 20 days after sowing in plastic pots filled with a mixture of vermiculite, perlite, peat moss and fine gravel in the proportions 2:2:1:1 (v/v). The pots were fertilized with 5 g of Magamp-K and 15 g of magnesia lime.

Soybean plants were grown for 35 days with complete nutrient solution aerated continuously in a growth chamber controlled at 25°C (day, 14 h) and 19°C (night, 10 h) with artificial light at about 40 klux from a metal halide lamp. The plants were well nodulated by inoculation of a commercial strain of *Rhizobium japonicum*. The composition of the nutrient solution was as follows (mg/l in deionized water): KNO_3, 18.1; $MgSO_4 \cdot 7H_2O$, 202.8; KH_2PO_4, 87.9; K_2SO_4, 16.6; $CaCl_2 \cdot 2H_2O$, 73.4; H_3BO_3, 2.86; $MnCl_2 \cdot 4H_2O$, 1.08; $ZnSO_4 \cdot 7H_2O$, 0.44; $CuSO_4 \cdot 5H_2O$, 0.04; $Na_2MoO_4 \cdot 2H_2O$, 0.10; $CoCl_2 \cdot 6H_2O$, 0.04; Fe-EDTA, 22.5; and pH, 5.8–6.2.

Whole plants of soybean and attached leaf (the fourth from lowest leaf) of corn were used for $^{13}CO_2$ assimilation. Assimilation chambers made of acrylic sheet designed for whole plants or attached leaves were set up in the growth cabinet with artifical light at 25 klux (for corn leaves) or 40 klux (for soybean plants). The temperature in the assimilation chamber was controlled at 25°C. After the plants or attached leaves had been introduced, the air in the chamber was purged with carbon dioxide-free air and then closed air-tight. $^{13}CO_2$ was generated from $Ba^{13}CO_3$ by reaction with 1 *N* hydrochloric acid. The concentration of carbon dioxide in the chamber was controlled at about 300–400 ppm by regulating manually the generation of $^{13}CO_2$, monitoring with an infrared carbon dioxide analyser. The abundance of ^{13}C in the air was denoted as that of the $Ba^{13}CO_3$ used.

After feeding of $^{13}CO_2$ for a certain period, the plants were immediately separated into the component parts and killed in liquid nitrogen or in a deep-freeze at −80°C. The frozen plant tissues were macerated with 80% (v/v) ethanol using a Waring blender or a mortar and pestle, followed by centrifugation at 3000 *g* for 30 min, then the pellet was washed twice with 80% ethanol. The supernatant and washings were combined and evaporated to remove ethanol. The resulting aqueous solution was passed through columns of Dowex 50 (H^+) and Dowex 1 ($HCOO^-$), and the neutral fraction eluted (containing carbohydrates) was evaporated and dried completely over phosphorus pentoxide, followed by the preparation of TMS derivatives.

Uniformally labelled [^{13}C]glucose

[U-^{13}C]Glucose containing 62.3 atom% of ^{13}C as an authentic value (Merck, Rahway, NJ, U.S.A.) was kindly supplied by Dr. S. Murayama of the Department of Soil Science, National Institute of Agricultural Sciences, Ibaraki, Japan.

Gas chromatograph–mass spectrometry

A Model JMS-D300 double-focusing mass spectrometer (JEOL, Tokyo, Japan) was equipped with a Model 5710A gas chromatograph (Hewlett-Packard, Avondale, PA, U.S.A.). For the separation of plant carbohydrates, a 1.8 m × 2 mm I.D. glass column packed with 3% OV-17 on 100–120-mesh Chromosorb W HP was used. The flow-rate of the carrier gas (helium) was 40 ml/min, the injector temperature was 250°C and the column temperature was programmed from 140 to 260°C at 2°C/min.

The chemical ionization (CI) method with isobutane as the reagent gas was used to obtain quasi-molecular ion peaks. The pressure of the reagent gas in the ionization chamber was kept at about 1 Torr, the ionization potential was 70 eV, the ion source temperature was 240°C and the ionization current was 300 μA. By using these conditions, the MH^+ ion peak was obtained as a base peak for the TMS

derivatives of any carbohydrate analysed in this experiment except sucrose. Mass spectra were obtained with repeat scanning over the mass range *m/e* 440–640 with a scanning speed of 0.6 sec and a scanning interval of 1.0 sec. The data for the intensity of each ion peak were stored for each scan in a JMA-2000 computer system and each mass number was integrated from the start to the end of one chromatographic peak. These integrated intensities of each mass number were recorded and used for calculation.

Liquid chromatography and ^{13}C analysis with an infrared absorption spectrometer

Soluble carbohydrates in corn leaves fed $^{13}CO_2$ were also separated by ion-exchange chromatography to measure the ^{13}C abundance by infrared absorption spectrometry. A Model JLC-6AH automatic liquid chromatograph (JEOL) was equipped with a water-jacketed glass column (280 × 8 mm I.D.) packed with LCR-3 anion-exchange resin. Borate–sodium hydroxide eluting buffers with the following concentrations were used: first, 0.11 *M* (pH 7.5); second, 0.25 *M* (pH 9.0); and third, 0.35 *M* (pH 9.5). The first buffer was changed after 130 min to the second buffer and after 310 min to the third buffer. The buffer flow-rate was 0.51 ml/min and the column temperature was constant at 55°C.

Carbohydrates (10–15 mg) were dissolved in 1 ml of the first buffer and loaded on the column with the automatic sample injector. The eluent was collected in 2-ml fraction tubes and aliquots of each fraction were heated with 1% orcinol in 96% sulphuric acid at 95°C followed by monitoring of the absorbance at 470 nm. The fractions corresponding to each carbohydrate were combined, evaporated, passed through a column of Dowex 50 (H^+) to remove sodium ions and concentrated so as to contain about 1 mg of carbohydrate in 0.1 ml of solution. A Model EX-130 infrared ^{13}C analyser (Japan Spectroscopic, Tokyo, Japan) was employed for the measurement of the ^{13}C abundance in carbohydrates. Borate saturating in the carbohydrate solution did not interfere in the ^{13}C analysis.

RESULTS

Analysis of authentic [^{13}C]glucose

Mass spectra of the TMS-oxime of glucose are shown in Fig. 1. The MH^+ (*m/e* 628) ion peak was a base peak in non-labelled glucose, whereas in authentic [U-^{13}C]glucose (62.3 atom%), an isotopic ion peak at *m/e* 634 exhibited the maximum intensity. Occasionally, a molecular ion peak (M^+, *m/e* 627) or another quasi-molecular ion peak ($M - H^+$, *m/e* 626) was detected with trace intensity. If the intensities of these peaks are relatively large, the effects of the isotopic species of these ion peaks on the peaks at *m/e* 628, 629, ..., etc., must be corrected, as discussed by Biemann[2]. However, in the experiment reported here, these peaks were usually very small or not detectable, and can then be neglected in the calculation.

Table I shows the relative intensities of the MH^+ ion and its isotopic species for the TMS-oxime of authentic glucose with ^{13}C in natural abundance. The ion multiplier corresponds to the gain control of the amplifier of the ion detector. Theoretical values were obtained by calculation from the natural abundance of isotopes of each element constituting the MH^+ ion (empirical formula $C_{24}H_{63}O_6NSi_6$) based on the assumption of random distribution of each isotope. The observed intensities above

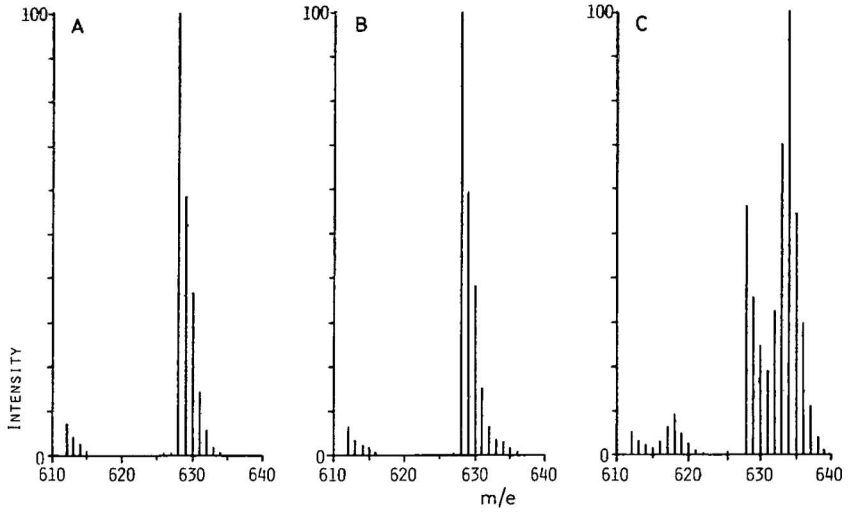

Fig. 1. Mass spectra (*m/e* 610–640) of TMS-oxime of authentic glucose containing ^{13}C in natural abundance (A), 3.84 atom% (B) and 62.3 atom% (C).

m/e 632 were higher to some extent than the theoretically expected values and the differences were much larger with high ion multiplying. This is considered to be caused by the fact that the small peaks suffered from a relatively large influence of electrical noise. The level of ion multiplying also affected to the deviation of the intensity of each ion peak, and the level required to detect small isotopic peaks depended on the amount of sample injected and also on the scanning speed per mass

TABLE I

RELATIVE INTENSITIES OF MH^+ ION PEAK AND ITS ISOTOPIC SPECIES OF TMS-OXIME OF GLUCOSE CONTAINING ^{13}C IN NATURAL ABUNDANCE

Data are expressed as mean ± standard deviation. $\sqrt{\Sigma (x - \bar{x})^2/n}$ ($n = 6$). Theoretical values were calculated by assumption of random distribution of ^{13}C, ^{2}H, ^{17}O, ^{18}O, ^{15}N, ^{29}Si and ^{30}Si each in natural abundance.

m/e	*Sample injected (μg)*			*Theoretical*
	5	*1*	*0.2*	
	Ion multiplier			
	1.10	*1.40*	*1.65*	
628	100.00	100.00	100.00	100.00
629	58.79 ± 0.36	58.43 ± 0.51	59.28 ± 0.57	58.98
630	38.04 ± 0.36	38.06 ± 0.37	38.43 ± 0.83	37.80
631	14.82 ± 0.09	14.73 ± 0.33	15.08 ± 0.41	14.46
632	5.69 ± 0.06	5.80 ± 0.05	5.98 ± 0.18	5.26
633	1.80 ± 0.02	1.85 ± 0.05	2.02 ± 0.09	1.47
634	0.63 ± 0.01	0.70 ± 0.03	0.75 ± 0.05	0.38

TABLE II

ABUNDANCE OF ISOTOPIC SPECIES OF T FOR MH^+ IONS OF TMS DERIVATIVES OF GLUCOSE AND FRUCTOSE OXIMES

T = $C_{18}H_{63}O_6NSi_6$. Data are expressed as mean ± standard error (n = 6).

Species	*Theoretial*	*Authentic*	*Corn leaves*	
		Glucose	*Glucose*	*Fructose*
T	0.4894	0.4855 ± 0.00083	0.4851 ± 0.00063	0.4858 ± 0.00059
T + 1	0.2558	0.2534 ± 0.00037	0.2508 ± 0.00063	0.2517 ± 0.00056
T + 2	0.1669	0.1668 ± 0.00058	0.1675 ± 0.00041	0.1660 ± 0.00067
T + 3	0.0590	0.0608 ± 0.00018	0.0617 ± 0.00033	0.0613 ± 0.00049
T + 4	0.0215	0.0237 ± 0.00011	0.0247 ± 0.00031	0.0245 ± 0.00037
T + 5	0.0056	0.0073 ± 0.00053	0.0076 ± 0.00018	0.0081 ± 0.00017
T + 6	0.0014	0.0025 ± 0.00004	0.0026 ± 0.00007	0.0025 ± 0.00004

unit. Under the analytical conditions adopted in this experiment, a level of 1.10 in the ion multiplier gave deviations within ±1.0% for the most of the peak intensities and then the amount of sample required was 5 μg or more.

Table II shows the abundance of isotopic species of T ($C_{18}H_{63}O_6NSi_6$) for MH^+ ions of TMS derivatives of glucose and fructose oximes. The measured abundances for authentic glucose and for glucose and fructose from corn leaves generally agreed well with theoretical values. However, the measured abundances for T + 4, T + 5 and T + 6 were significantly higher than the calculated values, reflecting the overestimation of small peak intensities in the mass spectra as shown in Table I. Thus, the use of theoretical values of the abundance of T for A_i in eqns. 1 resulted in some overestimation of the ^{13}C abundances. However, the atom excess percentage obtained by substracting the ^{13}C abundance in unenriched material determined by using

TABLE III

^{13}C ATOM% AND ISOTOPIC MOLECULAR ABUNDANCE OF AUTHENTIC [U-^{13}C]GLUCOSE

Original and diluted samples were expected to have 62.3 and 3.84 atom% as theoretical values, respectively.

Species	*Isotopic molecular abundance*		*Atom%*	
	Original	*Diluted*	*Original*	*Diluted*
M	0.2647 ± 0.0002	0.9058 ± 0.0004	60.77	3.72
M + 1	0.0227 ± 0.0004	0.0624 ± 0.0006	60.76	3.75
M + 2	0.0133 ± 0.0001	0.0014 ± 0.0009	60.89	3.67
M + 3	0.0397 ± 0.0001	0.0017 ± 0.0003	60.82	3.70
M + 4	0.1115 ± 0.0002	0.0052 ± 0.0003	60.94	3.65
M + 5	0.2529 ± 0.0003	0.0108 ± 0.0002	60.83	3.66
M + 6	0.2952 ± 0.0008	0.0127 ± 0.0001		
			Mean: 60.83 ± 0.045	3.69 ± 0.017

TABLE IV

ANALYSIS OF AUTHENTIC [^{13}C]GLUCOSE

Samples were obtained by dilution of [U-^{13}C]glucose (62.3 atom%). Data are expressed as mean ± standard error (n = 4).

Sample No.	*Atom%*	
	Expected	*Observed*
1	13.25	12.94 ± 0.062
2	7.87	7.82 ± 0.035
3	4.69	4.53 ± 0.059
4	2.95	2.92 ± 0.034
5	1.86	1.84 ± 0.020
6	1.49	1.51 ± 0.026

the same theoretical abundance of T was identical with the results obtained by using the measured abundance of T as the natural abundance of ^{13}C was 1.107 atom%. Therefore, it was considered to be preferable to use the measured abundance of T obtained from the analysis of unenriched material with the same conditions of measurement as for the analysis of enriched material.

The abundances of isotopic molecular species and ^{13}C (atom%) are shown in Table III for [^{13}C]glucose with 62.3 and 3.84 atom% of ^{13}C as authentic values. The measured ^{13}C contents were lower in both samples than the authentic values. A similar tendency was observed in the analysis of [^{13}C]glucose with a varying ^{13}C content, as shown in Table IV. The standard deviations varied from 0.2% of 60.83 atom% to 3.4% of 1.51 atom% [^{13}C]glucose. The isotopic molecular abundance of ^{13}C-enriched molecules provides information on the distribution of species of molecules containing a varying number of ^{13}C atoms. The results obtained for the original [U-^{13}C]glucose used in this experiment indicated that most of this sample consisted of non-labelled and labelled molecules with five or six ^{13}C atoms. The uniformity of labelling of this authentic [U-^{13}C]glucose will be discussed later.

Analysis of soluble carbohydrates in corn leaves fed $^{13}CO_2$

The total ion monitoring (TIM) mass chromatogram of the neutral fraction of corn leaves is shown in Fig. 2. Fructose, glucose and sucrose were the major components of this fraction. The abundances of ^{13}C obtained by GC–MS were compared with those obtained with the infrared ^{13}C analyser (Table V). The data from the two methods were nearly identical except for sucrose, which showed relatively high ^{13}C contents. For the analysis of sucrose, the fragment ion peak at m/e 451 was used because the MH^+ ion peak of the TMS derivative of sucrose (expected to show m/e 919) could not be obtained. This fragment ion was considered to contain two components from glucose and fructose residues of sucrose with the following mass fragmentation:

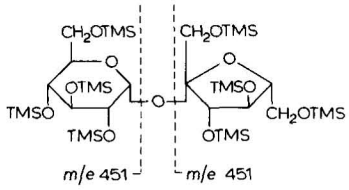

This interpretation was supported by a comparison of measured and theoretically calculated abundances of T for the empirical formula of this fragment ion (Table VI). Thus, if the ^{13}C abundances in glucose and fructose residues are not identical and also the contributions of these two components to this fragment are different, the resulting data on ^{13}C abundance would differ significantly from the ^{13}C abundance in sucrose. This is inevitable for the compound, which has a large molecular weight and for which molecular, quasi-molecular or fragment ion peaks containing all of the carbon atoms in original molecule cannot be obtained. Therefore, it should be noted that the data given for the ^{13}C abundance of sucrose in this paper possibly contain significant errors, probably giving lower values than the true ones.

Fig. 3 shows time course of the incorporation of ^{13}C into carbohydrates in corn leaves. The two experiments indicated that fructose and glucose were labelled more rapidly than sucrose in the short labelling period. However, the incorporation of ^{13}C into sucrose exceeded increasingly those of other two carbohydrates with increasing labelling period.

Labelling of carbohydrates with ^{13}C and their translocation in soybean plants

The incorporation of ^{13}C assimilated photosynthetically into soluble carbohy-

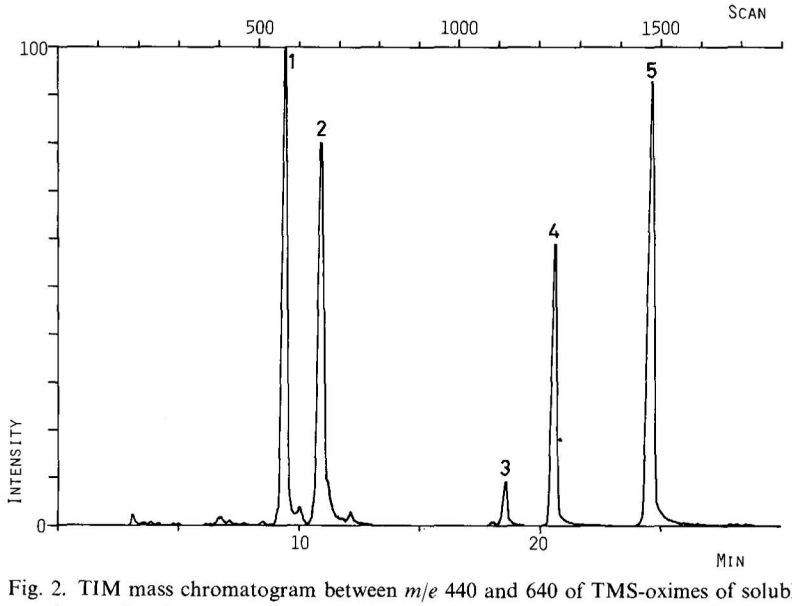

Fig. 2. TIM mass chromatogram between *m/e* 440 and 640 of TMS-oximes of soluble carbohydrates in corn leaves. 1 = Fructose; 2 = glucose; 3 = unknown; 4 = β-phenyl glucoside (internal standard); 5 = sucrose.

TABLE V

^{13}C ABUNDANCE OBTAINED BY GC–MS ANALYSIS AND INFRARED ABSORPTION SPECTROMETRY FOR SOLUBLE CARBOHYDRATES IN CORN LEAVES FED $^{13}CO_2$ UNDER VARIOUS CONDITONS

Carbohydrates were separated by ion-exchange chromatography (see text) followed by infrared analysis. Data are given as averages of three and four independent measurements for infrared and GC–MS analysis, respectively.

Sample	*Sample No.*	*Atom%*	
		IR	*GC–MS*
Sucrose	1	7.85 ± 0.069	7.09 ± 0.082
	2	3.58 ± 0.021	2.89 ± 0.038
	3	1.27 ± 0.010	1.24 ± 0.038
	4	1.16 ± 0.010	1.17 ± 0.033
Glucose	2	2.62 ± 0.115	2.56 ± 0.032
	3	1.61 ± 0.023	1.50 ± 0.047
	4	1.26 ± 0.006	1.27 ± 0.062
Fructose	3	1.50 ± 0.015	1.51 ± 0.062
	4	1.38 ± 0.015	1.37 ± 0.007

drates in soybean plants and their translocation to roots and nodules were investigated as an example of the application of the method presented here.

Soybean nodules contain large amounts of cyclitols, such as pinitol (5-O-methyl-D-inositol), (+)*chiro*-inositol, sequoyitol (2-O-methyl-*myo*-inositol) and *myo*-inositol[10]. These cyclitols form 60% or more of soluble carbohydrates in nodules and also are present in leaves, stems and roots at relatively low concentrations. The metabolism and physiological role of these cyclitols, especially in relation to the dinitrogen-fixing activity of soybean nodules, have not yet been elucidated.

Soybean plants were pre-treated in the dark for 48 h to reduce the endogenous pool of carbohydrates and then exposed to $^{13}CO_2$ (90 atom%) for 3 h under irradiance at about 40 klux. Plants were sampled 3, 9 and 23 h after the beginning of $^{13}CO_2$ exposure and the ^{13}C abundance of carbohydrates soluble in 80% ethanol was determined.

TABLE VI

ABUNDANCE OF ISOTOPIC SPECIES OF T FOR FRAGMENT ION (*m/e* = 451) OF TMS DERIVATIVE OF SUCROSE

T = $C_{12}H_{43}O_5Si_4$. Data are expressed as mean ± standard error (n = 6).

Species	*Theoretical*	*Observed*
T	0.6210	0.6135 ± 0.00189
T + 1	0.2152	0.2156 ± 0.00043
T + 2	0.1232	0.1287 ± 0.00047
T + 3	0.0299	0.0322 ± 0.00017
T + 4	0.0089	0.0065 ± 0.00176
T + 5	0.0016	0.0023 ± 0.00029
T + 6	0.0003	0.0010 ± 0.00017

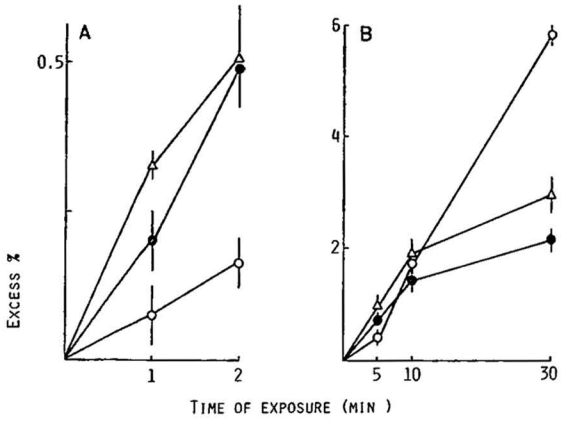

Fig. 3. Incorporation of ^{13}C into soluble carbohydrates in corn leaves fed $^{13}CO_2$ of 90 atom% (A) and 30 atom% (B). Data are given as averages of four or six independent measurements. Vertical lines = 2 × standard error. ○, Sucrose; ●, glucose; △, fructose.

The TIM mass chromatogram is shown in Fig. 4 for the nodule extract. Pinitol, (+)*chiro*-inositol, sequoyitol, glucose, *myo*-inositol and sucrose were the major components of this extract. Fructose was not completely separated from (+)*chiro*-inositol. Penta-TMS derivatives of pinitol and sequoyitol (mol.wt. 554) showed the MH^+ ion peak at *m/e* 555, and hexa-TMS derivatives of (+)*chiro*-inositol and *myo*-inositol (mol.wt. 612) showed the MH^+ ion peak at *m/e* 613, both as the base peak. Thus, these MH^+ ion peaks and their isotopic species were employed for ^{13}C analysis.

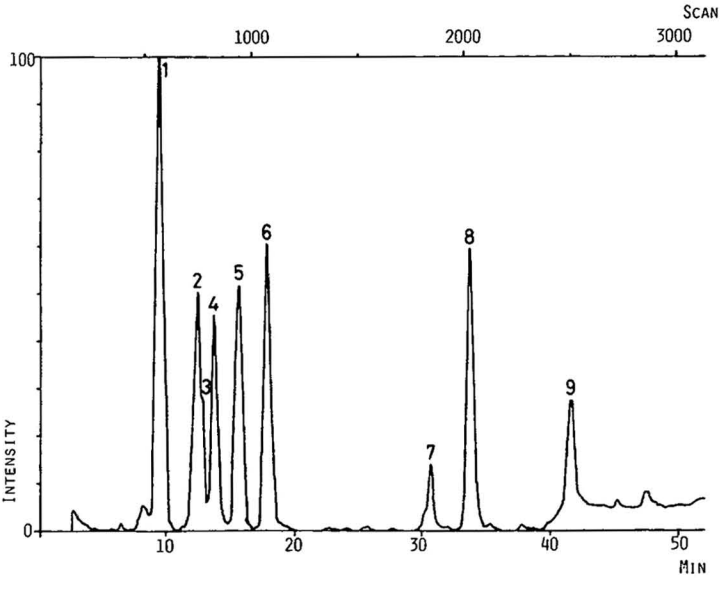

Fig. 4. TIM mass chromatogram of TMS-oximes of carbohydrates in 80% ethanol extract of soybean nodule. 1 = Pinitol; 2 = (+)*chiro*-inositol; 3 = fructose; 4 = sequoyitol; 5 = glucose; 6 = *myo*-inositol; 7 = unknown; 8 = β-phenyl glucoside (internal standard); 9 = sucrose.

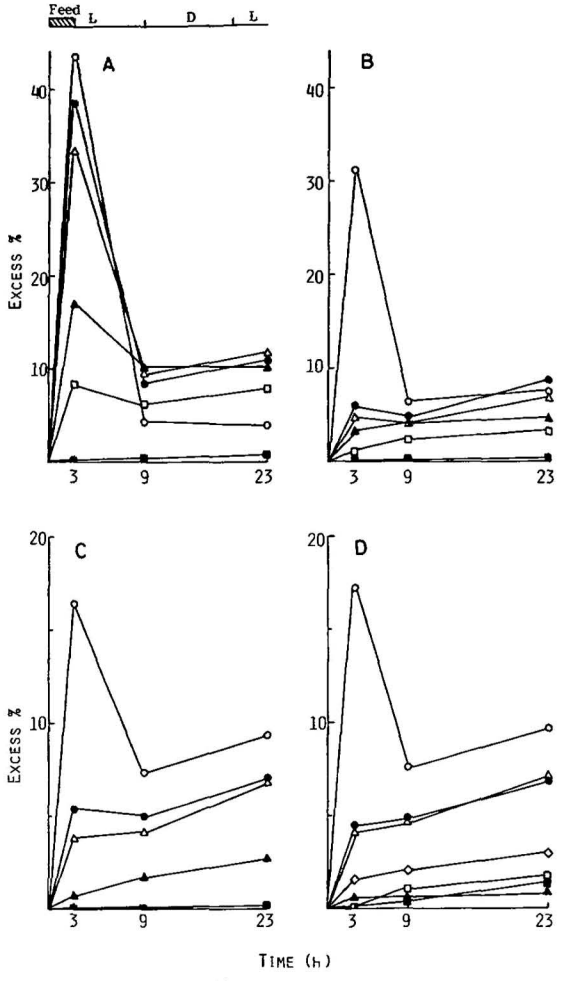

Fig. 5. Incorporation of ^{13}C into soluble carbohydrates in leaves (A), stems and petioles (B), roots (C) and nodules (D) of soybean plants following photosynthetic assimilation of $^{13}CO_2$ for 3 h. Data are given as averages of four independent measurements. Experimental conditions are briefly illustrated on the upper part of (A); L and D are light (40 klux) and dark, respectively. ○, Sucrose; ●, glucose; △, fructose; ▲, *myo*-inositol; □, sequoyitol; ■, pinitol; ◇, (+)*chiro*-inositol.

The results are shown in Fig. 5. The incorporation of ^{13}C into cyclitols other than *myo*-inositol and sequoyitol in leaves was much less than that into saccharides. In particular, pinitol, which occupied the largest part of cyclitols not only in nodule but also in other parts of the plant, exhibited little incorporation of ^{13}C. This result is contrary to the suggestion by Phillips and Smith[11] that pinitol may be one of the photosynthates that are translocated into the nodules. The results obtained in this experiment may indicate that sucrose is the major compound translocating carbon assimilated by photosynthesis into the root and also the nodules. The large amounts of cyclitols in the nodules are considered to be metabolically inactive as a whole. This suggests that these cyclitols may have a certain physiological role, different from the

intermediate metabolites supplying the energy fixed by photosynthesis to nodules for dinitrogen fixation.

It should be noted that the incomplete separation of fructose and (+)*chiro*-inositol may result in some errors in the measurement of ^{13}C abundance in (+)*chiro*-inositol. As shown in Fig. 1, the TMS-oxime of glucose (and also fructose) exhibited a small fragment ion peak at *m/e* 612 caused by the demethylation of the molecular ion, and isotopic species of this fragment ion are considered to overlap with MH^+ ion peaks of (+)*chiro*-inositol. For this reason, the ^{13}C abundance of (+)*chiro*-inositol was not measured in leaves, stems and roots. In nodule extracts the fructose content was very low and it seemed to be reasonable to neglect the contribution of fructose to the MH^+ ion peaks of (+)*chiro*-inositol. However, the possibility of overestimation of the ^{13}C abundance in (+)*chiro*-inositol was not removed completely because fructose showed a much higher ^{13}C abundance than (+)*chiro*-inositol.

DISCUSSION

For the calculation of the ^{13}C abundance in labelled compounds, it is essential that there is no contamination of the background or other impurities on the ion peaks to be measured. This assumption is considered to be satisfied completely for the quasi-molecular (MH^+) ion peak and its isotopic peaks obtained by the CI method. Some other inherent assumptions for the calculation of isotope abundance from GC–MS data together with the sources of error were discussed in detail by Biemann[2]. However, in ^{13}C-labelled compounds, the error caused by factors such as fractionation or loss of labelled molecules in the mass spectrometer is considered to be negligibly less than that in the deuterium-labelled compounds which Biemann mainly discussed.

In the analysis of authentic [^{13}C]glucose with varying abundance, the ^{13}C contents obtained by GC–MS were lower than the expected values (Tables III and IV). A satisfactory interpretation of these systematic differences is not given here, but

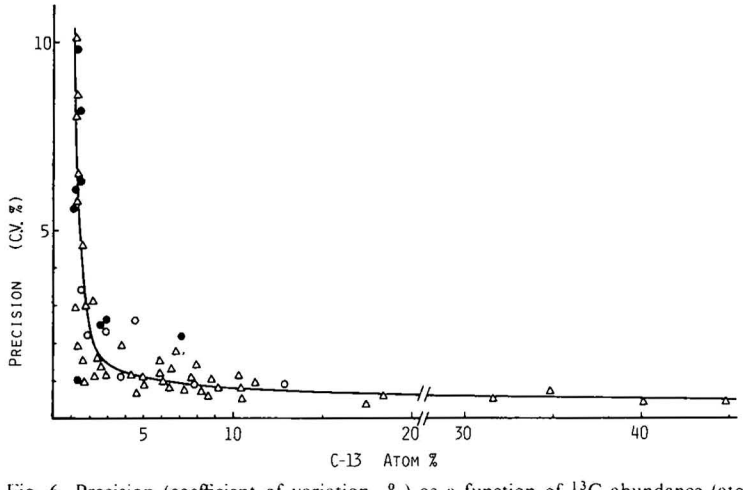

Fig. 6. Precision (coefficient of variation, %) as a function of ^{13}C abundance (atom%) for authentic [^{13}C]glucose (○) and ^{13}C-labelled carbohydrates in corn leaves (●) and in soybean plants (△).

the differences were not large in most instances and also were sufficiently reproducible.

The results of the analysis of authentic glucose (Tables I–IV) give an indication of the precision of the method. The variance of peak intensity (Table I) depends on the level of ion multiplying, and therefore on the amount of ions introduced into the detector. On the other hand, the scanning speed per mass unit and the number of repeat scans for one chromatographic peak were also important factors influencing the precision of measurement. The upper limit of the scanning speed permitted depends on the mass resolving power required for the measurement of the ion peaks concerned. In this experiment, the scanning speed was established at 0.6 sec for the mass range *m/e* 440–640, which included all of the MH^+ or fragment (for sucrose) ion peaks of carbohydrates analysed in this experiment. In addition, at least 0.4 sec was required for the dead time of data acquisition and for the reversion time of the magnetic field. Therefore, repeat scanning was conducted every 1.0 sec and then 40–80 scans were made from the start to the end of each chromatographic peak. If a very narrow mass range can be adopted, the scanning interval is less than 1.0 sec, and then the increase in the number of repeat scans may result in some improvement in precision, but a great improvement cannot be expected because the scanning interval cannot be less than 0.5 sec.

Fig. 6 shows the precision (coefficient of variation) of measurement as a function of ^{13}C atom%. The results indicate that a precision within about $\pm 2\%$ was achieved in the measurement of carbohydrates containing 2.0–10 atom% of ^{13}C, and less than $\pm 1\%$ for a ^{13}C abundance above 10 atom%. However, in the measurement of compounds containing below 2 atom% of ^{13}C, the variance of the data was much larger.

The precision achieved in this work is not necessarily sufficient for the ^{13}C analysis of biological compounds. However, as mentioned before, in other methods of stable isotope analysis with much better precision, it is difficult to avoid completely the errors caused by the complex purification procedure or degradation of materials. Therefore, in most tracer experiments, the present method seems to be suitable for the routine ^{13}C analysis of many biological compounds, as shown for example in the experiments on corn leaves and soybean plants fed $^{13}CO_2$.

A higher precision of measurement would permit the use of ^{13}C in a much lower enrichment experiment. Several workers[12] have reported other approaches for improving the precision of the peak intensity, but the level achieved was approximately $\pm 1\%$. Possible improvements may be achieved with the development of quadrupole-type GC–MS systems possessing improved sensitivity in the high mass region.

It is useful to discuss the uniformity of the distribution of isotopes in labelled molecules. For this purpose, the measured abundance of isotopic molecular species must be compared with the abundance obtained by calculation on the assumption of a random distribution of the isotopes. The distribution of labelled molecules in authentic [U-^{13}C]glucose (Table III) was very different from the theoretically uniform distribution of 60.83 atom% of ^{13}C (results of calculation not shown). The possibility that the sample is a mixture of unenriched glucose and enriched glucose with a uniform ^{13}C distribution was examined following the method of Heron[13] (Table VII). The measured abundance of enriched glucose was obtained as follows:

TABLE VII

COMPARISON OF MEASURED AND CALCULATED VALUES FOR ENRICHED FRACTION OF AUTHENTIC [U-^{13}C]GLUCOSE

Data were calculated from intensities of isotopic species of MH^+ ions of TMS-oximes of non-labelled and labelled (60.83 atom %) glucose according to the method of Heron[11].

Species	*Measured abundance*	*Calculated*		*Difference*
		Expression	*Abundance*	
M	0.00000*	$(1-x)^6$	0.00001	−0.00001
M + 1	0.00688	$6(1-x)^5x$	0.00025	0.00662
M + 2	0.01779	$15(1-x)^4x^2$	0.00399	0.01380
M + 3	0.05542	$20(1-x)^3x^3$	0.03336	0.02206
M + 4	0.15552	$15(1-x)^2x^4$	0.15695	−0.00143
M + 5	0.35274	$6(1-x)\,x^5$	0.39378	−0.04104
M + 6	0.41165	x^6	0.41165**	

* Assumed to be zero.

** This value was used for calculation of x: $x = \sqrt[6]{0.41165} = 0.8625$.

initially, it was assumed that all of the intensity at M (m/e = 628) was due to the unenriched glucose, and the observed intensities above m/e 629 were corrected for the contribution of the naturally occurring isotopic species of the TMS-oxime of unenriched glucose followed by the correction of intensities from isotopes other than ^{13}C from the enriched glucose. The results also indicate the significant differences from the values calculated on the assumption of uniformity. Thus, this sample of [U-^{13}C]glucose is considered to be significantly different from the uniform labelling.

ACKNOWLEDGEMENTS

The author thanks Dr. O. Ito and Dr. K. Okano of The National Institute for Environmental Studies (Tsukuba, Japan) for their help in obtaining the sample of $^{13}CO_2$-fed corn leaves and for ^{13}C analysis with the infrared ^{13}C analyser. This research was supported by a foundation grant from the Ministry of Agriculture, Forestry and Fisheries of Japan (GEP 56-II-2-2).

REFERENCES

1 K. Kumazawa and K. Yanagisawa, *Nippon Dojo Hiryogaku Zasshi*, 52 (1981) 74.
2 K. Biemann, *Mass Spectrometry, Organic Chemical Applications*, McGraw-Hill, New York, 1962, p. 204.
3 H. C. Hill, *Introduction to Mass Spectrometry*, Heyden, London, 1966.
4 T. Curstedt, *Eur. J. Biochem.*, 49 (1974) 355.
5 T. Cronholm, H. Matern, S. Matern and J. Sjövall, *Eur. J. Biochem.*, 48 (1974) 71.
6 R. M. Caprioli, W. F. Fies and M. S. Story, *Anal. Chem.*, 46 (1974) 453A.
7 M. Sano, Y. Yotsui, H. Abe and S. Sasaki, *Biomed. Mass Spectrom.*, 3 (1976) 1.
8 D. E. Matthews and J. M. Hayes, in E. R. Klein and P. D. Klein (Editors), *Proceedings of Third International Conference on Stable Isotopes*, Academic Press, New York, 1979, p. 95.
9 W. J. A. VandenHeuvel, J. L. Smith and J. S. Cohen, *J. Chromatogr. Sci.*, 8 (1970) 567.

10 J. G. Streeter, *Plant Physiol.*, 66 (1980) 471.
11 D. V. Phillips and A. E. Smith, *Can. J. Bot*, 52 (1974) 2447.
12 W. F. Holmes, W. H. Holland, B. L. Shore, D. M. Bier and W. R. Sherman, *Anal. Chem.*, 45 (1973) 2063.
13 E. J. Heron, in E. R. Klein and P. D. Klein (Editors), *Proceedings of the Second International Conference on Stable Isotopes*, 1975, p. 569.

Journal of Chromatography, 241 (1982) 325–332
Elsevier Scientific Publishing Company, Amsterdam — Printed in The Netherlands

CHROM. 14,836

HIGH-RESOLUTION GAS CHROMATOGRAPHY OF METHYLATED RIBONUCLEOSIDES AND HYPERMODIFIED ADENOSINES

EVALUATION OF TRIMETHYLSILYL DERIVATIZATION AND SPLIT AND SPLITLESS OPERATION MODES

THOMAS R. KEMP*
Department of Horticulture, University of Kentucky, Lexington, KY 40546 (U.S.A.)
ROGER A. ANDERSEN
Agricultural Research Service, U.S. Department of Agriculture, and Department of Agronomy, University of Kentucky, Lexington, KY 40546 (U.S.A.)
JAMES OH
Department of Chemistry, University of Kentucky, Lexington, KY 40546 (U.S.A.)
and
THOMAS H. VAUGHN
Agricultural Research Service, U.S. Department of Agriculture and Department of Agronomy, University of Kentucky, Lexington, KY 40546 (U.S.A.)
(First received January 21st, 1982; revised manuscript received February 20th, 1982)

SUMMARY

Methylated ribonucleosides and hypermodified adenosines were trimethylsilylated on chromatographed by high-resolution gas chromatography on a fused-silica capillary column operated in split and splitless modes. Evaluation of micro-silylation (50-μl volume) of methylated ribonucleosides showed that N,O-bis(trimethylsilyl)-trifluoroacetamide (BSTFA) and pyridine at 150°C gave greater yields than silylation with either BSTFA alone or BSTFA and pyridine at 75°C. N-Methyl-N-trimethylsilyltrifluoroacetamide gave lower yields of derivatives of N^6-substituted adenosines, such as N^6-methyladenosine, relative to those obtained with BSTFA. Methylated ribonucleosides generally gave sharp, symmetrical peaks on the SE-54 column operated in the split mode; however, the compounds were not as well resolved as the cytokinin-active hypermodified adenosines on the relatively non-polar SE-54 stationary phase. The splitless operation mode employing a cold trapping procedure (40°C initial temperature) yielded sharp peaks and nanogram quantities of N^6-methyladenosine were detectable. Most hypermodified adenosines separated well from other compounds, although several peaks of unknown composition eluted in the same chromatographic region as the methylated ribonucleosides when the cold trapping splitless technique was used.

INTRODUCTION

A large number of structural modifications of ribonucleosides are found in tRNA from plant, animal and microbial sources and in biological fluids[1–3]. These can

0021-9673/82/0000–0000/$02.75

range from simple methylation of a base or sugar moiety to more complex derivatizations as exemplified by the modified isopentyladenosines termed hypermodified ribonucleosides. The latter compounds function as cytokinins or plant cell division factors[2,3]. It was reported that changes in ribonucleoside methylation in tRNA in animals were associated with cellular differentiation processes and the development of tumorous or autonomous tissues[4,5]. Recent evidence has also indicated the presence of altered patterns of ribonucleoside methylation[6] and an additional cytokinin-active hypermodified adenosine[7] in tRNA of hormone-autonomous plant tissues. As part of a study of changes in ribonucleoside structural modifications in tRNA we are interested in methods of separation of these compounds.

Several investigations have dealt with methods of preparation and conditions for gas chromatographic (GC) separation of trimethylsilyl (TMS) derivatives of the parent nucleic acid bases and their corresponding ribonucleosides[8–15]. Lakings *et al.*[16] studied the efficiency of silylation and separation of several methylated bases. Hattox and McCloskey[17] studied chromatographic behavior of TMS derivatives of naturally occurring and synthetic modified ribonucleosides on two packed GC columns and Chang *et al.*[18] developed a GC method for quantitative analyses of two methylated ribonucleosides.

Cytokinin-active bases and ribonucleosides were silylated and separated on packed GC columns[19–21]. Claeys *et al.*[22] used capillary GC to resolve some permethylated cytokinin bases, and we recently reported[23] separation of cytokinin hypermodified bases and ribonucleosides by fused-silica capillary GC operated in split mode.

In the present investigation we studied reagents and reaction conditions for the preparation of TMS derivatives of ribonucleosides and chromatography of these compounds on high-resolution fused-silica capillary GC in split and splitless operation modes.

EXPERIMENTAL

Chemicals

trans-Ribosylzeatin (tZR), N^6-(Δ^2-isopentenyl)adenosine (IPA), phloretin (Ph), and methylated ribonucleosides including 1-methyladenosine (m^1A), N^6-methyladenosine (m^6A), N^6,N^6-dimethyladenosine (m^6_6A), 3-methylcytidine (m^3C), N^2-methylguanosine (m^2G), 1-methylinosine (m^1I), and 5-methyluridine (m^5U) were purchased from Sigma (St. Louis, MO, U.S.A.). The remaining cytokinin ribonucleosides were generously provided by Dr. J. Corse (USDA, ARS, Albany, CA, U.S.A.). N,O-Bis-(trimethylsilyl)trifluoroacetamide (BSTFA), BSTFA containing 1 % trimethylchlorosilane (TMCS), and N-methyl-N-trimethylsilyltrifluoroacetamide (MSTFA) were purchased from Pierce (Rockford, IL, U.S.A.). Pyridine and acetonitrile were obtained from Regis (Chicago, IL, U.S.A.). Methylene chloride and P_2O_5 were obtained from Fisher Scientific (Pittsburgh, PA, U.S.A.).

Preparation of modified ribonucleoside standards

Stock solutions used for evaluations of relative weight response (RWR) under various silylation conditions were prepared by dissolving 1 mg of each methylated ribonucleoside in 2 ml distilled water, except N^2-methylguanosine, which was dis-

solved in water adjusted to pH 1 with 1 *N* hydrochloric acid. The concentration of each solution was confirmed by calculations based on the UV absorbance at the λ_{max} for each compound and the published absorptivities[24].

Stock solutions of methylated ribonucleosides for long term storage in a freezer were made at the same concentration as above using 75% ethanol as solvent. Cytokinin-active hypermodified adenosines were dissolved in 95% ethanol at a concentration of 0.5 μg/μl.

Micro-silylation of methylated ribonucleosides

The following method was used for determination of RWR values and other chromatographic purposes: 50 μl of methylated ribonucleoside stock solution and 50 μl of IPA solution were concentrated to near dryness under a stream of nitrogen in a 1-ml screw-cap reaction vial. The sample was azeotroped with methylene chloride and then dried over P_2O_5 at 10^{-2} Torr overnight. A 50-μl volume of silylating reagent or 10 μl of solvent plus 40 μl of silylating reagent was added. Silylating reagents were either BSTFA, BSTFA containing TMCS (99:1, v/v) or MSTFA. The solvent was pyridine or acetonitrile. Vials were sealed with PTFE-lined screw caps and heated in an oil bath at 75 or 150°C for 30 min. Cytokinin-active hypermodified adenosines were silylated as described previously[23].

Determinations of RWR values for methylated ribonucleosides

RWR values for methylated ribonucleosides were determined on a Varian Aerograph Series 2100 gas chromatograph equipped with a Hewlett-Packard Model 3380 A integrator. A 0.5–1.0-μg sample of each compound plus IPA internal standard was silylated as described above and chromatographed on a 1.8 m × 2 mm I.D. glass column packed with 3% SP-2250 coated on 100–120 mesh Supelcoport (Supelco, Bellefonte, PA, U.S.A.). Nitrogen was used as carrier gas at a flow-rate of 30 ml/min. The injector temperature was 270°C, the flame ionization detector (FID) temperature was 280°C, and the column oven temperature was varied depending upon compound separation requirements. RWR values were calculated as follows:

$$\text{RWR} = \frac{\text{Peak area of silylated ribonucleoside}}{\text{Weight of silylated ribonucleoside}} \Big/ \frac{\text{Peak area of silylated IPA int. std.}}{\text{Weight of silylated IPA int. std.}}$$

If a methylated ribonucleoside yielded a shoulder or a secondary peak in addition to the major peak when chromatographed on the packed column, the area of the minor peak was included in the calculation of the RWR value. Earlier work on parent ribonucleosides showed that doublet peaks occurred that were composed of two silylated species of a given ribonucleoside[11,15].

Capillary GC of methylated ribonucleosides in split mode

Silyl derivatives of methylated ribonucleosides were chromatographed by high-resolution GC on a 30 m × 0.25 mm I.D. SE-54 (94% methyl, 5% phenyl, and 1% vinyl silicone) fused silica capillary column (J&W Scientific, Rancho Cordova, CA, U.S.A.) operated in the split mode. A microprocessor-controlled Hewlett-Packard 5880A gas chromatograph was used with inlet at 270°C, FID at 280°C, and the

column oven temperature-programmed from 180 to 265 C at 4 C/min after a 2-min initial hold. Helium was used as the carrier and makeup gas; the split ratio was 60:1 and the carrier linear velocity through the column was 31 cm/sec.

Capillary GC of modified ribonucleosides in splitless mode

For splitless operation mode the Hewlett-Packard gas chromatograph containing the SE-54 fused-silica capillary column was used with the inlet temperature at 270°C and FID at 280°C. The inlet purge flow was 1.2 ml/min and the carrier gas linear velocity was 31 cm/sec. The sample was injected with a purge inactivation time of 40 sec and an initial column oven temperature of 40°C. This procedure cold-trapped the silylation reagent (BSTFA) and the organic solvent containing the ribonucleoside sample. After 2 min, the oven was temperature-programmed at 10°C/min to 265°C and then maintained at 265°C for 60 min.

Mass spectrometry (MS)

The numbers of silyl moieties per molecule (molecular weights) of silylated hypermodified ribonucleosides were determined by electron impact using a Hewlett-Packard Model 5985 GC–MS instrument operated at 70 eV or by chemical ionization with a Finnegan Model 3300-6100 GC–MS instrument at 150 eV using methane as reagent gas.

RESULTS AND DISCUSSION

Conditions for silylation

Effects of temperature and solvent composition on the micro-silylation reaction of some methylated ribonucleosides with BSTFA are shown in Table I. Generally, compounds were silylated at 75°C in BSTFA with or without the inclusion of pyridine in the reaction mixture. However, increasing the reaction temperature to 150°C noticeably increased the yield of derivatives in several instances. The presence of pyridine in the reaction mixture at 150°C also improved the yield in several cases.

TABLE I

SOLVENT AND TEMPERATURE EFFECTS ON THE SILYLATION OF SOME METHYLATED RIBONUCLEOSIDES

Values, expressed as FID response (RWR)*

Ribonucleoside	*75°C*		*150°C*	
	BSTFA	*BSTFA–pyridine*	*BSTFA*	*BSTFA–pyridine*
1-Methyladenosine	0.44	0.67	0.84	1.07
N^6-Methyladenosie	1.15	1.10	1.04	1.18
N^6,N^6-Dimethyladenosine	1.53	1.47	1.60	1.66
3-Methylcytidine	0.82	0.82	0.89	1.05
N^2-Methylguanosine	0.51	0.54	0.55	0.59
3-Methyluridine	1.36	1.42	1.59	1.80
5-Methyluridine	0.79	0.76	0.94	0.91

* Relative to internal standard isopentenyladenosine. Each value is mean of two determinations.

Preliminary trials with acetonitrile–BSTFA or pyridine–BSTFA containing 1% TMCS gave results similar to those noted above. Among the compounds tested, methylated derivatives of adenosine and uridine frequently silylated more readily than methylated derivatives of cytidine or guanosine. Examples of compounds which silylated poorly under the micro-reaction conditions are 5-methylcytidine and 1-methylguanosine which yielded weak or nondetectable responses when chromatographed on the SE-54 capillary column. Chang *et al.*[18] reported a high yield for two methylated ribonucleosides, N^2,N^2-dimethylguanosine and 1-methylinosine using a relatively large volume (0.5 ml) of BSTFA and solvent for the silylation reaction.

Silylation of some modified ribonucleosides was also evaluated with MSTFA, also a strong silyl donor. Several compounds gave approximately equal yields of derivatives in both BSTFA and MSTFA at 150°C. However, N^6-substituted adenosines, such as N^6-methyladenosine gave a greater yield (2.8-fold) in BSTFA than in MSTFA. In contrast, when a relatively large amount of guanosine (125 μg) was treated with MSTFA, a 1.8-fold yield increase over that with BSTFA was obtained. A shift in the retention time of the guanosine product with MSTFA indicated the formation of a different silyl derivative.

Capillary GC in split mode

Results of chromatography of several representative silylated methylated ribonucleosides, prepared with BSTFA, on the SE-54 fused silica capillary column are shown in Fig. 1. Each compound (0.75 μg) was injected at a split ratio of 60:1. Most compounds gave sharp, symmetrical peaks in the split mode. However, the first emerging peak which corresponded to 3-methylcytidine was broader than the others. This may have resulted from the incomplete resolution of more than one silylated derivative of this ribonucleoside. The peak corresponding to N^2-methylguanosine was sharp and symmetrical, but the response was relatively low. This probably resulted from a less efficient silylation reaction for this compound. Tests with parent

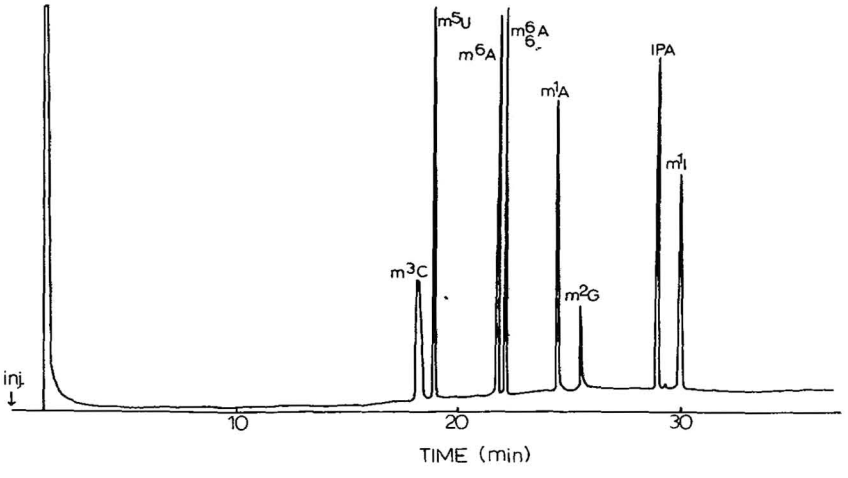

Fig. 1. Chromatogram of BSTFA-prepared silylated modified ribonucleosides on SE-54 fused-silica capillary column using split mode (60:1).

ribonucleosides showed that these compounds overlapped with some methylated ribonucleosides, for example, adenosine eluted with N^6-methyladenosine on the SE-54 column under the split condition. A more polar stationary phase may be useful for separation of these compounds in the split mode conditions. Earlier results[2,3] showed that hypermodified (cytokinin-active) adenosines were obtained longer and separated better on the SE-54 column; these compounds were structurally similar and relatively non-polar (*e.g.*, geometrical isomers of isopentenyl adenosine derivatives).

Capillary GC in splitless mode

The effect of inlet-purge inactivation time on the peak area of *trans*-ribosylzeatin was measured. It was found that a purge inactivation time of at least 20 sec was needed for maximum recovery of the compound under the GC conditions developed for temperature-programmed analysis of the modified ribonucleosides.

Table II lists relative retention times and number of silyl moieties as determined by MS (from molecular weights) of some representative hypermodified adenosines on the SE-54 column operated in the splitless mode. Generally, these compounds separated well using the cold-trapping splitless technique, except *cis*-ribosylzeatin and methylthioisopentenyladenosine which overlapped. Fig. 2 shows a chromatogram of 20 ng each of N^6-methyladenosine and *trans*-ribosylzeatin and the internal standard phloretin which were silylated with BSTFA and then separated on

TABLE II

SEPARATION OF HYPERMODIFIED ADENOSINES (CYTOKININ ACTIVE) BY COLD TRAPPING TECHNIQUE IN SPLITLESS MODE

Column: SE-54 fused-silica capillary.

Compound	*Adenosine substituents*		*No. of TMS moieties per molecule*	*Relative retention time**
	N^6-Amino site	*C-2 site*		
Isopentenyladenosine	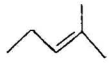	H	3	1.17
2-Methylthioisopentenyladenosine	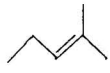	CH_3S-	3	1.59
Dihydroribosylzeatin	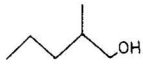	H	4	1.43
cis-Ribosylzeatin	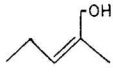	H	4	1.49
trans-Ribosylzeatin	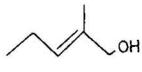	H	4	1.58
cis-2-Methylthioribosylzeatin	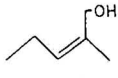	CH_3S-	4	2.17

* Relative to internal standard phloretin.

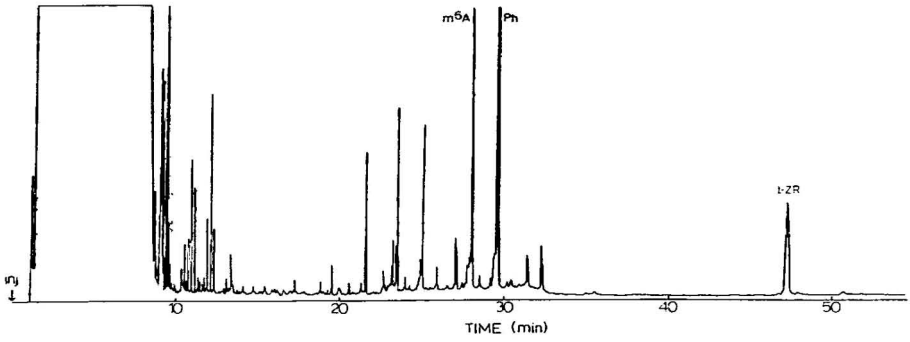

Fig. 2. Chromatogram of silylated derivatives of N^6-methyladenosine, *trans*-ribosylzeatin and the internal standard phloretin, 20 ng each, on SE-54 fused-silica capillary column using cold-trapping splitless technique.

the SE-54 column using the cold-trapping splitless technique. Results with N^6-methyladenosine as well as trials with other methylated ribonucleosides indicated that these compounds eluted in an area where interfering peaks of unknown composition appeared and therefore the method was not as useful for these compounds as for the hypermodified (cytokinin-active) adenosines. However, sharp, symmetrical peaks were obtained for both compounds and *trans*-ribosylzeatin separated well from all other peaks.

The relative FID response for silylated *trans*-ribosylzeatin in the splitless versus split mode of operation described above was 52-fold greater for the splitless operation. Injection of 2 ng of N^6-methyladenosine gave 25% of full scale deflection at maximum instrument sensitivity in the splitless mode.

ACKNOWLEDGEMENTS

The authors are indebted to Dr. Charles Hughes of the University of Kentucky Tobacco and Health Research Institute for GC–MS analyses, and Mary Lowe for technical assitance. This investigation is in connection with a project at the Kentucky Agricultural Experiment Station, and the results are published as Journal Article No. 82-10-3-7. Mention of a trademark, proprietary product, or vendor does not constitute a guarantee or warranty of the product by the U.S. Department of Agriculture and does not imply its approval to the exclusion of other products or vendors that may be suitable.

REFERENCES

1 R. H. Hall, *The Modified Nucleosides in Nucleic Acids*, Columbia University Press, New York, 1971.
2 F. Skoog and R. Schmitz, in G. Litvack (Editor), *Biochemical Actions of Hormones*, Vol. VI, Academic Press, New York, 1979, p. 335.
3 D. S. Letham, in D. S. Letham, P. B. Goodwin and T. J. V. Higgins (Editors), *The Biochemistry of Phytohormones and Related Compounds —A Comprehensive Treatise*, Vol. I, Elsevier, Amsterdam, 1978, p. 205.
4 E. Borek, *Cancer Res.*, 31 (1971) 596.
5 E. Borek and S. J. Kerr, *Advan. Cancer Res.*, 15 (1972) 163.

6 L. H. Jones and T. K. Scott, *Plant Physiol.*, 67 (1981) 535.
7 K. N. Pandey, T. R. Kemp, P. S. Sabharwal and R. A. Andersen, *In Vitro*, 15 (1979) 857.
8 R. I. Hancock and D. L. Coleman, *Anal. Biochem.*, 10 (1965) 365.
9 Y. Sasaki and T. Hashizume, *Anal. Biochem.*, 16 (1966) 1.
10 C. W. Gehrke and C. D. Ruyle, *J. Chromatogr.*, 38 (1968) 473.
11 M. Jacobson, J. F. O'Brien and C. Hedgcoth, *Anal. Biochem.*, 25 (1968) 363.
12 W. C. Butts, *Anal. Biochem.*, 46 (1972) 187.
13 V. Miller, V. Pacáková and E. Smolková, *J. Chromatogr.*, 119 (1976) 355.
14 C. W. Gehrke and A. B. Patel, *J. Chromatogr.*, 123 (1976) 335.
15 C. W. Gehrke and A. B. Patel, *J. Chromatogr.*, 130 (1977) 103.
16 D. B. Lakings, C. W. Gehrke and T. P. Waalkes, *J. Chromatogr.*, 116 (1976) 69.
17 S. E. Hattox and J. A. McCloskey, *Anal. Chem.*, 46 (1974) 1378.
18 S. Y. Chang, D. B. Lakings, R. W. Zumwalt, C. W. Gehrke and T. P. Waalkes, *J. Lab. Clin. Med.*, 83 (1974) 816.
19 B. H. Most, J. C. Williams and K. J. Parker, *J. Chromatogr.*, 38 (1968) 136.
20 J. G. Purse, R. Horgan, J. M. Horgan and P. F. Wareing, *Planta*, 132 (1976) 1.
21 N. Murai, B. J. Taller, D. J. Armstrong, F. Skoog, M. A. Micke and H. K. Schnoes, *Plant Physiol.*, 60 (1977) 197.
22 M. Claeys, E. Messens, M. van Montagu and J. Shell, in A. P. de Leenheer, R. R. Roncucci and C. van Peteghem (Editors), *Quantitative Mass Spectrometry in Life Sciences II*, Elsevier, Amsterdam, 1978, p. 409.
23 T. R. Kemp and R. A. Andersen, *J. Chromatogr.*, 209 (1981) 467.
24 D. B. Dunn and R. H. Hall, in G. D. Fasman (Editor), *Handbook of Biochemistry and Molecular Biology —Nucleic Acids*, Vol. 1, CRC Press, Cleveland, OH, 1975, p. 65.

Journal of Chromatography, 241 (1982) 333–344
Elsevier Scientific Publishing Company, Amsterdam — Printed in The Netherlands

CHROM. 14,774

INTERACTIONS BETWEEN CALMODULIN AND IMMOBILIZED PHENOTHIAZINES

APPLICATION TO THE PURIFICATION OF CALMODULIN FROM VARIOUS TISSUES BY AFFINITY CHROMATOGRAPHY*

CÉCILE ROCHETTE-EGLY
INSERM, Unité 61, Avenue Molière, 67200 Strasbourg (France)
EGISTO BOSCHETTI
IBF Pharmindustrie, 35 Avenue Jean-Jaurès, 92390 Villeneuve la Garenne (France)
PAUL BASSET
Centre de Neurochimie du CNRS, 5 Rue Blaise Pascal, 67000 Strasbourg Cédex (France)
and
JEAN-MARC EGLY*
INSERM, Unité 184, Laboratoire de Génétique Moléculaire des Eucaryotes du CNRS, 11 Rue Humann, 67085 Strasbourg (France)
(Received January 29th, 1982)

SUMMARY

The ability of a number of antipsychotic drugs such as phenothiazines to bind to calmodulin with high affinity in a calcium-dependent manner was applied to the study of the nature of their interactions with calmodulin. Thus, a series of phenothiazine derivatives and analogues were immobilized on agarose and examined for their binding characteristics to calmodulin. The binding of calmodulin to fluphenazine, perphenazine and 7-aminotriflupromazine involved on the one hand non-specific electrostatic interactions which are abolished by increasing the eluent salt concentration, and on the other hand, Ca^{2+}-dependent interactions which are reversed by EGTA addition. However, the Ca^{2+}-dependent binding of calmodulin was less specific with phenothiazine structural analogues (Neutral Red, diphenylamine) and was suppressed with other phenothiazine derivatives (thionine, Azure C, Toluidine Blue) or analogues (Brilliant Cresyl Blue). It is suggested that the calcium-dependent interactions between calmodulin and drugs involve a charge transfer π–π interaction which may be modulated by the electron donor–acceptor properties of the substituents of the aromatic ring. Affinity chromatography using immobilized fluphenazine was also used as the basis for the purification of calmodulin from a number of tissues in a rapid one-step procedure.

* Part of these results were presented at the *Fourth Symposium on Affinity Chromatography and Related Techniques, Veldhoven, The Netherlands, June 1981.*

0021-9673/82/0000–0000/$02.75

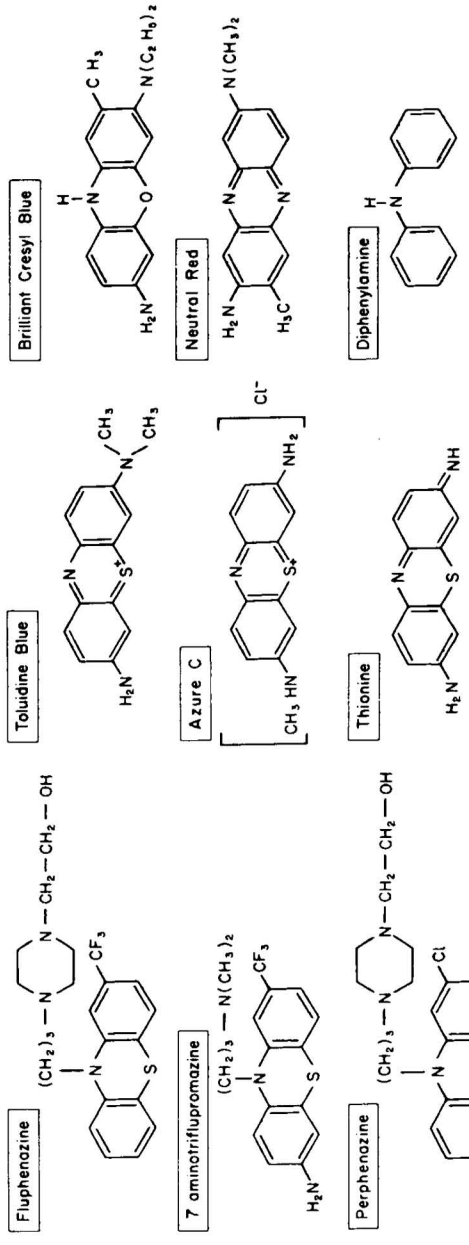

Fig. 1. Phenothiazine derivatives and structural analogues.

INTRODUCTION

The role of calcium ions in regulating the response of eukaryotic cells to external stimuli is now well established[1]. Calcium appears to exert its biological effects through binding to calcium-dependent proteins[2,3]. Recent studies have shown that an ubiquitous calcium-binding protein, calmodulin, exists in eukaryotic cells and regulates a number of enzymes, including 3′,5′ cyclic nucleotide phosphodiesterase[4], adenyl cyclase[5], myosin light chain kinase[6,7], membrane ATPase[8], phosphorylase kinase[9] and a nicotinamide adenine dinucleotide kinase[10].

Calmodulin is an acidic low-molecular-weight protein, composed of 148 amino acids. It lacks cysteine and tryptophan and contains one mole of the unusual amino acid N^{ϵ}-trimethyllysine[11]. Chemical and physical studies have shown that calmodulin binds 4 moles of calcium[12]. This binding produces large changes in calmodulin conformation[13–16] and makes the calmodulin–Ca^{2+} complex capable of activating the calmodulin-dependent systems. Another property ascribed to calmodulin is its ability to bind a class of neuroleptic drugs, the phenothiazines[17], in a calcium-dependent manner through a still unknown mechanism. In the present study, this interesting property was used as the basis (i) for improving the understanding of the nature of the interactions between phenothiazines and calmodulin and (ii) for designing an efficient support for affinity chromatography in order to purify calmodulin from various tissue extracts in a rapid one-step procedure. Thus, a series of phenothiazine derivatives and structural analogues were selected and tested for their ability to inhibit calmodulin activity. Then, after immobilization on a matrix, the characteristics of their binding to calmodulin were examined.

MATERIAL AND METHODS

Materials

Fluphenazine, perphenazine and 7-aminotriflupromazine were kindly provided by E. R. Squibb and Sons (Princeton, NJ, U.S.A.). Toluidine Blue, Azure C, Thionine, Brilliant Cresyl Blue, Neutral Red and diphenylamine were obtained from Aldrich-Europe (Beerse, Belgium). [8-^{3}H]cyclic GMP (38.7 Ci/mmole) was purchased from New England Nuclear Corporation (Boston, MA, U.S.A.). Agarose beads (Ultrogel A-6) were obtained from Reactifs-IBF, France, Acriflavin–Sephadex G-25 was prepared according to the previously described technique[18]. The scintillation mixture used for the radioactivity countings (Monophase 40) was from Packard Instruments International SA (Rungis, France) and ampholines from LKB (Bromma, Sweden). The Ram testis calmodulin used in this study was very generously provided by Dr. J. G. Demaille[19].

Preparation of gels for affinity chromatography

Phenothiazine derivatives and structural analogues (see Fig. 1) were immobilized on 6% agarose beads (Ultrogel A-6) according to the epichlorohydrin method of Sundberg and Porath[18,20]. The final conjugates thus obtained contained 1.5–10 μmoles of drug per ml of gel[21] by HCl titration. In particular, the fluphenazine Ultrogel conjugate used for the purification of calmodulin contained 3.7 μmoles of fluphenazine per ml of gel and had a binding capacity of 4 mg of calmodulin per ml of resin.

Affinity chromatography of calmodulin

Tissues (liver, heart, pancreas, etc.) were homogenized in three volumes of buffer A (20 m*M* Tris–HCl buffer pH 7.0, 1 m*M* $CaCl_2$, 1 m*M* 2-mercaptoethanol) and the homogenate was centrifuged at 100,000 *g* for 60 min. The supernatant was heat-treated at 90°C for 1 min. The resulting suspension was then recentrifuged for 20 min at 24,000 *g* and applied to a column (3 × 1.14 cm) of immobilized phenothiazine derivative or analogue which had been equilibrated with buffer A.

After the sample was applied, the column was washed with ten column volumes of buffer A, and then with the same buffer containing 0.3 *M* NaCl until the A_{280} of the eluent dropped to its baseline level. Calmodulin was then eluted by a buffer containing 20 m*M* Tris–HCl pH 7.0, 1 m*M* 2-mercaptoethanol, 0.3 *M* NaCl and 10 m*M* ethyleneglycol bis(β-aminoethyl ether)-N,N′-tetraacetic acid (EGTA). Fractions (3 ml) were collected at a flow-rate of 12 ml/h and aliquots (50 μl) were tested for their ability to activate the calmodulin-dependent phosphodiesterase. The active fractions were pooled, adjusted to 10 m*M* $CaCl_2$, extensively dialysed against buffer A and lyophilized. All operations were performed at 4°C.

Phosphodiesterase assay for calmodulin

Calmodulin was assayed by its ability to activate a standard quantity (5 μg) of a calmodulin-dependent phosphodiesterase from rat pancreas prepared according to Kakiuchi *et al.*[22].

The standard reaction mixture contained in a final volume of 0.1 ml: 50 m*M* Tris–HCl buffer (pH 7.5), 30 μ*M* Ca^{2+}, 200 m*M* NH_4Cl, 1 μ*M* [^{3}H]cyclic GMP ($1 \cdot 10^5$ cpm per 0.1 nmol), 5 μg phosphodiesterase and appropriate amounts of calmodulin. The reaction was initiated by addition of the substrate and carried out at 30°C for 10 min, then stopped by boiling for 1 min. The entire contents of the assay tube were applied onto acriflavin–Sephadex G-25 gel packed in 5-cm-high pasteur pipettes equilibrated in 0.2 *M* ethylmorpholine buffer (pH 7.0) containing 0.3 *M* NaCl. The 5′-GMP formed was eluted with the same buffer as previously described[23]. Results were calculated as nmoles of 5′-GMP formed per 10 min and per mg of enzyme.

Other methods

Sodium dodecyl sulphate (SDS) (0.1%), 10–20% linear gradient polyacrylamide gel electrophoresis was performed in slab gels with the buffer system described by Maizel[24]. Isoelectrofocusing (pH 3.6–5.2) was performed in 5% polyacrylamide gel slabs according to Basset *et al.*[25].

RESULTS

A number of antipsychotic phenothiazine drugs are capable of inhibiting several calmodulin-activated systems[17,26,27]. As shown in Fig. 2, phenothiazine derivatives such as fluphenazine, perphenazine and 7-aminotriflupromazine (see Fig. 1) antagonized the calmodulin-stimulated cyclic nucleotide phosphodiesterase. Concentrations as low as 10 μ*M* were sufficient to produce a 50% decrease in the activation of phosphodiesterase by calmodulin. However, other phenothiazine derivatives including Toluidine Blue, Azure C and thionine were without effect on phosphodiesterase

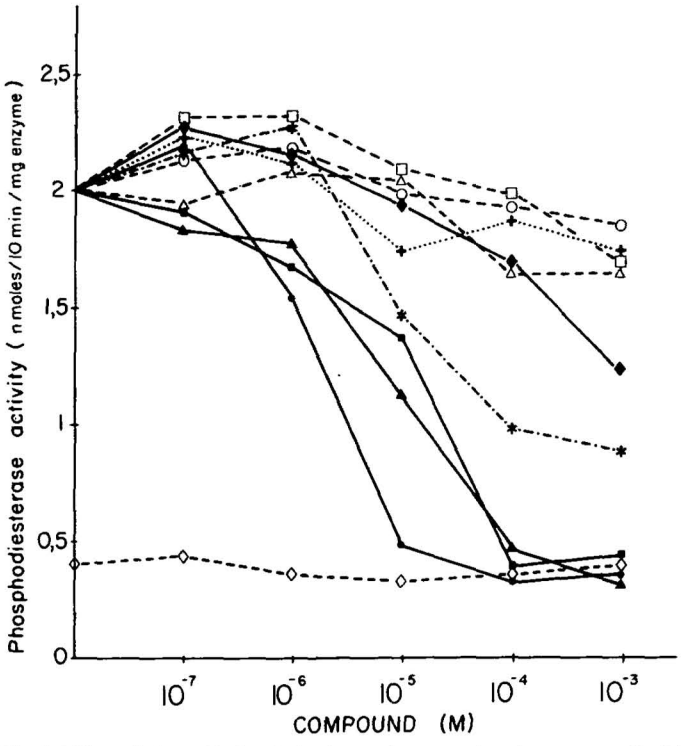

Fig. 2. Effects of phenothiazine derivatives and structural analogues on cyclic GMP phosphodiesterase in the presence of calmodulin. The assay medium contained 5 μg cGMP phosphodiesterase from rat pancreas, and 0.1 μg ram testis calmodulin. ◇--◇, Basal activity in the absence of calmodulin; ●—●, fluphenazine; ■—■, perphenazine; ▲—▲, 7-aminotriflupromazine; O – – O, Toluidine Blue; □ – – □, Azure C; △ – – △, thionine; + ·· +, Brilliant Cresyl Blue; ✳–·–✳, Neutral Red; ◆– ◆, diphenylamine. Each point is the mean from three experiments.

activity even at concentrations as high as 1 mM. In addition, structural analogues such as Brilliant Cresyl Blue and diphenylamine were also uneffective, whereas Neutral Red inhibited calmodulin activity by 50% at about 50 μM. None of the phenothiazine derivatives or analogues affected the phosphodiesterase activity in the absence of calcium (results not shown).

According to these results the phenothiazine derivatives and structural analogues mentioned above were also tested for their calmodulin-binding capacity. They were immobilized on 4% agarose beads using the epichlorhydrin method, which prevents secondary electrostatic interactions, in contrast to the cyanogen bromide method[28].

Affinity chromatography of calmodulin on immobilized phenothiazine derivatives

To compare the binding of calmodulin to phenothiazine derivatives, extracts prepared from rat liver were applied to immobilized phenothiazines in the presence of $CaCl_2$. Fig. 3A illustrates a typical elution profile for the chromatography of rat liver calmodulin on fluphenazine–agarose. With extensive washing of the column in the presence of Ca^{2+}, most of the applied protein was eluted and the absorbance of the

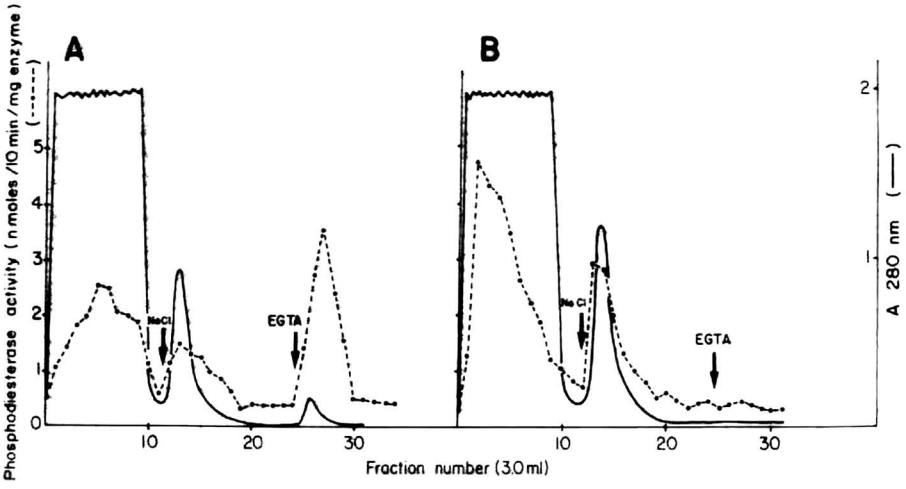

Fig. 3. Phenothiazine–agarose chromatography of rat liver calmodulin. A heat-treated extract of rat liver was applied on a phenothiazine column as described in Materials and methods. The column was washed with the equilibration buffer (buffer A) followed by the same buffer containing 0.3 *M* NaCl and then eluted by replacement of calcium by 10 m*M* EGTA in the buffer. Column: 3 × 1.14 cm. Flow-rate: 12 ml h. 3-ml fractions were collected. Chromatography was followed spectrophotometrically at 280 nm. Aliquots (50 µl) were tested for their ability to activate the calmodulin-dependent phosphodiesterase. A, Fluphenazine–agarose; B, Azure C–agarose.

eluent dropped to zero. As shown by the phosphodiesterase test (Fig. 3A) and by SDS polyacrylamide gel electrophoresis (Fig. 4), some calmodulin eluted during the salt wash. When buffer containing 10 m*M* EGTA was applied to the column, a small peak was eluted. Fractions from this peak were shown by gel electrophoretic analysis to contain a single low-molecular-weight polypeptide (Fig. 4) which stimulated the calmodulin-dependent phosphodiesterase preparation (Fig. 3A).

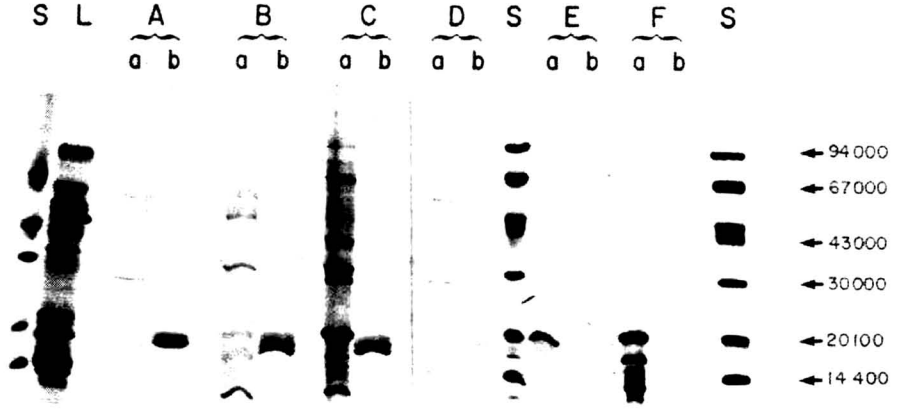

Fig. 4. 0.1 % SDS, 10–20 % polyacrylamide linear gradient gel electrophoresis of NaCl (a) and EGTA (b) peaks eluted from immobilized phenothiazine derivatives. S = Standards; L = rat liver extract; A = fluphenazine–agarose; B, perphenazine–agarose; C = 7-aminotriflupromazine agarose; D = Toluidine Blue–agarose; E = Azure C–agarose; F = thionine–agarose.

Similar chromatographic profiles were obtained with immobilized perphenazine and 7-aminotrifluprom azine, these compounds differing from fluphenazine by the halogen in position 2 for the former, and the N(10) lateral chain for the latter. As shown by electrophoresis on SDS–polyacrylamide gels (Fig. 4), some calmodulin was eluted during the salt wash, but most was recovered as a single protein in the EGTA elution peak.

By contrast, with other immobilized phenothiazine derivatives such as Toluidine Blue, Azure C and thionine which lack halogen of the 2 position and lateral chain at N(10), the elution profiles showed a different pattern (Fig. 3B). Some calmodulin was retained on the column without calcium dependence and was eluted during the salt wash, simultaneously with other components, but none was recovered in the EGTA fractions (Fig. 4).

Affinity chromatography of calmodulin on immobilized phenothiazine structural analogues

Phenothiazine analogues such as Brilliant Cresyl Blue and Neutral Red differing from phenothiazines by the substituents on the aromatic ring were also immobilized on agarose beads. As shown in Fig. 5, with Brilliant Cresyl Blue, some calmodulin was retained on the column without calcium dependence and eluted during the salt wash, but none was recovered in the EGTA fractions. However, with im-

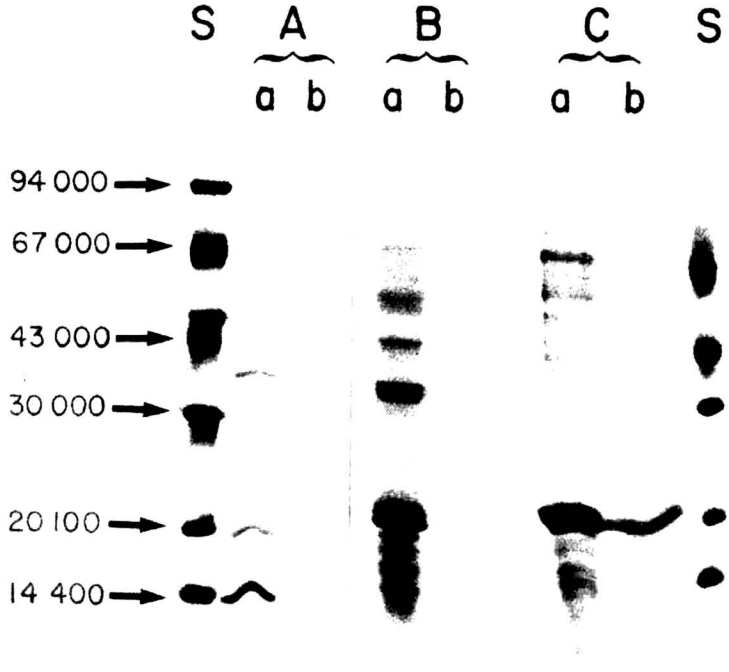

Fig. 5. 0.1 % SDS, 10–20 % polyacrylamide gradient gel electrophoresis of NaCl (a) and EGTA (b) peaks eluted from immobilized phenothiazine structural analogues. S = Standards; A = Brilliant Cresyl Blue–agarose; B = Neutral Red–agarose; C = diphenylamine–agarose.

mobilized Neutral Red and diphenylamine some calmodulin was retained on the column and eluted with EGTA, but several other components coeluted with calmodulin (Fig. 5).

Properties of calmodulins purified by affinity chromatography on fluphenazine–agarose

According to the above results, immobilized fluphenazine was used as the basis for the purification of calmodulin from a number of tissues by affinity chromatography. By this method, homogeneous calmodulin was obtained from bovine brain, rat liver, rat pancreas or rat heart. As isolated, in the presence of 10 m*M* EGTA, all calmodulins migrated with the same mobility as standard ram testis calmodulin, showing a single Coomassie Blue staining band in polyacrylamide gels, corresponding to an apparent molecular weight of approximately 19,500 (Fig. 6). In addition, as previously reported by Burgess *et al.*[29] and by Autric *et al.*[19], these calmodulins showed a different migration rate when electrophoresis was carried out in the presence of calcium. When subjected to isoelectrofocusing in 5% polyacrylamide gels, all calmodulins migrated as single bands with a p*I* of about 4.2 (Fig. 7).

A widely used functional test for calmodulin is its ability to activate preparations of calmodulin-dependent cyclic nucleotide phosphodiesterase in a calcium-dependent manner. Fig. 6 shows that the activation curves for the various calmodulins obtained by affinity chromatography are very similar to that obtained for standard ram testis calmodulin. The calmodulins increased the activity of the phosphodiesterase preparation 4–5-fold. No stimulation occurred in the absence of calcium (data not shown).

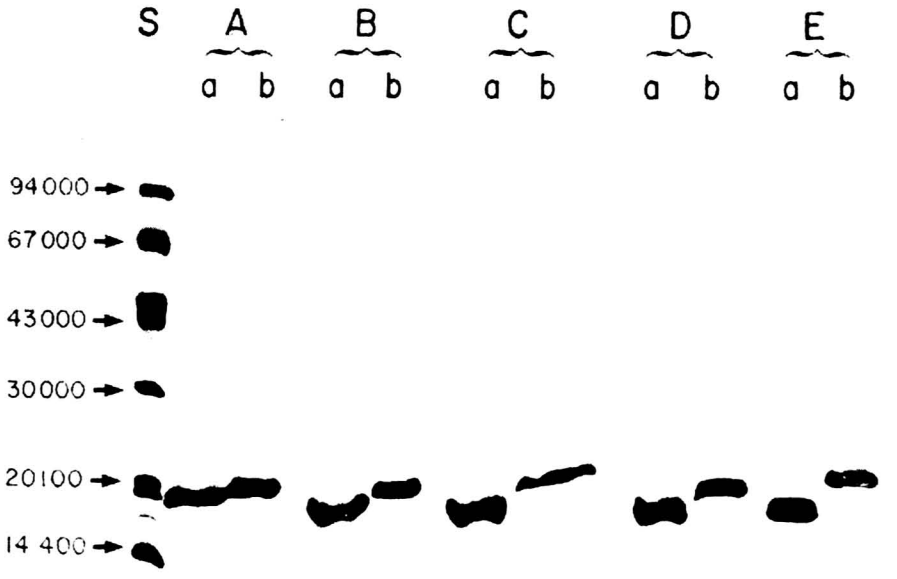

Fig. 6. 0.1% SDS, 10–20% polyacrylamide linear gradient gel electrophoresis of purified calmodulins (5 μg) in the presence of 10 m*M* $CaCl_2$ (a) or 10 m*M* EGTA (b). S = Standards; A = ram testis calmodulin; B = bovine brain calmodulin; C = rat liver calmodulin; D = rat pancreas calmodulin; E = rat heart calmodulin.

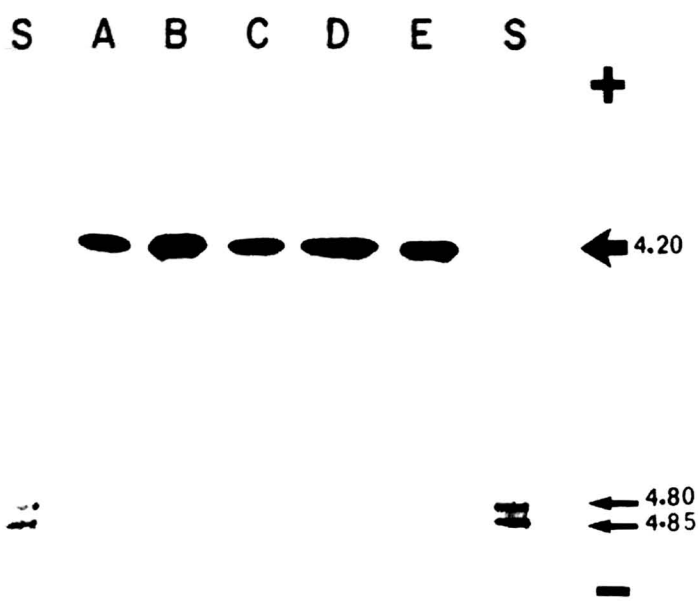

Fig. 7. Isoelectrofocusing (pH 3.6–5.2) of purified calmodulins (10 μg) on 5% polyacrylamide gels. S = Standard albumin; A–E as in Fig. 6.

DISCUSSION

The present report describes the use of affinity chromatography for studying the interactions between phenothiazines or analogues and calmodulin. By this method, immobilized phenothiazine derivatives substituted by an halogen in position 2 and a lateral chain at N(10) (fluphenazine, perphenazine, 7-aminotriflupromazine) were found to have a similar chromatographic behaviour and to bind calmodulin with high affinity and specificity. This binding involves, on the one hand, non-specific electrostatic interactions which are abolished by increasing the eluent salt concentration, and on the other hand, Ca^{2+}-dependent interactions which are reversed by EGTA addition. Although various non-specifically bound proteins were eluted simultaneously with calmodulin by increasing the salt concentration, calmodulin obtained by EGTA elution was homogeneous.

The use of immobilized phenothiazine derivatives and structural analogues was helpful in the understanding of the nature of the interactions between calmodulin and phenothiazines. When the halogen substituents (electron donors) were suppressed and NH_2, $NHCH_3$ or $N(CH_3)_2$ groups (electron acceptors) were introduced in the molecule, the phenothiazine derivatives thus obtained (Toluidine Blue, Azure C, thionine) did not bind calmodulin in a calcium-dependent manner, since no calmodulin was obtained by EGTA elution. However, they kept their ability to bind calmodulin through non-specific electrostatic interactions. Further suppression of the sulphur in the heterocycle and its replacement by oxygen (as in Brilliant Cresyl Blue) did not alter these electrostatic interactions. However, when the sulphur was replaced by nitrogen in the heterocycle (as in Neutral Red) the calcium-dependent interactions

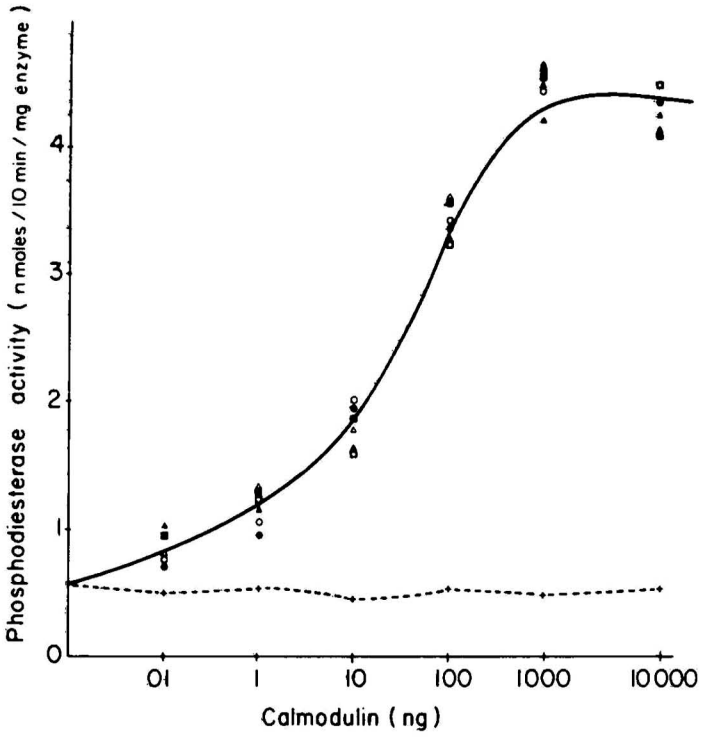

Fig. 8. Activity of rat pancreas cyclic GMP phosphodiesterase in the absence (+--+) and in the presence of various amounts of calmodulin from rat testis (●), bovine brain (▲), rat brain (■), rat liver (○), rat pancreas (△) and rat heart (□). All assays contained 30 μM calcium and 5 μg phosphodiesterase. Each point is the mean from three experiments.

were restored but the affinity and the specificity of the binding remained poor, since contaminants coeluted with calmodulin at the EGTA step. The same phenomenon was observed with diphenylamine which lacks electron acceptor–donor substituents and the sulphur.

From these results, two aromatic rings joined by a nitrogen as in diphenylamine seem necessary for drugs to interact in a calcium-dependent manner with calmodulin. Furthermore, electron donor (halogen) substituents increase the affinity and the specificity of the calcium-dependent binding of calmodulin. By contrast, electron attractor (amino) substituents decrease these properties. Therefore, the calcium-dependent interactions between calmodulin and drugs seem to involve a charge transfer π–π interaction which may be modulated by the electron donor–acceptor properties of the substituents of the aromatic rings. According to these results, the drugs which bind calmodulin in a calcium-dependent manner with the highest affinity and specificity are the phenothiazine derivatives substituted by an halogen (fluphenazine, perphenazine, 7-aminotriflupromazine). Furthermore, these drugs have the highest capacity to antagonize the calmodulin-stimulated systems. These results are in agreement with recent reports[14,16] providing evidence that, when binding to calmodulin, calcium induces conformational transitions affecting a number of aromatic residues (phenylalanine). These conformational changes would be responsible for the

binding of certain aromatic ligands such as phenothiazines[13–16] which then antagonize the interaction of calmodulin with its target enzymes.

Affinity chromatography using immobilized antipsychotic drugs is a valuable tool not only for studying the nature of the interactions between calmodulin and drugs but also for the search for new calmodulin-binding drugs. Furthermore, this procedure can also be used for the purification of calmodulin from various tissues as previously described by Jamieson and Vanaman[30] and by Charbonneau and Cormier[31]. In the present study, with fluphenazine coupled to the agarose matrix by the epichlorhydrin method[18], which avoids the non-specific electrostatic secondary interactions displayed by the cyanogen-bromide coupling method[28,30], homogeneous calmodulin was rapidly obtained from a number of tissue sources in only one step. All preparations of calmodulin prepared by fluphenazine–agarose affinity chromatography showed physical and chemical properties (molecular weight, acidity, heat stability and biological activity) similar to those of previously characterized mammalian calmodulins[32,33], suggesting that this procedure can be employed for the purification of calmodulin from any tissue source.

ACKNOWLEDGEMENTS

The authors are indebted to Dr. J. G. Demaille for reading the manuscript and to Professor J. Porath for many valuable suggestions for performing experiments. They also wish to thank J. L. Plassat for the SDS–polyacrylamide gels and Squibb and Sons Inc. for the gift of fluphenazine, perphenazine and 7-aminotriflupromazine.

REFERENCES

1 M. J. Berridge, *Advan. Cyclic Nucl. Res.*, 6 (1975) 1–98.
2 W. Y. Cheung, *Science*, 207 (1980) 19–27.
3 A. R. Means and J. R. Dedman, *Nature (London)*, 285 (1980) 73–77.
4 W. Y. Cheung, *J. Biol. Chem.*, 246 (1971) 2859–2869.
5 C. O. Brostrom, Y. C. Huang, B. M. Cl. Breckenridge and D. J. Wolff, *Proc. Nat. Acad. Sci. U.S.*, 72 (1975) 64–68.
6 R. Dabrowska, J. M. F. Sherry, D. K. Aromatorio and D. J. Hartshorne, *Biochemistry*, 17 (1978) 253–258.
7 M. P. Walsh, B. Vallet, F. Autric and J. G. Demaille, *J. Biol. Chem.*, 254 (1979) 12136–12144.
8 H. W. Jarrett and J. T. Penniston, *J. Biol. Chem.*, 253 (1978) 4676–4682.
9 P. Cohen, A. Burchell, J. G. Foulkes, P. T. W. Cohen, T. C. Vanaman and A. C. Nairn, *FEBS Lett.*, 92 (1978) 287–293.
10 J. M. Anderson, H. Charbonneau, H. P. Jones, R. O. McCann and J. M. Cormier, *Biochemistry*, 19 (1980) 3113–3120.
11 C. B. Klee, *Calcium and Cell Function*, 1 (1980) 59–77.
12 T. M. Crouch and C. B. Klee, *Biochemistry*, 19 (1980) 3692–3698.
13 D. C. Laporte, B. M. Wierman and D. R. Storn, *Biochemistry*, 19 (1980) 3814–3819.
14 K. B. Seamon, *Biochemistry*, 19 (1980) 207–215.
15 T. Tanaka and H. Hidaka, *J. Biol. Chem.*, 255 (1980) 11078–11080.
16 C. B. Klee, *Biochemistry*, 16 (1977) 1017–1024.
17 B. Weiss and R. M. Levin, *Advan. Cyclic Nucl. Res.*, 9 (1978) 285–302.
18 J.-M. Egly and J. Porath, *J. Chromatogr.*, 168 (1979) 35–47.
19 F. Autric, C. Ferraz, M. C. Kilhoffer, J. C. Cavadore and J. G. Demaille, *Biochim. Biophys. Acta*, 631 (1980) 139–147.
20 L. Sundberg and J. Porath, *J. Chromatogr.*, 90 (1974) 87–98.
21 E. Boschetti, unpublished results.

22 S. Kakiuchi, R. Yamazaki, Y. Teshima, K. Uenishi and E. Miyamoto, *Biochem. J.*, 146 (1975) 109–120.
23 C. Rochette-Egly and J. M. Egly, *J. Cyclic Nucl. Res.*, 6 (1980) 335–345.
24 J. V. Maizel, *Methods Virol.*, 5 (1971) 180.
25 P. Basset, Y. Beuzard, M. C. Garel and J. Rosa, *Blood*, 51 (1978) 971–982.
26 K. Gietzen, A. Mansard and H. Bader, *Biochem. Biophys. Res. Commun.*, 94 (1980) 674–681.
27 B. D. Roufogalis, *Biochem. Biophys. Res. Commun.*, 98 (1981) 607–613.
28 R. Jost, T. Miron and M. Wilchek, *Biochim. Biophys. Acta*, 362 (1974) 75–82.
29 W. H. Burgess, D. K. Jemiolo and R. H. Kretsinger, *Biochim. Biophys. Acta*, 623 (1980) 257–270.
30 G. A. Jamieson and M. J. Vanaman, *Biochem. Biophys. Res. Commun.*, 90 (1979) 1048–1056.
31 H. Charbonneau and M. J. Cormier, *Biochem. Biophys. Res. Commun.*, 90 (1979) 1039–1047.
32 C. B. Klee, T. H. Crouch and P. G. Richman, *Annu. Rev. Biochem.*, 49 (1980) 489–515.
33 D. M. Watterson, P. A. Mendel and T. C. Vanaman, *Biochemistry*, 19 (1980) 2672–2676.

Journal of Chromatography, 241 (1982) 345–359
Elsevier Scientific Publishing Company, Amsterdam — Printed in The Netherlands

CHROM. 14,724

AMINO ACID ANALYSES BY HIGH-PERFORMANCE LIQUID CHROMATOGRAPHY

AN EVALUATION OF THE USEFULNESS OF PRE-COLUMN Dns DERIVATIZATION

CATHARINA DE JONG and GRAHAM J. HUGHES
Laboratorium für Biochemie der Eidgenössischen Technischen Hochschule, ETH-Zürich, CH-8092 Zürich (Switzerland)
and
ERIKA VAN WIERINGEN and KENNETH J. WILSON*
Biochemisches Institut der Universität Zürich, Rämistrasse 74, CH-8001 Zürich (Switzerland)
(Received January 13th, 1982)

SUMMARY

The utility of pre-column amino acid Dns derivatization, liquid chromatographic separation and subsequent quantitation has been evaluated. Relative to the more conventional method, *e.g.*, the chromatography of free amino acids on ion-exchange resins and post-column detection, the techniques are equally suitable when beginning with nanomole amounts of material. At the lower picomole level, an area where few if any analyzers can perform routinely, the results are significantly better. Not only is the amino acid composition expected from an investment of 100–300 pmol of peptide but also the identification of the amino-terminal residue. The Dns modifications have been performed under conditions very similar to those described by Tapuhi *et al.* (*J. Chromatogr.*, 205 (1981) 325–337 and *Anal. Biochem.*, 115 (1981) 123–129) which ensure complete modification. Reversed-phase high-performance liquid chromatography was carried out on a Brownlee Aquapore RP-300 column, employing a gradient of methyl ethyl ketone–2-propanol at 55°C, under conditions which allow for the separation of all Dns derivatives expected from a "normal" peptide/protein hydrolysate.

INTRODUCTION

The quantitation of amino acid concentrations from such widely differing sources as grains, physiological fluids and hydrolyzed peptides/proteins has for years relied on the method developed by Spackman *et al.*[1]. Here the amino acids are chromatographically separated on a cation-exchange resin, mixed with ninhydrin as they are eluted, and heated; the absorbance of the Ruhemann's purple complex is then measured photometrically. Concentrations are calculated by comparing the

0021-9673/82/0000–0000/$02.75

TABLE I

RECENT METHODOLOGY FOR AMINO ACID ANALYSIS UTILIZING HPLC EQUIPMENT

	Chromatographic conditions		*Detection*	*Sensitivity limits (pmol)*	*Analysis times (min)*	*Remarks*	*Ref.*
	Column support	*Buffers**					
I	Free amino acids						
	1 NH_2-bonded phase	KH_2PO_4–AN gradient	200 nm (UV)	Not given	30	N, Q and G poorly separated	4
	2 RP-18	Ion-pairing-AN–MeOH	Post-column (OPA)	< 40	30	E, G and T poorly separated	5
	3 Cation exchange	Sodium formate, step gradient	Post-column (OPA)	10	45	All amino acids separated	3
II	Dns-amino acid derivatives						
	1 RP-8	Sodium acetate–phosphate–AN gradient	Fluorescence	>1000	58	Adequate separation; low *M* value	6
	2 RP-18	MeOH–THF–AcOH–TEA gradient	Fluorescence	Not given	40	Good separation of all amino acids; comment that can be used for pico- and femtomole ranges	7
III	OPA-amino acid derivatives						
	1 RP-18	Na_2HPO_2–AN gradient	Fluorescence	5	45	T and G not separated	8
	2 Several RP-supports	TEA–AcOH–AN gradients	Fluorescence	25	50	Chromatographic conditions with several different supports tested	9

* Abbreviations: AcOH = acetic acid; AN = acetonitrile; MeOH = methanol; TEA = triethylamine; THF = tetrahydrofuran.

peak areas in the sample with those for known concentrations of the same amino acids in a standard. Instruments utilizing this basic method have been improved over the years from the standpoints of both sensitivity and shorter analysis times. Changes in resin synthesis and sizing methods, reduction of the column dimensions, advances in photometer design and higher chemical purity have all been significant contributing factors toward improving the technique. The introduction of fluorescence detection methods have, in turn, provided another 5–10 fold increase in sensitivity (see Benson[2] for a review of some of these points). Most commercially available instruments are currently capable of performing routine analyses at the *ca.* 500 pmol level within 60–90 min.

Recent advances in high-performance liquid chromatography (HPLC) technology have also provided instrumentation suitable for utilization in amino acid analysis (see Table I). In a previous report[3] the conversion of a dual-pump, automated HPLC instrument into a highly sensitive (> 10 pmol), quick (60 min) analyzer was described. The chromatography was carried out on a Durrum DC-4A resin, and *o*-phthalaldehyde (OPA) was used as the detection reagent. A variable-temperature water-bath, buffer selector valve, fluorometer and microprocessor interfacing unit were the additional items required. We have subsequently improved upon these results through the substitution of Kontron AS-70 (7 μm) resin and the utilization of either isocratic or gradient programmes for amino acid elution[10].

Other approaches have been to use various silica derivatives as the chromatographic support material (Table I). Free amino acids have been separated using a gradient on NH_2 silica employing UV detection[4], and on reversed-phase (RP) supports with post-column OPA derivatization[5]. Pre-column derivatizations with Dns chloride (Dns-Cl)[6,7,11–14] followed by RP-HPLC have also been investigated. Although yielding fluorescent amino acid derivatives which reportedly can be detected in the low femtomole range by chemiluminescence[15], there appear to be a number of serious drawbacks inherent to using a pre-column reaction with either Dns-Cl or OPA[8,9]: (1) no reaction, incomplete reaction, and/or formation of secondary peaks from the same amino acid; (2) lack of stability of the derivatives with respect to time, solvent or exposure to light; (3) widely differing detector responses for equal amounts of derivative; and (4) introduction of contamination in the form of amino acids or reaction byproducts during the derivatization process. None of these needs serious consideration when a post-column reaction is used.

The purpose of this communication is to compare the suitability of (a) pre-column Dns derivatization and subsequent RP-HPLC separations of the derivatives with (b) post-column OPA or ninhydrin detection of amino acids separated by ion-exchange chromatography. As will be shown, each method has its own advantages, and their utilities depend on the specific application.

EXPERIMENTAL

Chemicals and buffers

Dns-Cl, Li_2CO_3 and methylamine–HCl were purchased from Fluka (Buchs, Switzerland), methyl ethyl ketone "LiChrosolv" from Merck (Darmstadt, G.F.R.) and HPLC-quality 2-propanol from J. T. Baker (Gross-Gerau, G.F.R.). Both free amino acids and their Dns derivatives were from Sigma (St. Louis, MO, U.S.A.).

Additionally, a type H amino acid standard solution from Hamilton (Bonaduz, Switzerland) was used. Water was quartz bi-distilled.

The following peptides were obtained from Bachem (Dubendorf, Switzerland): (1) D-leu^6-renin inhibitor (His-Pro-Phe-His-Leu-Leu-Val-Tyr), (2) angiotensin II (Asp-Arg-Val-Tyr-Ile-His-Pro-Phe), (3) lys^8-vasopressin (Cys-Tyr-Phe-Gln-Asn-Cys-Pro-Lys-Gly-amide), (4) iodo-phe^1-experimental allergic encephalitogenic peptide (iodo-Phe-Ser-Trp-Gly-Ala-Glu-Gly-Gln-Arg), (5) eledoisin (Pyr-Pro-Ser-Lys-Asp-Ala-Phe-Ile-Gly-Leu-Met-amide), (6) physalaemine (Pyr-Ala-Asp-Pro-Asn-Lys-Phe-Tyr-Gly-Leu-Met-amide), (7) γ-MSH (Tyr-Val-Met-Gly-His-Phe-Arg-Trp-Asp-Arg-Phe-Gly), (8) D-arg^6-dynorphin-(1–13) (Tyr-Gly-Gly-Phe-Leu-Arg-Arg-Ile-Arg-Pro-Lys-Leu-Lys), (9) somatostatin (Ala-Gly-Cys-Lys-Asn-Phe-Phe-Trp-Lys-Thr-Phe-Thr-Ser-Cys) and (10) des-tyr-γ-endorphin (Gly-Gly-Phe-Met-Thr-Ser-Glu-Lys-Ser-Gln-Thr-Pro-Leu-Val-Thr-Leu). The homogeneity of each peptide was checked by RP-HPLC in a $NaClO_4$–acetonitrile buffer system[16] prior to acid hydrolysis.

The stock solution used in buffer preparation consisted of 37.5 ml of 1 *N* NaOH, 2.5 ml of formic acid and 3.75 ml acetic acid per litre of quartz bi-distilled water. For the buffers used in Dns-amino acid separations the stock solution was made 10% (v/v) in methyl ethyl ketone for *A* buffer and 3% (v/v) methyl ethyl ketone–35% 2-propanol (v/v) for *B* buffer.

Instrument

The HPLC unit consisted of two Altex Model 110 pumps (Beckman, Berkeley, CA, U.S.A.), a Kontron Model 200 microprocessor (Kontron, Zürich, Switzerland), and a WI-SP sampler (Waters, Milford, MA, U.S.A.). Effluent monitoring was with a Fluoro-Monitor from Aminco (Silver Spring, MD, U.S.A.), which was equipped with a 70-μl flow-through cell and filters for fluram detection, and was operated with the damping switch in the ON position. Similarly, an Uvikon 725 Spectrophotometer (Kontron) with an 8-μl flow-through cell was employed for UV-visible detection. The output of either detector was plotted by a two-channel recorder (Model 600, W + W Electronic, Basel, Switzerland) and peak areas determined using a 3390 A integrator from Hewlett-Packard (Avondale, PA, U.S.A.). A stainless-steel pressure coil (*ca.* 200 cm × 0.25 mm I.D.) was connected to the detector outlet in order to prevent degassing and bubble formation in the flow-through cell.

Separations were carried out at 0.8 ml/min on columns thermostated at 55°C in a stainless steel jacket using a Haake type FJ water-bath (Karlsruhe, B.R.D.). The columns (250 × 4.6 mm I.D.) tested were: RP-8 (10 μm), RP-18 (5 μm), RP-18 (10 μm) and RP-300 (10 μm) from Brownlee (Santa Clara, CA, U.S.A.); Partisil-10 ODS-2 and ODS-3 from Whatman (Clifton, NJ, U.S.A.); Zorbax ODS from DuPont (Wilmington, DE, U.S.A.); and a 150 × 4.6 mm I.D. column of Ultrasphere-ODS (5 μm) from Altex.

Methods

Dns derivatization was carried out under conditions similar to those used by Tapuhi *et al.*[7], using Dns-Cl in acetonitrile (1.5 mg/ml, 5.56 m*M*) and Li_2CO_3 (40 m*M*) as the buffer. The ratio of Dns-Cl to buffer was 1:2 and the volume used dependent on the *total* concentration of amino groups present in the sample to be dansylated. For example, standards were reacted at 37°C for 60 min in the following

volumes: 20 μl of standard solution (1 nmol per amino acid/μl), 800 μl of buffer and 400 μl of Dns-Cl. The reaction was terminated by the addition of 40 μl of 2% methylamine and a further 5 min incubation at 37°C; the total volume was 1260 μl. Reaction volumes were decreased progressively by a factor of two for each halving of the standard concentrations, *e.g.*, 630 μl for 10 nmol, 315 μl for 5 nmol, 165 μl for 1 nmol and 85 μl for 500 pmol (in the latter two the standard concentration was diluted 10-fold to 0.1 nmol/μl). For samples with total concentrations of 10 nmol amino groups or less a final volume of 85 μl was employed, the minimal amount which we could conveniently manipulate. The derivatized samples were diluted into a sufficient amount of buffer *A* to lower the pH to *ca.* 4.0 and injected automatically. Peptides and proteins were hydrolyzed in distilled 6 *N* hydrochloric acid for 22 h at 110°C under vacuum. A Durrum D-500 analyzer (Dionex, Sunnyvale, CA, U.S.A.) was used for determining amino acid compositions/concentrations by "standard" methods. All glassware that came in contact with the reagents for Dns derivatization was carefully washed; tubes (60 × 5 mm I.D.) for hydrolyses were heated at 500°C for *ca.* 4 h to pyrolyze any organic material present. Solutions were transferred with automatic pipettes using polypropylene tips, and Dns derivatization reactions were carried out in micro sample tubes with caps (250 μl or 1.5 ml total volume) made of the same material. No attempts were made to clean either the tips or sample tubes.

RESULTS AND DISCUSSION

When the first report by Tapuhi *et al.*[7] on the utilization of Dns derivatization and subsequent separation of the Dns-amino acids by HPLC appeared, we thought that this might well be a technique suitable for determining the amino acid compositions of peptides which were being isolated at below the nanomole level using RP-HPLC techniques[16–19]. Their use of Dns-Cl in acetonitrile, a Li_2CO_3 reaction buffer and methylamine (for terminating the reaction) were directly applied. We were not, however, able to utilize the large volumes (3 ml total) or the apparent high amino acid concentrations (exact values not given) which they were. This was based on the necessity to develop a method which would allow one both to identify the amino terminus of a peptide and to determine its amino acid composition by using less than 200 pmol of starting material. Numerous experiments led to the final reaction conditions (see Experimental), which maintain a ratio range of [Dns-Cl]:[amino acid] of between 6:1 and 8:1, for *total* amino acid concentrations from *ca.* 20 to 400 nmol. For peptide hydrolysates or for unhydrolyzed peptides, where the *total* primary amino group concentrations are usually much less (0.1–5 nmol), the ratio increases to values far in excess of 8:1. It is interesting to note that a similar ratio range (5:1 to 10:1) was reported by Tapuhi *et al.* in a later publication[14].

Dns-amino acids were separated by Tapuhi *et al.*[7] on a 5-μm C_{18} Hypersil column (150 × 4.6 mm I.D.) employing a methanol gradient at pH 4.0. Since such a column was not available we checked a number of other C_8 and C_{18} packings from both the same and different suppliers (see Experimental). The only one found which gave acceptable results, *i.e.* good peak shape and separation of *all* Dns derivatives found in hydrolysates of "normal" proteins, was the Brownlee RP-300 resin. This support material has also recently been shown to be useful for both peptide and protein HPLC[20].

It was during the search for another suitable HPLC resin that the methyl ethyl

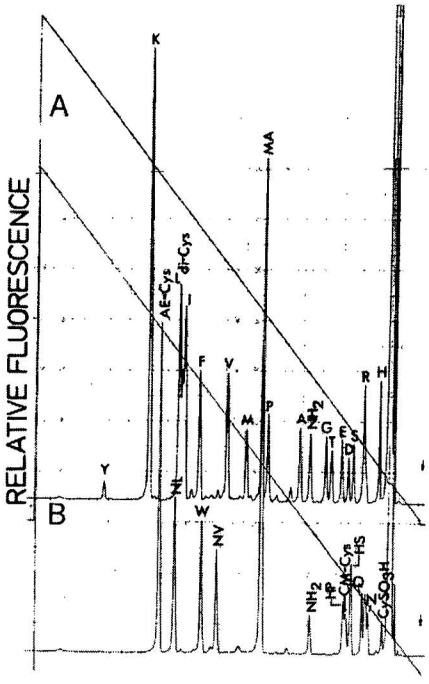

Fig. 1. Reversed-phase HPLC of Dns-amino acids. A, Dns derivatives of the amino acids found in protein hydrolysates; B, Dns derivatives of amino acids often resulting from chemical modifications, cleavages at specific side-chains or used as internal standards. Amount per derivative, *ca.* 200 pmol; photomultiplier setting, 30; 20-mV recorder range. The one-letter code for the amino acids is used except for the following abbreviations: NH_2 = amide; MA = methylamine; di-Cys = cystine; $CySO_3H$ = cysteic acid; HS = homoserine; CM-Cys = carboxymethylcysteine; HP = hydroxyproline; NV = norvaline; NL = norleucine; AE-Cys = aminoethylcysteine.

ketone–2-propanol-based gradient system was developed (Fig. 1). The gradient is started at 0% buffer *B* in order to achieve maximum separation between Dns-His, as well as Dns-$CySO_3H$, and the polar reaction by-products which elute with the void volume of the column. Elution can be commenced at higher values (12–15% buffer B), in order to shorten run times, but Dns-His and often Dns-Arg are lost when the concentration ratio of by-products to amino groups is too high. The ammonia originating from the acid deamination of Asn and Gln, as well as that contaminating the HCl used for hydrolysis, yields the Dns-NH_2 derivative during modification. Since we were unable to separate this derivative from that of Glu using the methanol gradient of Tapuhi *et al.*[7] on the RP-300 resin, it was necessary to develop the indicated system. Separations of Dns-Pro and Dns-MA are sometimes problematic and will be discussed later. The elution of Dns-di-Cys between Dns-Ile and Dns-Leu is not thought detrimental since most samples are either alkylated or oxidized prior to hydrolysis, thereby converting Cys and/or di-Cys residues into acid-stable derivatives.

In comparison with the other amino acid derivatives (see Fig. 2A), the amount of Dns-Tyr observed is low and represents one of the potential problems of employing pre-column Dns derivatization for quantitative analysis. The sample chromato-

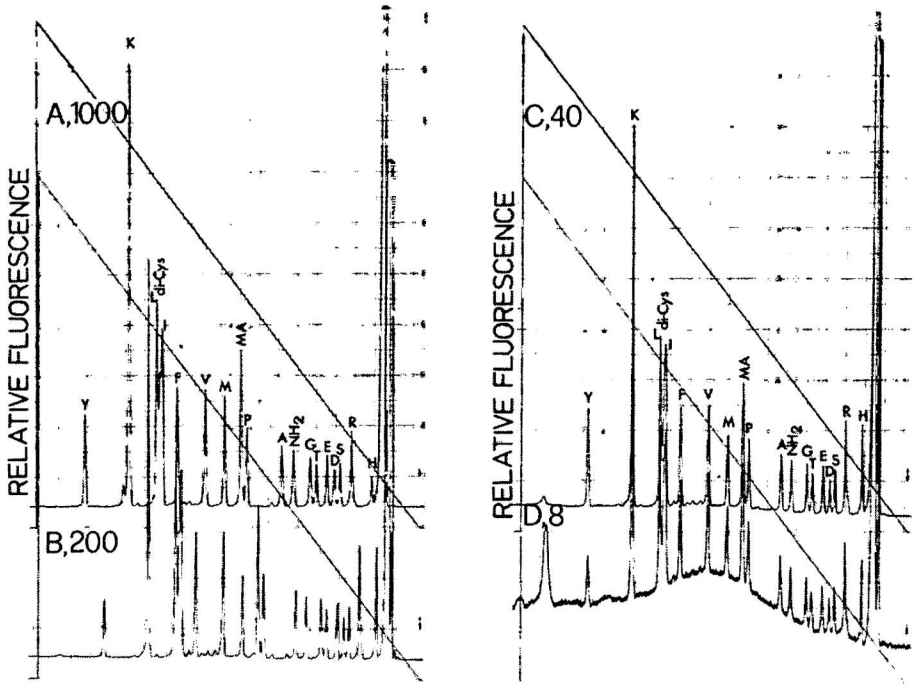

Fig. 2. Chromatography of various concentrations of Dns-amino acids. The amounts (picomoles of each derivative) are indicated on the chromatograms. Photomultiplier setting was held constant at 30 while recorder sensitivity was progressively increased, *i.e.*, 100 mV (A), 20 mV (B), 5 mV (C) and 1 mV (D). Sample volumes injected from a stock solution (5 pmol per derivative per μl) were 200 μl (A), 40 μl (B), 8 μl (C) and 8 μl from a five-fold dilution of the original solution (D).

graphed here (Fig. 1) was allowed to remain for a few (4–5) days at room temperature (diluted into the *A* buffer for HPLC) and exposed to the light in the laboratory, both natural and from overhead irridescent lamps. This loss is not observable when the samples are analyzed within a reasonable time (1 day) after Dns derivatization while remaining somewhat protected from direct light, *i.e.*, as in the micro-injection vials for many automatic sampling systems. However, for greatest accuracy, it is recommended that injections be carried out as soon as possible following sample preparation. A second problem concerning Dns-Tyr stability was observed while testing the chromatographic properties of the various C_8/C_{18} columns and utilizing the tetrahydrofuran (THF) containing buffer system of Tapuhi *et al.*[7]. Decreased amounts, or even total lack, of this derivative were often noted and attributed to the presence of oxidants in the reagent. Thus, instead of attempting to purify the reagent, our gradient system was developed employing methyl ethyl ketone as a substitute for the THF.

Fig. 1B illustrates the elution positions of the Dns derivatives of Norleu and Norval, analogues often used as internal/external standards, and of those amino acids which are normally destroyed during HCl hydrolysis, *e.g.*, Asn and Gln (for reasons discussed above) and Trp. Similarly, the positions of three Cys derivatives, namely cysteic acid, carboxymethyl- and aminoethylcysteines, are indicated. Dns-homoserine, a product arising from the CNBr cleavage at Met residues, co-chromato-

TABLE II

AMINO ACID COMPOSITIONS OF PEPTIDES DETERMINED BY (1) PRE-COLUMN Dns DERIVATIZATION AND RP-HPLC SEPARATION WITH (2) THOSE DETERMINED BY CATION-EXCHANGE SEPARATION AND NINHYDRIN DETECTION*

Italicized values indicate which amino acid was used for calculations of composition.

Peptide	*No. residues*	*Analysis method*	*Amino acid*																		*Amount (pmol/μl)*
			D	*T*	*S*	*E*	*P*	*G*	*A*	*C*	*V*	*M*	*I*	*L*	*Y*	*F*	*H*	*K*	*R*	*W*	
1	8	1					1.0				0.8			2.0	0.6	*1.0*	1.5				188
		2					1.0				0.6			2.1	0.8	*1.0*	1.9				184
2	8	1	1.2				*1.0*				1.2		0.6		0.6	1.0	1.1		1.1		520
		2	0.9				*1.0*				0.8		0.8		0.8	0.9	0.8		0.9		508
3	9	1	1.1			1.0	1.0	1.1		ND					0.6	*1.0*		1.0			392
		2	0.9			1.0	1.0	0.9		ND					0.7	*1.0*		0.8			430
4	9	1			*1.0*	2.1		1.9	0.9							0			1.0	0	267
		2			*1.0*	2.2		2.1	1.1							0			1.0	0	224
5	11	1	1.4		1.2	1.1	1.1	1.1	1.2			1.0	0.6	1.0		*1.0*		0.9			572
		2	1.1		0.9	1.1	1.1	1.0	1.0			0.9	0.9	1.0		*1.0*		0.9			587
6	11	1	2.1			1.2	1.2	1.1	1.2			1.1		1.0	0.9	1.1		*1.0*			390
		2	1.7			1.0	1.1	1.0	0.8			1.0		1.0	0.9	0.8		*1.0*			421
7	12	1	1.3					2.1			1.2	1.1			1.0	*2.0*	0.6		2.1	0	660
		2	0.8					1.9			1.0	1.1			1.0	*2.0*	0.8		1.7	0	601
8	13	1					1.1	2.1					0.7	2.0	0.6	*1.0*		2.1	3.1		336
		2					1.1	2.0					1.0	2.0	0.9	*1.0*		2.2	2.9		356
9	14	1	*1.0*	1.7	1.2			1.2	1.3	ND						3.0		1.9		0	334
		2	*1.0*	2.0	0.9			1.1	0.9	ND						3.2		1.9		0	283
10	16	1		2.6	2.2	2.3	1.3	2.1			1.0	0.8		2.1		*1.0*		1.0			204
		2		3.0	1.9	2.0	1.1	1.8			1.0	1.0		2.1		*1.0*		0.8			213

* Peptides hydrolyzed were: 1 = renin inhibitor; 2 = angiotensin II; 3 = Lys^8-vasopresin; 4 = iodo-Phe^1-experimental allergic encephalitogenic peptide; 5 = eledoisin; 6 = physalaemine; 7 = γ-MSH; 8 = D-Arg^6-dynorphin (1–13); 9 = somatostatin; 10 = des-Tyr-γ-endorphin. See Experimental for their respective sequences. The amounts or concentrations of the peptides are given in the last column and have been determined by the respective methods.

graphs with the Asp derivative, and 4-hydroxyproline, present in high amounts in collagen, with Dns-Glu.

The concentrations of Dns derivatives which can be easily chromatographed with the present system range from *ca.* 25 nmol down into the low picomole levels. Fig. 2 shows a concentration series of 1000, 200, 40 and 8 pmol of each Dns-amino acid. The extended elution time for the 1000 pmol sample (Fig. 2A), as compared with the others (Fig. 2B–D), was due to a slightly lower flow-rate being delivered from both HPLC pumps. At the 8-pmol level the signal-to-noise ratio ranges from *ca.* 70:1 for Dns-Lys down to 7.5:1 for Dns-Asp. For this reason, as well as that of amino acid contamination of specially distilled 6 *N* hydrochloric acid and cleaned glassware, attempts are seldom made to carry out analyses at much below the 50-pmol level. Note that at the 8 pmol level the Dns-Tyr peak is significantly lower than would be expected. This appears not to be due to irradiation, since the samples were injected consecutively, but rather to an apparent loss or destruction during chromatography. For a series of 200-pmol injections the elution times of the Dns derivatives were found to be extremely reproducible (maximum deviations between 0.01 and 0.04 min, depending on the particular derivative). Similarly, the standard deviations for the Dns-amino acids range between 2 and 5 pmol.

In addition to fluorescence detection, the absorption properties of the methyl ethyl ketone–2-propanol buffers are such that the elution of the Dns derivatives can be followed using the ultraviolet range between 320 and 340 nm. The variations in peak-area ratios for the different Dns-amino acids, a factor of *ca.* 13 when comparing the fluorescence yields of Dns-Lys and Dns-Ser, are much less pronounced. Although its use is between 10 and 100 times less sensitive, depending on the Dns derivative, nanomole concentrations can be conveniently detected and should be considered as an alternative in those laboratories where either a fluorometer is not available or analyses in the picomole range are not required.

The utility of the Dns derivatization reaction and subsequent RP-HPLC of the products is indicated in Table II. Here, various amounts of the peptides (2–12 nmol) were hydrolyzed in distilled 6 *N* hydrochloric acid and dried by rotary evaporation, and the resultant amino acids were dissolved in a known volume of water. Aliquots containing *ca.* 1 nmol of hydrolyzed peptide were required for determining the indicated compositions by cation-exchange-based amino acid analysis (denoted as 2 under *Analysis method* in Table II). To have carried out the analyses on either of our Durrum instruments at significantly lower concentrations would have required a formidable effort, *i.e.* running the instrument at elevated detection levels, readjustment or replacement of photometer lamp(s), etc. In a similar manner, aliquots of 200–500 pmol of hydrolysate were derivatized and analyzed at the 100–300 pmol range (see Figs. 3A and B for representative chromatograms). Although the compositions determined by the two methods are seen to agree rather well (compare 1 and 2 under *Analysis method* in Table II), there are exceptions: Asp values in peptides 5 and 7, due to poor integration; Pro value in peptide 6, poor peak integration due to large amount of Dns-MA (see later discussion); His value in peptide 7, reduced due to excessive amounts of polar by-product material eluting just prior to the amino acid derivative. The peptide concentrations as determined by both methods (last column, Table II) also agree reasonably well. This result contrasts with the latest report of Tapuhi *et al.*[14], where significant differences between the two types of analysis were

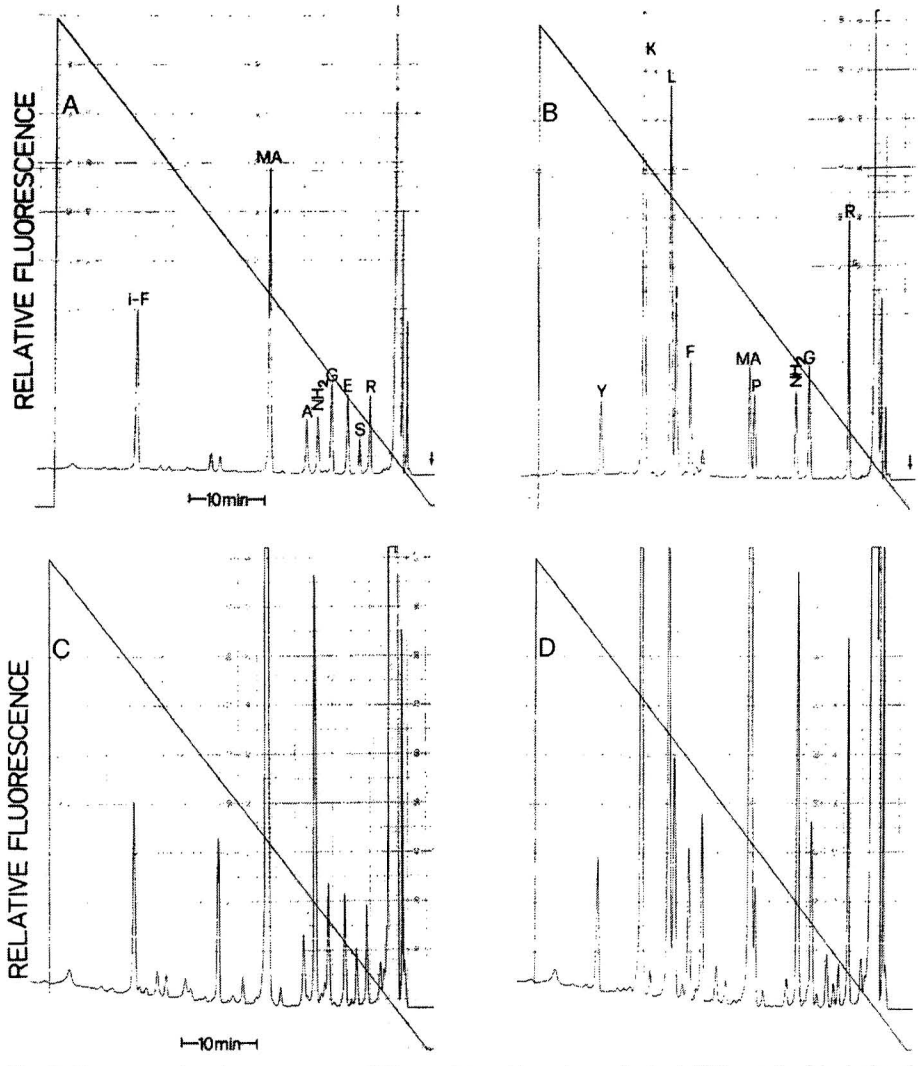

Fig. 3. Representative chromatograms of Dns-amino acid analyses. A, 1 μl (224 pmol) of hydrolyzed peptide 4 was Dns derivatized and 50% (112 pmol) chromatographed. B, 1 μl (514 pmol) of hydrolyzed peptide 8 was Dns derivatized and 50% (257 pmol) chromatographed. For both A and B the photomultiplier setting was 30 and the recorder sensitivity was 20 mV. C, 298.6 pmol of peptide 4 were Dns derivatized and two-thirds of the sample hydrolyzed for 18 h. Dns derivatization was repeated and 25% (*i.e.* one-sixth of original sample or 49.8 pmol) chromatographed. D, 457 pmol of peptide 8 were processed in the same manner as for C (above), 76.2 pmol being chromatographed. Fluorometer photomultiplier and recorder settings were 10 and 20 mV, respectively.

observed. However, as they pointed out, this might well have been due to the sample undergoing analysis (fermentation broth) and/or manipulations required prior to the analysis itself.

As stated in the introduction, one prime objective was to find conditions which would allow the simultaneous determination of amino acid compositions and identifi-

cation of amino-terminal residues on as small an amount of material as possible. To this end it was necessary to determine the rate at which Dns derivatives are destroyed under the conditions employed for peptide/protein hydrolysis. Table III indicates the percentages of Dns-amino acids remaining after exposure to hydrolysis conditions (6 *N* hydrochloric acid at 110°C under vacuum) for various times. The results clearly indicate why a short hydrolysis time is necessary when Pro is the amino-terminal residue. The decrease in the values for Dns-Ile represents the destruction of Dns-di-Cys (since they co-elute it was not possible to give separate values); the reason for the low Dns-Met percentages are presently not yet clear. Thus, during the hydrolysis of a Dns-peptide not only are the labeled residues (N-terminal and ε-Lys) being released through peptide-bond cleavage, but destruction of the Dns derivatives also occurs. For these reasons a Dns-peptide is usually hydrolyzed for both 4 h and 18 h and the chromatographic results compared (see below).

TABLE III
PERCENTAGE OF Dns-AMINO ACID REMAINING AFTER ACID HYDROLYSIS
Duplicate samples of Dns-amino acids (737 pmol each) were dried following Dns derivatization and hydrolyzed in 150 µl of distilled 6 N hydrochloric acid under vacuum for the indicated time. Following evaporation the hydrolysates were dissolved in buffer A and a portion (207 pmol of each) analyzed. The averaged peak areas for the duplicates of each time period were then compared with those of an unhydrolyzed sample of identical concentration and expressed as percentage of Dns derivative remaining.

Amino acid	*Hydrolysis time (h)*				
	1	*2*	*4*	*8*	*18*
Asp	97	101	105	117	121
Thr	100	96	90	79	58
Ser	96	92	75	58	29
Glu	100	101	94	92	79
Pro	85	58	18	0	0
Gly	96	89	74	57	31
Ala	97	100	91	80	57
Val	100	92	89	84	68
Met	35	27	43	51	38
Ile	130	103	100	94	76
Leu	101	91	91	85	72
Tyr	85	–	109	–	94
Phe	100	91	92	92	79
His	100	97	90	85	77
Lys	97	75	94	92	58
Arg	100	89	76	72	61

The chromatograms illustrated in Fig. 3C and D are examples of where a relatively small amount of starting material (300 and 457 pmol of peptides 4 and 8, see Table II) was used for both compositional and amino-terminal analyses. Following Dns derivatization, a portion of each (one third) was hydrolyzed for 4 h and the remaining (two-thirds) for 18 h. Each 18-h hydrolysate was divided equally; on one half derivatization was repeated and aliquots (49.8 and 76.2 pmol, respectively) were injected. A comparison of Fig. 3A with 3C and 3B with 3D thus represents the difference between the derivatization of the amino acids in a peptide hydrolysate and those

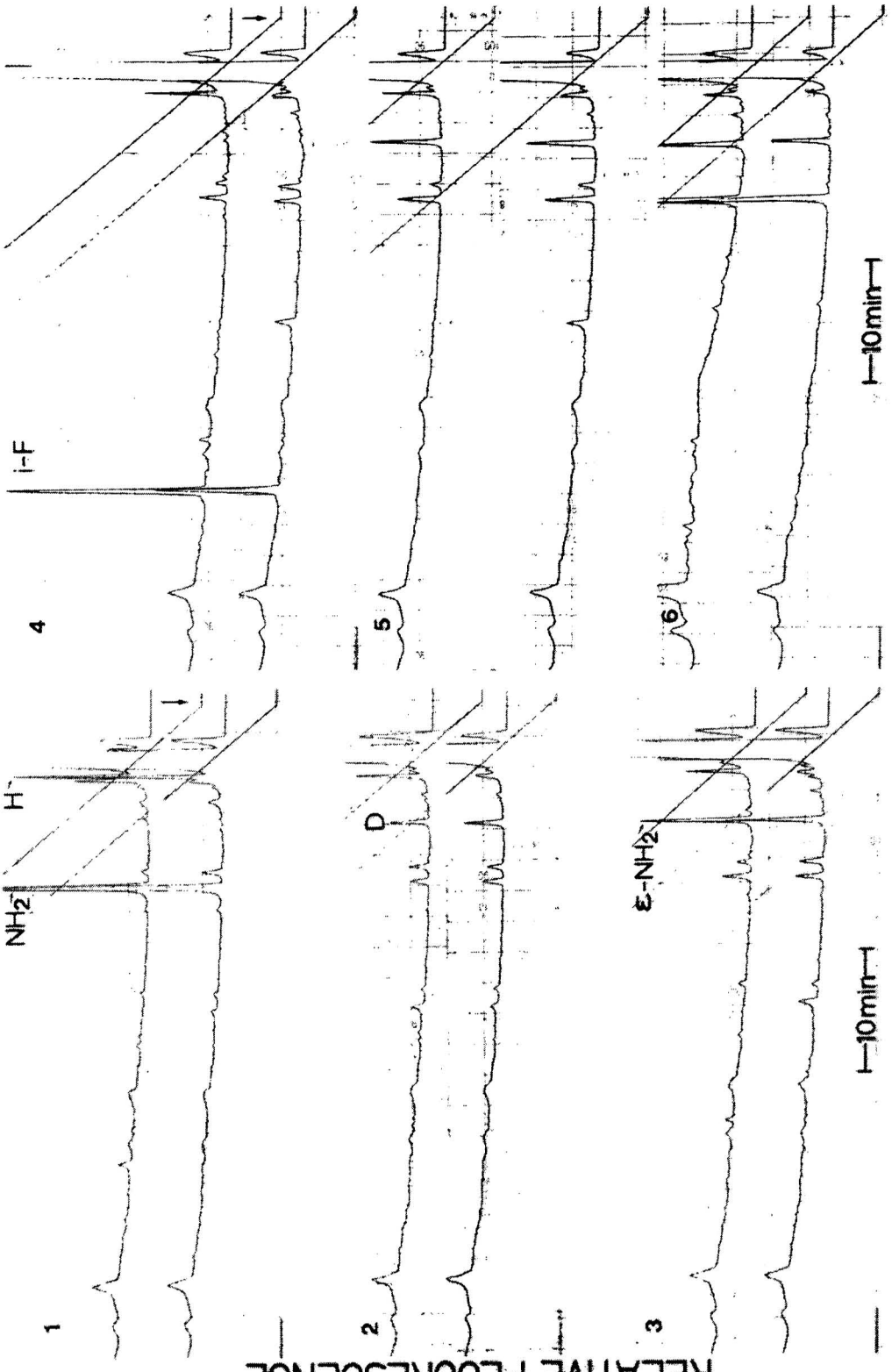

Fig. 4.

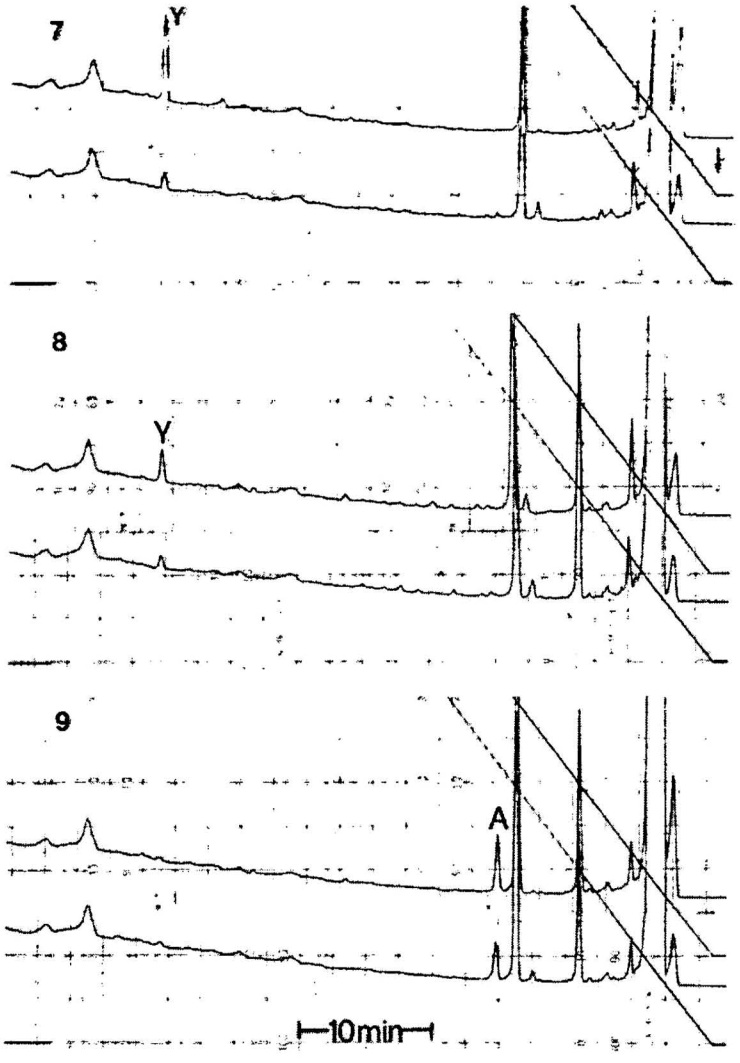

Fig. 4. Amino-terminal analyses of various peptides. Aliquots of known amounts of peptides 1–9 (see Table II) were Dns derivatized, one-third was hydrolyzed for 4 h and 50% of the hydrolysate (*i.e.* one-sixth of original) was chromatographed (upper chromatogram for each peptide). Hydrolysis for 18 h was carried out on the remaining two-thirds; the sample was divided equally and 25% (again one-sixth of original) chromatographed (lower chromatogram). The remaining sample was Dns derivatized, and the results were compared with those given in Table II (results not given). The amounts (pmol) of Dns-peptide chromatographed following both 4 h and 18 h of hydrolysis were: 1, 81.8; 2, 56.4; 3, 63.7; 4, 49.8; 5, 58.7; 6, 56.1; 7, 133.6; 8, 76.2; and 9, 58.4. Fluorometer photomultiplier and recorder settings were 10 and 20 mV, respectively. Additional abbreviations used; ε-NH_2 = Dns-ε-Lys; i-F = Dns-iodo-Phe.

arising from the hydrolysate of a peptide which had been previously dansylated at the available primary amino groups. From the latter it is apparent that more peaks are visible (perhaps from the hydrolyzed by-products of the first derivatization or from the second derivatizaton of degradation products thereof) and that the relative ratios between the Dns-amino acids and Dns-MA, as well as the reaction by-products

eluting at the beginning of each chromatogram, are quite low. However, the ratios between each of the peaks agree well with those noted when only a single derivatization of the hydrolyzed peptide was performed. In fact the amino acid compositions of the peptides agreed extremely well with the values given in Table II, *i.e.*, for peptide 4: *1.0 Ser*, 1.94 Glu, 2.05 Gly, 0.80 Ala and 0.79 Arg; and Peptide 8: 1.90 Gly, 0.65 Ile, 2.08 Leu, 0.84 Tyr, *1.0 Phe*, 1.84 Lys and 2.62 Arg. No value for Pro is given for peptide 8 and, as can be seen from the chromatogram (Fig. 3D), is a consequence of the peak not being detected for integration, *e.g.*, due to the large Dns-MA peak partially obscuring the Dns-Pro derivative. By comparing the relative peak heights, however, it is clear that the peak area approximates the value expected.

All of the other peptides given in Table II were similarly Dns derivatized, hydrolyzed, re-Dns derivatized and chromatographed as outlined above (results not given). Although integration problems were noted with each peptide containing a prolyl residue, the amino acid compositions were in good agreement with the given compositions (Table II), exceptions being the Met values which were constantly below average (40–50%). In those cystine-containing peptides (numbers 3 and 9) no Dns derivatives of the amino acid or degradation products thereof were observed. Values for those residues which were capable of Dns derivatization, *e.g.*, primary amino groups at the amino-termini and the ε-amino groups of lysyl side-chains, were not, as might have been expected, low. This suggests that although destruction of the Dns derivatives occurs during acid hydrolysis (Table III) the resulting free amino acid is subsequently capable of being re-Dns derivatized.

The chromatograms from those portions of peptides 1–9 which were derivatized and subsequently hydrolyzed for either 4 h or 18 h are shown in Fig. 4. For those peptides not blocked at the amino terminus (5 and 6) or involved in disulphide formation (3), a single discrete peak was observed which correctly identified the first residue. In those peptides containing internal lysyl residues an additional peak was observed, with a retention time slightly less than that of Dns-Asp, which has been identified as the Dns-ε-Lys derivative. Since even on new columns these two derivatives are poorly separated, it can be expected that, as the column ages, identification will become more and more difficult. We have found that washing (regeneration) with a few column volumes of a 1:1 mixture of chloroform and methanol often improves subsequent performance. However, if this fails then either the elution gradient must be changed or a "newer" column used for the reanalysis. A comparison of those peptides containing amino acids which are deaminated during acid hydrolysis (*e.g.*, Asn, Gln and/or carboxy-terminal amides) with those lacking such residues, indicates little correlation between the relative sizes of the Dns-NH_2 peaks and the amount of peptide hydrolyzed. Thus, the contaminating NH_3 must be coming from other sources, such as the buffer used for originally dissolving the peptides, the bi-distilled water used for diluting them and/or the distilled hydrochloric acid employed for hydrolysis.

In summary the above examples demonstrated that the Dns derivatization reaction, and subsequent separation of the derivatives via RP-HPLC, is well suited to quantitative peptide amino acid analysis. The lower limits for which the methods can be utilized are principally defined by the amount of contamination present in/on all solutions/surfaces which come in contact with the sample during handling. Practical amounts, or those with which it is convenient to work, have been shown to be in the 100–300-pmol range. Such amounts provide sufficient material for both determi-

nation of the amino acid composition and identification of the amino-terminal residue. However, it should be strongly emphasized that the usefulness depends on assuring near-quantitative derivatization and the availability of an instrument equipped for fluorescence detection and, preferably, automatic injection as well as peak integration. Such an instrument is then useable for not only amino acid analysis as shown but also for analyses based on either isocratic[3,10] or gradient[10] elutions of cation-exchange resins. In these cases either a motorized selector valve for the buffers/regeneration solutions or a third pump for post-column OPA transfer are additional requirements. Thus, for specialized protein laboratories which are interested in determining amino acid compositions and/or amino terminal residues on low picomole amounts of material, or for those laboratories requiring only a few analyses per given time period, and not wishing to buy an extra pump or valve, then this method must be considered essential.

ACKNOWLEDGEMENTS

We thank Dr. P. Grogg of Bachem for supplying the synthetic peptides. This research was supported (in part) by grant 0.330.077.98-3 from the Eidgenössische Technische Hochschule, Zürich. The additional support from Kontron International and the Sandoz-Stiftung, Sandoz AG, is also recognized.

REFERENCES

1 D. H. Spackman, W. H. Stein and S. Moore, *Anal. Chem.*, 30 (1958) 1190–1206.
2 J. R. Benson, in R. N. Perham (Editor), *Instrumentation in Amino Acid Sequence Analysis*, Academic Press, New York, 1975, pp. 1–39.
3 G. J. Hughes, K. H. Winterhalter, E. Boller and K. J. Wilson, *J. Chromatogr.*, 235 (1982) 417–426.
4 R. Schuster, *Anal. Chem.*, 52 (1980) 617–620.
5 M. K. Radjai and R. T. Hatch, *J. Chromatogr.*, 196 (1980) 319–322.
6 D. C. Olson, G. J. Schmidt and W. Slavin, *Chromatogr. Newslett.*, 7 (1979) 22–25.
7 Y. Tapuhi, N. Miller and B. L. Karger, *J. Chromatogr.*, 205 (1981) 325–337.
8 D. W. Hill, F. H. Walters, T. D. Wilson and J. D. Stuart, *Anal. Chem.*, 51 (1979) 1338–1341.
9 B. R. Larsen and F. G. West, *J. Chromatogr. Sci.*, 19 (1981) 259–265.
10 G. J. Hughes and K. J. Wilson, *J. Chromatogr.*, 242 (1982) in press.
11 E. Bayer, E. Grom, B. Kaltenegger and R. Uhmann, *Anal. Chem.*, 48 (1976) 1106–1109.
12 K.-T. Hsu and B. L. Currie, *J. Chromatogr.*, 166 (1978) 555–561.
13 S. Weiner and A. Tishbee, *J. Chromatogr.*, 213 (1981) 501–506.
14 Y. Tapuhi, D. E. Schmidt, W. Lindner and B. L. Karger, *Anal. Biochem.*, 115 (1981) 123–129.
15 S. Kobayashi and K. Imai, *Anal. Chem.*, 52 (1980) 424–427.
16 K. J. Wilson, A. Honegger and G. J. Hughes, *Biochem. J.*, 199 (1981) 43–51.
17 G. J. Hughes, K. H. Winterhalter and K. J. Wilson, *FEBS Letts.*, 108 (1979) 81–86.
18 A. Honegger, G. J. Hughes and K. J. Wilson, *Biochem. J.*, 199 (1981) 53–59.
19 G. J. Hughes, C. De Jong, R. W. Fischer, K. H. Winterhalter and K. J. Wilson, *Biochem. J.*, 199 (1981) 61–67.
20 K. J. Wilson, E. van Wieringen, S. Klauser, M. W. Berchtold and G. J. Hughes, *J. Chromatogr.*, 237 (1982) 407–416.

Journal of Chromatography, 241 (1982) 361–370
Elsevier Scientific Publishing Company, Amsterdam — Printed in The Netherlands

CHROM. 14,736

AMINO ACID MICROANALYSIS OF PROTEINS EXTRACTED FROM SPOTS OF FIXED, STAINED, TWO-DIMENSIONAL GELS

TAKASHI MANABE*, OSAMU ODA and TSUNEO OKUYAMA
Department of Chemistry, Faculty of Science, Tokyo Metropolitan University, Setagaya-ku, Tokyo 158 (Japan)
(First received October 23rd, 1981; revised manuscript received December 17th, 1981)

SUMMARY

A method for the extraction of proteins from fixed, stained, two-dimensional polyacrylamide gels and subsequent amino acid microanalysis was described. Human serum proteins were separated by two-dimensional electrophoresis, the stained spots were punched out and the proteins in each piece of gel were extracted with 0.1 *M* sodium hydroxide–2% thiodiglycol. The extracted proteins were hydrolysed and applied to an amino acid analyser equipped with a fluorimeter for detection of the reaction products with *o*-phthaldialdehyde. By reducing the amount of background contaminants, amino acid analysis of 1 μg or less of extracted proteins became possible. The amino acid composition of the proteins was compared with reported compositions of serum proteins by calculating correlation coefficients, which we designated "similarity indices of amino acid composition". These indices were useful for the identification of the extracted proteins.

INTRODUCTION

In previous reports, we described a technique of two-dimensional electrophoresis in the absence of denaturing agents[1,2] and its applications to the analysis of human immunoglobulin myeloma proteins[3] and human α-amylase isoenzymes[4]. With this technique, p*I* values and approximate molecular weights of 128 human plasma protein spots were determined and about 80 spots were identified as known plasma proteins[5].

During the course of the identifications of plasma proteins, we intended to extract proteins from the fixed, stained, slab gels and to analyse their amino acid compositions. Extraction of proteins from polyacrylamide gel and subsequent amino acid analysis have been reported[6–9]. However, we found that these existing methods were not sufficiently sensitive for our purpose[6,7] or had complicated extraction steps[8,9].

We report here a simple method for the amino acid microanalysis of proteins extracted from fixed, stained, two-dimensional polyacrylamide gels. The method is useful for the subsequent analysis of proteins separated by two-dimensional electrophoresis.

0021-9673/82/0000–0000/$02.75

EXPERIMENTAL

Materials

o-Phthaldialdehyde (OPA) (analytical-reagent grade), 6 *M* hydrochloric acid for amino acid sequence analysis and other reagents for amino acid analysis were obtained from Wako (Tokyo, Japan). Amino acid standards were obtained from Takara Kosan (Tokyo, Japan). Ampholines, pH 3.5–10 and 3.5–5, were purchased from LKB (Bromma, Sweden). Other reagents for electrophoresis were of special grade or better from Wako Nakarai Chemicals (Kyoto, Japan). Water for the preparation of acidic and basic buffers for amino acid analysis and for solutions used in the extraction procedure (7% acetic acid and 0.1 *M* sodium hydroxide–2% thiodiglycol) were prepared with a system consisting of an ion-exchange column and a glass distillation apparatus and was collected directly from the distillation condenser.

Two-dimensional electrophoresis

Human serum (50 μl) was subjected to two-dimensional electrophoresis as described earlier[1,2]. The second-dimension slab gel was a 4–21% (or 4–17%) linear acrylamide gradient gel and was 16 cm wide, 12 cm high and 0.4 cm thick. The gels were stained with 0.025% Coomassie Brilliant blue R-250–50% (v/v) methanol–7% (v/v) acetic acid overnight and destained in 7% (v/v) acetic acid at 80°C for 4 h and in two changes of 7% (v/v) acetic acid at room temperature for 2 days.

Extraction of proteins from polyacrylamide gel matrix

A two-dimensional electrophoretic slab gel that had been stained and destained was placed in a plastic container, 1 l of 7% (v/v) acetic acid was added to the container and the gel was allowed to stand for 1 h in the container with a lid. Then the acetic acid solution was removed by decanting the container (the gel was held using a polyethylene disposable glove). Stained spots on the gel were punched out with a stainless-steel tube (inner diameter 2 mm, commonly used in immunoelectrophoresis for making sampling holes on agar gel plates). The piece of gel was pushed out with a thin glass rod into a Pyrex test-tube (100 × 12 mm I.D., calcined at 500°C for 3 h), 0.2 ml of freshly prepared 0.1 *M* sodium hydroxide–2% thiodiglycol was added with a glass micropipette and the tube was allowed to stand for 10 min at 40°C, then the solution was removed with the micropipette and discarded. A further 0.2 ml of 0.1 *M* sodium hydroxide–2% thiodiglycol was added to the test-tube, the mixture was allowed to stand for 10 min at 40°C, then the solution was transferred into another calcined hydrolysis tube (100 × 12 mm I.D. or 55 × 4 mm I.D.).

Preparation of samples for amino acid analysis

The solution was freeze-dried and 0.5 ml of 6 *M* hydrochloric acid was added to the test-tube. The tube was evacuated for 5 min and sealed, and hydrolysis was performed at 110°C for 24 h. The tube was then opened and 150 μl of 0.1 *M* hydrochloric acid–1% thiodiglycol were added. The tube was agitated on a mixer for 10 sec and 100 μl of the solution were subjected to amino acid analysis.

Amino acid analysis

Analyses were performed with a Nikon–Rank Hilger Chromaspek J-180

amino acid analyser (Rank Precision Industries, Westwood, Great Britain), which was equipped with a column (350 mm × 3.0 mm I.D.) packed with divinylbenzene–styrene cation-exchange resin (6 ± 1 μm), and a fluorimeter for detection of OPA reaction product. A schematic diagram of the modified flow system of the amino analyser is shown in Fig. 1. The buffers for elution and for fluorescence development were modified as follows. The acid buffer contained 42.0 g of citric acid, 25.4 g of lithium chloride, 14.0 ml of 10% Brij 35, 0.8 ml of *n*-caproic acid, 2.5 ml of thiodiglycol and 4 l of water. The basic buffer contained 42.0 g of citric acid, 50.4 g of lithium hydroxide monohydrate, 35.2 g of boric acid, 14.0 ml of 10% Brij 35, 0.4 ml of *n*-caproic acid and 4 l of water. The gradient elution was controlled with a programmer.

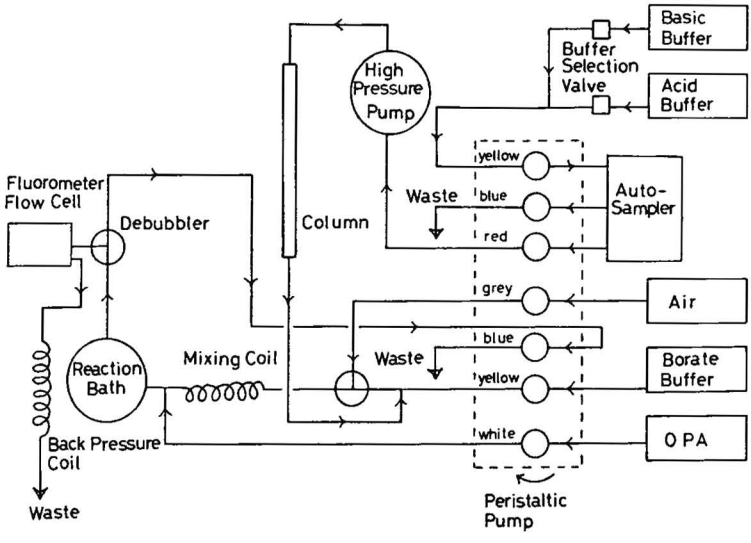

Fig. 1. Schematic diagram of the amino acid analyser equipped with a fluorimeter for detection of reaction product.

Samples for analysis were introduced into the column via a filling device adjusted to accomodate 100 μl of sample. The column temperature was controlled from 40 to 96°C during one analysis. Borate buffer, which contained 370.8 g of boric acid, 10 *M* potassium hydroxide solution added to give pH 10.5 and made up to 4 l with water, was mixed with the column effluent, passed through a mixing coil (50 cm × 1.0 mm I.D.; coil radius 6 mm), mixed with OPA solution which contained 3.2 g of OPA, 80 ml of ethanol, 8 ml of 2-mercaptoethanol, 8 ml of 15% sodium hypochlorite and 4 l of water, and then passed through a reaction coil at 44°C. The effluent was passed into a fluorimeter, with an excitation wavelength of 350 nm and an emission wavelength of 450 nm. Amino acids were quantitated by measuring their peak areas with a Shimadzu Chromatopak C-E1 B integrator (Shimadzu, Kyoto, Japan).

Calculation of correlation coefficients

The amino acid composition of the protein in a piece of stained gel was calculated by subtracting the amounts of amino acids in a piece of background gel from those of the piece of stained gel. The correlation coefficients between the measured

amino acid composition of an extracted protein and the reported compositions of serum proteins, which we called "similarity indices" (γ), were calculated according to the equation

$$\gamma = \frac{n\Sigma x_i y_i - \Sigma x_i \Sigma y_i}{\sqrt{[n\Sigma x_i^2 - (\Sigma x_i)^2]\,[n\Sigma y_i^2 - (\Sigma y_i)^2]}}$$

where x_i represents the measured content of an amino acid (i), y_i the content in the literature of the same amino acid (i) and n is the number of (x_i, y_i) pairs (number of amino acid species) used for the calculation. The calculated similarity indices were sorted with a microcomputer NEC PC-8001 (Nippon Electric, Tokyo, Japan). The amino acids used for the calculation were Asp, Thr, Ser, Glu, Pro, Gly, Ala, Val, Ile, Leu, Tyr, Phe, Lys, His and Arg. The serum proteins, the amino acid compositions of which were used to calculate the correlation coefficients, were: C1 inactivator[10], prealbumin[11], transferrin[12], albumin[13], C1q complement[14], C3 complement[15], Gc-globulin[16], thyroxin-binding globulin[17], haemopexin[16], α_1-antitrypsin[18], α_1-antichymotrypsin[18], inter-α-trypsin inhibitor[18], anti-thrombin[19], α_2-macroglobulin[20], proteinase inhibitor[20], low-density lipoprotein (LDL)[21], apo-high-density lipoprotein[22], kininogen[23], ceruloplasmin[24], α_1-acid glycoprotein[25], α_1-glycoprotein easily precipitating[18], α_2-HS glycoprotein[18], histidine-rich α_2-glycoprotein[26], Ba-α_2-glycoprotein[27], α_2-β_1-glycoprotein 4S[28], β_1-glycoprotein[29], β_2-glycoprotein[18], fibrinogen[30], α_{2H}-globulin[31] and α_1-α_2-globulin urate binding[32].

RESULTS

Method of extraction

Before examining extraction methods, direct hydrolysis of the piece of gel that contained stained proteins was examined. However, amino acid analysis of the hydrolysate showed a large amount of ammonia derived from the hydrolysis of polyacrylamide gel, and the broad ammonia peak overlapped the peaks of lysine and arginine. Moreover, tailing of the ammonia peak enhanced the baseline fluorescence of the next analysis. As direct hydrolysis of the gel was not successful, we tried to extract stained proteins from the polyacrylamide gel matrix.

We chose extraction with 0.1 *M* sodium hydroxide–2% thiodiglycol as described under Experimental. Fig. 2 shows how the amount of extracted protein change on repeating the extraction cycle. Purified human albumin (2 mg) was subjected to two-dimensional electrophoresis and a gel punched from the albumin spot and that from background gel position were compared. The solution obtained after each extraction cycle was freeze-dried and hydrolysed and the hydrolysate was subjected to amino acid analysis. The protein content of the solution was calculated by adding the amounts of amino acids. In the first cycle of extraction, the pH of the extraction solution was about neutral, as the slab gel had been soaked in 7% (v/v) acetic acid. The amounts of proteins obtained in this extraction step from the albumin gel and the background gel were almost the same. In the second cycle of extraction, the amount of protein extracted from the albumin gel was about 8 times greater than that from the background gel. The pH of the extraction solution after the second extraction cycle was about 13. When the extraction cycle was repeated further, the

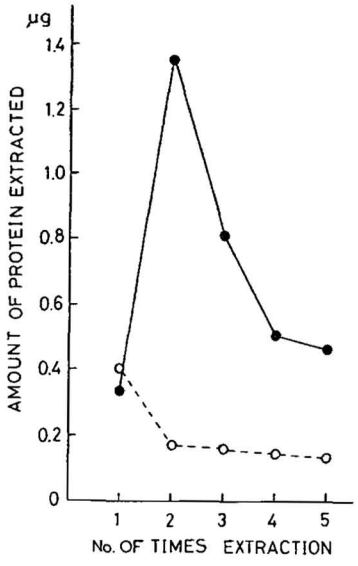

Fig. 2. Change in the amount of protein extracted on repeating the extraction cycle for a piece of gel punched out from the albumin spot (●) and for a piece of background gel (○).

recovery of protein from the albumin gel decreased and then the ratio of protein content of albumin gel extract to background gel extract decreased. Therefore, the first cycle was actually the step of washing the piece of gel and the second cycle was the step of protein extraction.

Amino acid microanalysis

Fig. 3 shows one of the two-dimensional polyacrylamide slab gels used to punch out gel pieces. The holes on the slab gel show the positions where the pieces of gel were punched out with a stainless-steel tube. The arrows show the positions where background gel pieces were taken out. Because the procedure is simple, extraction from 25 gel pieces could be done within 2 h.

Fig. 4 shows the relative peak heights of equimolar (250 pmol) amounts of amino acids, determined by the OPA method with a Nikon–Rank Hilger amino acid analyser. An integrator was used to calculate peak areas of amino acids and individual amino acids in amounts as small as 5 pmol could be determined.

Fig. 5 shows two examples of amino acid analysis of the gel extract. Fig. 5A and B show the elution patterns of amino acids of the extract from a piece of gel positioned at spot 80 (Fig. 3) and that extracted from a piece of background gel, respectively. The spot number corresponded to that in the "normalized map" of plasma proteins, which illustrated the standard distribution of the proteins on two-dimensional electrophoretic gels[5]. The amounts of amino acids found in the hydrolysate of the background gel extract were subtracted from those in the hydrolysate of the sample gel extract and the amino acid composition of the extracted protein was calculated.

Table I shows three examples of the amino acid compositions of extracted protein. The amino acid compositions of protein extracted from spots 80, 81 and 82

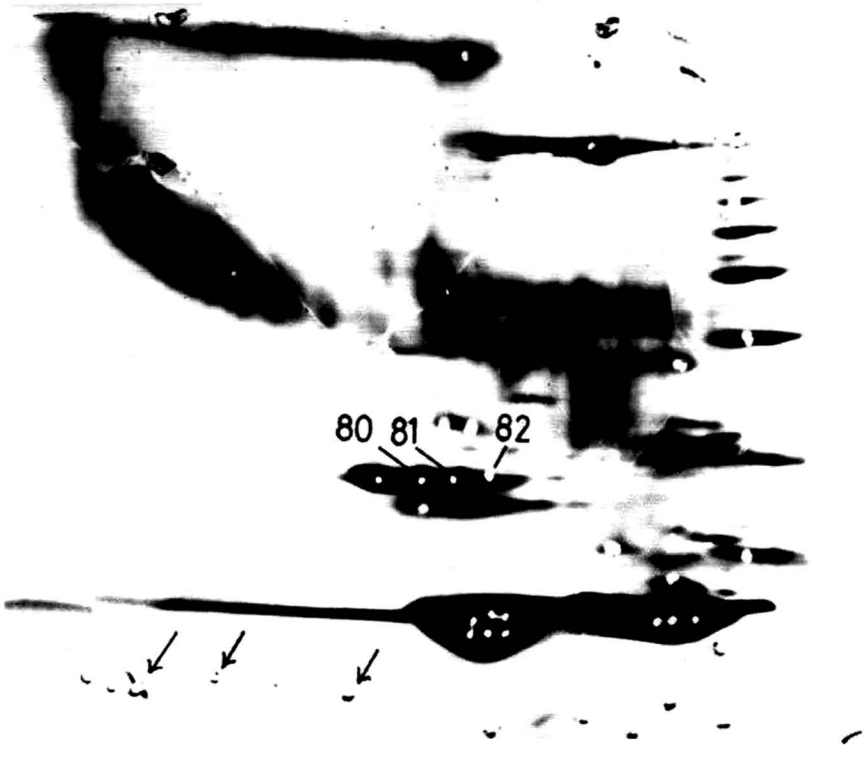

Fig. 3. Two-dimensional polyacrylamide slab gel used to punch out stained gel pieces. Spot numbers corresponded to those in the "normalized map" of human plasma proteins[5] and the amino acid compositions of the proteins extracted from the numbered spots are shown in Table I. The arrows show the positions where pieces of background gel were punched out.

resembled that of transferrin[12]. However, the contents of cysteine and methionine of the extracted proteins were much lower than the reported values, suggesting that these amino acids have been oxidized. The amounts of protein extracted were 0.92 μg from spot 80, 0.72 μg from spot 81 and 0.50 μg from spot 82. The considerable differences in the amounts of glycine and histdine in spot 82 from the reported values may be due to the relatively high background level of these amino acids (Fig. 5B). The maximal amount of protein extracted from one piece of gel was about 1.5 μg (from the albumin spot) and about 0.6–1.0 μg of protein was extracted from the pieces of gel positioned at the spots of major serum proteins (those which have serum concentrations exceeding 40 mg/dl).

The similarity indices of the amino acid composition of the extracted protein and the compositions of 30 human serum proteins were calculated using a microcomputer, in an attempt objectively to describe the "degree of similarity" between amino acid compositions. Table II shows some of the results of the calculation for the amino acid compositions of spots 80, 81 and 82 (Table I). Although the microcomputer was programmed to calculate similarity indices with 30 serum proteins simultaneously, only the highest and next to highest "similarity indices" are listed in the table in order

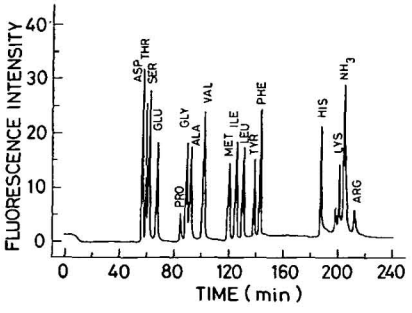

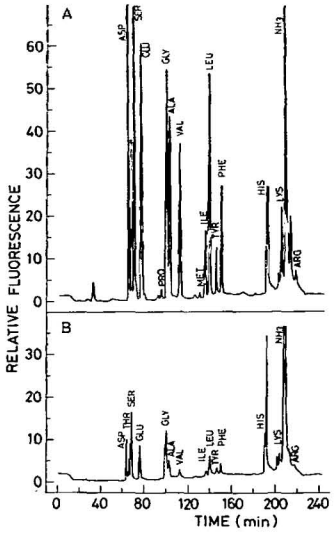

Fig. 4. Relative peak heights of equimolar (250 pmol) amounts of amino acids determined by the OPA method.

Fig. 5. Two examples of amino acid analysis of the gel extract. (A) Elution pattern of amino acids of the extract from a piece of gel positioned at spot 80 (Fig. 3); (B) elution pattern of background gel extract.

TABLE I

THREE EXAMPLES OF AMINO ACID COMPOSITIONS OF EXTRACTED PROTEINS

Extracts from spots 80, 81 and 82. The reported compositions of transferrin[12] is also listed. The reported number of alanine residues was used to compare the amino acid compositions.

Amino acid	*Protein extracted*			*Transferrin reported*[12]
	From spot 80 (0.92 μg)	*From spot 81 (0.72 μg)*	*From spot 82 (0.50 μg)*	
Asp	69.8	66.7	67.2	71
Thr	24.6	25.5	24.7	25
Ser	35.4	28.9	31.1	35
Glu	53.2	59.1	66.0	53
Pro	25.8	29.4	26.9	36
Gly	47.0	46.3	64.5	46
Ala	*51*	*51*	*51*	*51*
Cys/2	0	0	0	30
Val	39.4	40.9	39.2	40
Met	0	3.1	0	8
Ile	13.7	14.6	17.0	14
Leu	57.0	57.0	55.4	52
Tyr	23.6	23.4	19.5	24
Phe	29.7	27.0	27.6	27
Lys	42.0	44.6	47.9	49
His	17.1	23.1	27.3	17
Arg	22.7	19.4	20.5	23

TABLE II

RESULTS OF CALCULATION OF "SIMILARITY INDEX" BETWEEN THE AMINO ACID COMPOSITION OF EXTRACTED PROTEIN AND 30 REPORTED COMPOSITIONS OF SERUM PROTEINS

Only the serum proteins that showed the highest and next to highest "similarity indices" are listed.

Protein extracted	*Similarity index between amino acid compositions*	*Serum protein*
From spot 80	0.970	Transferrin
	0.829	α_1-Glycoprotein easily precipitated
From spot 81	0.960	Transferrin
	0.855	α_1-Glycoprotein easily precipitated
From spot 82	0.910	Transferrin
	0.848	Haemopexin

to avoid complexity. As shown in Table II, each protein extracted from spots 80–82 showed the highest similarity index with transferrin. Among the three spots, spot 80 showed the highest similarity index with transferrin and the results are in accordance with the fact that the largest amount of protein was extracted from spot 80. We used these results to identify serum proteins on the two-dimensional electrophoretic gels. A similarity index exceeding 0.95 was our standard of identification.

DISCUSSION

In preliminary studies, we examined various procedures for the extraction of protein from the gel matrix and found that every solution and item of glassware used in the extraction steps contained contaminants. Even ion-exchanged and doubly distilled water contained contaminants when it had been stored in a reservoir. The stored water did not show detectable free amino acids but when hydrolysed, amino acids at concentrations up to 3 μg/ml were detected. These results suggest that the contaminants in water are macromolecular substances, such as spores of moulds. Therefore, fresh water taken directly from the condenser of the distillation apparatus was used to prepare extraction solutions. Test-tubes were also sources of contamination. Methods for washing test-tubes with detergents or concentrated hydrochloric acid were examined. However, some contaminants remained in the washed test-tubes in amounts that were not reproducible, possibly because these methods needed water in the last step of washing. Therefore, we calcined the test-tubes without washing them. This was an effective method of removing contaminants.

As shown in Fig. 2, the background gel extract contained about 0.4 μg of contaminants in the first cycle of extraction; the amount was reduced by repeating the cycle, and it became constant at about 0.1 μg. A blank test-tube subjected to the procedures of extraction and hydrolysis in the absence of a piece of gel also contained about 0.1 μg of contaminants. Possibly the contaminants come from air that enters

the test-tubes during the extraction steps. In fact, the amount could be reduced when smaller (55 × 4 mm I.D.) test-tubes were used.

The amino acid compositions of the contaminants found in stored water, in washed test-tubes and in background gel extracts were similar, with high levels of serine and glycine (for example, see Fig. 5B). Results of the amino acid analyses of the contaminated substances will be presented elsewhere.

We used 0.1 *M* sodium hydroxide solution for extraction of proteins. The concentration of sodium hydroxide in the extraction solution was chosen to neutralize a piece of gel that had been soaked in 7% (v/v) acetic acid in the first cycle. Protein was not extracted in the first cycle, so this step served to wash the piece of gel. In the second cycle, the pH of the gel piece increased to 13 and protein was extracted as shown in Fig. 2. Therefore, the second cycle was the actual extraction step. The reason why protein was not extracted in the first cycle is unclear. Possibly fixed and stained proteins could not be solubilized by just neutralizing the pH of the gel, because the rate of the conformation change of the proteins at neutral pH was low.

As shown in Tables I and II, the similarity indices were useful for comparing the amino acid compositions. The values listed in Table II were calculated by comparing 15 amino acids. However, as shown in Fig. 5, the degree of background contribution differs for each amino acid; the measured value of valine is more reliable than that of glycine. Therefore, for the calculation of similarity indices, the reliability of the measured values of each amino acid must be taken into account, especially when the amount of the extracted protein is small.

REFERENCES

1 T. Manabe, K. Tachi, K. Kojima and T. Okuyama, *Seibutsu Butsuri Kagaku*, 22 (1978) 171.
2 T. Manabe, K. Tachi, K. Kojima and T. Okuyama, *J. Biochem.*, 85 (1979) 649.
3 T. Manabe, N. Takahashi, K. Kojima, T. Shinoda and T. Okuyama, *J. Biochem.*, 87 (1980) 451.
4 T. Kadofuku, T. Manabe and T. Okuyama, *Seibutsu Butsuri Kagaku*, 24 (1981) 319.
5 T. Manabe, K. Kojima, S. Jitzukawa, T. Hoshino and T. Okuyama, *J. Biochem.*, 89 (1981) 841.
6 L. L. Houston, *Anal. Biochem.*, 44 (1971) 81.
7 K. Sreekrishna, C. E. Jones, K. A. Guetzow, M. R. Presad and V. C. Joshi, *Anal. Biochem.*, 103 (1980) 55.
8 W. E. Brown and G. C. Howard, *Anal. Biochem.*, 101 (1980) 294.
9 D. G. Drescher and K. S. Lee, *Anal. Biochem.*, 84 (1978) 559.
10 H. Haupt, N. Heimburger, T. Kranz and G. Schwick, *Eur. J. Biochem.*, 17 (1970) 254.
11 P. A. Peterson, *J. Biol. Chem.*, 246 (1971) 34.
12 W. F. Line, D. Grohlich and A. Bezkorovainy, *Biochemistry*, 6 (1967) 3393.
13 R. H. McMenamy, H. M. Dintzis and F. Watson, *J. Biol. Chem.*, 246 (1971) 4744.
14 K. Yonematsu, R. M. Stroud, W. Niedermeier and W. T. Butler, *Biochem. Biophys. Res. Commun.*, 43 (1971) 1388.
15 D. B. Budzko, V. A. Bokisch and H. J. Muller-Eberhard, *Biochemistry*, 10 (1971) 1166.
16 N. Heimburger, K. Heide, H. Haupt and H. E. Schultze, *Clin. Chim. Acta*, 10 (1964) 293.
17 N. A. Giogrio, Jr. and M. Tabachnick, *J. Biol. Chem.*, 243 (1968) 2247.
18 H. G. Schwick, N. Heimburger and H. Haupt, *Z. Int. Med.*, 21 (1966) 193.
19 N. Heimburger, H. Haupt and H. G. Schwick, in H. Fritz and H. Tschesche (Editors), *Proceedings of the International Research Conference on Proteinase Inhibitors*, De Gruyter, Berlin, 1971, p. 1.
20 K. Hochstrasser, H. Feuth and O. Steiner, *Hoppe-Seyler's Z. Physiol. Chem.*, 354 (1974) 927.
21 K. Simons, C. Ehnholm, O. Renkonen and B. Bloth, *Acta Pathol. Microbiol. Scand.*, 78B (1970) 459.
22 M. Ayrault-Jarrier, G. Lastra, D. Pastier, J. Burdin and J. Polonovski, *Biochimie*, 54 (1972) 973.
23 J. V. Piers, *Fed. Proc., Fed. Amer. Soc. Exp. Biol.*, 27 (1968) 52.
24 L. Ryden, *Int. J. Protein Res.*, 3 (1971) 131.

25 W. E. Marshall and J. Porath, *J. Biol. Chem.*, 240 (1964) 209.
26 H. Heimburger, H. Haupt, T. Kranz and S. Baudner, *Hoppe Seyler's Z. Physiol. Chem.*, 353 (1972) 1133.
27 K. Schmid and W. Burgi, *Biochim. Biophys. Acta*, 47 (1961) 440.
28 T. Iwasaki and K. Schmid, *J. Biol. Chem.*, 245 (1970) 1814.
29 J. Labat, M. Ishiguro, Y. Fujisaki and K. Schmid, *J. Biol. Chem.*, 244 (1969) 4975.
30 E. Triantaphyllopoulos and D. Triantaphyllopoulos, *Biochem. J.*, 105 (1967) 393.
31 J. Cejka and M. D. Poulik, *Arch. Biochem. Biophys.*, 144 (1971) 775.
32 K. Slejten, I. Aakisson and J. O. Alosaker, *Nature New Biol.*, 231 (1971) 118.

Journal of Chromatography, 241 (1982) 371–379
Elsevier Scientific Publishing Company, Amsterdam — Printed in The Netherlands

CHROM. 14,761

ANALYSIS OF QUINIC ACID ESTERS OF HYDROXYCINNAMIC ACIDS IN PLANT MATERIAL BY CAPILLARY GAS CHROMATOGRAPHY AND HIGH-PERFORMANCE LIQUID CHROMATOGRAPHY

BIRGIT MÖLLER* and KARL HERRMANN

Institut für Lebensmittelchemie der Universität Hannover, Wunstorfer Strasse 14, D-3000 Hannover 91 (G.F.R.)

(Received January 20th, 1982)

SUMMARY

Capillary gas chromatographic (GC) and high-performance liquid chromatographic (HPLC) methods for separation and determination of *cis* and *trans* isomers of nine caffeoyl-, *p*-coumaroyl- and feruloylquinic acids in plant extracts are presented and compared. GC analysis requires highly deactivated SE-30 capillaries because of the sensitivity of the silylated compounds and the high temperatures involved. The production of these capillaries is described. HPLC analysis is performed with an RP-18 column and a gradient elution with 2% acetic acid–methanol. Both methods allow the separation of the *trans* isomers and most of the *cis* isomers. For the various samples, quantitative results of GC and HPLC separation agree well.

INTRODUCTION

Quinic acid esters of hydroxycinnamic acids[1] are of interest in plant physiology and food chemistry because of their ubiquitous occurrence in plants. The most common compounds of the class are esters of caffeic acid, especially chlorogenic acid and neochlorogenic acid. They are often found together with *p*-coumaric acid and ferulic acid esters. In contrast, sinapic acid esters are rare, except in a few plant families like Brassicaceae. Table I lists the investigated substances. The old and not the IUAPAC nomenclature has been chosen to allow a simple comparison to former investigations.

Because of the chemical similarity of the different cinnamoylquinic acids and their possible isomers, high separation efficiency is needed to resolve all compounds. For each acid there are three positional isomers each having two *cis–trans* isomers. Capillary gas chromatography (GC) and high-performance liquid chromatography (HPLC) have been shown to be the appropriate methods. So far, GC[2–5] and HPLC[6,7] have only been used to determine some of the hydroxycinnamoylquinic acids. Moreover, none of these studies considered *cis* isomers, which are formed by brief exposure to UV light during sample preparation and storage.

0021-9673/82/0000–0000/$02.75

TABLE I

INVESTIGATED CINNAMOYL QUINIC ACIDS

Quinic acid

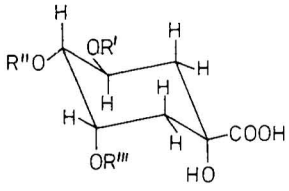

R_1 = Caffeic acid

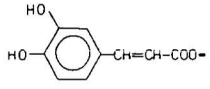

R_2 = *p*-Coumaric acid

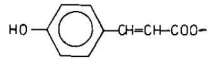

R_3 = Ferulic acid

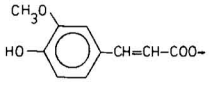

Compound	*R'*	*R''*	*R'''*
3-Caffeoylquinic acid (chlorogenic acid)	R_1	H	H
4-Caffeoylquinic acid (cryptochlorogenic acid)	H	R_1	H
5-Caffeoylquinic acid (neochlorogenic acid)	H	H	R_1
3-*p*-Coumaroylquinic acid	R_2	H	H
4-*p*-Coumaroylquinic acid	H	R_2	H
5-*p*-Coumaroylquinic acid	H	H	R_2
3-Feruloylquinic acid	R_3	H	H
4-Feruloylquinic acid	H	R_3	H
5-Feruloylquinic acid	H	H	R_3

EXPERIMENTAL

Reference samples

Only chlorogenic acid is commercially available (Roth, Karlsruhe, G.F.R.). By heating chlorogenic acid with a buffer of pH 7 its isomerization yielded the other caffeoylquinic acids[8]. The *p*-coumaroylquinic acids were isolated from unripe apples by paper chromatography, as were the feruloylquinic acids from green Robusta coffee. They were isomerized in the same way as chlorogenic acid. All compounds were affirmed by mass and NMR spectroscopy.

Sample extraction and prepurification

A 100-g amount of fruit material was twice extracted with 1 l of 80% methanol for 30 min in an atmosphere of nitrogen at room temperature. The combined extracts were concentrated to about 350 ml in a rotary vacuum evaporator at less than 40°C and then purified in a preliminary way by polyamide column chromatography.

About 50 g of polycaprolactam powder (MN-Polyamid-SC-6, 0.05–0.16 mm; Macherey, Nagel & Co, Düren, G.F.R.) were suspended in methanol–water (1:1), packed into a 250 × 35 mm I.D. tube, first washed with 1 l of methanol–formic acid (995:5) and then with 1 l of water. The aqueous extract was added to the polyamide column, which then was rinsed with 800 ml of water followed by 800 ml of methanol. The hydroxycinnamoylquinic acids were eluted with 800 ml of methanol–formic acid

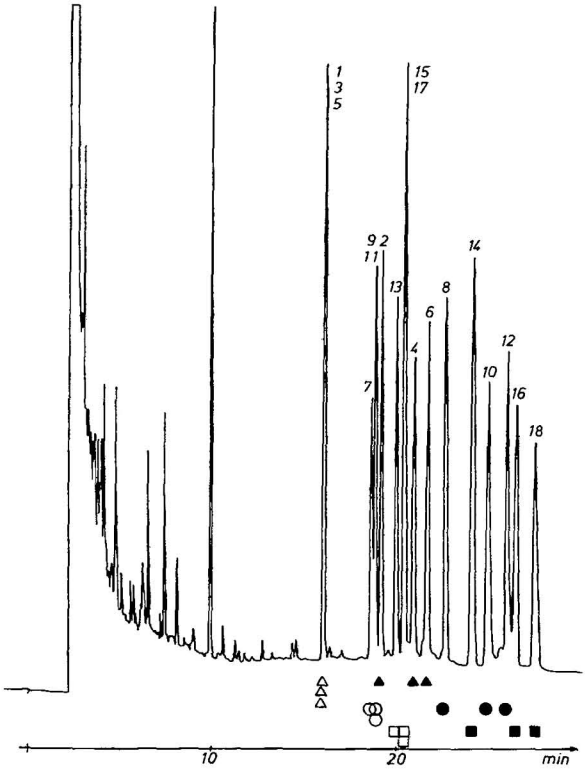

Fig. 1. Gas chromatogram of hydroxycinnamoylquinic acids (trimethylsilyl derivatives). Column: SE-30 (wall-coated open tubular column, 37 m × 0.27 mm I.D.), temperature 220–270°C at 4°C/min. Injector and detector temperatures: 300°C. Carrier gas: nitrogen, 0.9 ml/min. Attenuation: 1 × 32. Splitting ratio: 1:20. Chart speed: 40 cm/h. Quinic acids: 1 = *cis*-3-*p*-coumaroyl; 2 = *trans*-3-*p*-coumaroyl; 3 = *cis*-4-*p*-coumaroyl; 4 = *trans*-4-*p*-coumaroyl; 5 = *cis*-5-*p*-coumaroyl; 6 = *trans*-5-*p*-coumaroyl; 7 = *cis*-3-feruloyl; 8 = *trans*-3-feruloyl; 9 = *cis*-4-feruloyl; 10 = *trans*-4-feruloyl; 11 = *cis*-5-feruloyl; 12 = *trans*-5-feruloyl; 13 = *cis*-3-caffeoyl; 14 = *trans*-3-caffeoyl; 15 = *cis*-4-caffeoyl; 16 = *trans*-4-caffeoyl; 17 = *cis*-5-caffeoyl; 18 = *trans*-5-caffeoyl; △, *cis*-, ▲, *trans*-*p*-coumaroyl; ○, *cis*-, ●, *trans*-feruloyl; □, *cis*-, ■, *trans*-caffeoyl.

(995:5). The eluate was concentrated to 50 ml at 40°C under vacuum. This served as a stock solution for analysis by GC and HPLC.

Capillary GC

GC analysis was performed with a Carlo Erba 2150 gas chromatograph equipped with a Grob splitter, a glass capillary and a flame ionization detector. Borosilicate glass capillaries (0.27 mm I.D., 0.8 mm O.D.) were leached, flushed and dehydrated according to Grob *et al.*[9]. A simple and excellent deactivation is achieved by silylation with N,O-bis(trimethylsilyl)acetamide (BSA). Nine tenths of the capillary were filled with BSA and the ends were sealed in a flame. The capillary was kept at 110 C for 20 h, then flushed with toluene and pentane (2 ml of each for a 50-m capillary) and dried at 100°C in a nitrogen flow for about 30 min. The capillary was coated by the static method[10] using a 0.2% solution of the coating material in pentane. 3 m at both ends were discarded.

Derivatization of the samples. A 0.5-mg amount of (+)-catechin (Roth) was added as an internal standard to 2–10 ml of the stock solution depending on its concentration, and the sample was evaporated to dryness. Derivatization was performed with 1 ml of BSA–trimethylchlorosilane (TMCS) (20:1) at 70°C for 1 h.

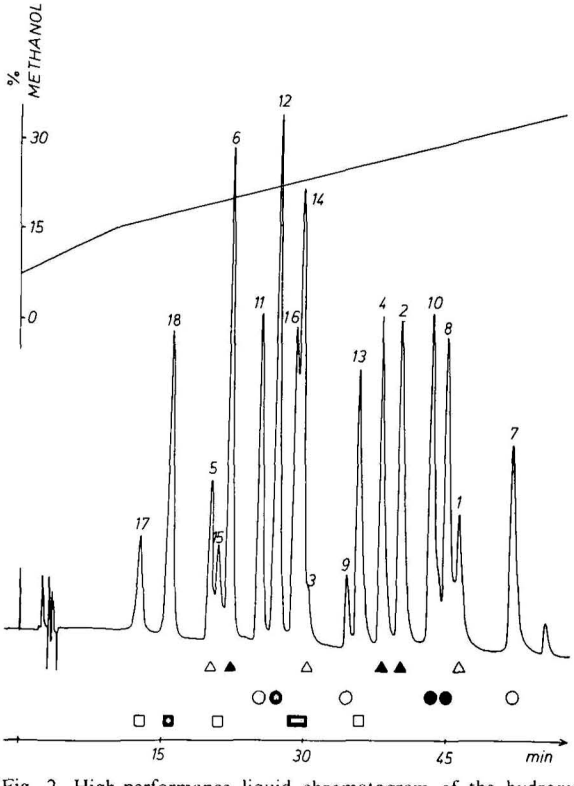

Fig. 2. High-performance liquid chromatogram of the hydroxycinnamoylquinic acids. Column: LiChrosorb RP-18. Detection: 320 nm. Flow-rate: 0.8 ml/min. Gradient elution: solvent A = 2% acetic acid, B = methanol; from 7% B to 15% B in 10 min, then from 15% B to 35% B in 50 min. Peaks as in Fig. 1.

Quantitative analysis of the chromatograms was done with a Hewlett-Packard 3390 A integrator. Each compound was calibrated with chlorogenic acid. With an injection volume of 1 μl and splitting ratio of 1:20, the detection limit for each substance is 10 ng, that means 1 ppm for the original concentration in the fruit.

HPLC

HPLC analysis was performed with a Pye Unicam HPLC chromatograph (LC XPD pump, LC XP gradient programmer, LC UV detector) equipped with a Rheodyne 7125 injection valve (10 μl) and a reversed-phase C_{18} column (LiChrosorb RP-18, 5 μm, 250 × 4 mm I.D.; E. Merck, Darmstadt, G.F.R.). The stock solutions can be used without modification although in some cases dilution was useful.

For quantitative analysis the HP 3390 A integrator was used. Calibration was done with the free acids (caffeic, *p*-coumaric and ferulic acid) and their mass concentrations were calculated with respect to their molecular weights.

RESULTS AND DISCUSSION

Prepurification

Polyamide columns are generally used to isolate phenolic compounds from plant extracts. Because of their carboxyl group in addition to the phenolic structure the hydroxycinnamoylquinic acids are strongly adsorbed by polyamide. On one hand this fact permits their separation from other phenolics like hydroxycinnamoylglucose and most of the flavonoids. On the other it poses the problem of desorption without modification or decomposition.

The usual method of desorption by an alkaline solution cannot be applied because of the formation of positional isomers and rapid oxidation, especially of caffeic acid esters. We have tried an elution with methanol–0.05 *N* HCl (9:1), but when concentrating the eluate we observed that the increase in concentration of the acid caused a methylation.

Both problems are avoided by eluting with methanol–formic acid (995:5). Using this method no modification of any compound was found. This was shown in the case of chlorogenic acid with a recovery of 98%.

For GC analysis this preliminary purification is absolutely necessary because otherwise perturbating substances would be silylated in a similar way. It is also important for HPLC because it simplifies the chromatograms, which means an increase in reliability.

Derivatization

When performing the derivatization for GC by use of pure BSA, a permutation of positional isomers takes place in some cases. Probably this is due to the alkaline nature of BSA and is avoided by the addition of the strongly acidic TMCS.

Capillary GC

As silyl derivatives of hydroxycinnamoylquinic acids are very sensitive to contact with incompletely deactivated surfaces, a high degree of inertness even at high temperatures was required. Most commercially available capillaries did not provide either the required inertness or the separation efficiency, especially after longer periods

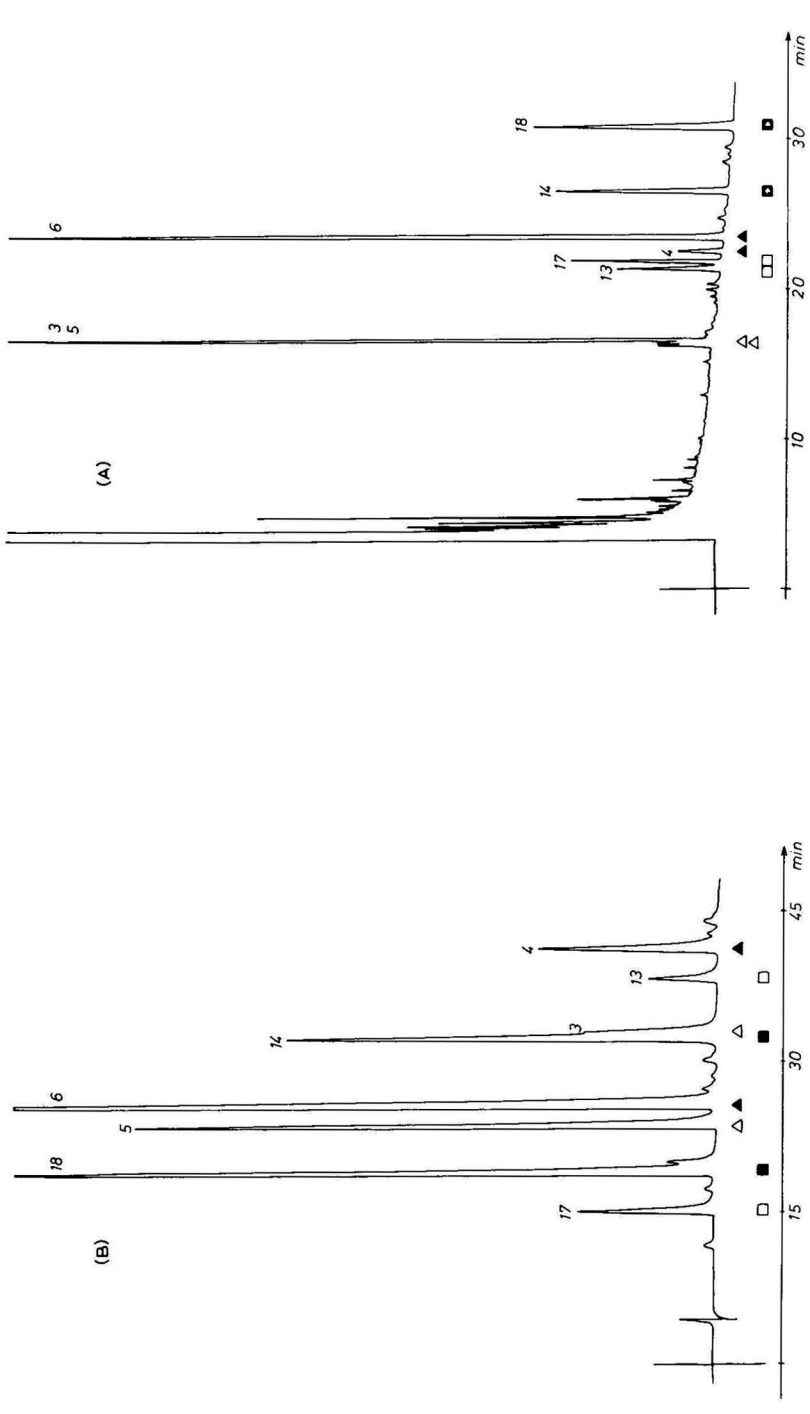

Fig. 3. GC (A) and HPLC (B) separation of an extract of the morello cherry "Schattenmorelle Bockelmann". Peaks and conditions as in Figs. 1 and 2.

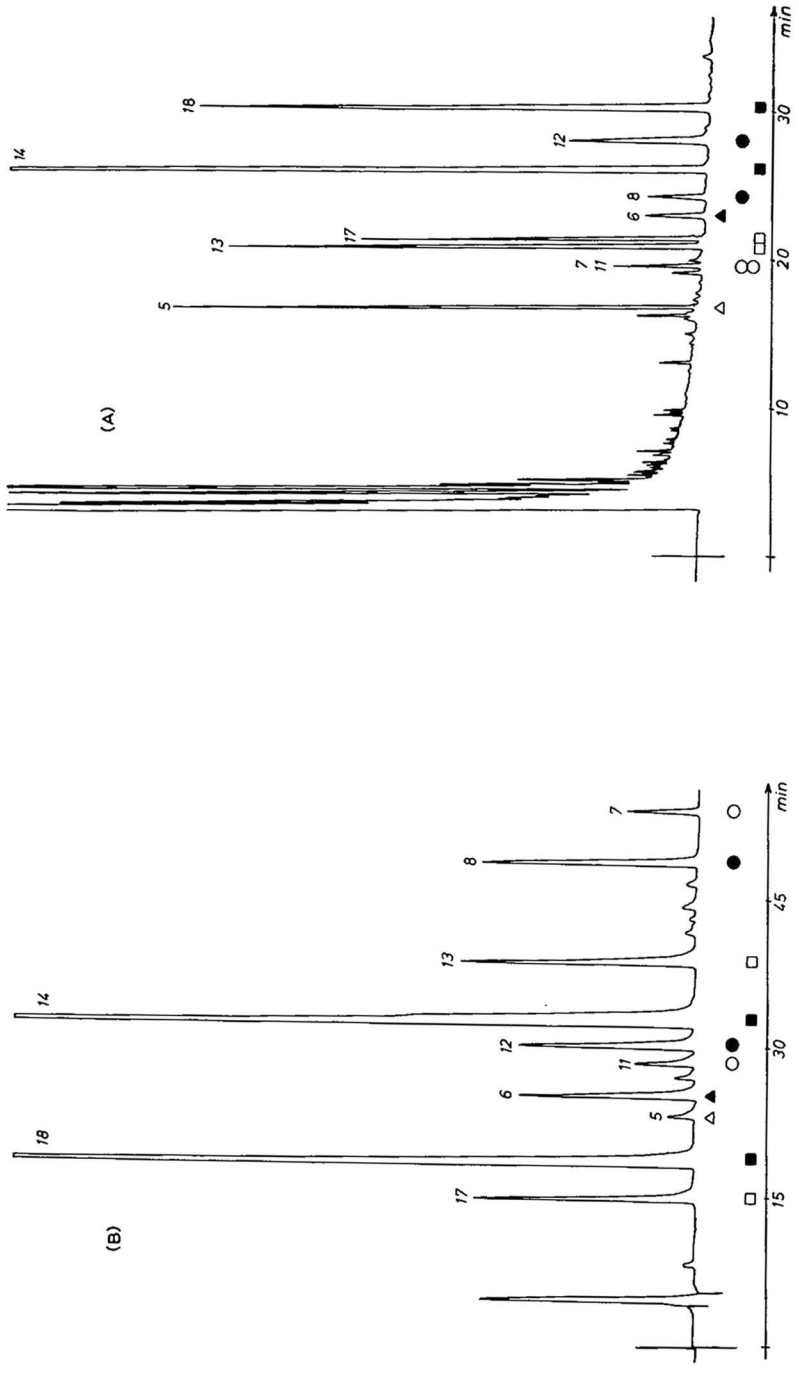

Fig. 4. GC (A) and HPLC (B) separation of an extract of the apricot "Mombacher Frühe". Peaks and conditions as in Figs. 1 and 2.

of use. Therefore a procedure has been developed which guaranties suitable capillaries of constant quality. These capillaries (≈ 40 m) had a separation number according to Kaiser[11] (determined with undecane and dodecane at 90°C) between 35 and 45 and their quality could be maintained for more than half a year.

A comparison of the different stationary phases SE-30, SE-52, Dexsil 300 and 400 revealed that the less polar phase SE-30 showed the best separation. For all hydroxycinnamoylquinic acids and for all stationary phases the three *cis* isomers were eluted before the *trans* isomers and the positional isomers in the sequence 3-, 4-, 5-.

HPLC

In contrast to GC, HPLC does not require derivatization nor specially prepared columns.

On RP-18 the positional isomers were eluted contrary to GC in the sequence 5-, 4-, 3- when using a gradient elution with 2% acetic acid and methanol. The *cis* and *trans* isomers are grouped together. Surprisingly the sequence of the *cis* and the *trans* isomers differs for each positional isomer. For all hydroxycinnamoylquinic acids the *cis* isomers are eluted first for the 4- and 5-isomers, while the *trans* isomers are eluted first for the 3-isomers.

Quantitation

For both GC and HPLC, calibration could not be performed by the reference samples since sufficient amounts of pure substances were not available. Therefore in GC all compounds are calibrated with chlorogenic acid. It is assumed that the response of the compounds varies only slightly, because the structures and the molecular weights are very similar. In HPLC the free hydroxycinnamic acids in *trans* form have been used for calibration because the UV-absorption is believed to be the same for the free acids and the esters. Between chlorogenic acid and caffeic acid a difference of 4% was found. The results were corrected neither for this difference nor for the possible difference of the extinction of the *cis* and *trans* isomers.

Both chromatographic techniques have been applied to 20 different fruit samples and the results from the two methods agreed within 10%. This value is the maximum deviation that has been observed and there seems to be no systematic difference. The agreement is evidence that the assumptions made for calibration are reasonable and that no important effects have been negelected. The concentrations of the hydroxycinnamoylquinic acids found in pome and stone fruit, will be reported elsewhere.

HPLC may be preferred because there is no danger of decomposition and because it is easier to apply. On the other hand GC allows coupling with a mass spectrometer which provides a quick and reliable identification.

ACKNOWLEDGEMENT

The work was supported by a grant from Deutsche Forschungsgemeinschaft which is gratefully acknowledged.

REFERENCES

1 K. Herrmann, *Prog. Chem. Organ. Nat. Prod.*, 35 (1978) 73.
2 J. L. Wilson, W. J. Dunlap and S. H. Wender, *J. Chromatogr.*, 35 (1968) 329.
3 J. T. Kung, W. S. Ryder and J. R. Feldman, *Assoc. Sci. Int. Cafe*, (1968) 223.
4 A. Fleuriet and J. J. Macheix, *J. Chromatogr.*, 74 (1972) 339.
5 E. Bombardelli, B. Gabetta and E. M. Martinelli, *Fitoterapia*, 48 (1977) 143.
6 J. Krause and D. Strack, *J. Chromatogr.*, 176 (1979) 465.
7 L. Nagels, W. van Dongen, J. de Brucker and H. de Pooter, *J. Chromatogr.*, 187 (1980) 181.
8 M. L. Scarpati and P. Esposito, *Ann. Chim. (Rome)*, 54 (1964) 56.
9 K. Grob, G. Grob and K. Grob, Jr., *J. High Resolut. Chromatogr. Chromatogr. Commun.*, 2 (1979) 31.
10 J. Bouche and M. Verzele, *J. Gas Chromatogr.*, 6 (1968) 501.
11 R. Kaiser, *Chromatographie in der Gasphase, II Kapillar-Chromatographie, Dünnfilm- and Dünnschichtkapillar-GC*, Bibliographisches Institut, Mannheim, Wien, Zürich, 1975.

Journal of Chromatography, 241 (1982) 381–389
Elsevier Scientific Publishing Company, Amsterdam — Printed in The Netherlands

CHROM. 14,750

TRACE ENRICHMENT AND SEPARATION OF CHOLESTEROL OXIDATION PRODUCTS BY ADSORPTION HIGH-PERFORMANCE LIQUID CHROMATOGRAPHY

ISTVAN CSIKY
Department of Analytical Chemistry, University of Lund, POB 740, S-22007 Lund (Sweden)
(First received September 25th, 1981; revised manuscript received January 18th, 1982)

SUMMARY

A method for the liquid chromatographic determination of some oxidation products of cholesterol is described. The oxygenated sterols were concentrated on a short pre-column of Nucleosil NO_2 with hexane as the mobile phase. The separation was performed on a longer column with the same stationary phase but with a hexane–propanol or a hexane–butanol gradient.

Cholest-5-ene-3β,20α-diol, cholest-5-ene-3β,25-diol cholest-5-ene-3β,7α-diol, cholest-5-ene-3β,7β-diol, 3β-hydroxycholest-5-ene-7-one and cholest-5-en-3β-ol were detected at levels as low as 10^{-8} mole $\cdot l^{-1}$. The method was also used for the determination of oxidation products of cholesterol in butter and in heated butter.

INTRODUCTION

Cholesterol is generally recognized as a possible risk factor in the occurrence and progression of coronary heart disease and atherosclerosis. Cholesterol is easily oxidized in the presence of air, especially when heated[1,2]. Some of the oxidized sterols may accumulate in the walls of arteries[3–6], and animal feeding experiments indicate a connection between dietary intake of cholesterol oxidation products and atherosclerosis[7–9]. It is also known that a substantial amount of cholesterol is obtained from the diet and that much food is exposed to heat before consumption. Despite great interest in cholesterol itself, information on its oxidation products and their occurrence, *e.g.*, in foods, is limited. This may be due to the lack of adequate purification and concentration methods. Extraction followed by gas chromatography[3] produced a number of peaks suspected to be oxidation products; however, some of them were found to be artifacts[4] due to the exposure of the samples to air and high temperature. Efficient high-performance liquid chromatography (HPLC) separations of mixtures of oxygenated sterols have been described[10–12] and HPLC separation in combination with enzymatic detection has been suggested[12]. The latter method gives improved detection of sterols with low UV absorption, but its application is restricted to aqueous or alcoholic samples. In the common case of low concentrations in lipid matrices it seems necessary to include a pre-concentration and preferably an enrichment pro-

0021-9673/82/0000–0000/$02.75

cedure. In an unpublished method[13] the triglycerides were removed by freezing and with this procedure the oxidation products could easily be lost by coprecipitation.

This paper describes a method for the determination of oxygenated sterols in foods. It employs a concentration column connected on-line with a separation column. A preliminary study of the formation of some oxygenated sterols in heated butter was made.

EXPERIMENTAL

A sterol mixture containing cholest-5-ene-3β,20α-diol (20α-hydroxycholesterol) ($3 \cdot 10^{-4}$ *M*), cholest-5-ene-3β,25-diol (25-hydroxycholesterol) ($3 \cdot 10^{-4}$ *M*), cholest-5-ene-3β,4β-diol (4β-hydroxycholesterol) ($3 \cdot 10^{-4}$ *M*), cholest-5-ene-3β,7α-diol (7α-hydroxycholesterol) ($4 \cdot 10^{-4}$ *M*), cholest-5-ene-3β,7β-diol (7β-hydroxycholesterol) ($3 \cdot 10^{-4}$ *M*), 3β-hydroxycholest-5-ene-7one (7-ketocholesterol) ($4 \cdot 10^{-4}$ *M*) and cholest-5-ene-3β-ol (cholesterol) ($3 \cdot 10^{-4}$ *M*) was prepared by dissolving the reference substances in hexane–propanol (99.9:0.1) and further diluting with hexane. This mixture will be referred to as "sterol mixture A".

The hydroxycholesterols and 7-ketocholesterol were purchased from Steraloids (Pawling, NJ, U.S.A.). Cholesterol and triolein (glyceryl trioleate) were obtained from Sigma (St. Louis, MO, U.S.A.).

A gradient liquid chromatograph (Spectra Physics SP 8000) was used in all experiments. Spectrophotometric detection was carried out with two UV detectors, an LKB 2138 Uvicord S at 206 nm and with an LDC Spectromonitor III at 210 nm. The detector sensitivities were set to 0.2 a.u.f.s.

The concentration and separation columns were made of stainless steel, with dimensions 40 × 3.9 mm I.D. and 200 × 2.9 mm I.D., respectively. Both columns were packed with 5 μm Nucleosil NO_2 bonded phase material.

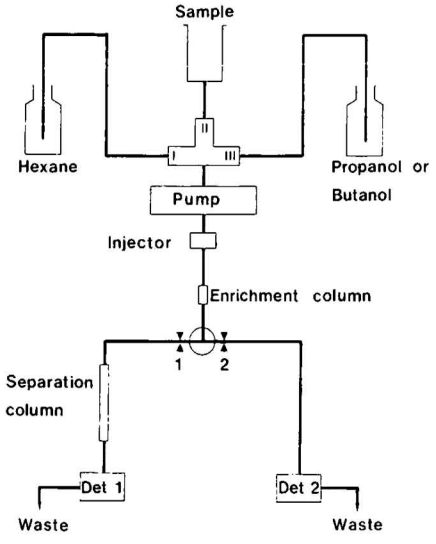

Fig. 1. Chromatographic set-up. 1, 2 = Needle valves; I, II, III = microprocessor-controlled gradient mixing valves.

The experimental set-up, shown in Fig. 1, was used in three modes of operation, each involving changes in mobile phase composition.

Concentration step

The sample was introduced through one of the three mobile-phase inlets of the SP 8000 microprocessor-controlled gradient mixing valves. By appropriate programming, sample volumes of 1.0–1000 ml were injected. Sample volumes of less than 1.0 ml were injected by the valve injector with a syringe. The injection medium was hexane. The outlet from the concentrating column could be directed either to detector 2 or to the separation column by means of a T-connection and two needle valves. During the concentration step valve 1 (to the separation column) was closed and valve 2 was open. Detector 2 (210 nm) gave useful information about components in the sample which were not retarded by the concentration column and about the time needed for a certain sample volume to pass through.

Separation step

Needle valve 1 was opened and needle valve 2 was closed when the signal from detector 2 returned to the baseline. A linear gradient programme from 0 to 5% propanol in hexane or from 0 to 10% butanol in hexane for 30 min at 2.5 ml/min was then activated. Cholesterol and the oxygenated sterols were gradually eluted with increasing proportions of alcohol and were detected at 206 nm.

Re-equilibration

Before the next injection, the system was re-equilibrated with hexane at 2.5 ml/min. Stripping the column with alcohol was completed after about 40 min.

RESULTS

The concentration procedure was studied with a model system which consisted of the diluted sterol mixture A. The chromatograms were evaluated by peak-height measurements. In order to facilitate comparison of peak heights, the results were normalized to the peak height of 7-ketocholesterol.

Pumping speed

Sterol mixture A was diluted to $3 \cdot 10^{-7}$–$4 \cdot 10^{-7}$ *M* and 40.0 ml of the diluted mixture were injected at different pumping speeds. Separations were carried out at 40°C with a linear gradient from 0 to 5% propanol in hexane for 30.0 min at a flow-rate of 2.5 ml/min.

The results in Table I indicate that the enrichment of the sterols is independent of the pumping speed up to at least 7 ml/min. The apparent decrease at 10 ml/min may be due to an error in the volume injected caused by failure of the pumping programme to cope with this high speed. The peak-height variation at pumping speeds below 7.0 ml/min is only slightly higher than that for repeated injections of the same sample volume at constant pumping speed.

Temperature effect

The effect of temperature on the concentration and separation was also ex-

TABLE I

INFLUENCE OF PUMPING SPEED ON CONCENTRATION EFFICIENCY

Pumping speed (ml/min)	*Peak height relative to 7-ketocholesterol*							*Absolute peak height (mm) for 7-keto-chol*
	Chol	*20α-OH-chol*	*25-OH-chol*	*4β-OH-chol*	*7α-OH-chol*	*7β-OH-chol*	*7-keto-chol*	
2.0	0.59	0.60	0.70	0.15	0.86	0.80	1.00	66.3
3.0	0.58	0.61	0.62	0.15	0.86	0.81	1.00	66.0
4.0	0.63	0.68	0.64	0.14	0.84	0.81	1.00	65.5
5.0	0.53	0.64	0.67	0.12	0.87	0.84	1.00	64.5
6.0	0.48	0.60	0.66	0.12	0.90	0.82	1.00	66.8
7.0	0.65	0.67	0.68	0.15	0.85	0.83	1.00	63.0
10.0	0.55	0.59	0.67	0.12	0.79	0.76	1.00	58.0
S (%)*	10	6	4	10	4	3	–	5

* S = Relative standard deviation.

plored. Three temperature settings were used: 75, 40 and 15°C. Separations were carried out as before, but with a constant pumping speed of 1.0 ml/min. A 1.0-ml volume of sterol mixture A diluted to 10^{-5} M was injected.

At 75°C both concentration and separation were affected in a negative way. The peak-height variation for cholesterol, which is the first peak in the chromatogram, was very large and the peaks were also distorted. The recovery, as estimated from peak-height measurements, was 20–30% less than at either 40 or 15°C.

At both 40 and 15°C the concentration was quantitative and the separation was sufficient. The peak-height variation for cholesterol was 10% at 40°C and 7% at 15°C. The peaks were narrower, higher and more symmetrical at the lower temperature. Thus, a temperature of 15°C was chosen for the subsequent experiments.

Concentration effect

One of the most important features of concentration system is its ability to concentrate very dilute solutions with an acceptable recovery. To explore this for the present system the following experiment was carried out.

Five samples, containing the same amount of sterol mixture A (100 μl, 1.0, 10.0, 100.0 and 1000 ml), were prepared. The concentration thus varied from about $3 \cdot 10^{-3}$ to $3 \cdot 10^{-8}$ M. The pumping speed was 5.0 ml/min. Separations were carried out as before. Table II shows that the relative peak heights are independent of dilution, whereas the absolute peak heights show a small decrease due to band broadening in the concentration column. For the most dilute solution several minor "unknown" peaks appeared in the chromatograms. Considering the facile oxidation of cholesterol in dilute solutions[1], it is possible that the peaks may be due to oxidation products other than those contained in sterol mixture A.

Interference from excess of cholesterol

Sterol mixture A was diluted to $3 \cdot 10^{-7}$–$4 \cdot 10^{-7}$ M with hexane in three flasks. Cholesterol was added to total concentrations of $2 \cdot 10^{-6}$, $6 \cdot 10^{-6}$ and $6 \cdot 10^{-5}$ M,

TABLE II

DEPENDENCE OF CONCENTRATION EFFICIENCY ON SAMPLE DILUTION

*Concentration (M)**	*Injection volume (ml)*	*Peak height relative to 7-ketocholesterol*							*Absolute peak height (mm) for 7-keto-chol*
		Chol	*20α-OH-chol*	*25-OH-chol*	*4β-OH-chol*	*7α-OH-chol*	*7β-OH-chol*	*7-keto-chol*	
$a \cdot 10^{-4}$	0.1	0.79	0.62	0.73	0.25	0.82	0.81	1.00	69
$a \cdot 10^{-5}$	1.0	0.93	0.63	0.69	0.24	0.80	0.84	1.00	64
$a \cdot 10^{-6}$	10.0	0.92	0.64	0.69	0.24	0.81	0.78	1.00	61
$a \cdot 10^{-7}$	100.0	0.84	0.71	0.73	0.23	0.82	0.79	1.00	58
$a \cdot 10^{-8}$	1000	0.90	0.79	0.72	0.23	0.86	0.85	1.00	56

* $a = 3$ for cholesterol, 20α-hydroxycholesterol, 25-hydroxycholesterol, 4β-hydroxycholesterol and 7β-hydroxycholesterol; $a = 4$ for 7-ketocholesterol and 7α-hydroxycholesterol.

respectively. Samples of 100 ml were injected. The results, which were obtained under the same conditions as above, are presented in Table III. It can be seen that this excess of cholesterol does not influence the concentration of the other sterols. The chromatogram obtained when cholesterol was present in the largest excess is shown in Fig. 2. The resolution is still very good, and it is not affected by the large cholesterol peak at the beginning of the chromatogram.

Interference from triglycerides

Glycerol triolate represents about 3 % of the lipids in butter and was selected as a model substance for the examination of the concentration selectivity. The most common triglyceride, glycerol tristearate, could not be dissolved in hexane. The gradient mixing valve controlling the flow of propanol (valve III, see Fig. 1) was temporarily connected to a solution of glycerol trioleate in hexane (90.0 mg/ml) during the concentration step. The concentration programme was altered so that the interfering material could be added independently through valve III. Sterol mixture A, diluted to $3 \cdot 10^{-6}$–$4 \cdot 10^{-6}$ *M*, was introduced through valve II. The sample was diluted by the streams through valves I and III. These two valves controlled the ratio of hexane to triolein solution in the enrichment medium. The sample flow-rate was 2.5 ml $\cdot$ min^{-1}, the total flow-rate through the concentration column was 5.0 ml/min and the sample volume was 10.0 ml. The propanol tubing was reconnected and the

TABLE III

DEPENDENCE OF CONCENTRATION EFFICIENCY ON THE AMOUNT OF CHOLESTEROL IN THE ENRICHMENT MEDIUM

Cholesterol (M)	*Peak height relative to 7-ketocholesterol*						*Absolute peak height (mm) for 7-keto-chol*
	20α-OH-chol	*25-OH-chol*	*4β-OH-chol*	*7α-OH-chol*	*7β-OH-chol*	*7-keto-chol*	
$2 \cdot 10^{-6}$	1.00	1.05	0.33	1.00	0.98	1.00	62
$6 \cdot 10^{-6}$	1.05	0.96	0.28	1.02	1.03	1.00	66
$6 \cdot 10^{-5}$	0.95	0.99	0.32	0.99	0.98	1.00	67

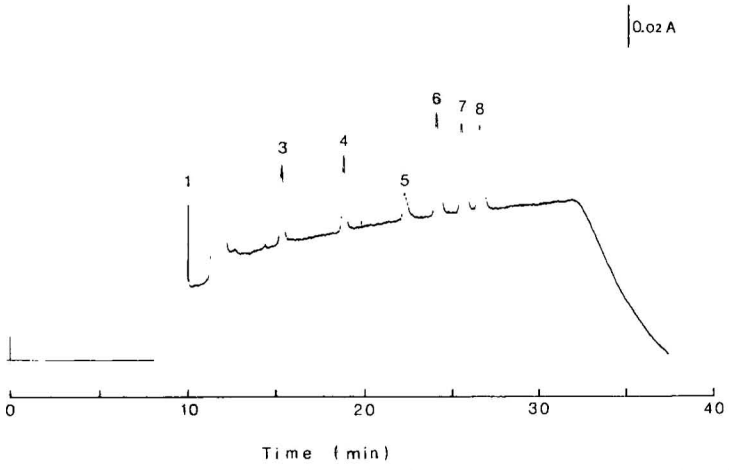

Fig. 2. Concentration and separation of a mixture of oxidized sterols (*ca.* $3 \cdot 10^{-7}$ *M*) with excess of cholesterol ($6 \cdot 10^{-5}$ *M*) in the sample solution. Peaks: 1 = peak due to displacement effect; 2 = cholesterol; 3 = 20α-hydroxycholesterol; 4 = 25-hydroxycholesterol; 5 = 4β-hydroxycholesterol; 6 = 7-ketocholesterol; 7 = 7α-hydroxycholesterol; 8 = 7β-hydroxycholesterol.

original programme was restarted when the concentration had been completed.

A small fraction from the triglyceride solution was also retarded on the concentration column and worsened the separation on the main column. An improvement was achieved when butanol was used instead of propanol and the gradient shape was adjusted. The separation gradient was from 0 to 10% butanol in hexane for 30 min at a flow-rate of 2.5 ml/min. The results from runs with glycerol trioleate levels in the concentration medium of 4.5, 22.5 and 45 mg/ml, respectively, are shown in Table IV.

It was found that the level of triglyceride in the concentration medium affected both the concentration and the separation. The recovery of the early sterol peaks, such as cholesterol and 20α-hydroxycholesterol, decreased with increasing level of triglyceride. The explanation may be that the less polar sterols spread over a larger part of the concentration column owing to a competitive effect of the triglyceride solution. This leads to band broadening and a decreased utilization of the concentration column. The concentration column should therefore have a large over-capacity.

TABLE IV

DEPENDENCE OF CONCENTRATION EFFICIENCY ON THE AMOUNT OF TRIOLEIN IN THE ENRICHMENT MEDIUM

Triolein (mg/ml)	*Peak height relative to 7-ketocholesterol*							*Absolute peak height (mm) for 7-keto-chol*
	Chol	*20α-OH-chol*	*25-OH-chol*	*4β-OH-chol*	*7α-OH-chol*	*7β-OH-chol*	*7-keto-chol*	
0	1.29	1.06	0.91	0.34	0.99	1.02	1.00	72
4.5	0.96	0.67	0.81	0.30	1.00	0.99	1.00	72
22.5	0.85	0.69	0.79	0.29	0.94	0.93	1.00	70
45.0	0.75	0.81	0.78	0.31	0.99	0.95	1.00	70

The separation on the main column was also worsened by components from the trioleate solution, reatained on the concentration column. A broad peak appearing at the front of the chromatogram increased with increasing amount of triglyceride. Prior purification of the triolein solution removes the interference. The competition in the concentration column, on the other hand, seems to be caused by the triglyceride itself. Apart from the additional peak there is, of course, a band broadening when a triglyceride is present during the concentration step, caused by the broader distribution in the concentration column. The separation was acceptable when the level of unpurified trigylceride in the sample solution was below 45 mg/ml.

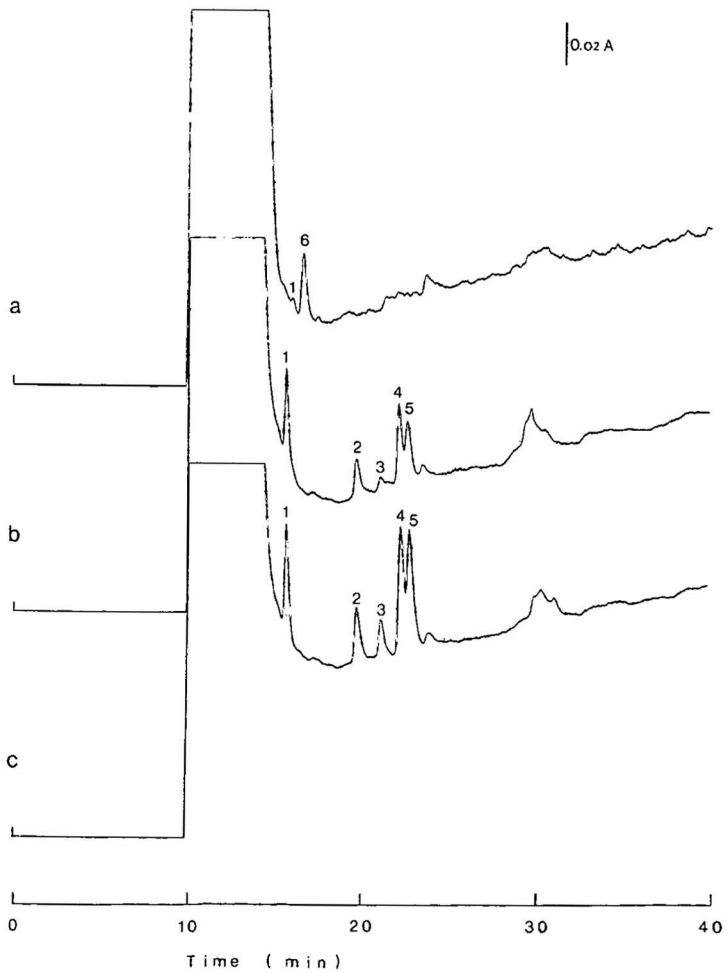

Fig. 3. Concentration and separation of oxidized sterols in heated and unheated butter. (a) Unheated butter; (b) butter heated at 180°C for 5 min; (c) same as b but with standard addition of reference mixture A. Peaks: 1 = 25-hydroxycholesterol; 2 = 4β-hydroxycholesterol; 3 = 7-ketocholesterol; 4 = 7α-hydroxycholesterol; 5 = 7β-hydroxycholesterol; 6 = unknown.

Oxidized cholesterol in butter

The method described above was used for determining oxidized cholesterol in unheated and heated butter. Butter (1.0 g) was heated for 5 min in an open glass vessel kept at 180°C. The butter was dissolved in 100 ml of hexane and the solutions were centrifuged to remove water and filtered to remove particles. Volumes of 25 ml were injected at a pumping speed of 5.0 ml/min. Separations were carried out with a linear gradient from 0 to 10% butanol in hexane for 30 min at a flow-rate of 2.5 ml/min and a temperature of 15°C.

Some of the resulting chromatograms are presented in Fig. 3. Chromatogram a was obtained when a solution of natural butter and b when a solution of heated butter was injected. Chromatogram c was obtained with the same solution as for b, but with addition of reference mixture A.

The separation of the oxidized sterols is still efficient, although the large interfering peak from triglycerides, cholesterol and possibly other compounds in the samples makes UV detection of 20α-hydroxycholesterol impossible. The identity of peak 6 from the unheated butter is not known. Some variation in retention time was sometimes observed. This could be due to a varying degree of displacement of sterols during the concentration step. The amounts of oxidized cholesterol found in heated and unheated butter are given in Table V. The amount of cholesterol in butter is about 2.50 mg/g. Thus about 4% of the cholesterol was oxidized during 5 min at 180°C. The interference from the matrix increased when the heating was prolonged.

DISCUSSION

Trace components can normally be recovered from complex matrices only after lengthy multi-step work-up procedures. Cholesterol and similar lipids in food are usually analysed by chromatographic methods after group separation by different extraction procedures[14–17]. Apart from being laborious these methods are less suitable for the determination of oxidation products as there is a pronounced risk of oxidation during sample preparation. The single-step trace concentration described here is adequate for butter that has been only slightly oxidized. After prolonged heating, there is further degradation, resulting in products that interfere in the method. The nature of these interfering substances is not known, but mass spectrometry has shown that the amount of cholesterol esters with fatty acids increases con-

TABLE V

OXIDIZED CHOLESTEROL CONTENT IN HEATED AND UNHEATED BUTTER

Sample	*Concentration (ug/g)*				
	25-OH-chol	*4β-OH-chol*	*7-keto-chol*	*7α-OH-chol*	*7β-OH-chol*
Unheated	2.6	–	–	–	–
Heated for 5 min at 180°C	34.0	25.6	5.2	19.6	8.4
Heated for 10 min at 180°C	–	5.2	11.2	52.2	19.7

siderably. The selectivity of the concentration step is not sufficient. When some other samples, such as eggs, were analysed, a number of broad peaks appeared in the chromatogram and the determination of trace amounts of oxidized sterols became impossible.

The chromatographic system described is capable of quantitative concentration and separation, even when cholesterol is present in large excess. Triglycerides can be tolerated only in limited concentrations.

ACKNOWLEDGEMENTS

The author thanks Dr. Lars Haraldson for valuable discussions and continuous support and Professor Gillis Johansson for his interest and review of the manuscript. In addition, support from Swedish National Food Administration is acknowledged.

REFERENCES

1 S. Bergström, *Ark. Kemi, Mineral. Geol.*, 16A, No. 10 (1942) 1.
2 L. L. Smith, W. S. Matthews, J. C. Pride, R. C. Bachmann and B. Reynolds, *J. Chromatogr.*, 27 (1967) 187.
3 J. E. Van Lier, L. L. Smith, *Biochemistry*, 6 (1967) 3269.
4 L. L. Smith and J. E. Van Lier, *Atherosclerosis*, 12 (1970) 1.
5 L. L. Smith and N. L. Pandya, *Atherosclerosis*, 17 (1973) 21.
6 J. I. Teng and L. L. Smith, *Texas Rep. Biol. Med.*, 33 (1975) 2.
7 K. T. Lee, H. Imai, N. T. Werthessen and C. B. Taylor, *Atherosclerosis*, 1 (1978) 648.
8 H. Imai, N. T. Werthessen, C. B. Taylor and K. T. Lee, *Arch. Pathol. Lab. Med.*, 100 (1976) 565.
9 H. Imai, N. T. Werthessen, V. Subramanyam, P. W. LeSuesne, A. H. Soloway and M. Kanisawa, *Science*, 207 (1980) 651.
10 G. A. S. Ansari and L. L. Smith, *J. Chromatogr.*, 175 (1979) 307.
11 L. S. Tsai and C. A. Hudson, *J. Amer. Oil Chem. Soc.*, 58 (1981) 931.
12 L. Ógren, I. Csiky, L. Risinger, L. G. Nilsson and G. Johansson, *Anal. Chim. Acta*, 117 (1980) 71.
13 L. B. Croon, Swedish National Food Administration, personal communication.
14 E. G. Bligh, W. J. Dyer, *Can. J. Biochem. Physiol.*, 37 (1959) 911.
15 J. K. Punwar, *J. Ass. Offic. Anal. Chem.*, 58 (1975) 804.
16 W. D. Hubbard, A. J. Sheppard, D. R. Newkirk, A. R. Prosser and T. Osgood, *J. Amer. Oil Chem. Soc.*, 54 (1977) 81.
17 A. J. Sheppard, D. R. Newkirk, W. D. Hubbard and T. Osgood, *J. Ass. Offic. Anal. Chem.*, 60 (1977) 1302.

Journal of Chromatography, 241 (1982) 390–391
Elsevier Scientific Publishing Company, Amsterdam — Printed in The Netherlands

CHROM. 14,784

Note

Convenient apparatus for methylating small samples with diazomethane

M. A. WALKER, D. R. ROBERTS and E. B. DUMBROFF*
Department of Biology, University of Waterloo, Waterloo, Ontario N2L 3G1 (Canada)
(Received January 28th, 1982)

Schlenk and Gellerman[1] introduced a method for small-scale esterification of fatty acids with diazomethane in 1960. Methylation by that procedure is now commonly used to increase the volatility and improve the chromatographic chracteristics of a wide range of acidic organic compounds. However the explosive and toxic nature of diazomethane[2] mandates a sealed but flexible system that minimizes leakage and glassware breakage yet provides for convenient attachment and removal of sample and reaction vials to the methylation system. Contaminants from non-inert surfaces, such as rubber stoppers, should also be eliminated in order to achieve accurate quantitative results with modern, high-performance, chromatographic columns. Experience in our laboratory has shown that previously described apparatus[1,3] used in the production of diazomethane lack one or more of these requirements. As a result we have modified the Schlenk and Gellerman system and have developed a simple, inert and tightly-sealed unit that allows for convenient methylation of small samples.

The completely assembled apparatus consists of four identical units (Fig. 1) connected in series with PTFE tubing. A stream of nitrogen is passed through 8 ml of diethyl ether in the first unit and then into the diazomethane generating unit (unit 2) that contains 1.1 ml of diethyl ether, 1.1 ml (2-(2-ethoxyethoxy) ethanol (Aldrich, Milwaukee, WI, U.S.A.), 0.9 ml of 10 *M* NaOH and 0.8 g of N-methyl-N-nitroso-*p*-toluene sulfonamide (Diazald, Aldrich). Ethereal diazomethane is swept into unit three which, initially, contains 3 ml of diethyl ether. When the ether turns yellow, the vial is replaced with one containing a sample dissolved in 3 to 6 ml of methanol or another appropriate solvent. Derivatization is complete upon development of a light yellow color in the sample vial. Excess diazomethane passes into unit 4 and is neutralized in 8 ml of glacial acetic acid. Six to eight samples of μg to mg quantities can be esterified in about 10 min. The reaction in unit 2 is stopped by adding 3 ml of acetic acid, and the reagents are replaced before repeating the procedure with additional samples.

Each unit consists of a 6 mm O.D. gas delivery tube (g) with the inlet tapered to allow attachment of narrow-bore PTFE tubing. All cut glass is fire polished to avoid reactive surfaces[2]. The delivery tube is held in place with a bored vial cap (a), and a closed, leak-proof system is assured by using PTFE-backed, silicone, sealing rings (b, 15 mm O.D., 6 mm I.D. and d, 22 mm). The flanged, double screw-cap (e, 22 mm) facilitates rapid changing of sample vials (f). Excess diazomethane leaves the unit via

0021-9673/82/0000–0000/$02.75

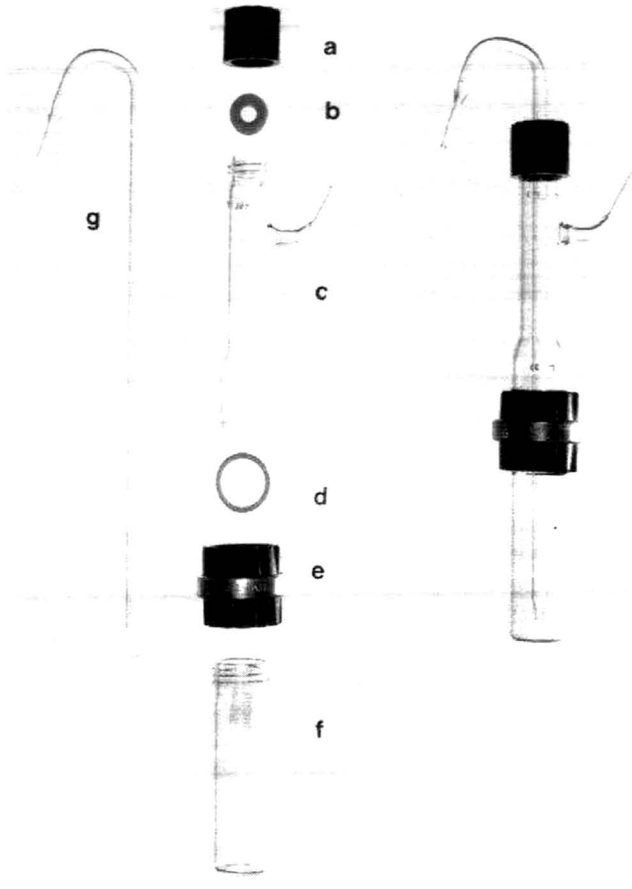

Fig. 1. An assembled methylation unit and individual components. Description in text.

the tapered outlet of part c which consists of two fused, glass screw joints (22 and 15 mm). All parts of the apparatus are available from Sovirel Laboratory Glassware (Levallois-Perret, France) or from Pegasus Industrial Specialties (Agincourt, Ontario, Canada) and modifications are simple and readily made by a competent glassblower.

ACKNOWLEDGEMENTS

The authors are indebted to our glassblower, Mr. George Hill, for his ingenuity and helpful suggestions, and support from the Natural Sciences and Engineering Research Council of Canada is gratefully acknowledged.

REFERENCES

1 H. Schlenk and J. L. Gellerman, *Anal. Chem.*, 32 (1960) 1412.
2 D. R. Knapp, *Handbook of Analytical Derivation Reactions*, Wiley, New York, 1979.
3 M. J. Levitt, *Anal. Chem.*, 45 (1973) 618.

Journal of Chromatography, 241 (1982) 392–394
Elsevier Scientific Publishing Company, Amsterdam — Printed in The Netherlands

CHROM. 14,801

Note

Analysis of anions by ion chromatography using ultraviolet detection

R. A. COCHRANE* and D. E. HILLMAN
Materials Quality Assurance Directorate, Royal Arsenal East, London SE18 6TD (Great Britain)
(Received February 10th, 1982)

Single-column anion chromatography has been reported by Gjerde *et al.*[1,2] as a method for the analysis of anions. Separation is performed on a low-capacity, silica-based ion-exchange column and is achieved by using a very dilute solution of an aromatic acid salt (*e.g.* potassium hydrogen phthalate) as the eluent. An electrical conductivity detector is used to monitor the anion peaks. The system is simple to operate but is less sensitive than the two column system marketed by Dionex Corporation[3] where the use of a suppressor column eliminates the background conductivity.

This note describes the use of an ultraviolet detection system which relies on the decrease in the background ultraviolet absorption of the potassium hydrogen phthalate buffer as the individual anions are eluted. The sensitivity of this system is approximately one order of magnitude greater than with the conductance detector.

EXPERIMENTAL

The chromatographic system consisted of the following parts in series: (1) Milton Roy mini pump set at a flow-rate of 1.5 ml/min; (2) a Rheodyne 7120 sample injection valve fitted with a 100-μl sample loop; (3) Vydac 302 column, 25 cm × 4.6 mm I.D. (Separations Group); (4) LDC Model 701 conducto monitor used in the differential mode at the most sensitive setting (× 10); (5) Schoeffel SF770 variable-wavelength UV detector set at 308 nm detection wavelength and the zero suppression at −2 (maximum −5); (6) Servoscribe dual-pen recorder, set at 10 mV output and 1 cm/min chart speed.

Potassium hydrogen phthalate solution ($5 \cdot 10^{-3}$ *M*) at pH 4.6, filtered through a Millipore 0.65-μm filter (type DA) was used as eluent. Sample solutions were prepared from analytical grade reagents dissolved in the eluent.

RESULTS AND DISCUSSION

UV detection of anions is not generally applicable except at very low wavelengths such as 215 nm[4]. An alternative method of detection of non-UV-absorbing species is to add a low level of UV-absorbing substance to the eluent. The emergence of a component is then shown by a negative detector response.

This effect is easily achieved in the ion chromatography system where the preferred buffer solution (potassium hydrogen phthalate) has a strong UV response

0021-9673/82/0000–0000/$02.75

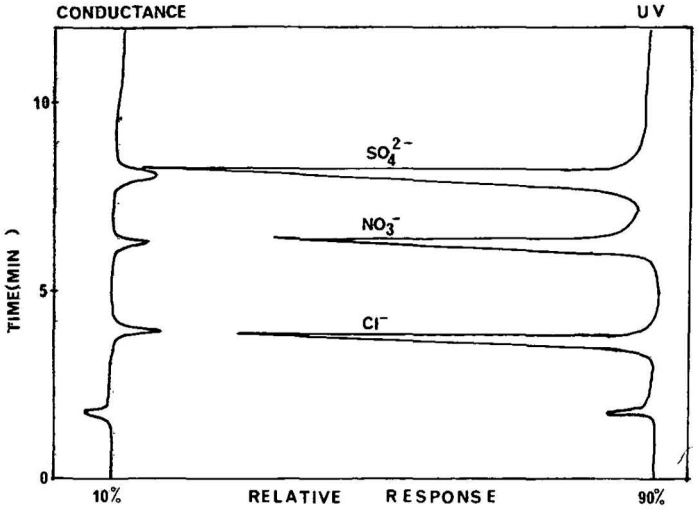

Fig. 1. Separation of chloride (10 ppm), nitrate (25 ppm) and sulphate (25 ppm) with UV and conductance detection.

with λ_{max} at 280 nm. At this wavelength the excessively strong absorbance will not allow adequate zero suppression, and the wavelength was therefore increased to a much less absorbing region (308 nm) where the background response could be backed-off sufficiently for the detector to be used at maximum sensitivity. A comparison of the conductivity and UV detectors showed that:

(1) The response is greater for UV detection by a factor of 5–30 (see Fig. 1 and

TABLE I

LIMITS OF DETECTION FOR A NUMBER OF ANIONS USING THE CONDUCTANCE AND UV DETECTORS

Anion	*Limits of detection (ppm)**	
	Conductance	*UV*
Chloride	1	0.1
Bromide	1	0.2
Nitrite	1	0.2
Chlorate	2	0.2
Nitrate	3	0.3
Sulphate	3	0.3
Iodide	3	0.5
Phosphate	4	0.3
Bromate	5	0.2
Acetate	9	0.4
Formate	10	0.5
Iodate	12	0.4

* This is equivalent to twice the noise level at the most sensitive setting for both detectors.

TABLE II

LINEARITY RANGES FOR SOME ANIONS

Anions	*Linearity range (ppm) (upper limit)*	
	Conductance	*UV*
Chloride	25	50
Nitrate	60	60
Sulphate	80	100

Table I). A relatively stronger, negative UV response occurs for weakly acidic anions because there is no dependence on their ionisation.

(2) Linearity ranges using UV detection are greater than those for conductance (Table II).

(3) Conductance detection may give positive or negative peaks depending on eluent concentration and pH (ref. 2). UV detection of non-UV-absorbing ions gives a response in one direction only.

A number of water extracts have been analysed using the two detectors in series. The ultraviolet detection system has extended the range of application of single-column ion chromatography by overcoming one of the main limitations of the single-column system *i.e.* the level of sensitivity for trace analysis.

REFERENCES

1 D. T. Gjerde, J. S. Fritz and G. Schmuckler, *J. Chromatogr.*, 186 (1979) 509.
2 D. T. Gjerde, G. Schmuckler and J. S. Fritz, *J. Chromatogr.*, 187 (1980) 35.
3 C. A. Pohl, E. L. Johnson, *J. Chromatogr. Sci.*, 18 (1980) 442.
4 R. N. Reeve, *J. Chromatogr.*, 177 (1979) 393.

Journal of Chromatography, 241 (1982) 395–398
Elsevier Scientific Publishing Company, Amsterdam — Printed in The Netherlands

CHROM. 14,785

Note

Affinity electrophoresis in an isotachophoretic discontinuous buffer system

VÁCLAV HOŘEJŠÍ* and TAPOSH KUMAR DATTA*
Institute of Molecular Genetics, Czechoslovak Academy of Sciences, Vídeňská 1083, 142 20 Prague 4 (Czechoslovakia)
and
MARIE TICHÁ
Department of Biochemistry, Charles University, Albertov 2030, 120 00 Prague 2 (Czechoslovakia)
(Received January 25th, 1982)

Affinity electrophoresis[1,2] is based on a combination of electrophoretic separation and specific interaction with an immobilized ligand incorporated into the gel support medium for electrophoresis. Various modifications of affinity electrophoresis can be used for detection and identification of ligand-binding proteins, verifying the homogeneity of the binding proteins and estimation of the strength of protein–ligand interactions. It is usually necessary to employ conditions under which the mobility of the protein is sufficiently high for the difference in mobilities observed on the control (non-interacting) gel and on the affinity gel to be great enough (at least 50%). Also, the presence of various protein impurities which do not interact with the ligand may obscure the results of an affinity electrophoresis, especially, when the specific ligand-binding protein is only a minor component of the sample and when some of the "impurities" have low mobilities. In the present communication we demonstrate the applicability of affinity isotachophoresis (AITP) which in some cases may be useful in avoiding these complications.

Isotachophoresis of proteins in gel media[3] is based on the choice of leading and terminating ions, so that the mobility of all charged molecules in the sample is higher than that of the terminating ion and lower than that of the leading ion. In such a system the proteins present in the sample will migrate within a stack between the boundaries of the zones of leading and terminating ions and will be separated into individual tandemly arranged zones according to their mobilities within the stack. If no "spacer" substances are added [such as ampholyte isoelectric focusing (IEF) carriers] which may aid in the separation of the individual protein components, the experimentally observable result after protein fixation and staining is that the sample migrates as a single sharp zone usually with little or no resolution of the individual components.

We expected that if isotachophoresis were to be performed in a gel containing

* Present address: Indian Institute of Chemical Biology, 4, Raja Subodh Mullick Road, Jadavpur, Calcutta-700032, India.

0021-9673/82/0000–0000/$02.75

immobilized ligand capable of complex formation with a component of the sample, this component would, as a result of the interaction, leave the stack and emerge near the top of the gel. The following results verify this expectation.

MATERIALS AND METHODS

Materials

Agarose L was obtained from LKB (Bromma, Sweden) and chemicals for polyacrylamide gel preparation from Serva (Heidelberg, G.F.R.). Soluble O-glycosyl polyacrylamide copolymers were prepared by copolymerization of acrylamide and allyl glycosides of the respective sugars[4]; the carbohydrate contents of the α-D-mannosyl- and α-D-galactosyl copolymers were 14.1 and 6.7%, respectively. Crude pea seed lectin (PSA) was the protein fraction precipitated from pea seed meal extract by $(NH_4)_2SO_4$ (350 g/l); crude soybean lectin (SBA) was the protein fraction precipitated from soy bean extract by $(NH_4)_2SO_4$ (650 g/l). Heterogeneity of the samples was revealed by IEF performed in 5% polyacrylamide gel[5] containing 2% Ampholine 3.5–10 (LKB).

Isotachophoresis

Separating gels (60 × 2.5 mm; either 2% agarose L or 5% polyacrylamide gel) contained 0.125 *M* Tris–HCl pH 6.8. Affinity gels also contained corresponding O-glycosyl polyacrylamide copolymers (up to 5 mg/ml) and in some cases also free sugars. The electrode buffer contained 25 m*M* Tris and 192 m*M* glycine. Samples (20 μg of the protein) were loaded on the top of the gels in 20 μl of 25 m*M* Tris–HCl pH 6.8, containing glycerol (0.1 ml per ml) and bromophenol blue (10 mg/l). Isotachophoresis was performed at 60 V until bromophenol blue reached a distance of approximately 50 mm from the top of the gel. Proteins were stained by Coomassie Blue R 250.

RESULTS

The results of PSA and SBA are shown in Figs. 1 and 2. Clearly, PSA interacts specifically with α-D-mannosyl residues immobilized in the agarose gel whereas inactive impurities present in the sample remain in the stack migrating with the dye front. Similarly, SBA is retarded due to its interaction with α-D-galactosyl residues immobilized in the polyacrylamide gel. SBA specifically interacts also with the unmodified agarose gel matrix and this interaction can be abolished by free D-galactose (Fig. 1b). The degree of PSA or SBA retardation in affinity gels is dependent on the concentration of immobilized ligand (Fig. 2). The PSA isolectins are well resolved on the affinity gels containing lower concentrations of immobilized α-D-mannosyl residues.

DISCUSSION

In the present communication we have demonstrated the applicability of AITP to two lectins interacting with carbohydrates immobilized in affinity gels. This variant of affinity electrophoresis may possess certain advantages for qualitative detection of

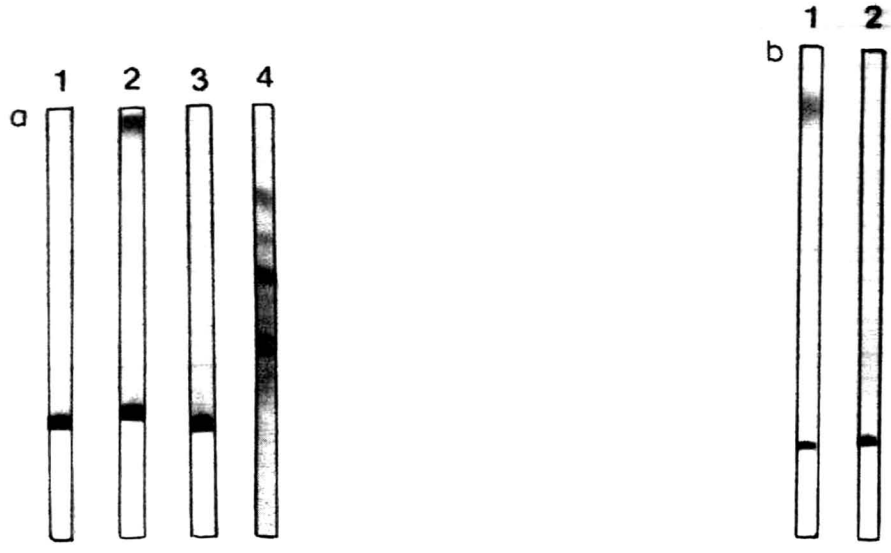

Fig. 1. Affinity isotachophoresis of PSA and SBA. a, Crude PSA on 5% polyacrylamide gels. 1 = Control gel; 2 = affinity gel containing 1% α-D-mannosyl polyacrylamide copolymer; 3 = the same as gel 2 but also containing 2% D-mannose; 4 = isoelectric focusing of crude PSA (for demonstration of the degree of heterogeneity of the sample). Note: Similar results to those obtained in gels 1–3 were also found with 2% agarose L instead of polyacrylamide gels (not illustrated). b, Crude SBA on 2% agarose gel. 1 = Pure 2% agarose L gel; 2 = as in 1 but the gel also contained 2% D-galactose.

ligand-binding proteins. Thus, all the inactive ballast proteins migrate rapidly in a single zone with the dye front and the specific binding protein is "extracted" from this single band on the affinity gel so that it is localized near the top of the gel. There is no interference with zones of ballast proteins in this region and the specific protein may be clearly identified, presumably even if present only in relatively low amount in the crude mixture. The interaction with immobilized ligand is clearly observable because of the marked difference in the rate of electrophoretic migration on control and affinity gels, respectively. Isotachophoresis can be used to "force" a protein to migrate relatively long distances in a control gel; this should be favourable for quantitative estimation of the strength of interaction of the protein with the immobilized ligand, but the fact that the protein migrates under different ionic conditions in the control gel (*i.e.*, within the stack) and in affinity gels (in terminating buffer) will probably affect the accuracy of such measurements. Thus, AITP is suggested for qualitative analytical purposes, similarly to affinity isoelectric focusing[6].

Although the technique clearly works in the above examples, it remains to be seen what are its limitations. For example, we were not able to demonstrate an interaction of defatted bovine serum albumin with immobilized Cibacron Blue F3GA (*i.e.*, affinity gels containing Blue Dextran T 2000) in the ITP buffer system used in this study (not illustrated), whereas specific interaction of the same protein with this ligand could be clearly demonstrated by affinity electrophoresis[7,8]. It seems likely that the removal of the protein from the stack and its retardation in affinity gel as a result of its interaction with immobilized ligand will depend on the actual balance between the counteracting effects of electrophoretic mobility of the protein, stacking properties of the buffer system and the strength of the protein–ligand interaction.

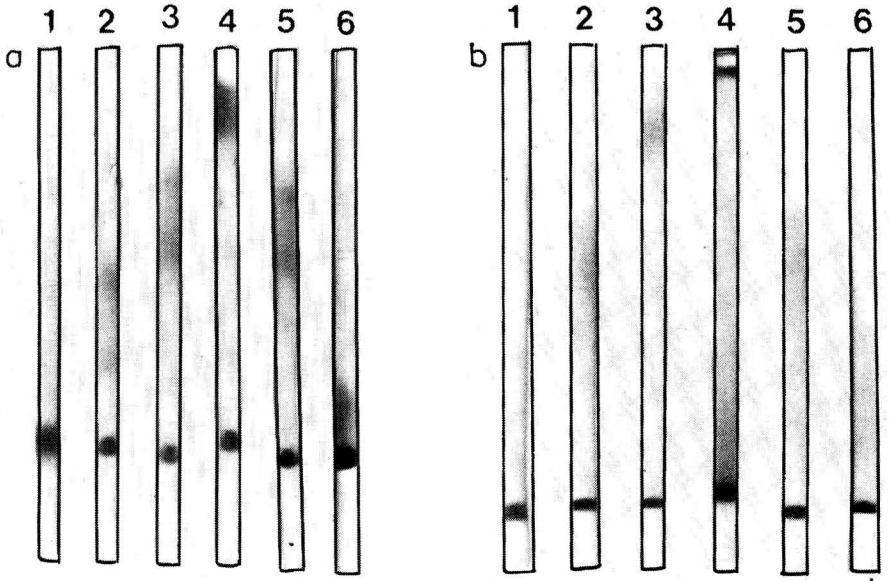

Fig. 2. Dependence of specific retardation of PSA (a) and SBA (b) on the concentration of immobilized and free sugars in 5% polyacrylamide gel during AITP. a: 1–4 = Gels containing 0, 0.1, 0.2 and 0.5% α-D-mannosyl polyacrylamide copolymer, respectively; 5, 6 = affinity gels containing 0.5% α-D-mannosyl polyacrylamide copolymer and 0.5 or 1% free D-mannose, respectively. b: 1–4 = affinity gels containing 0, 0.2, 0.5 and 1% α-D-galactosyl polyacrylamide copolymer, respectively; 5, 6 = affinity gels containing 1% α-D-galactosyl polyacrylamide copolymer and 0.5% or 1% free D-galactose, respectively.

We are aware that there may be formal objections to the designation of the technique as "affinity isotachophoresis" because the zone of the protein interacting with the immobilized ligand leaves the stack and migrates under the conditions of zone electrophoresis, while only the non-interacting proteins migrate isotachophoretically. However, we feel that this designation, although possibly inaccurate, correctly reflects the combination of the principles of isotachophoresis and biospecific affinity interaction which is the rationale of this method.

ACKNOWLEDGEMENTS

We are indebted to Drs. J. Turková and Z. Prusík for critical reading of the manuscript and to Mrs. L. Vyhnálková for its careful typing.

REFERENCES

1 V. Hořejší, *Anal. Biochem.*, 112 (1981) 1–8.
2 T. C. Bøg-Hansen, in J.-M. Egly (Editor), *Affinity Chromatography and Molecular Interactions, Les Colloques de l'INSERM*, Vol. 86, INSERM, Paris, 1979, pp. 399–416.
3 P. J. Svendsen and C. Rose, *Sci. Tools*, 17 (1970) 13–17.
4 V. Hořejší, P. Smolek and J. Kocourek, *Biochim. Biophys. Acta*, 538 (1978) 293–298.
5 P. G. Righetti and J. W. Drysdale, *Biochim. Biophys. Acta*, 236 (1971) 17–28.
6 V. Hořejší and M. Tichá, *Anal. Biochem.*, 116 (1981) 22–26.
7 M. Tichá, V. Hořejší and J. Barthová, *Biochim. Biophys. Acta*, 499 (1978) 301–308.
8 S. J. Johnson, E. C. Metcalf and P. D. G. Dean, *Anal. Biochem.*, 109 (1980) 63–69.

Journal of Chromatography, 241 (1982) 399–403
Elsevier Scientific Publishing Company, Amsterdam — Printed in The Netherlands

CHROM. 14,782

Note

Gas chromatographic assay of atropine and phenobarbital in pharmaceutical preparations containing Valeriana liquid extract

PÁL MAJLÁT
National Institute for Pharmacy, Zrinyi u. 3, H-1051 Budapest (Hungary)
(Received January 28th, 1982)

Currently there are thousands of commercially available dosage forms with both antispasmodic and sedative actions. Some of them contain phenobarbital and a small quantity of atropine in a relatively large amount of Valeriana extract.

The aim of this work was to develop sensitive and reproducible methods for quantification of atropine and phenobarbital in the presence of valepotriates —the main active substances in Valeriana— and other natural products.

Previous procedures of assaying dosage forms for atropine and phenobarbital relied largely on titrimetry. These methods lack specificity and the required sensitivity in this case. Spectrophotometric measurements cannot be carried out, even after a lot of separation procedures, because of interfering coloured materials and other substances. Furthermore, atropine has little absorption in the UV region. On the basis of these facts, gas chromatography (GC) was chosen for solving the problem.

Both the British Pharmacopoeia 1980 (ref. 1) and the United States Pharmacopoeia XX[2] recommend GC for quantification of atropine in pharmaceutical formulations. Determination of the extracted atropine base is carried out by the official GC procedures. Neither of these methods is applicable in the presence of Valeriana liquid extract because of co-extracted interfering substances. With these considerations in mind the most likely approach was the GC analysis of one of the hydrolysis products of atropine. Quercia *et al.*[3] reported a GC method for assaying atropine in the form of tropine in pharmaceutical preparations, and Grabowski *et al.*[4] developed a GC procedure for quantitating homatropine methyl bromide based on the analysis of mandelic acid produced upon its hydrolysis. The first method does not distinguish between atropine and its main decomposition product, apoatropine, as the alcohol component of both compounds is tropine. A technique, based on the same principles as the second method[4], has now been developed for determination of the very small amount of atropine (0.05%) in Valeriana liquid extract.

Due to the polar characters of 5,5-disubstituted barbituric acids, their GC determination was accompanied by certain difficulties. However, since the introduction of derivatization procedures their GC analysis has been greatly simplified. In this work the phenobarbital, present in an amount forty-fold greater than that of atropine, has been methylated and analysed in the preparation —without previous extraction— by GC.

0021-9673/82/0000–0000/$02.75

EXPERIMENTAL

The preparation comprised atropine sulphate (0.0075 g), menthol (0.3 g), phenobarbital (0.45 g) and Valeriana liquid extract (total solid 10%, w/v, 14.24 g).

Instrumentation and procedure

A Carlo Erba Model GV gas chromatograph, equipped with a flame ionization detector, was used. The column was a glass tube (1.0 m × 3.0 mm I.D.) packed with 1.5% OV-101 on silanized Gas-Chrom P (100–120 mesh). Nitrogen was used as carrier gas at a flow-rate of 40 ml/min and the column was operated at 140°C for tropic acid and at 165°C for phenobarbital. Chromatograms were recorded on a Speedomax Model G recorder and integrated by a Carlo Erba Model 75 electronic integrator. The chart speed was 12.7 mm/min.

All reagents were of analytical grade and the drug substances used were of pharmacopoeial standard.

Analysis of atropine sulphate

The internal standard was a solution of 24 mg 2-naphthol in 10.00 ml of anhydrous diethylether.

To about 5.000 g of the preparation (equivalent to about 2.5 mg atropine sulphate) were added 10.0 ml of water. The solution was extracted with three 10-ml portions of chloroform and one 10-ml portion of anhydrous ether. Vigorous shaking was avoided. The chloroform and ether extracts along with any emulsion were discarded. The aqueous solution was acidified to pH 2 with 10% hydrochloric acid and the solution was extracted with three 10-ml portions of anhydrous ether. Vigorous shaking was again avoided. The ether extracts were discarded. The aqueous solution was adjusted to pH 13 with 10% sodium hydroxide solution and heated to boiling for 30 min. Following cooling, the solution was adjusted to pH 2.2 by using 10% hydrochloric acid and extracted with three 20-ml portions of anhydrous ether. To the combined filtered (through cotton–anhydrous sodium sulphate) extract was added 1.00 ml of 2-naphthol internal standard solution. The solution was evaporated to dryness on a water-bath. The residue was dried over silica gel and dissolved in 200 μl of N,O-bis(trimethylsilyl)acetamide (BSA) and the solution was allowed to stand at room temperature for 20 min. A 0.5-μl volume was injected into the GC column.

Analysis of phenobarbital

The methylating reagent, 0.05 *M* trimethylphenylammonium acetate solution, was prepared from N,N-dimethylaniline and methyl iodide according to Mráz and Šedivec[5]. The internal standard was a solution of 60 mg hexobarbital in 10.00 ml of 0.5 *M* trimethylphenylammonium acetate solution.

In a 10-ml volumetric flask about 1.000 g of the preparation (equivalent to about 3 mg of phenobarbital) was dissolved in 5.00 ml of hexobarbital internal standard solution and diluted to the mark with 0.5 *M* trimethylphenylammonium acetate solution. A 0.5-μl volume was injected into the GC column.

RESULTS AND DISCUSSION

Direct GC determination of atropine —without previous extraction— cannot be carried out due to the preponderant concentrations of various natural components in the preparation. Attempts to decrease the attenuation in order to increase the peak of atropine have not been successful. The usual extraction procedure for atropine base did not eliminate interfering co-extracted substances that elute at and near the retention time of atropine.

These inadequacies prompted us to investigate other GC routes. Applying the method of Grabowski *et al.*[4] to atropine seemed to be most promising. However, under the circumstances of the hydrolysis[4], atropic acid —besides tropic acid— was always formed and the hydrolysis was not complete. To avoid the formation of atropic acid the hydrolysis was tried at room temperature, on a water-bath, on a hot-plate and by varying the pH of the solution. The presence and amount of atropic acid as well as the extent of hydrolysis were checked by GC and paper chromatography[6].

Complete hydrolysis takes place in 30 min at pH 13 on a hot-plate. Degradation of atropine to apoatropine and/or tropic acid to atropic acid is negligible under these circumstances. The rate of hydrolysis of atropine is proportional to the hydroxide ion concentration and is enhanced by increased temperature[7]. The high rate of hydrolysis may prevent the formation of atropic acid in this case.

The extraction procedure described in the Experimental effectively separates atropine and tropic acid successively from all interfering substances. In Fig. 1 a chromatogram of tropic acid obtained from the preparation is shown.

Although the introduction of derivatization techniques removed the disadvantages of irreproducible adsorptions and tailings previously experienced in GC of 5,5-

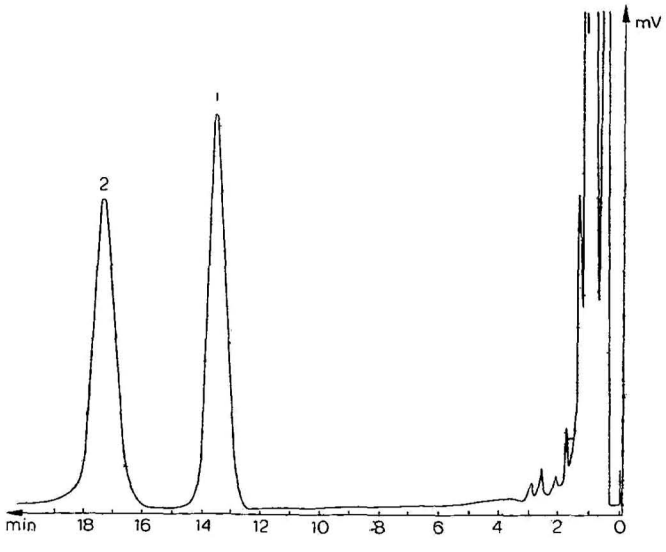

Fig. 1. Chromatogram of the preparation of silylated 2-naphthol (1) and silylated tropic acid (2). Column: 1.0 m × 3 mm, 1.5% OV-101 on Gas-Chrom P. Temperatures: injector 150°C, oven 140°C, detector 160°C. Nitrogen flow-rate: 40 ml/min.

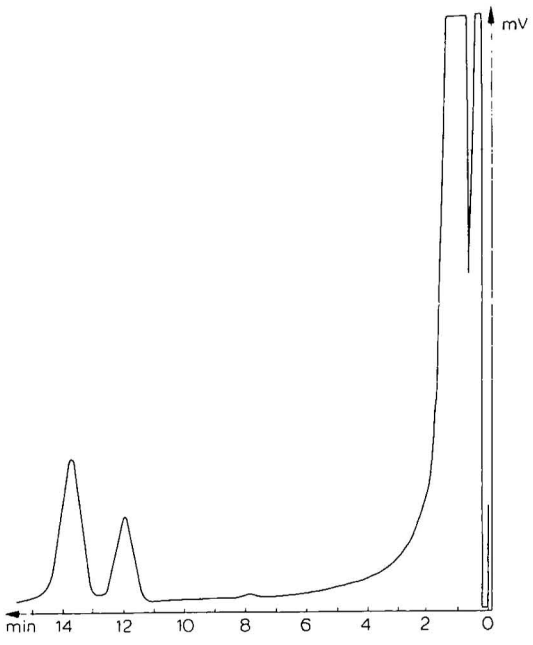

Fig. 2. Chromatogram of the preparation of methylated hexobarbital (1) and methylated phenobarbital (2). Temperatures: injector 180°C, oven 165°C, detector 200°C. Other conditions as in Fig. 1.

disubstituted barbituric acids, the composition of the derivatizing reagents remained a problem. Trimethylphenylammonium hydroxide, N,N,N-trimethylanilinium hydroxide and N,N-dimethylformamide (DMF) dialkylacetals[8,9] were often used as alkylating and acetal-forming agents. Methylation with the strongly basic quaternary ammonium bases produced cleavage of the barbiturate molecule[10] and/or formation of lower methylated products[11]. Impurities are very common in DMF and can interfere with peaks of barbitúrates.

Mráz and Ševic[5] proposed neutral reagents for methylation of barbiturates, the use of which produced the 1,3-dimethyl derivative of the corresponding barbituric acid without formation of by-products. This method has been applied with satisfactory results to methylate phenobarbital.

TABLE I

ACCURACY OF THE METHOD

Recovery experiments were carried out on laboratory-prepared mixtures of atropine and phenobarbital in 15.0 ml of ethanol. Results are means of the analysis of three samples, each of which was chromatographed six times.

Drug substance	*Weight (mg)*	*Found mean, $\bar{x}$ (mg)*	*Recovery, $\bar{x}$ (%)*
Atropine sulphate	7.50	7.35	98.0
Phenobarbital	450.00	448.00	99.0

TABLE II

PRECISION OF THE METHOD

The means, relative standard deviations and 95% confidence limits were determined by the analysis of three samples each of which was chromatographed six times.

Drug substance	*Label claim (mg)*	*Mean $\bar{x}$ (mg)*	*S_r (%)*	*95% Confidence limits (mg)*
Atropine sulphate	7.50	7.15	3.37	7.15 ± 0.12
Phenobarbital	450.00	441.00	1.53	441.00 ± 3.36

Methylated phenobarbital and methylated hexobarbital, the internal standard, are analysed directly in the dosage form. Previous extraction of phenobarbital is rendered unnecessary since there are no interfering peaks on the chromatogram of the preparation. Fig. 2 displays a chromatogram of hexobarbital and phenobarbital (both methylated).

The internal standrd method was used for quantitative evaluation. The ratio of the area of the peak of interest to the area of the internal standard peak was measured. Detector response factors relative to the internal standards were determined previously. Detector response linearities to tropic acid and phenobarbital were confirmed in the concentration ranges 0.5–2 mg/ml and 2–4 mg/ml, respectively.

Accuracy data for quantified components are given in Table I. Table II shows the precision data.

The procedure presented here for the assay of atropine and phenobarbital may provide an approach for their determination in other complex mixtures of pharmaceutical interest, too.

ACKNOWLEDGEMENT

The author thanks Mrs. Zsuzsanna Dvorák-Balogh for her technical assistance.

REFERENCES

1 *british Pharmacopoeia 1980*, The University Press, Cambridge, 1980, pp. 567, 571, 583, 737.
2 *United States Pharmacopoeia 20th Revision*, Mack Publishing Company, Easton, 1979, pp. 59, 60, 66–68.
3 V. Quercia, C. Cardini and B. Tucci, *Boll. Chim. Farm.*, 107 (1968) 373.
4 B. F. Grabowski, B. J. Softly, B. L. Chang and W. G. Hanley, *J. Pharm. Sci.*, 62 (1973) 806.
5 M. Mráz and V. Šedivec, *Collect. Czech. Chem. Commun.*, 42 (1977) 1338.
6 I. Bayer and P. Majlát, *Acta Pharm. Hung.*, 34 (1964) 65.
7 P. Zvirblis, I. Socholitsky and A. A. Kondritzer, *J. Pharm. Sci.*, 45 (1956) 450.
8 R. D. Budd, *J. Chromatogr.*, 192 (1980) 212.
9 A. S. Christophersen and K. E. Rasmussen, *J. Chromatogr.*, 192 (1980) 363.
10 G. W. Stevenson, *Anal. Chem.*, 38 (1966) 148.
11 E. Brochman-Hanssen and T. O. Oke, *J. Pharm. Sci.*, 58 (1969) 370.

Journal of Chromatography, 241 (1982) 404–408
Elsevier Scientific Publishing Company, Amsterdam Printed in The Netherlands

CHROM. 14,763

Note

Bestimmung von Gardona in pflanzlichen Produkten unter Anwendung der Gas–Flüssigkeitschromatographie

P. WASSILEVA-ALEXANDROVA*, A. NEJITSCHEVA, E. KOVATSCHEVA und G. MARUDOV
Hochschule für Lebensmittelindustrie, Plovdiv (Bulgarien)
(Eingegangen am 29. Dezember 1981)

Das Pestizid Gardona (2-Chlor-1-(2,4,5-Trichlorphenyl)-Vinyldimethoxylphosphat) weist eine gute selektive Insektizidaktivität und eine niedrige Warmblütertoxizität auf und gehört zur Gruppe der langsam zerfallenden phosphororganischen Insektizide. Es wird vielfach als Schädlingbekämpfungsmittel bei Obst, Gemüse und Futtermitteln eingesetzt. Die Bestimmung dieses Insektizids erfolgt durch Dünnschichtchromatographie[1,2], Gaschromatographie[3,4] und spektrophotometrische Verfahren. Am zuverlässigsten ist jedoch die Methode der Gas–Flüssigkeitschromatographie, die durch hohe Empfindlichkeit gekennzeichnet ist. In unserer Arbeit setzten wir uns deshalb zum Ziel, ein analytisches Verfahren auszuarbeiten, das sich zur Serienbestimmung von Gardonarückständen in Pflanzenprodukten eignet und effektive Extraktion, Reinigung und günstige gaschromatographische Bedingungen miteinschliesst.

EXPERIMENTELLES

Substanzen und Reagenzien

Wir verwendeten Gardona (98.8 % β-Isomer), ethanolische Lösungen in Konzentrationen 10, 25 und 50 $\mu g/cm^3$ (Shell), Chloroform, Aceton, Petrolether und Acetonitril. All eingesetzten Reagenzien sind p.a. Qualität.

Geräte

Ein Gaschromatograph GCV (Pye Unicam) wurde verwendet.

Arbeitsweise

Nicht mit Gardona behandelte Äpfel der Sorte Goldennoble werden mit einem Mixer homogenisiert. Dem erhaltenen Brei werden Proben zu 50–100 g entnommen und mit entsprechend 10, 25 und 50 g Gardona durch Zugabe von 1 cm^3 Lösung in Konzentrationen von 10, 25 und 50 $\mu g/cm^3$ angereichert. Die Extraktion des Pestizids erfolgt durch Behandlung der Probe mit 50 cm^3 Acetonitril innerhalb von 15 min auf Schüttelapparat und Abfiltrieren über Silikagelschicht. Das Filtrat wird zu 100 cm^3 einer 5 %igen Natriumchlorid-Lösung in einen Scheidetrichter gegeben. Das Pestizid wird aus der erhaltenen Lösung zweimal mit je 50 cm^3 Chloroform extrahiert. Die vereinigten Chloroformextrakte werden über Natriumsulfat im Laufe von 10 min

0021-9673/82/0000–0000/$02.75

getrocknet und durch Blauband-Filter abfiltriert. Das Filtrat wird bei 40°C zur Trockne gedampft. Die Reinigung der Pflanzenextrakte erfolgt nach zwei Verfahren: durch Säulenchromatographie und durch Einfrieren bis −20°C. Die säulenchromatographische Reinigung der Pflanzenextrakte erfolgt durch eine quantitative Übertragung des fast zur Trockne eingedampften Rückstandes mit Chloroform auf eine 10-mm Säule und 5 g Adsorbens (10 g bei 130°C aktiviertes Phlorizin, 8 g Zylit, 1 g Aktivkohle und 10 g wasserfreies Natriumsulfat). Die adsorbierten Stoffe werden mit Chloroform bei einer Geschwindigkeit von 3 cm^3/min eluiert. Die ersten 5 cm^3 Eluat werden weggeschüttet und die nachfolgenden 35 cm^3 bei 40°C zur Trockne eingedampft. Der Trockenrückstand wird in einer Hexanmenge derart aufgelöst, dass Lösungen mit einer Konzentration von etwa 10 $\mu g/cm^3$ erhalten werden.

Die Reinigung der Pflanzenextrakte durch Gefrieren bis −20°C erfolgt wie bereits eingehend in Lit. 5 beschrieben.

Aliquote der gereinigten Lösungen werden gaschromatographisch nach Gardonagehalt unter folgenden Bedingungen untersucht: eine 2 m × 2 mm Glassäule; stationäre Phase 3% SE-30, auf Chromosorb-Füller VV (100–120 Maschen).

Die Detektionssysteme sind: (1) Elektroneneinfangdetektor; Säulentemperatur 210°C; Detektortemperatur 300°C und Injektortemperatur 210°C; Geschwindigkeit des Trägergases Stickstoff 75 cm^3/min. (2) Flammenphotometrischer Detektor mit einem Aufsatz zur Phosphorbestimmung; Säulentemperatur 190°C; Detektortemperatur 200°C und Injektortemperatur 210°C. Geschwindigkeit des Trägergases Stickstoff 75 cm^3/min und die von Wasserstoff 30 cm^3/min.

Als Anzeigerreagens wird die Lösung des Gardonas in Hexan in einer Konzentration von 10 $\mu g/cm^3$ herangezogen. Die Mikrospritzen zum Einspritzen von Proben aus Pflanzenprodukten und der Anzeiger haben Volumen von 1–10 μl.

ERGEBNISSE UND DISKUSSION

Die quantitative Bestimmung der Pestizide in Pflanzenprodukten ist von der Art ihrer Extraktion, von den Reinigungsbedingungen der Extrakte und den die endgültige Bestimmung hindernden Stoffen abhängig. Um die optimale Extraktionsmenge an Gardona in Pflanzenprodukten zu bestimmen, führten wir die Extraktion mit unterschiedlichen in der Literatur beschriebenen Lösungsmitteln[1,6,7] durch, die für phosphororganische Pestizide am geeignetesten erscheinen: Hexan, Petrolether, Aceton und Chloroform. Die vergleichende Untersuchung zeigte einen hohen Extraktionsgrad mit jedem der bereits angeführten Lösungsmittel. Wir bevorzugten jedoch das Chloroform als mehr zugänglich und weniger toxisch.

Leitet man in ein Pestizid enthaltendes Polarlösungsmittel Wasser und anschliessend nichtpolares Lösungsmittel ein, so geht das Pestizid ins nichtpolare Lösungsmittel über, während im polaren der grösste Teil der Verunreinigungen zurückbleibt[8,9]. Aus diesem Grunde untersuchten wir die Reaktion des Gardonas mit Chloroform aus dem System Acetonitril–Wasser. Die erhaltenen Ergebnisse vergleichen wir mit jenen der nur mit Chloroform durchgeführten Extraktion (Tabelle I). Wie aus der Tabelle hervorgeht, ist eine bessere Extraktion des Gardonas durch Chloroform aus dem System Acetonitril–Wasser zu erzielen. Durch die Umlagerung des Gardonas vom Acetonitril–Wasser-Medium in Chloroform wird auch eine gewisse Reinigung des primären Extraktes erreicht.

TABELLE I

EXTRAKTION DES GARDONAS AUS ÄPFELN

Extraktion aus 100 g Äpfeln	*Gardona (µg)*		*% der Nachweisbarkeit*
	Zugesetzt	*Gefundenen Mittelwert von 20 Bestimmungen*	
Chloroform	25.0	22.8	91.2
Chloroform aus dem System Acetonitril–Wasser	25.0	23.8	95.2

Die auf die beschriebene Weise gewonnenen Pflanzenextrakte enthalten immer noch grosse Mengen an Wachsen, Pigmenten und anderen Stoffen, die die quantitative Bestimmung des Insektizids wesentlich erschweren. Zu deren Trennung von den das Pestizid enthaltenden Extrakten setzten wir die Methode der Säulenchromatographie und des Einfrierens bei niedrigen Temperaturen ein.

Zur Ermittlung der Bedingungen für die beste Reinigung durch Säulenchromatographie prüften wir unterschiedlich zusammengesetzte, auch von anderen Autoren[3,4,10] empfohlene Adsorbentia. Den besten Prozentsatz der Nachweisbarkeit ergab die Reinigung der Pflanzenextrakte durch die im Experimentellen bereits beschriebene Säule 1 und durch eine Säule mit 5 g Phlorizin, über das ein Gemisch aus 2.5 g Al_2O_3, 2.5 g Phlorizin und 2 g wasserfreiem Natriumsulfat (Säule 2) eingeleitet wurde. Die in Tabelle II angeführten Ergebnisse zeigen, dass sich beide Chromatographiesäulen zur Reinigung der grosse Mengen an Wachsen enthaltenden Extrakte aus Äpfeln und Birnen eignen. Bei der Reinigung mit der bisher in der Literatur nicht erwähnten Säule 2 erhielten wir stets farblose Extrakte.

Die beste säulenchromatographische Reinigung der Pflanzenextrakte verglichen wir mit der Reinigung durch Gefrieren bis $-20°C$. Die Paralleluntersuchungen erfolgten mit gleichen oder kleineren Gardonamengen als die in Pflanzenobjekten zulässigen Insektizidrückstände. Die in Tabelle III angeführten Ergebnisse weisen darauf hin, dass der Prozentsatz der Nachweisbarkeit bei der Anwendung der Säulenchromatographie etwas höher ist. Da jedoch die Reinigung durch Gefrieren bis $-20°C$ eine kürzere Prozedur und einen kleineren Verbrauch an Reagenzien erfordert, betrachten wir beide Methoden als gut geeignet für die Reinigung von Obstextrakten.

Die endgültige quantitative Bestimmung des Gardonas in den gereinigten Pflanzenextrakten erfolgte durch Gas–Flüssigkeitschromatographie. Als Anzeigesy-

TABELLE II

GEHALT AN GARDONA IN ÄPFELN BEI REINIGUNG DER EXTRAKTE DURCH SÄULENCHROMATOGRAPHIE

Reinigung der Extrakte durch	*Gardona, zugesetzt zu 100 g Äpfeln (µg)*	*Gardona, gefunden (µg)*	*% der Nachweisbarkeit*
Säule 1	25.0	23.8	95.2
Säule 2	25.0	23.5	94.0

TABELLE III

GEHALT AN GARDONA IN ÄPFELN, BESTIMMT MIT GAS-FLÜSSIGKEITSCHROMATOGRAPHIE BEI UNTERSCHIEDLICHER REINIGUNG DER EXTRAKTE

Reinigung durch	*Gardona, zugesetzt zu 100 g Äpfeln (μg)*	*Gardona, gefunden (μg)*	*% der Nachweisbarkeit*
(a) Gefrieren bei −20°C			
Probe 1	50.0	47.3	94.6
Probe 2	25.0	23.4	93.6
Probe 3	10.0	9.1	91.0
(b) Säulenchromatographie			
Probe 1	50.0	48.4	96.8
Probe 2	25.0	23.8	95.2
Probe 3	10.0	9.2	92.0

steme benutzten wir Elektroneneinfang- und flammenphotometrischen Detektor. Um eine geeignete stationäre Phase auszuwählen, erprobten wir drei flüssige Phasen mit unterschiedlicher Polarität: QF-1 (5%); OV-17 (3%) und SE-30 (3%). An den drei gaschromatographischen Säulen erzielten wir bei fast gleicher Empfindlichkeit der Bestimmung eine gute Trennung des Gardonas von den restlichen störenden Stoffen. Die stationäre Phase SE-30 (3%) wurde wegen der günstigeren Arbeitsbedingungen (Temperatur 190°C) vor den flüssigen Phasen 3% OV-17 (240°C) und 5% QF-1 (250°C) bevorzugt. Die ermittelten optimalen gaschromatographischen Bedingungen für die Bestimmung des Gardonas unter Anwendung von Elektroneneinfang- und flammenphotometrischem Detektor sind oben angeführt. Fig. 1 zeigt die bei der

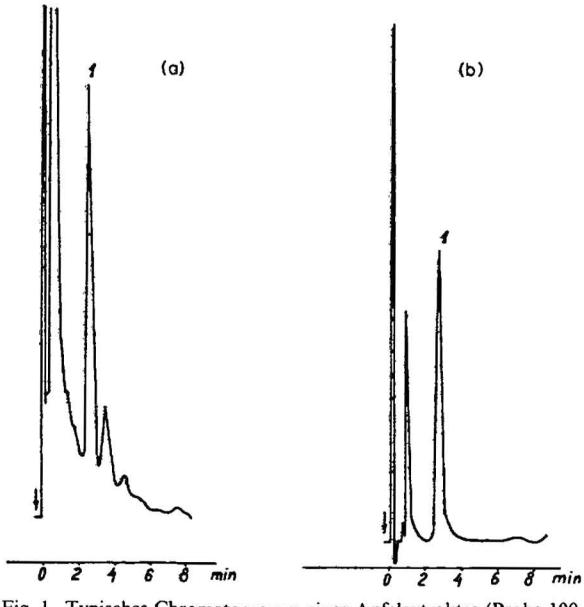

Fig. 1. Typisches Chromatogramm eines Apfelextraktes (Probe 100 g), angereichert mit 25 μg Gardona, nach Reinigung durch Säulenchromatographie: (a) unter Benutzung von Elektroneneinfangdetektor und (b) unter Benutzung von Flammenphotometrischen Detektor. 1 = Gardona.

Analyse des Gardonas im Extrakt aus Äpfeln unter Einsatz der erwähnten Detektoren erhaltenen Chromatogramme. Daraus lässt sich ersehen, dass die Empfindlichkeit des flammenphotometrischen Detektors gegen die störenden Stoffe niedriger ist im Vergleich zu dem Elektroneneinfangdetektor, was eine kürzere analytische Prozedur der Reinigung der Pflanzenextrakte (durch Gefrieren bis $-20°C$) und der angewendeten Lösungsmittel erlaubt.

Die Empfindlichkeit der Bestimmung unter Benutzung beider Detektorsysteme ist hoch (0.0025 mg/kg bei dem flammenphotometrischen Detektor und 0.0005 mg/kg bei dem Elektroneneinfangdetektor) und ermöglicht eine quantitative Bestimmung unter den zulässigen Gardonarückständen in Pflanzenprodukten (0.5 mg/kg).

Die Reproduzierbarkeit und die Genauigkeit der Methode unter Anwendung der Gas–Flüssigkeitschromatographie (flammenphotometrischen Detektors) wurde durch 20 Parallelbestimmungen des Gardonagehaltes in 100 g nach der Methode der Säulenchromatographie gereinigten und an 25 g Gardona angereicherten Äpfelextrakten bestimmt.

Die erhaltenen Ergebnisse wiesen nach statistischer Bearbeitung zufriedenstellende Genauigkeit (Relativfehler 4.8%) und Reproduzierbarkeit (relative Standardabweichung 5.2%) auf.

LITERATUR

1 G. F. Wjilegschanina und L. S. Kejiser, *Zh. Anal. Khim.*, 3 (1975) 590.
2 L. G. Gwosdikova, *Konserv i ovost, prom-st*, 12 (1977) 34.
3 G. F. Vjilegschanina, R. G. Kalmjikova und L. S. Kejisler, *Tr. 2-oe vses. sovestanie po isledovaniju ostatkov pestizidov i profilaktike sagrjasnenija imi produktov pitanija, kormov i vneschnoii sredji, Tallin*, (1971) 151.
4 I. E. Fahey, P. E. Nelson und D. L. Ballee, *J. Agr. Food Chem.*, 18 Nr. 5, (1970) 866.
5 P. S. Wassileva-Alexandrova und A. Nejitscheva, *Nahrung* (1981) im Druck.
6 J. Desmarchelier, *Pestic. Sci.*, 8 (1977) 473.
7 R. M. Stimac, *J. Ass. Offic. Anal. Chem.*, 62 (1979) 85.
8 T. Lipowska, S. Kubacki und W. Coshch, *Pr. Inst. Lab. Badaw. Przem. Spozyw.*, 25 (1975) 3.
9 R. W. Storherr, P. Qtt und R. R. Watts, *J. Ass. Offic. Anal. Chem.*, 54 (1971) 513.
10 H. P. Burchfield und E. E. Storrs, *J. Chromatogr. Sci.*, 13 (1975) 202.

Journal of Chromatography, 241 (1982) 409–412
Elsevier Scientific Publishing Company, Amsterdam — Printed in The Netherlands

CHROM. 14,758

Note

Rapid assay for oxalate oxidase using reversed-phase high-performance liquid chromatography

PIERGIORGIO PIETTA*, ALMA CALATRONI and MARIO PACE
Istituto di Chimica Organica ed Analitica, Università di Milano, Via Celoria 2, 20133 Milan (Italy)
(Received January 20th, 1982)

Oxalate oxidase from barley seedlings (oxalate: oxygen oxidoreductase, E.C. 1.2.3.4) has been recently purified and used[1] for the assay of oxalic acid in biological fluids. The activity of this enzyme is usually measured by the colorimetric determination of hydrogen peroxide enzymatically produced according to

$$(COOH)_2 + O_2 \xrightarrow{\text{oxalate oxidase}} 2\,CO_2 + H_2O_2$$

$$H_2O_2 + DH_2 \xrightarrow{\text{peroxidase}} 2\,H_2O + D$$

where DH_2 are different chromogenic systems, such as 3,5-dichloro-2-hydroxybenzenesulphonic acid–4-aminophenazone[2], 3-methyl-2-benzothiazolinone hydrazone hydrochloride–N,N-dimethylaniline[1] and *o*-dianisidine[3].

High-performance liquid chromatography (HPLC) represents a useful alternative to the colorimetric methods for enzyme assays, because of its selectivity, sensitivity and reliable quantitation[4–6]. Therefore we have developed an HPLC method for the assay of oxalate oxidase, which measures the formation of 2,2′-dihydroxy-3,3′-dimethoxybiphenyl-5,5′-diacetic acid (II) from 4-hydroxy-3-methoxyphenylacetic acid (homovanillic acid, I)[7]:

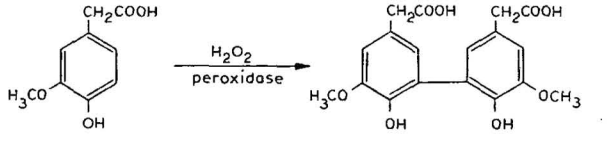

I II

This analytical approach, based upon reversed-phase HPLC, is of wide utility, as demonstrated by its application to other oxidases in the presence of different chromogenic systems[8].

0021-9673/82/0000–0000/$02.75

EXPERIMENTAL

A Model 6000A solvent delivery system, Model U6K universal injector, Model 440 ultraviolet detector and Model 730 data module, all from Waters Assoc. (Milford, MA, U.S.A.), were used in all determinations.

A prepacked, stainless-steel column of μBondapak C_{18} (30 cm × 4.0 mm I.D., particle size 10 μm) was obtained from Waters Assoc. A precolumn of Bondapak C_{18} Corasil (2 cm × 4 mm I.D.) was used.

Reagents

Homovanillic acid (I), nicotinic acid, tris(hydroxymethyl)aminomethane (Tris) and peroxidase (Type II) were purchased from Sigma (St. Louis, MO, U.S.A.); reagent-grade diammonium hydrogen phosphate and succinic acid were from E. Merck (Darmstadt, G.F.R.), and hydrogen peroxide was from Montedison–Carlo Erba (Milan, Italy).

Water used for the preparation of eluents and solutions was distilled, deionized and filtered through Millipore membrane filters, pore size 0.45 μm (Millipore, Bedford, MA, U.S.A.). Methanol was of HPLC (Chromasolv; Riedel-De Haën, Hannover, G.F.R.).

A homovanillic acid solution (2.4 mg/ml) was prepared by dissolving the acid in water. The buffer 0.1 *M* Tris, was obtained by adding the amine (1.211 g) to 100 ml of water and adjusting the pH to 7.8 with 0.1 *M* HCl. A 10 m*M* hydrogen peroxide solution and an aqueous peroxidase solution (1.15 mg/ml) were employed. Nicotinic acid, as internal standard (IS), was dissolved in water to give a concentration of 50 μg/ml. This solution was used within 24 h.

Oxalate oxidase from barley seedlings

Barley seed (*Hordeum vulgare* L. var. distichon Alefeld) was supplied by Malteria Adriatica (Mestre, Italy) and seedlings were used as enzyme source after 8 days at 24°C.

Barley seedlings (1 kg) were homogenized and extracted with 1 l of water. The extract was heated at 80°C for 3 min at 4°C. To the resulting supernatant was added solid ammonium sulphate to give a 60% saturated solution which was allowed to stand for 1 h at 0°C. After centrifugation at 100 *g* for 15 min at 4°C, the precipitate was collected and dissolved in distilled water. The enzyme solution was dialyzed overnight against distilled water at 4°C and then lyophilized. Yield: 100 mg. Specific activity: 0.03–0.1 units per mg of protein. K_M (Michaelis constant, from the Lineweaver–Burk plot) = $4 \cdot 10^{-4}$ *M*.

Chromatographic conditions

Samples were eluted isocratically using 0.01 *M* diammonium hydrogen phosphate buffer–methanol (68:32). After mixing, the buffer was brought to pH 4.9 with 20% phosphoric acid and filtered through a 0.45-μm membrane filter (Type HA, Millipore).

The flow-rate was 1.5 ml/min, and the temperature was ambient in all cases. Chromatographic peaks were monitored at 254 nm. The range setting was fixed at 0.005 a.u.f.s.

Calibration curve

A 50-μl volume of a solution of I and 25 μl of peroxidase solution were added to 1.35 ml of 0.1 *M* Tris buffer, spiked with hydrogen peroxide in the range of 0.0–

0.18 μmol. Then 0.25 ml of nicotinic acid solution were added. Replicate injections of 5 μl were made for each sample.

Oxalate oxidase activity

A 100-μl volume of enzyme solution (10 mg/ml) was added to 100 μl of oxalic acid solution (11 m*M* in 50 m*M* succinate buffer, pH 3.6). The resulting mixture was incubated at 37°C for different times. The reaction was stopped by the addition of 1.35 ml of 0.1 *M* Tris, 50 μl of the solution of I and 25 μl of peroxidase solution. After adding 0.25 ml of nicotinic acid solution, the solution was filtered through a 0.45-μm filter (Millipore), and 5 μl of the filtrate were injected into the chromatograph.

RESULTS AND DISCUSSION

For the determination of II (2,2′-dihydroxy-3,3′-dimethoxybiphenyl-5,5′-diacetic acid) an isocratic elution mode of reversed-phase HPLC was used. The separation of a synthetic mixture of the reference compounds I, II and IS detected at 254 nm is shown in Fig. 1. The minimum detection limits were ≈30 ng for I, ≈30 ng for II and ≈5 ng for IS. A series of standard samples each containing 0–0.18 μmol hydrogen peroxide were prepared according to the procedure described under *Calibration curve*. Chromatographic results showed that the peak area ratio, II/IS, *versus* amount of hydrogen peroxide amount is linear up to 0.20 μmol.

The amount of the enzymatically liberated hydrogen peroxide can be obtained directly from

$$y = 0.11\,x + 0.189;\ r = 0.998$$

where y and x represent the μmol of hydrogen peroxide and the peak area ratio, respectively.

Prior to the chromatographic assay, the enzymatic reaction was stopped by raising the pH from 3.6 (optimum value for oxalate oxidase activity) to 7.8 and the samples were filtered to avoid column contamination.

The activity of oxalate oxidase was calculated from the amount of the en-

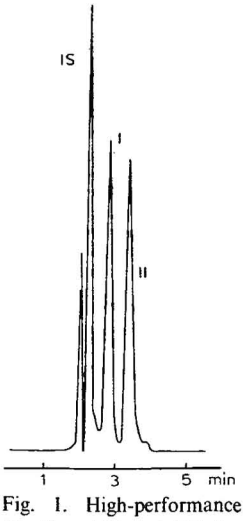

Fig. 1. High-performance liquid chromatogram of homovanillic acid (I), 2,2′-dihydroxy-3,3′-dimethoxybiphenyl-5,5′-diacetic acid (II) and nicotinic acid (IS).

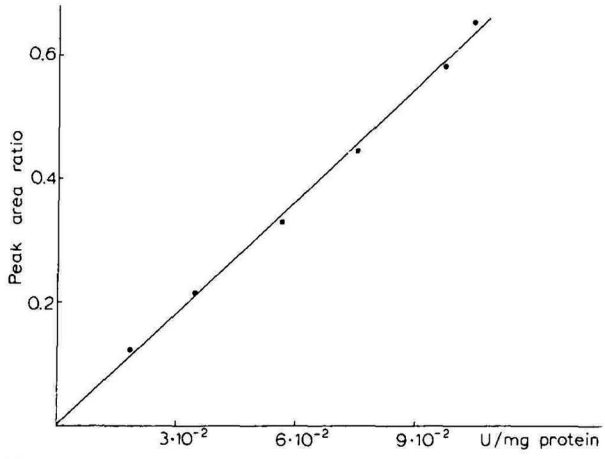

Fig. 2. Assay of oxalate oxidase activity.

zymatically produced hydrogen peroxide, using the following formula:

$$\text{Activity (U/mg protein)} = \frac{\mu\text{mol } H_2O_2}{\text{incubation time} \cdot \text{mg protein}}$$

As shown in Fig. 2, there is a good correlation of the amount of II produced in 5 min to oxalate oxidase activity, in the range of $2 \cdot 10^{-2}$–$1 \cdot 10^{-1}$ U/mg of oxalate oxidase.

CONCLUSIONS

The described reversed-phase HPLC determination of oxalate oxidase activity offers several advantages over colorimetric assays. The analysis time, after incubation, is short (4 min) and the separation is free from interference.

Moreover, the II produced might be measured flurometrically (λ_{ex} 315 nm; λ_{em} 425 nm), which makes the assay even more sensitive ($\approx$5 ng) than the UV detection.

Finally, this reversed-phase HPLC procedure can be successfully extended to the determination of small amounts of other oxidases by the use of synthetic substrates with UV or fluorometric absorption[8].

ACKNOWLEDGEMENT

This study was supported by the National Research Council of Italy (Progetto Finalizzato Chimica Fine e Secondaria).

REFERENCES

1 M. Sugiura, H. Yamamura, K. Hirano, Y. Ito, M. Sasaki, M. Morikawa, M. Ynoue and M. Tsuboi, *Clin. Chim. Acta*, 105 (1980) 393.
2 D. Barham and P. Trinder, *Analyst (London)*, 97 (1972) 142.
3 M. Pace, A. Varallo, P. G. Pietta and A. Burlina, *IRCS Clin. Biochem.*, 8 (1980) 237.
4 A. M. Krstulovic and C. Matzura, *J. Chromatogr.*, 176 (1979) 217.
5 K. Zaitsu, Y. Okada, H. Nohta, K. Kohashi and Y. Ohkura, *J. Chromatogr.*, 211 (1981) 129.
6 S. Soeda, J. Abe and A. Nagamatsu, *J. Liquid Chromatogr.*, 4 (1981) 713.
7 G. G. Guibault, P. Brignac, Jr. and M. Zimmer, *Anal. Chem.*, 40 (1968) 191.
8 P. G. Pietta, A. Calatroni and R. Colombo, *J. Chromatogr.*, 243 (1982) in press.

Journal of Chromatography, 241 (1982) 413–415
Elsevier Scientific Publishing Company, Amsterdam — Printed in The Netherlands

CHROM. 14,797

Note

Detection of binding between transfer RNA and RNA polymerase by high-performance liquid chromatography

SALLY AMERO*
Division of Plant Science, West Virginia University, Morgantown, WV 26506 (U.S.A.)
(First received April 14th, 1981; revised manuscript received February 3rd, 1982)

Recent *in vitro* transcription assays indicate that a specific association between *E. coli* transfer RNA and *E. coli* RNA polymerase should be readily demonstrable[1]. Preliminary sucrose density gradient analyses of mixtures of transfer RNA and RNA polymerase suggest that binding between the two molecules does occur. However, examination of this molecular association in the proportions and conditions employed in the original transcription assays requires detection of minute amounts of complex formation in a system that is saturated with transfer RNA, and the density gradient technique affords neither precise measurement of complex formation nor maintenance of isotonic conditions. Therefore, high-performance liquid chromatographic (HPLC) columns were devised which would exclude the bound complex but retain free transfer RNA, so that complex formation could be monitored indirectly as the reduction in the single elution peak from transfer RNA. The simple high performance exclusion technique affords highly reproducible, quantitative results and greater sensitivity and rapidity than is afforded by conventional exclusion chromatography.

EXPERIMENTAL

Sample preparation

E. coli transfer RNA from strain W and *E. coli* RNA polymerase Type 1 (E.C. 2.7.7.6) from strain K12 were purchased from Sigma Chemical (St. Louis, MO, U.S.A.). The polymerase was shipped, at a concentration of 1.69 mg/ml, in a solvent consisting of 60% glycerol and 40% 50 m*M* Tris buffer, pH 8.0, 0.2 m*M* dithioerythritol, 0.1 m*M* EDTA, 10 m*M* $MgCl_2$, and 0.45 *M* $(NH_4)_2SO_4$. This buffer was substituted, with and without glycerol, for polymerase as indicated in the Table. The tRNA was mixed at a concentration of 1 mg/ml in 0.01 *M* Tris–HCl buffer, pH 7.9, with 0.02 *M* $MgCl_2$, 1 m*M* EDTA, and 0.1 *M* KCl. To 100-μl aliquots of tRNA were added 11-μl volumes of (1) Sigma *E. coli* RNA polymerase, (2) Tris buffer without polymerase, (3) Tris buffer with 60% glycerol, (4) maize polymerase of unknown concentration in buffer (prepared as described in ref. 2), and (5) bovine serum albumin (BSA) in Tris buffer.

* Present address: Department of Biology, University of Virginia, Charlottesville, VA 22901, U.S.A.

0021-9673/82/0000–0000/$02.75

HPLC

Quantitation of tRNA was carried out on a Waters Assoc. Model 201 HPLC (Waters Assoc., Milford, MA, U.S.A.) equipped with a Varichrom variable-wavelength detector (Varian Assoc., Palo Alto, CA, U.S.A.) and a Coleman Model 165 strip-chart recorder. A 55 cm × 7 mm I.D. stainless-steel column was dry packed with equal parts of Corning glycophase-G in 100 Å CPG-10 and uncoated 75 Å CPG-10 controlled pore glass (Corning, Medfield, MA, U.S.A.). The mobile phase was 0.01 *M* Tris–HCl buffer formulated as above. All analyses were carried out at a wavelength of 260 nm, a flow-rate of 3 ml/min, and a recorder chart speed of 5 mm/min. Since peak width at half-height was a constant, all data were recorded as peak height in mm.

RESULTS AND DISCUSSION

This study was undertaken to determine whether transfer RNA can bind to, and thereby regulate, *E. coli* RNA polymerase in the context of *in vitro* transcription assays wherein transfer RNA seemingly functions as an effector molecule[1]. It was important that the experimental design accomodate the ionic conditions and the ratio of transfer RNA to polymerase established in the original transcription studies, which contained insufficient polymerase for direct spectrophotometric detection at 280 nm. The single molecular species that could be detected spectrophotometrically was transfer RNA.

As shown in Table I, the peak area of transfer RNA eluted from the HPLC column decreases significantly with the addition of glycerol-stabilized *E. coli* RNA polymerase. Table I further demonstrates that approximately 20% of the initial 27% decrease in peak height may be attributed to the effect of glycerol in the mix. The 20% reduction caused by glycerol, however, is static over a 10× range of glycerol concentrations, and so does not account for the final 7% decrease in the transfer RNA peak. The experiments were repeated with BSA and maize polymerase, with no apparent effect on the transfer RNA peak height.

The glycerol effect has not been characterized for this study. The control experiments with glycerol were performed since viscous solutions such as glycerol may sufficiently reduce operating pressures to affect elution properties[3,4]. The observations that the reductions in the transfer RNA peak are constant over a 10× range of

TABLE I

PEAK HEIGHTS OF VARIOUS TRANSFER RNA MIXTURES

Sample	*Peak height (mm)*	*% of control*
tRNA + water	125.7	120.0
tRNA + buffer	126.0	120.0
tRNA + buffer + glycerol**	104.7	100.0
tRNA + buffer + glycerol + polymerase	96.7	92.3
tRNA + buffer + BSA	128.0	122.0
tRNA + buffer + maize polymerase	128.3	122.0

* Buffer = 50 m*M* Tris, pH 8.0 (see text).

** Control.

glycerol concentrations, and that the retention time for transfer RNA is unchanged, indicate that the glycerol effect does not result primarily from changes in viscosity. The control experiments do indicate that the glycerol effect is observed in the absence of RNA polymerase and must, therefore, involve either transfer RNA or the column matrix. Although it is possible for glycerol to stabilize single-stranded nucleic acids, transfer RNA contains a high degree of secondary structure and its conformation is relatively stable. Glycerol in these concentrations does not affect the absorptivity of transfer RNA in polymerase buffer. However, it is interesting to note the glycophase matrices are coated with glyceropropylsilyl moieties in order to reduce non-specific absorption[4,5], and I speculate that glycerol interacts with the glycophase matrix. On this basis, I would expect other polyalcohols to produce similar effects.

As the association between transfer RNA and RNA polymerase reported here appears quantitatively reproducible within reasonable estimates of error, a molar binding ratio can be calculated. Although the RNA polymerase bound to transfer RNA cannot be directly measured by this monitoring technique, a minimal binding ratio can be estimated by assuming total saturation of polymerase by transfer RNA. Therefore, 7% reduction in the transfer RNA elution peaks represents a molar ratio of 6 transfer RNA molecules per polymerase molecule, assuming molecular weights of 25,000 and 390,000, respectively. On the basis of filter-binding assays, Pongs and Ulbrich[6] report a 1:1 complex between *E. coli* RNA polymerase and *E. coli* fMet-$tRNA_f^{Met}$ and a 5:1 molar ratio of *B. stearothermophilus* rMet-$tRNA_f^{Met}$ and *E. coli* polymerase. As these studies were conducted under much different conditions (3 m*M* $MgCl_2$), and with formylated, aminoacylated tRNA species, a direct analogy to this report is unwarranted. RNA polymerase may be expected to bind to nucleic acids, particularly to template DNA or to RNA products, but it is surprising to encounter such high binding ratios in systems where RNA polymerase is actively transcribing.

Nucleic acids are not generally amenable to HPLC; the macromolecules tend to clog columns and are denatured by sheer forces. However, accommodation of small samples and precise detection of each molecular species involved in a reaction are obvious advantages of HPLC for studies of polynucleotide-binding reactions, compared to conventional methods such as ultracentrifugation, electron microscopy, or filter retention[7,8]. HPLC may therefore be applicable to other analyses of specific polynucleotide interactions, such as template recognition, competitive inhibition, or hybridizations.

REFERENCES

1 S. Amero, *Dissertation*, West Virginia University, Morgantown, WV, 1979.
2 M. E. Epperly, *Dissertation*, West Virginia University, Morgantown, WV, 1979.
3 L. R. Snyder and J. J. Kirkland, *Introduction to Modern Liquid Chromatography*, 2nd ed., Wiley, New York, 2nd ed., 1979, pp. 487–500.
4 W. W. Yau, J. J. Kirkland and D. D. Bly, *Modern Size-Exclusion Chromatography*, Wiley-Interscience, New York, 1979.
5 F. E. Regnier and R. Noel, *J. Chromatogr. Sci.*, 14 (1976) 316–320.
6 O. Pongs and N. Ulbrich, *Proc. Nat. Acad. Sci. U.S.*, 73 (1976) 3064.
7 G. Hatfield and R. Burns, *Proc. Nat. Acad. Sci. U.S.*, 66 (1970) 1027.
8 M. J. Chamberlain, in R. Losick and M. Chamberlain (Editors), *RNA Polymerase*, Cold Spring Harbor Laboratory, 1976, p. 159.

Journal of Chromatography, 241 (1982) 416–418
Elsevier Scientific Publishing Company, Amsterdam — Printed in The Netherlands

CHROM. 14,756

Note

Analysis of nitrobenzoic acid isomers by high-performance liquid chromatography

TSUNG-TSAN SU* and YU-CHEN CHENG

Union Industrial Research Laboratories, Industrial Technology Research Institute, P.O. Box 100, Hsinchu (Taiwan)

(First received September 29th, 1981; revised manuscript received January 22nd, 1982)

p-Nitrobenzoic acid is a valuable chemical in many areas of industry and research. It is commercially prepared by oxidation of *p*-nitrotoluene. However, the nitration of toluene produces less than 40% of the desired *para* isomer. Thus, a procedure yielding a higher purity of *p*-nitrobenzoic acid is necessary.

In order to investigate the purity of *p*-nitrobenzoic acid obtained from different procedures, it is necessary to develop a sensitive method for the analysis of isomeric nitrobenzoic acids.

A literature search reveals many separations of isomeric nitrobenzoic acids[1–8]. However, these are primarily thin-layer[1,2], ion-exchange[3,4] or gas chromatographic analyses[5]. Thin-layer chromatography is a convenient method used in separation and detection, but not in quantitation of isomers; the separations achieved on ion-exchange resins were by means of traditional column chromatography. Although a quantitation of isomeric nitrobenzoic acids can be accomplished by gas chromatographic separation of their methyl esters, the necessity of transforming isomeric nitrobenzoic acids into their esters may lead to inaccuracies in the analysis due to the various esterification rates of the acids. Since high-performance liquid chromatography (HPLC) offers a rapid and sensitive technique, its use in the analysis of isomeric nitrobenzoic acids is expected to be very valuable.

EXPERIMENTAL

Standards and sample

The standards of isomeric nitrobenzoic acids, used in the construction of calibration curves, were purified by recrystallization of reagent-grade samples from water or benzene.

The procedure used to prepare the sample of *p*-nitrobenzoic acid from polystyrene was similar to that described by Rondestvedt *et al.*[9].

Apparatus and chromatographic conditions

A Model ALC/GPC 244 liquid chromatograph (Waters Assoc., Milford, MA, U.S.A.) equipped with a Model 6000 solvent delivery system was used. The chromatographic columns were LiChrosorb RP-18, 5 and 10 μm, obtained from E. Merck,

0021-9673/82/0000–0000/$02.75

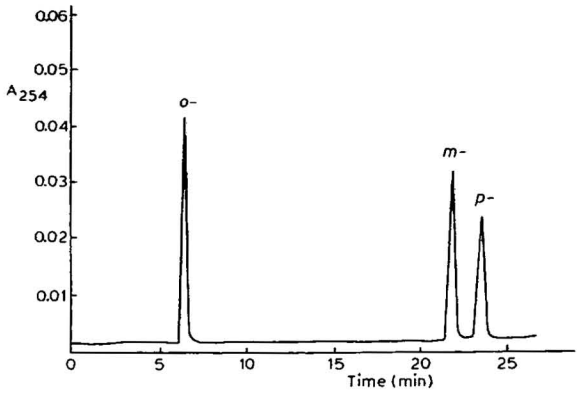

Fig. 1. Separation of isomeric nitrobenzoic acids on LiChrosorb RP-18, 5 μm, with methanol–water (30:70) containing 1 % acetic acid as the mobile phase. The flow-rate was 0.7 ml/min.

VerCopak C_{18}, 10 μm, obtained from Vertex Co. (Taiwan) and μBondapak C_{18}, 10 μm, obtained from Waters. A fixed-wavelength (254 nm) ultraviolet (UV) detector was employed and the chromatograph was operated at ambient temperature. The flow-rate was 0.7–1 ml/min at an operating pressure of 3000 p.s.i. (LiChrosorb RP-18, 5 μm) or 1000 p.s.i. (VerCopak C_{18}, LiChrosorb RP-18 and μBondapak C_{18}, 10 μm). Chromatograms were recorded on an Omniscribe at a chart speed of 0.5 cm/min.

Quantitations were performed on a Shimadzu LC-3A. The chromatographic column used was Zorbax ODS, 5 μm, obtained from DuPont and the chromatograph was operated at 40°C.

RESULTS AND DISCUSSION

Using different methanol–water mixtures containing 1 % acetic acid as the mobile phase, the separation of isomeric nitrobenzoic acids was studied. When VerCopak C_{18}, 10 μm, was used and the mobile phase was methanol–water (70:30) containing 1 % acetic acid, the retention times of *p*- and *m*-nitrobenzoic acids are the same, although *o*-nitrobenzoic acid is well separated from them. In order to separate *p*-nitrobenzoic acid from the *m*-isomer, a column of LiChrosorb RP-18, 5 μm, was tried. Good separation was not achieved when the mobile phase was the same as before. However, by changing to methanol–water (30:70) containing 1 % acetic acid, improved separation of *p*-nitrobenzoic acid from the *m*-isomer can be achieved. In order to separate *p*-nitrobenzoic acid from the *m*-isomer, the flow-rate should be reduced from 1 to 0.7 ml/min. The chromatogram obtained is shown in Fig. 1.

Under the above conditions, no separation of the *m*- and *p*-isomers was obtained on VerCopak C_{18}, 10 μm, μBondapak C_{18}, 10 μm, or LiChrosorb RP-18, 10 μm. This suggests that the mean particle size of the packing material in the column has an important effect on the separation of isomeric nitrobenzoic acids.

Using the conditions to achieve complete separation of isomeric nitrobenzoic acids on LiChrosorb RP-18, 5 μm, the calibration curves can be obtained (Fig. 2). The peak heights were linearly related to the amount injected. The results can be used

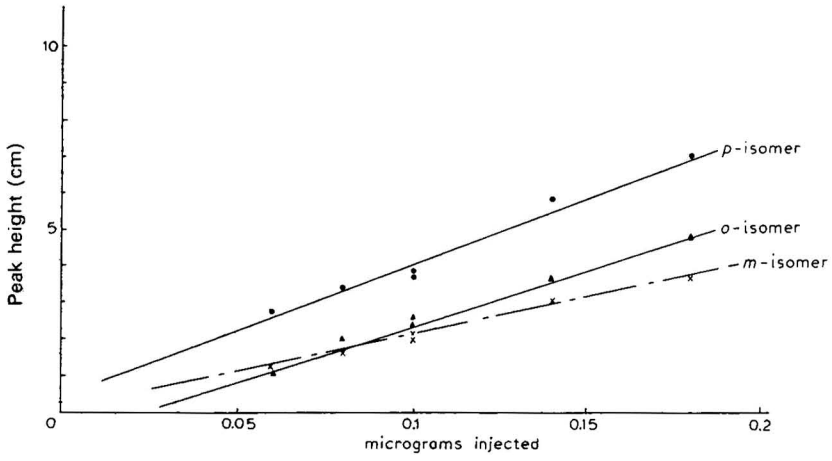

Fig. 2. Calibration curves of isomeric nitrobenzoic acids.

for the quantitation of isomeric nitrobenzoic acids. By comparing the chromatogram of crude *p*-nitrobenzoic acid obtained from polystyrene and the calibration curves, the purity of the crude acid was estimated to be 91%. The precision was determined by repeatedly assaying the sample of *p*-nitrobenzoic acid. The standard deviation was 1.5%. This result showed that the purity of *p*-nitrobenzoic acid prepared from polystyrene was much better than that prepared by the traditional method (oxidation of nitrotoluene).

ACKNOWLEDGEMENT

The authors are grateful to San Kwang Instruments Co., Ltd., especially to Mr. K. T. Chen for valuable discussions.

REFERENCES

1 G. Coppi, *Boll. Chim. Farm.*, 101 (1962) 225.
2 S. Hashimoto and T. Yamashita, *Kogyo Kagaku Zasshi*, 70 (1967) 1450.
3 O. R. Skorokhod and M. L. Tabulo, *Ionoobmen Tekhnol., Akad. Nauk SSSR, Inst. Fiz. Khim.*, (1965) 186; *C.A.*, 63 (1965) 10648.
4 O. R. Skorokhod and M. L. Tabulo, *Geterogennye Reaktsii i Reakts. Sposobnost sb.*, (1964) 26; *C.A.*, 64 (1966) 11906.
5 A. Smith and F. Vernon, *J. Chromatogr.*, 43 (1969) 503.
6 B. Flurscheim and E. L. Holmes, *J. Chem. Soc., London*, (1938) 1242.
7 W. Wittenberger, *Chem.-Ztg.*, 77 (1953) 536.
8 A. P. Krashkov and L. A. Tumovskii, *Tr. Mosk. Khim.-Tekhnol. Inst.*, 58 (1968) 294; *C.A.*, 71 (1969) 27294.
9 C. S. Rondestvedt, J. R. Jefrey and J. E. Miller, *Ind. Eng. Chem., Prod. Res. Develop.*, 16 (1977) 309.

Journal of Chromatography, 241 (1982) 419–422
Elsevier Scientific Publishing Company, Amsterdam — Printed in The Netherlands

CHROM. 14,800

Note

Efficient clean-up of fat samples by Sep-Pak cartridges for polybrominated biphenyl analysis

L. ALICE HU*, G. A. S. ANSARI, MARY TREINEN MOSLEN and EDWARD S. REYNOLDS
Chemical Pathology Laboratory, The University of Texas Medical Branch, Galveston, TX 77550 (U.S.A.)
(Received January 26th, 1982)

Measurement of polybrominated biphenyl (PBB) contamination in fat samples from humans or animals by gas chromatography generally involves preliminary column chromatography on Florisil for removal of neutral fat[1–4]. This clean-up step is time consuming and requires large volumes of solvents, but in the end allows the PBBs in the sample to be concentrated. We have found that sequential extraction of fat samples through Florisil and C_{18} disposable cartridges (Sep-Pak) provides a rapid and efficient method to remove neutral fat prior to PBB analysis.

EXPERIMENTAL

Materials

All solvents were pesticide grade (Burdick and Jackson, Muskegon, MI, U.S.A.) [^{14}C]2,4,5,2′,4′,5′-hexabromobiphenyl (HBB) (10.2 mCi/mmole) of 98+% purity was obtained from New England Nuclear, Boston, MA, U.S.A. Aldrin (99% purity) was obtained from Analabs, North Haven, CT, U.S.A. Florisil and C_{18} Sep-Pak cartridges were obtained from Waters Assoc., Milford, MA, U.S.A. Human fat samples were obtained at autopsy.

Fat preparation

Fat samples containing 10 or 1000 ppb* were prepared by combining 0.5 g fat with 5.0 or 500 ng [^{14}C]HBB. A 5-ml volume of hexane and 0.5 g anhydrous Na_2SO_4 were added and the mixture was homogenized for 5 min. The hexane layer was removed and the residue reextracted by homogenization two more times with hexane (5 ml each time). The hexane fractions were pooled and evaporated to dryness under vacuum at room temperature.

Sep-Pak chromatography

Dried fat was dissolved in 1 ml of acetonitrile or hexane containing 0.1 μg aldrin as an internal standard for C_{18} or Florisil Sep-Pak chromatography, respectively. The dissolved sample was placed on the Sep-Pak cartridge with a syringe. The cartridge was eluted with 40 ml of additional acetonitrile or 10 ml of hexane. Preliminary

* Throughout this article, the American billion (10^9) and trillion (10^{12}) is meant.

0021-9673/82/0000–0000/$02.75

studies of the needed elution volume of C_{18} and Florisil Sep-Pak cartridges demonstrated that the [^{14}C]HBB radioactivity was eluted with the first 40 ml of acetonitrile or the first 10 ml of hexane.

If the fat was to be chromatographed through a second Sep-Pak cartridge, the eluate was dried under vacuum at room temperature, the residue redissolved in 1 ml of the appropriate solvent, placed on the second cartridge and eluted with 40 ml of acetonitrile or 10 ml of hexane.

[^{14}C]HBB and fat recoveries

The final Sep-Pak eluate was dried under vacuum at room temperature in a tared vial and weighed to determine fat recovery. [^{14}C]HBB recovery was determined by dissolving the residue in 1 ml hexane, suspending an aliquot in Scintiverse (Fisher, Fair Lawn, NJ, U.S.A.) and measuring the radioactivity levels with a Packard Mark III liquid scintillation counter (Searle Analytics, Des Plains, IL, U.S.A.). Quench correction was made according to an external standard. Aliquots of the suspended residue were also analyzed by gas chromatography.

Gas chromatography

Gas chromatography was carried out on a Varian Model 3700 equipped with a ^{63}Ni electron-capture detector, a Varian CDS 111 chromatography data system and a fused-silica capillary column (30 m × 0.25 mm) coated with 0.25 μm DB-1 phase (J & W Scientific, Rancho Cordova, CA, U.S.A.). Nitrogen carrier flow-rate was 1 ml/min, and make-up rate was 20 ml/min. Split ratio was 1:100. Injector temperature was 270°C. Detector temperature was 350°C. Oven temperature was programmed to increase from 230°C to 300°C at a rate of 1°C/min.

RESULTS AND DISCUSSION

Recovery of [^{14}C]HBB after homogenization and hexane extraction averaged 98%. As detailed in Table I, fat removal was four times higher with C_{18} Sep-Pak elution than with Florisil Sep-Pak elution. Sequential elution through both types of Sep-Pak cartridges in either sequence removed all but 4 to 6% of the fat. Recoveries of 1000 ppb [^{14}C]HBB after single or sequential Sep-Pak clean-up ranged from 96 and 99% (Table I). [^{14}C]HBB recoveries from samples containing 10 ppb HBB were similarly high and ranged from 97 to 99%.

TABLE I

RECOVERY OF 1000 ppb [^{14}C]HBB AND FAT FOLLOWING SEP-PAK CHROMATOGRAPHY

Extraction	*[^{14}C]PBB recovery (%)*	*Fat recovery (%)*
C_{18}	96.5 ± 0.8*	19.8 ± 0.6
Florisil	99.7 ± 0.3	78.2 ± 1.0
C_{18}–Florisil	96.3 ± 0.4	3.1 ± 0.3
Florisil–C_{18}	97.2 ± 1.1	5.5 ± 0.4

* Mean ± S.E.M. of 3–5 determinations.

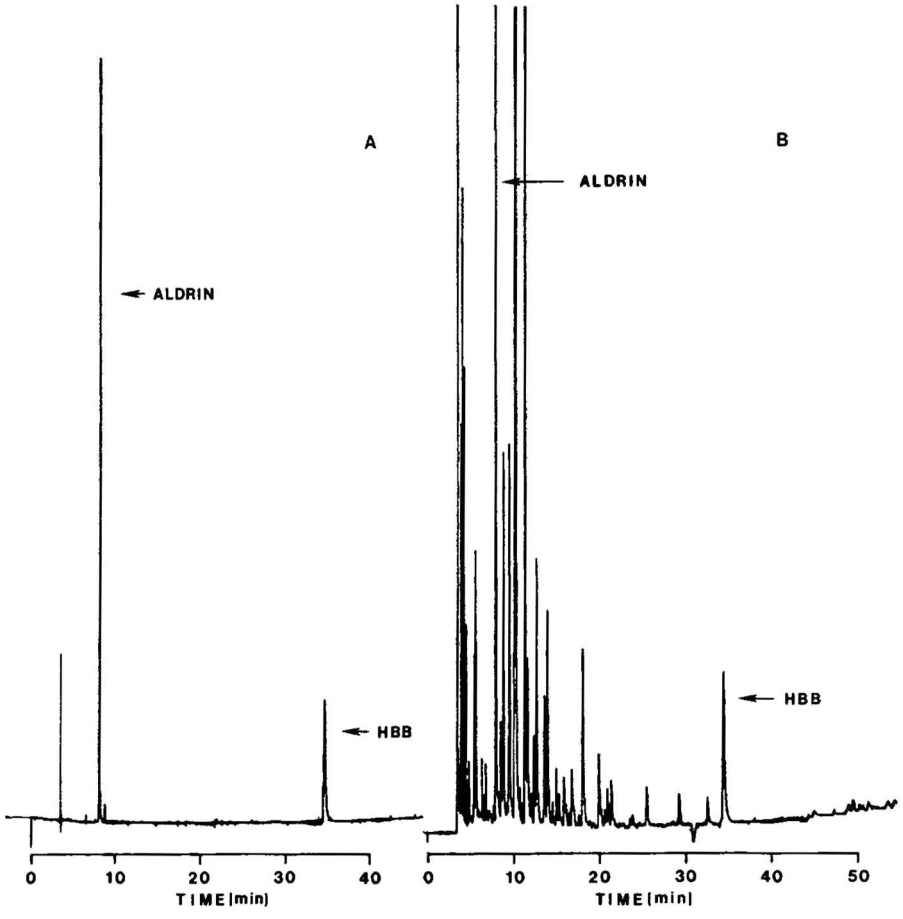

Fig. 1. Gas chromatograms of HBB and aldrin: A, Sep-Pak eluate of standard mixture of 100 ng aldrin and 30 ng HBB in 1 ml hexane; B, Sep-Pak eluate of human body fat (0.5 g) plus 100 ng aldrin and 30 ng HBB in 1 ml hexane.

The sequential Sep-Pak elution procedure provided a clean extract as illustrated by the relatively flat base lines of the chromatograms in Fig. 1A and B. In other studies to be described elsewhere[5] we have identified some of the other peaks in the human fat sample (Fig. 1B) as polyhalogenated aromatics.

In conclusion, sequential elution through C_{18} and Florisil Sep-Pak cartridges provides a convenient and rapid method to clean-up fat samples prior to gas chromatographic analysis of PBB contents. The achieved fat removal of 94% and HBB recovery of 96% are equivalent or better than that achieved with other methods[1–3]. The method is equally efficient for samples containing low (10 ppb) levels such as have been found in eagle carcasses in multiple states[4] or for samples containing higher (1000 ppb) levels such as were found in PBB exposed workers[3]. We estimate that fat samples could be concentrated using this efficient clean-up procedure to allow detection of PBBs at ppt levels.

REFERENCES

1 H. B. Matthews, S. Kato, N. M. Morales and D. B. Tuey, *J. Toxicol. Environm. Hlth.*, 3 (1977) 599.
2 L. B. Willett, C. J. Brumm and C. L. Williams, *J. Agr. Food Chem.*, 26 (1978) 122.
3 M. S. Wolff, H. A. Anderson, F. Camper, M. N. Nikaido, S. M. Daum, N. Haymes and I. U. Selikoff, *J. Environm. Pathol. Toxicol.*, 2 (1979) 1397.
4 T. E. Kaiser, W. L. Reichel, L. N. Locke, E. Cromartie, A. J. Krynitsky, T. G. Lamont, B. M. Mulhern, R. M. Prouty, C. J. Stafford and D. M. Swineford, *Pestic. Monit. J.*, 13 (1980) 145.
5 E. S. Reynolds, L. A. Hu, G. A. S. Ansari, M. T. Moslen, in preparation.

Journal of Chromatography, 241 (1982) 423–427
Elsevier Scientific Publishing Company, Amsterdam — Printed in The Netherlands

CHROM. 14,776

Note

Method for high-performance liquid chromatographic measurement of N-nitrosamines in food and beverages

R. C. MASSEY*, C. CREWS and D. J. McWEENY

Ministry of Agriculture, Fisheries and Food, Food Science Laboratory, Queen Street, Norwich NR2 4SX (Great Britain)

(Received January 29th, 1982)

Trace analysis of N-nitrosamines by high-performance liquid chromatographic (HPLC) methods has hitherto been limited to non-polar N-nitrosamines[1], polar nitrosamines such as N-nitrosodiethanolamine[2] and only those ionisable N-nitrosamines (*e.g.* N-nitrosoamino acids) where the ionisation can be suppressed by the solvent[3]. Routine analysis of even these compounds is further hampered by problems associated with the cold traps[4] normally used with the thermal energy analyser (TEA) which has been used as detector. The limitation on HPLC analysis of non-volatile N-nitrosamines is due to (i) the loss of performance of the catalytic pyrolysis tube if inorganic buffers or ion-pairing agents are used and (ii) the seriously adverse effect on base-line stability of the detector when solvents containing more than trace amounts of water are used. Recent work[5] provides at least a partial solution to these problems by the use of reversed-phase microbore HPLC using an organic ion-pairing agent and a post-column acetone make-up solvent prior to a TEA detector. The present work involves a very simple clean-up procedure which allows routine determination of polar N-nitrosamines in cured meats and beverages. The method involves a "Preptube" extraction stage and avoids the need for liquid–liquid extractions and centrifugation of the resultant emulsions.

EXPERIMENTAL

Materials

"Preptubes" (Thermo-Electron Corp., Waltham, MA, U.S.A.) for non-volatile N-nitrosamine analysis were conditioned with either 20 g 2 *N* sulphuric acid containing 1 g ammonium sulphamate and 3.5 g sodium chloride or 20 g 1.0 *M*, pH 7.0, phosphate buffer containing 0.2 g sodium azide and 3.5 g sodium chloride (for acidic or neutral extracts, respectively) and then eluted sequentially with 100 ml acetone and 100 ml ethyl acetate prior to use.

Reagent blanks were regularly analysed for the volatile and non-volatile N-nitrosamine analyses and found to be negligible in all cases. All solvents were glass distilled before use.

0021-9673/82/0000–0000/$02.75

Methods

Volatile N-nitrosamines in beer were determined by a gas chromatographic (GC) method in which sodium azide (0.5 g) and internal standard (N-nitrosodipropylamine) were added to beer (45 g) which was then adsorbed on three Preptubes prewetted with dichloromethane and eluted with 6 × 8 ml of this solvent. Concentration to 1.0 ml in a Kuderna–Danish evaporator at 55°C was followed by GC analysis with 20% Carbowax 20M terephthalic acid (TPA) + 2% KOH on Chromosorb W AW at 190°C using a TEA detector. Recoveries were 85–100%.

Extracts of non-volatile N-nitrosamines from cured meats (20 g) were prepared by homogenising for 3 minutes at 45°C with 20 g Celite and 90 ml of *either* 2 *N* sulphuric acid containing 5 g ammonium sulphamate (for acidic extracts) *or* 1 *M* phosphate buffer (pH 7.0) containing 1 g sodium azide (for neutral extracts). After cooling to 5°C, the mixture was filtered and 50 g of the filtrate saturated with sodium chloride. The filtrate (3 × 15 g) was absorbed onto three Preptubes and each Preptube eluted with 100 ml ethyl acetate. The eluates were combined and concentrated to dryness on a rotary evaporator at 35°C. The residue was suspended in 2 × 50 ml acetone and concentrated to dryness at 35°C to remove traces of water. The residue was suspended in 5 ml acetone, filtered, the filtrate blown down to dryness with nitrogen and redissolved in 0.5 ml acetone.

Extracts of non-volatile N-nitrosamines from beer (50 g) were prepared by adding 10 g of sodium chloride and *either* 5 ml 10 *N* H_2SO_4 containing 2.5 g ammonium sulphamate *or* 0.5 g sodium azide and sufficient 2 *N* sodium hydroxide (ca. 2 ml) to adjust the pH to 7.0. The sample (3 × 15 g) was absorbed onto three Preptubes and treated as described for cured meats.

Acidic extracts (20 μl aliquots) were analysed with a Spherisorb 5 silica column (25 cm × 5 mm) pre-conditioned with 1 l of 10% acetic acid in acetone. The mobile phase was linearly programmed from 98:1:1 to 89:10:1 hexane–ethanol–acetic acid over 20 min at 2 ml/min. N-Nitrosopipecolic acid was used as internal standard and eluted after 11.8 min.

Neutral extracts (20 μl aliquots) were analysed with a Spherisorb 5 silica column (25 cm × 5 mm) pre-conditioned with 1 l of 2% acetic acid in acetone. The mobile phase was linearly programmed from 2:98 to 98:2 acetone–hexane over 30 min at 2 ml/min.

The HPLC analyses were performed using a TEA Model 502 chemiluminescence detector. The TEA pyrolyser was operated at 550°C and two sets of cold traps (isopropanol–solid carbon dioxide and liquid nitrogen) were used to trap the vapourised mobile phase.

Total N-nitrosamine levels were measured using a procedure[6] in which beer (1 g) was added to refluxing ethyl acetate (50 ml) containing α-tocopherol (0.5 g) and treated sequentially with 2 ml acetic acid and then 2 ml 15% HBr in acetic acid. The reaction mixture was connected in series via two 6 *N* KOH traps, a solid carbon dioxide–isopropanol trap, a needle valve and a liquid nitrogen trap to the reaction chamber of the TEA operating at 7 mmHg.

RESULTS AND DISCUSSION

Using the Preptube extraction methods described in the Experimental section

TABLE I

N-NITROSAMINE CONTENT OF BEER

Assuming stoichiometric release of NO from all N-nitrosamines; for NDMA 0.014 μmol/kg is equivalent to 1.0 μg/kg.

Sample	*Concentration (μmol/kg)*			
	N-Nitroso-dimethylamine	*N-Nitroso-proline*	*Major neutral N-nitrosamine*	*Total N-nitrosamine*
1	0.014	0.162	0.25	17.4
2	0.012	0.052	0.17	6.0
3	0.014	0.040	0.01	1.1
4	0.012	0.012	0.01	0.2

the recovery of N-nitrosoproline added to cured meat at 50 μg/kg was 76% (S.D. = 9.3; $n = 6$), detection limit 5 μg/kg; the recovery of N-nitrosoproline added to beer at 20 μg/kg was 91% (S.D. = 14.4, $n = 12$), detection limit 1 μg/kg. These data compare favourably with other analytical methods for N-nitrosoproline[7–9] and the use of Preptubes facilitates the extraction stage by eliminating liquid–liquid extractions and centrifugation of resultant emulsions. Using the procedures described above measurements were made of N-nitrosodimethylamine (NDMA), acidic and neutral non-volatile N-nitrosamines and total N-nitrosamines in beer. Results from four samples are given in Table I. N-Nitrosoproline eluted in the acidic extract as twin peaks corresponding to the two conformational isomers and was the major component; no other N-nitrosoamino acids were detected. The chromatograms from the neutral extract of sample 1 showed a peak which was much greater than those found in the other samples. All results are expressed as μmol/kg of NO assuming that each of the N-nitrosamines present gives a stoichiometric yield of NO in the catalytic pyrolyser of the TEA. All samples were light beers; the NDMA levels correspond to 0.9–1.1 μg/kg and are at the upper end of the range encountered in beer on sale in Great Britain early in 1981 (levels were typically around 0.4 μg/kg). It is notable that levels of total N-nitrosamines are much greater than can be accounted for in terms of the chromatographic peaks obtained from the extracts. The amount of material unaccounted for can be relatively large. The microbore HPLC method[5] will provide information about ionic N-nitrosamines which would not be extracted by the procedures reported here. It is also notable that whereas the amounts of total N-nitrosamine and of the major neutral N-nitrosamine are highest in sample 1 and decrease in samples 2 and 3 to the lowest in sample 4 there is no simple correlation between these figures and those for NDMA and N-nitrosoproline.

The HPLC–TEA chromatogram of the acidic fraction of sample 2 is shown in Fig. 1; with the exception of N-nitrosoproline no N-nitrosoamino acids were detected in any of the samples. The HPLC–TEA chromatogram of the neutral non-volatile fraction of sample 1 is shown in Fig. 2. Treatment of this neutral fraction with acetic acid and also with HBr–acetic acid[10] showed all the peaks to be unaffected by acetic acid but destroyed by the HBr–acetic acid reagent, thus indicating the presence of the N-nitroso functional group. Further studies are being conducted to establish the identities of these unknown compounds.

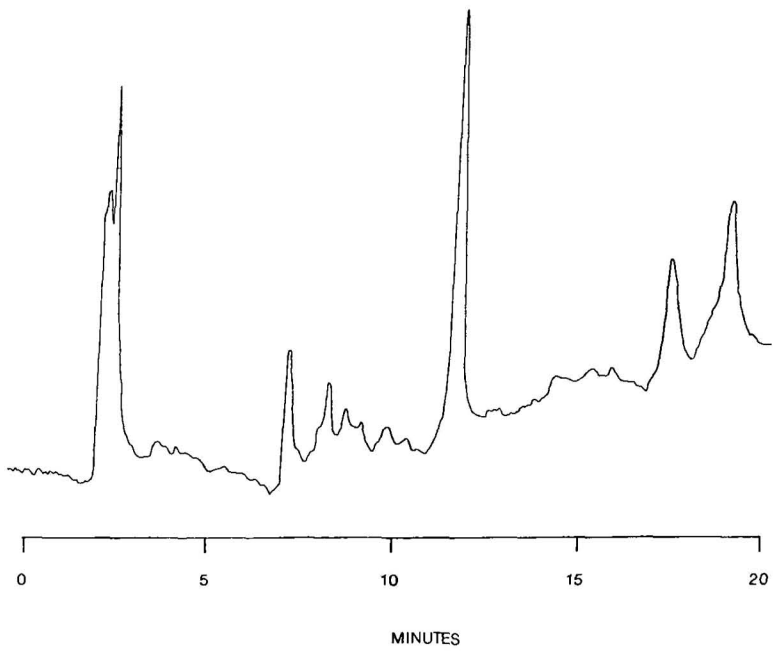

Fig. 1. HPLC–TEA Chromatogram of acidic beer extract with N-nitrosopipecolic acid internal standard (elution time 11.8 min). TEA attenuation ×16.

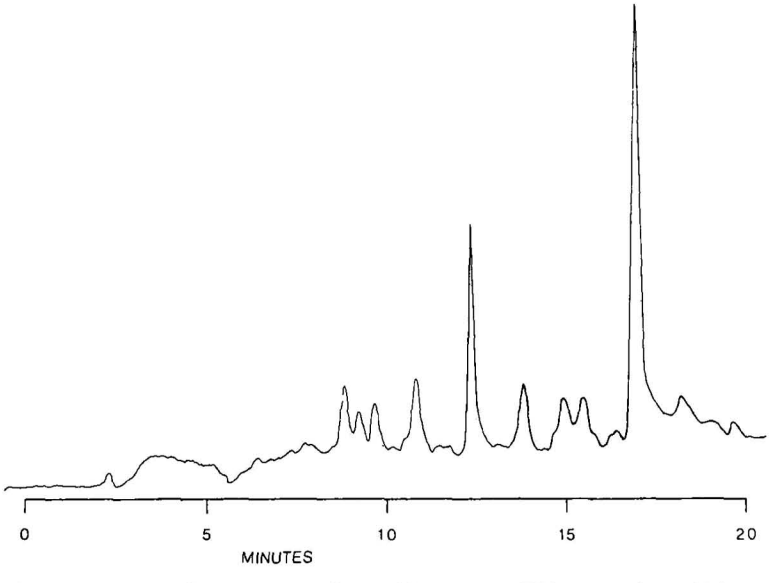

Fig. 2. HPLC–TEA Chromatogram of neutral beer extract. TEA attenuation ×64 for main peak, otherwise ×16.

It is known that malt is the only significant source of NDMA in beer but it remains to be established whether or not the same relationships hold with respect to the other nitrosamines. If malt is the source then the reasons for lack of correlation between the abundances of the various classes of nitrosamine in different beers will have to be sought in terms of differences in malting practice and in the various palliative measures applied in ensuring low levels of NDMA. The method described here is capable of being used on a routine basis for investigations of this sort or for quality control purposes.

REFERENCES

1 D. H. Fine, D. P. Rounbehler, A. Silvergleid and R. Ross, in B. J. Tinbergen and B. Krol (Editors), *Proc. Second Int. Symp. Nitrite in Meat Products, Zeist, 1976*, Wageningen PUDOC, 1977, pp. 191–198.
2 D. Klein, A. M. Girard, J. DeSmedt, Y. Fellion and G. Debry, *Food Cosmet. Toxicol.*, 19 (1981) 233.
3 I. S. Krull, T. Y. Fan, M. Wolf, M. Ross and D. H. Fine, in G. L. Hawk (Editor), *Biological/Biomedical Applications of Liquid Chromatography*, Marcel Dekker, New York, 1979, p. 443.
4 W. F. Tully and W. C. Kuryla, *Microchem. J.*, 24 (1979) 62.
5 R. C. Massey, C. Crews, D. J. McWeeny and M. E. Knowles, *J. Chromatogr.*, 236 (1982) 527.
6 C. L. Walters, M. J. Downes, M. W. Edwards and P. L. R. Smith, *Analyst (London)*, 103 (1978) 1127.
7 C. Janzowski, G. Eisenbrand and R. Preussmann, *Food Cosmet. Toxicol.*, 16 (1978) 343.
8 J. K. Baker and C.-Y. Ma, *J. Agr. Food Chem.*, 26 (1978) 1253.
9 N. P. Sen, S. Seaman and M. McPherson, in E. A. Walker, L. Griciute, M. Castegnaro and M. Borzsonyi (Editors), *N-Nitroso Compounds: Analysis, Formation and Occurrence, IARC Scientific Publication No. 31*, Lyon (1980) 457.
10 I. S. Krull, E. U. Goff, G. G. Hoffman and D. H. Fine, *Anal. Chem.*, 51 (1979) 1706.

Journal of Chromatography, 241 (1982) 428–431
Elsevier Scientific Publishing Company, Amsterdam — Printed in The Netherlands

CHROM. 14,775

Note

Separation of diacyl and plasmalogen phospholipids of rat brain synaptosomal membranes on chromarods

MARIAN FOOT and MICHAEL T. CLANDININ*

Department of Nutritional Sciences, Faculty of Medicine, University of Toronto, 150 College Street, Toronto, Ontario M5S 1A8 (Canada)

(Received January 29th, 1982)

Plasmalogen phospholipids are important components of central nervous system membranes[1], red blood cells[2] and many other vertebrate tissues[3]. Such phospholipids are difficult to separate and quantify as they chromatograph with their diacyl form. Separation of the two species involves mild acid hydrolysis and extensive thin-layer chromatography (TLC).

Separation of polar lipids on silica-coated quartz rods coupled with a flame ionization detector (FID) has already been reported for some lipid mixtures[4,5]. We wish to report a simple and fast method for quantifying synaptosomal lipids containing both diacyl- and 1-alk-1[1]-enyl, 2-acyl-phosphatidylethanolamine. The present report is an adaptation of the reactional two-dimensional TLC system of Horrocks[6] replacing up to three TLC stages and quantitation of separated phospholipids by inorganic phosphorus determination. The application of this method to complex lipid extracts of biological origin containing such plasmalogen phospholipids is demonstrated.

EXPERIMENTAL

Synaptosomal membranes were isolated from rat brain[7] and total lipids extracted with 20 volumes of chloroform–methanol (2:1) followed by 20 volumes of chloroform–methanol–28% aqueous ammonia (35:5:2). Extracts were evaporated to dryness at 40°C under nitrogen and dissolved in 300 μl chloroform, containing 10 mg/ml nonadecane as an internal standard, to give a final phospholipid concentration of *ca.* 5 mg/ml. Chromarods (type S, Technical Marketing, Mississauga, Canada) were stored in 10 *N* sulphuric acid and washed at least four times in distilled water prior to use. The rods were dried 5 min at 110°C and then activated by passage through the FID (Iatroscan Model TH10 obtained from Technical Marketing). Lipid extracts (1 μl) were applied to each chromarod using a 1-μl syringe (Precision Sampling, Baton Rouge, LA, U.S.A.). The rods were developed 20 min in light petroleum (b.p. 50–110°C)–diethyl ether (85:15) to separate neutral lipids and the nonadecane internal standard. The rods were air dried 5 min, then dried 5 min at 70°C and transferred to the FID scanning frame. Rods were scanned to the beginning of the phospholipid band which remained at the origin of the chromarod.

0021-9673/82/0000–0000/$02.75

Half the rods were then placed in a glass frame and exposed to hydrochloric acid fumes for 5 min by positioning the frame over concentrated hydrochloric acid in a TLC tank in such a way that the phospholipid band was approximately 4–5 cm from the level of the acid. The rods were dried 5 min at 70°C and then reactivated by scanning the upper portion of the rod a second time. Phospholipids were separated by development for 40 min in chloroform–methanol–water (80:35:3). The rods were air dried 5 min, then oven dried 5 min at 70°C and scanned in full.

Chromarods were scanned through the FID at 30 sec per rod utilizing Gear No. 40. The hydrogen flow-rate was 80 ml/min and the air flow-rate 2 l/min. The FID was used in combination with a Hewlett-Packard (Avondale, PA, U.S.A.) 3390A reporting integrator. This integrator was also used to plot chromatograms at a chart speed of 10 cm/min, peak width 0.01, threshold 3 and attenuation 6 utilising a full scale deflection of 64 mV (Fig. 1).

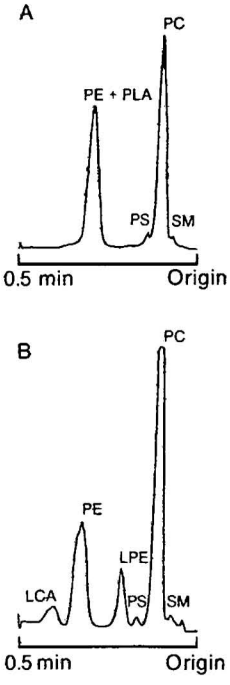

Fig. 1. Phospholipid separation from a sample of rat brain synaptosomal membrane on Chromarod S rods. The sample in Fig. 1B was exposed to HCl fumes prior to development on the chromarod as explained in the text. LCA = Long-chain aldehydes; PE = phosphatidylethanolamine; PLA = ethanolamine plasmalogen; LPE = lysophosphatidylethanolamine; PS = phosphatidylserine; PC = phosphatidylcholine; SM = sphingomyelin.

The FID response to each lipid was determined from purified standards. The concentration of each standard was confirmed by phosphorus analysis[8].

RESULTS AND DISCUSSION

Following acid hydrolysis of the phospholipid mixture two new peaks appear

on the chromatogram: lysophosphatidylethanolamine and long chain aldehydes. The phosphatidylethanolamine peak was also reduced in size relative to phosphatidylcholine. The phospholipids were hydrolysed for up to 10 min but no increase in the plasmalogen: phosphatidylethanolamine ratio was observed after the first few minutes of hydrolysis. This chromatographic system is capable of separating neutral lipids, phosphatidylethanolamine, lysophosphatidylethanolamine, phosphatidylserine, phosphatidylcholine and sphingomyelin within 3 hours of lipid extraction (Fig. 1A and B).

Conventional methods for separation of lipid mixtures containing plasmalogens are considerably more time consuming. Phospholipids are separated from neutral lipids and then subjected to 2-dimensional TLC. The total phosphatidylethanolamine fraction may then be acid hydrolysed and the resulting mixture of aldehydes, phosphatidylethanolamine, and lysophosphatidylethanolamine separated by further TLC[2]. Alternatively the two-dimensional reactional TLC of Horrocks[6] may be employed where phospholipids are acid-hydrolysed after separation in the first dimension. These TLC methods have been well characterized but require larger quantities of membrane lipid, involve several TLC stages, loss of lipid during recovery from TLC plates and chemical analysis for inorganic phosphorus.

Because of rod variability response factors were calculated for each lipid on each rod (Fig. 2). The standard deviation of FID response to 10 μg nonadecane was 13.7% when data from all 10 rods were used but was 3–5% when a single rod was examined. For this reason regression equations were routinely calculated for each lipid type on each rod (Fig. 2). Values of $r \geq 0.99$ indicate that these analyses are highly reproducible within the lipid concentrations tested.

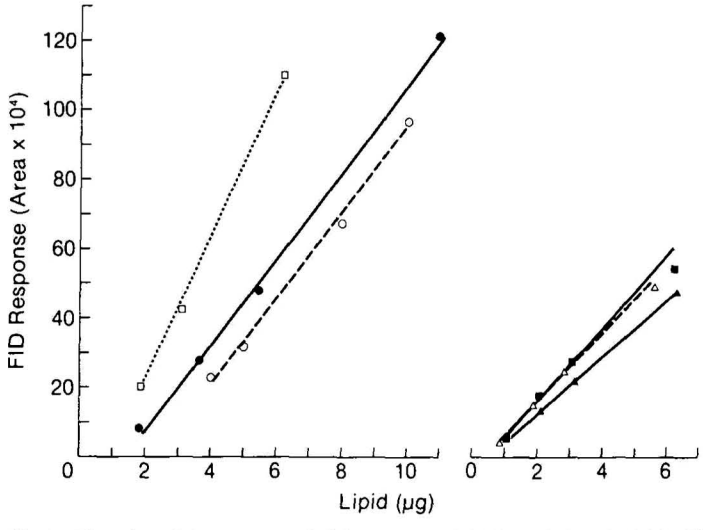

Fig. 2. Linearity of the response of different neutral lipids and phospholipids. □, cholesterol; △, phosphatidylcholine; ■, sphingomyelin; ●, phosphatidylethanolamine; ▲, lysophosphatidylethanolamine; ○, nonadecane. The following regression equations were determined for each line and in each case $r \geq 0.99$ for $n = 10$. □, $y = 20.92x - 20.87$; △, $y = 10.86x - 5.8$; ■, $y = 10.94x - 6.38$; ●, $y = 12.36x - 17.59$; ▲, $y = 8.23x - 4.07$; ○, $y = 12.47x - 29.25$.

TABLE I

POLAR LIPID COMPONENTS IN SYNAPTOSOMAL MEMBRANES OF WEANLING RATS

Values represent the average ± s.d. for three separate synaptosomal preparations from weanling rats. Each sample was analysed in triplicate.

Lipid	*nmoles lipid/mg synaptosomal protein*
Phosphatidylcholine	284 ± 26.6
Sphingomyelin	79 ± 6.7
Phosphatidylethanolamine	198 ± 14.3
Plasmalogen (ethanolamine)	168 ± 10.9
Phosphatidylserine	< 50
Cholesterol	480 ± 32

Quantitative application of this method of analysis is illustrated for syaptosomal membrane prepared from brains of three groups of weanling rats (Table I). The speed and reproducibility of this method of analysis indicates that it has quantitative advantages for routine accurate determination of naturally occurring polar lipid constituents present in complex lipid extracts of biological origin.

ACKNOWLEDGEMENTS

These studies were supported by the Natural Sciences and Engineering Research Council, The Agricultural Research Council of Alberta and the Medical Research Council of Canada.

REFERENCES

1 G. Y. Sun and A. Y. Sun, *Biochim. Biophys. Acta*, 280 (1972) 306.
2 V. Rogiers, *J. Chromatogr.*, 182 (1980) 27.
3 M. H. Hack and F. M. Helmy, *J. Chromatogr.*, 151 (1978) 432.
4 S. M. Innis and M. T. Clandinin, *J. Chromatogr.*, 205 (1981) 490.
5 J. K. Kaitaranta and N. Nicolaides, *J. Chromatogr.*, 205 (1981) 339.
6 L. A. Horrocks, *J. Lipids Res.*, 9 (1968) 469.
7 T. F. Cruz and J. W. Gurd, *J. Biol. Chem.*, 253 (1978) 7314.
8 C. H. Fiske and Y. Subbarowe, *J. Biol. Chem.*, 66 (1925) 375.

Journal of Chromatography, 241 (1982) 432–433
Elsevier Scientific Publishing Company, Amsterdam – Printed in The Netherlands

CHROM. 14,777

Letter to the Editor

Applied headspace gas chromatography

Sir,

J. Novák's review of the book "*Applied Headspace Gas Chromatography*", edited by B. Kolb [*J. Chromatogr.*, 209 (1981) 494] included misleading remarks about a new technique for collecting headspace volatiles. This technique, which was developed by A. Rapp and W. Knipser, is discussed in Chapter 8 of the book under review.

Rapp and Knipser's method is new only in the trapping and concentration of headspace volatiles. The method of sweeping volatiles from a sample by gas extraction, as used traditionally in headspace methods, is unaltered. Thus the reviewer's question "One might ask why the authors did not extract the wine directly with Freon 11", suggests a fundamental lack of understanding of the difference in composition of volatiles obtained by headspace analysis and by simply solvent extracting a sample. Such differences, in the specific case of wine volatiles, have been discussed in the literature[1].

The method of Rapp and Knipser involves a three-phase partitioning of entrained headspace volatiles between the extracting gas, Freon 11, and an aqueous phase. Because of the limited solubility of ethanol in Freon 11, when partitioned against water[2], most of the unwanted ethanol goes into the aqueous phase. But most importantly, the volatile headspace components are efficiently trapped in the Freon F11 free from water and ethanol. Rapp and Knipser have elsewhere[3] discussed the precision and trapping efficiency of their technique.

The method has been used in our own laboratories for almost three years and in this time several hundred headspace analyses have been carried out. We have abandoned older methods of concentrating headspace volatiles on porous resins and this says much for the Rapp and Knipser technique, since we had earlier devoted considerable time to the development of a porous resin method for our research[4]. Reasons for adopting the new method include: (a) simplicity of both apparatus and technique, (b) several gas chromatographic analyses of the same headspace collection can be made, (c) there are no problems with selectivity of porous resin adsorbents distorting the composition of collected headspace volatiles[5], (d) there are no problems with artefacts from the decomposition of porous resins generated during thermal desorption of volatiles[6]. In our hands the technique has proved valuable not only for the analysis of volatiles from wines and other alcoholic beverages but also for fruit juices and plant tissue homogenates.

It is my hope in writing this to correct a wrong impression given of a new technique and to encourage all those interested in headspace analysis to look again at the Rapp and Knipser method. It is the first major advance in headspace trapping and concentration since Jennings *et al.*[7] introduced the porous resin technique in 1972.

The Australian Wine Research Institute, Private Mail Bag, Glen Osmond, S.A. 5064 (Australia)

P. J. WILLIAMS

0021-9673/82/0000–0000/$02.75

1 P. J. Williams and C. R. Strauss, *J. Inst. Brew. (London)*, 84 (1978) 148.
2 P. J. Hardy, *J. Agr. Food Chem.*, 17 (1969) 656.
3 A. Rapp and W. Knipser, *Chromatographia*, 13 (1980) 698.
4 P. J. Williams and C. R. Strauss, *J. Inst. Brew. (London)*, 83 (1977) 213.
5 K. E. Murray, *J. Chromatogr.*, 135 (1977) 49.
6 M. J. Lewis and A. A. Williams, *J. Sci. Food Agr.*, 31 (1980) 1017.
7 W. G. Jennings, R. Wohleb and M. J. Lewis, *J. Food Sci.*, 37 (1972) 69.

(Received October 12th, 1981)

Journal of Chromatography, 241 (1982) 434
Elsevier Scientific Publishing Company, Amsterdam - Printed in The Netherlands

CHROM. 14.778

Letter to the Editor

Applied headspace gas chromatography

Sir,

There are several points in Dr. Williams' letter which deserve a reply. Leaving apart questions such as whether my remark on the paper by Rapp and Knipser necessarily suggests a fundamental lack of understanding of the problem and whether the method indeed is the first major advance in headspace trapping and concentrating since 1972, I shall concentrate on the heart of the dispute. As Dr. Williams' arguments stated in the second paragraph of his letter are not quite clear, I would first recapitulate the situation.

Rapp and Knipser's method, as described in the book I have reviewed, consists in bubbling a stream of inert gas at a flow-rate of 50 ml/min through a 400-ml sample of wine at 20°C for 20 h, entraining the gaseous extract into a container with 10% aqueous ethanol thereby absorbing the volatiles swept from the wine, continuous extraction of the volatiles dissolved in the ethanolic solution by Freon 11, condensing the final extract and chromatographing the concentrate by capillary gas chromatography. My comment on this procedure was: "An unusual, but probably questionable method of measuring the profiles of volatile compounds in wine, consisting in.... One might ask why the authors did not extract the wine directly with Freon 11".

What the authors actually do is transfer volatiles from a sample of wine to 10% aqueous ethanol, *i.e.*, to a liquid the composition of which is very similar to that of the matrix of wine, and then extract the volatiles from the aqueous ethanol with Freon 11. Regarding the chemical similarity of 10% aqueous ethanol and wine matrix, it seems obvious that essentially the same results would be obtained when using the procedure described by Rapp and Knipser and when extracting a sample of wine directly with Freon 11. Compounds such as sugars, acids and tannins would remain largely in the aqueous phase. The only appreciable difference may be lower contents of some volatiles in the aqueous ethanol as compared with their contents in the sample of wine due to their incomplete transfer by stripping. Hence, my remark on Rapp and Knipser's procedure is hardly likely to mislead anyone. Rather, the abridged version of the procedure that I suggested may yield better results with much simpler instrumentation and in a much shorter time. It would not be difficult to check this experimentally.

Institute of Instrumental Analytical Chemistry,
Czechoslovak Academy of Sciences, Leninova 82,
61142 Brno (Czechoslovakia)

JOSEF NOVÁK

(Received January 29th, 1982)

0021-9673/82/0000–0000/$02.75

Author Index

PUBLICATION SCHEDULE FOR 1982

Journal of Chromatography (incorporating *Chromatographic Reviews*) and *Journal of Chromatography, Biomedical Applications*

MONTH	J	F	M	A	M	J	J	A	S	O	N	D
Journal of Chromatography	234/1 234/2 235/1 235/2	236/1 236/2	237/1 237/2 237/3	238/1 238/2 239	240/1 240/2 241/1	241/2 242/1 242/2	243/1 243/2 244/1 244/2	The publication schedule for further issues will be published later.				
Chromatographic Reviews		251/1		251/2								
Biomedical Applications	227/1	227/2	228	229/1	229/2	230/1	230/2					

INFORMATION FOR AUTHORS

(Detailed *Instructions to Authors* were published in Vol. 209, No. 3, pp. 501–504. A free reprint can be obtained by application to the publisher.)

Types of Contributions. The following types of papers are published in the *Journal of Chromatography* and the section on *Biomedical Applications:* Regular research papers (Full-length papers), Short communications and Notes. Short communications are preliminary announcements of important new developments and will, whenever possible, be published with maximum speed. Notes are usually descriptions of short investigations and reflect the same quality of research as Full-length papers, but should preferably not exceed four printed pages. For review articles, see page 2 of cover under Submission of Papers.

Submission. Every paper must be accompanied by a letter from the senior author, stating that he is submitting the paper for publication in the *Journal of Chromatography*. Please do not send a letter signed by the director of the institute or the professor unless he is one of the authors.

Manuscripts. Manuscripts should be typed in double spacing on consecutively numbered pages of uniform size. The manuscript should be preceded by a sheet of manuscript paper carrying the title of the paper and the name and full postal address of the person to whom the proofs are to be sent. Authors of papers in French or German are requested to supply an English translation of the title of the paper. As a rule, papers should be divided into sections, headed by a caption (*e.g.*, Summary, Introduction, Experimental, Results, Discussion, etc.). All illustrations, photographs, tables, etc., should be on separate sheets.

Introduction. Every paper must have a concise introduction mentioning what has been done before on the topic described, and stating clearly what is new in the paper now submitted.

Summary. Full-length papers and Review articles should have a summary of 50–100 words which clearly and briefly indicates what is new, different and significant. In the case of French or German articles an additional summary in English, headed by an English translation of the title, should also be provided. (Short communications and Notes are published without a summary.)

Illustrations. The figures should be submitted in a form suitable for reproduction, drawn in Indian ink on drawing or tracing paper. Each illustration should have a legend, all the *legends* being typed (with double spacing) together on a *separate sheet*. If structures are given in the text, the original drawings should be supplied. Coloured illustrations are reproduced at the author's expense, the cost being determined by the number of pages and by the number of colours needed. The written permission of the author and publisher must be obtained for the use of any figure already published. Its source must be indicated in the legend.

References. References should be numbered in the order in which they are cited in the text, and listed in numerical sequence on a separate sheet at the end of the article. Please check a recent issue for the lay-out of the reference list. Abbreviations for the titles of journals should follow the system used by *Chemical Abstracts*. Articles not yet published should be given as "in press", "submitted for publication", "in preparation" or "personal communication".

Proofs. One set of proofs will be sent to the author to be carefully checked for printer's errors. Corrections must be restricted to instances in which the proof is at variance with the manuscript. "Extra corrections" will be inserted at the author's expense.

Reprints. Fifty reprints of Full-length papers, Short communications and Notes will be supplied free of charge. Additional reprints can be ordered by the authors. An order form containing price quotations will be sent to the authors together with the proofs of their article.

News. News releases of new products and developments, and information leaflets of meetings should be addressed to: The Editor of the News Section, Journal of Chromatography/Journal of Chromatography, Biomedical Applications, Elsevier Scientific Publishing Company, P.O. Box 330, 1000 AH Amsterdam, The Netherlands.

Advertisements. Advertisement rates are available from the publisher on request. The Editors of the journal accept no responsibility for the contents of the advertisements.